TIME DELAY TRACKING USING CORRELATION TECHNIQUES

BY

BIJAN KIANI-SHABESTARI

A thesis submitted to the Faculty of Science of the University of Edinburgh for the degree of Doctor of Philosophy.

Department of Electrical Engineering

June 1983

To My Dear

Parents

ABSTRACT

Correlation function implementation methods are reviewed and their performance under non-stationary signal condition described. Transit time measurement techniques based on methods for detecting the most significant peak position of a cross-correlation function are described and dynamic performance, defined by the sample data nature of the output indication is noted as a major deficiency. Simple analogue, negative feedback, time delay tracking loops offer an acceptable dynamic performance, but in practice these may track spurious peaks.

Improvements have been made to the basic tracking circuit which results in the most significant peak always being tracked and hence a reliable transit time measurement system is formed, with a good dynamic performance, which is suitable for use in industrial correlation flow meters. Flow measurement is noted as an important application area for this work.

Parameters affecting the performance of this correlation based measurement system , in particular under non-stationary signal conditions, have been reviewed. A detailed analysis of the performance of the tracking loop is presented. Transfer function analysis of the loop has shown it to be a first order system. Experimental results have closely confirmed predictions derived from the linear transfer function.

A flow noise simulator was designed and constructed to investigate the performance of the improved circuit. Performance of the improved tracking circuit under changing signal conditions was investigated and the results obtained indicates that it can be designed to offer industrially acceptable performance.

ACKNOWLEDGEMENTS

The programme of the research reported in this thesis was commenced in November 1980. I would like to thank Professor J.Collins, Chairman of School of Engineering , University of Edinburgh, and Taylor Instrument Ltd., for providing the opportunity and facilities to carry out this work.

I would like to express my sincere gratitude to my supervisor, Dr. J.R. Jordan for his help, friendship, advice and encouragement. The success of this project is in a large measure, due to his skill in providing the necessary stimulus to progress when the working conditions became difficult.

Special mention should be made of Dr. G.Coghill who was always willing to assist with any computing difficulties. His invaluable advice to interface the experimental system to the Departments main-frame computer is acknowledged.

I would also like to thank the staff and colleagues in the Instrumentation and Digital Systems Lab., Department of Electrical Engineering for their friendship and help during the research programme.

The author would like to take this opportunity to express his grateful thanks to the following in the Taylor Instrument Ltd.

1. Mr. R.Modie (Technical Director, Servomex Ltd., Crowborough), for his support, friendship, and helpful discussions during his visits to Edinburgh.

2. Mr. K.Bowdell (Industrial Engineering Manager, Stevenage), and his research team for arranging a visit to Taylor Instrument Ltd. branch in Stevenage, and providing all the facilities needed to design a highly reliable IEEE bus interface circuit.

3. Mr. T.Murphy (Taylor Instrument Ltd.,USA), for his helpful comments during his visit to Edinburgh, and providing the necessary information needed during the research programme.

Financial support of the UK SERC during the first two years of the research programme, and Taylor Instrument Ltd. is gratefully acknowledged.

Finally I would like to thank Miss M.Mitchell, who patiently and carefully typed the reports on this thesis, and Miss Yvette Wood for her tremendous encouragement and support during periods of difficulty.

L I S T O F C O N T E N T S

		Page No.
Title Page		(i)
Abstract		(ii)
Declaration of Originality		(iii)
Acknowledgements		(iv)
List of Contents		(vi)
CHAPTER 1	INTRODUCTION	1
1-1	Correlation Based Measurement Systems	1
1-2	Correlation Flow Measurement	2
1-3	The Program of Research	5
1-4	Thesis Format	6
CHAPTER 2	CORRELATION THEORY AND IMPLEMENTATION	8
2-1	The Correlation Function	8
2-1-1	Digital Correlation Algorithms	11
2-2	Implementation of Correlators	14
2-2-1	Serial Correlator	15
2-2-2	Parallel Correlator	15
2-2-3	Serial Parallel Correlator	15
2-2-4	Overloading Counter Correlator	17
2-2-5	Tracking Correlators	18
2-2-6	Single Chip Customised Correlators	27
2-2-7	Micro-computer Based Correlators	31
2-3	Performance of the Correlators	35

List of Contents Continued Page No.

2-3-1 Errors due to the Practical realisation of the Correlation Flow-meter 38

2-3-2 Errors due to the Physical Nature of the Flow Noise Signal 42

CHAPTER 3 THE NOISE SIMULATOR 52

3-1 Introduction 52

3-2 The Flow Noise Simulator 54

3-2-1 Programmable PRBN Signal Generator 56

3-2-2 Programmable Delayed PRBN Generator 59

3-2-3 The Digital Non-recursive FIR Filter 60

3-2-4 Uncorrelated Noise Generator 61

3-3 Flow Noise Simulation 66

3-3-1 Bandwidth of the Simulated Flow Noise Signals 66

3-3-2 Time Delay Setting 70

3-3-3 Correlation Function Significance 74

3-4 Calibration of the Flow Noise Simulator 78

3-5 Experimental System 79

CHAPTER 4 IMPROVED CONSTRAINED PEAK TRACKING CORRELATOR 82

4-1 Introduction 82

4-2 Improved Constrained Peak Tracking Correlator 83

4-3 ICPT Correlators Circuit Design 107

4-4 Coarse Correlators 113

4-4-1 The TRW TDC 1004J Based Correlator 114

4-4-2 Micro-computer Based Correlator 120

List of Contents Continued Page No.

4-5 Experimental System 125

CHAPTER 5 PERFORMANCE OF THE ICPT CORRELATOR 128

5-1 Introduction 128

5-2 Performance of the Tracking Correlator 133

5-2-1 Dynamic Performance of the Tracking Correlator 136

5-2-2 Static Performance of the Tracking Correlator 189

5-3 Performance of the Coarse Correlators 195

5-4 Performance of the ICPT Correlator 200

5-4-1 Dynamic Performance of the ICPT Correlator 201

5-4-2 Static Performance of the ICPT Correlator 209

CHAPTER 6 CONCLUSIONS AND RECOMMENDATIONS 213

REFERENCES 223

APPENDIX 1 Deriving Delayed Sequences From Pseudo Random Binary Noise Generators using Exclusive-NOR Feedback. 236

APPENDIX 2 A FIR Filter For Generating Multilevel Signals From Single Bit Noise Sequences. 242

APPENDIX 3 An Assembled Listing of the Program used to Estimate and Find the Peak of the Correlation Function using 6809 Based Micro-computer. 245

CHAPTER 1 INTRODUCTION

1-1 Correlation Based Measurement Systems

Correlation based measurement systems are potentially useful in a wide range of applications in measurement, telecommunications, and control systems. Due to the growing advances in micro-electronic technology the practical implementation of the correlation function and its applications have been reported by several authors, for example Bendat and Piersol (1980). The range of problems which can be solved using correlation measuring techniques are extremely wide.

The major measurement applications for correlation have been, and will probably continue to be found, in correlation flow-meters. The correlation flow-meter is based on measuring the transit time of naturally occurring flow disturbances between two points, a known distance apart, in the direction of flow. It should be noted that careful transducer design is required to ensure that the correlation function relating transducer outputs has a significant amplitude and symmetrical shape. Different types of transducers for example, hot-wire, capacitive, ultrasonic and optical have been reported to monitor the flow noise disturbances for flow measurement applications.

Velocity measurement using correlation techniques have been reported by several investigators, for example, Townsend (1947), Batterfield, Brigand and Downing (1961), Fisher and Davies

(1963) and Komiya (1966). Other measurement situations are being investigated where noise signals are inherently generated that are suitable for correlation analysis. For example, water and gas leaks generate acoustic noise, this noise can be monitored by positioning receiving transducers at a number of points and the cross-correlations obtained relating the transducers outputs. The geometry of the receiving transducers and peak positions of the measured cross-correlation functions are then used to locate the position of the leak.

Other application of the transit time measurement using correlation techniques are described by several investigators, for example, distance measurement - Spilker and Magill (1961), gas chromatography - Godfrey and Derenish (1968), system identification - Sheppard (1973), bio-medical engineering - Tompkins, Monti and Intaglietta (1974), communication and radar - Forrest and Price (1978), and sonar - Adams, Kuhn, Whyland (1980). A survey of possible application areas for correlation function based measurement systems has been given by Massen (1982).

1-2 Correlation Flow Measurement

The majority of industrial flow systems are highly turbulent so that the flow may be regarded as consisting of a large number of naturally occurring disturbances moving with the flow. Important factors appearing in a flow measurement system specification can be listed as, accuracy, reliability, response time, range, and cost. An obviously desirable feature of any type of flow-meter is that it should offer little or no obstruction to

the flow stream.

Industrial correlation flow metering can be applied to fluids, gasses and particles in suspended flow. This is often combined with density measurement in order to achieve a mass per unit time in volumetric applications. The open channel flow measurement application of the correlation based measurement systems has been described by Kaghazchi and Beck (1977).

Despite recent advances in low cost micro-electronic circuits the correlation flow— meter has not achieved a commercially attractive selling price. In addition a long measurement time is required to achieve statistically acceptable results but this leads to a display which jumps in discreet steps from reading to reading under changing signal conditions. This is generally thought to be a bad feature for industrial applications.

Correlation function theory is generally only valid for stationary signal conditions. Experimentally however it can be observed that the function peak height is reduced and its width increases if the flow noise signal is changed during the integration period. Very little work has been reported on the accuracy of correlation based measurement systems under changing signal conditions.

Due to the relatively low cost of implementation, coarsely quantised time delay axis based measurement systems have been developed by several investigators for flow measurement

applications. Reported, commercially developed, correlation flow-meters are based on the above technique. The Endress and Hauser Co. (1982), have developed a commercially available correlation based measurement system for flow measurement applications. In addition the commercially developed correlator have been successfully employed for the location of the position of water and gas leaks. Other reported developments are the prototype KPC multichannel correlation signal processor developed by Kent Instruments Ltd., Keech (1982), and the prototype correlation flow-meter developed by Taylor Instruments Ltd. (1976).

Under changing, i.e. non-stationary flow noise signal conditions it is likely that the tracking correlators will perform better than coarsely quantised time delay axis based correlation flow-meters. In addition tracking correlators are not complex and expensive to implement. But they do not have a good reputation for industrial applications. Major obstacles for industrial application, and in particular for flow measurement applications, is the possibility of tracking spurious peak which could lead to inaccurate estimation of transit time.

Consequently the major part of this thesis is concerned with the development of a peak tracking system for industrial flow measurement applications. An improved constrained peak tracking ICPT correlator has been designed and constructed to give reliable and accurate estimation of flow velocity with a fast response time. The performance of the ICPT correlator was investigated

under changing signal conditions, and the results obtained indicates that the ICPT correlator can be designed to offer an industrially acceptable performance.

1-3 The Programme of the Research

The primary objective of the research programme was to investigate methods for improving the accuracy and dynamic performance of correlation based measurement systems, particularly under changing signal conditions. This part of the research programme has resulted in the design and construction of the improved constrained peak tracking (ICPT) correlator, and its performance was optimised for flow measurement applications.

The improved constrained peak tracking correlator is comprised of three correlators operating in parallel. A micro-computer based coarse correlator was designed to constrain the tracking loop to track the most significant peak of the correlation function. The variance of the peak position estimate of the micro-computer based correlator is poor and can set the delay shift register length of the loop through a coarse position latch. The tracking loop is free to track the most significant peak of the correlation function within its linear lock range. A window comparator is used to control the coarse position latch through a logic control, and is enabled once the tracking loops error voltage is beyond its linear lock range. A single bit polarity serial correlator is used to indicate the out of lock mode of the tracking correlator.

A secondary objective of the research programme was to design and construct a programmable flow noise simulator, which could be used to evaluate the performance of the prototype ICPT correlator. The designed and constructed flow noise simulator has characteristic very similar to flow generated noise signals.

An IEEE bus interface circuit was designed and constructed for the flow noise simulator and the ICPT correlator. The experimental measurement system was controlled through the IEEE bus by an HP-85 computer. This computer controlled arrangement was proved to be invaluable for the large number of long term, statistical, experiments carried out to evaluate the performance of the experimental system.

A detailed experimental study of the performance of the tracking loop revealed that for linear and reliable operation of the ICPT correlator additional circuits such as the window comparator and coarse position latch were required. The prototype model of the tracking system was found to operate exactly as predicted by its first order transfer function. The experimental results obtained for the performance of the ICPT correlator indicate that the ICPT correlator can be considered as one approach to the future realisation of industrially acceptable correlation flow-meters.

1-4 Thesis Format

Chapter 2 gives the theoretical and practical background necessary to understand and implement correlation based

measurement systems. A review of published works on the performance of correlators and some of the techniques available to estimate the correlation function under non-stationary signal conditions is also presented.

Design of the micro-computer based flow noise simulator is described in chapter 3. The second part of this chapter describes the performance of the flow noise simulator.

Chapter 4 describes design of the prototype ICPT correlator. The design of the TRW TDC1004J based coarse correlator and the micro-computer based coarse correlator are also presented in this chapter.

The detailed investigation of the performance of the tracking correlator is given in the first part of chapter 5. The second part of chapter 5 is devoted to an assessment of the overall performance of the ICPT correlator.

Chapter 6 summarises the conclusions of the thesis and suggests some extensions to the research programme.

CHAPTER 2 CORRELATION: THEORY AND IMPLEMENTATION

2-1 The Correlation Function

The correlation function relating two random variables describes the dependence of one random signal on the other one as a function of the time delay between the two signals. The cross-correlation between two random signals, x(t) and y(t), can be described by the mathematical expectation:-

$$R_{dyx}(t,\tau) = E\,[\, y(t) \cdot x(t-\tau)\,] \qquad (2\text{-}1)$$

where $R_{dyx}(t,\tau)$ is the cross-correlation function between x(t) and y(t) with a time difference τ, and E is the ensemble average. For a stationary random process this average will only depend on the time difference between two signals and the cross-correlation function can be expressed as:-

$$R_{dyx}(\tau) = \lim_{T\to\infty} \frac{1}{T}\int_0^T y(t) \cdot x(t-\tau)\, dt \qquad (2\text{-}2)$$

The correlation function integral can be implemented as shown in figure 2-1.

The normalised correlation function, $\rho(\tau)$, is given by:-

$$\rho(\tau) = \frac{R_{dyx}(\tau)}{R_{dxx}(0) \cdot R_{dyy}(0)} \qquad (2\text{-}3)$$

Where $R_{dxx}(\tau)$ and $R_{dyy}(\tau)$ are the auto-correlation functions of x(t) and y(t). The auto-correlation function of the random processes x(t) and y(t) are given by:-

$$R_{dxx}(\tau) = \frac{1}{T}\int_0^T x(t) \cdot x(t-\tau)\, dt \qquad (2\text{-}4)$$

and

$$R_{dyy}(\tau) = \frac{1}{T}\int_0^T y(t) \cdot y(t-\tau)\, dt \qquad (2\text{-}5)$$

with $R_{dxx}(0)$ = mean square value of x,

and $R_{dyy}(0)$ = mean square value of y.

In recent years correlators have been widely used in flow measurement applications. A schematic diagram of a correlation flow-meter is shown in figure 2-2. Two transducers are clamped to the pipe wall at a distance L apart, and generates electrical noise signals which are related to flow turbulence and conveyed particles. The signal at the down-stream transducer y(t) will be, approximately, a delayed version of the signal, x(t), being monitored by the up-stream transducer. The time delay between up-stream and down-stream signals is found from the position of the peak of the correlation function estimate.

Therefore flow velocity within the pipe is given by:-

$$V = \frac{L}{\tau} \qquad (2\text{-}6)$$

Time domain estimation of the correlation function integral can be performed using one of the three methods given below:-

i) Direct correlation methods: the direct correlation function is estimated with both signals in their analogue form.

ii) Stieltjes correlation methods: where one input signal is quantised and the other input signal to the correlator is analogue, Watts,(1962). The simplest form in this classification is known as the relay correlator, where one input signal is quantised to two levels.

(iii) Digital correlation methods: The digital correlation function is estimated with both signals quantised. In the most extreme case both signals are quantised to two levels and is referred to as polarity correlation.

Significant improvements in the cost of estimation of the correlation function can be achieved using digital algorithms. Due to the growing capability and the availability of low cost and fast digital integrated circuits, digital techniques to estimate correlation functions have been extensively investigated.

2-1-1 Digital Correlation Algorithms

If the digital techniques are used to estimate the correlation function, input signals must first be sampled and quantised. The digital sampled-data correlation function, R_{Dyx}, algorithm is given by:-

$$R_{Dyx}(j) = \frac{1}{N} \sum_{k=1}^{N} y_k \cdot x_{k-j} \qquad j=0,1,2,\ldots,M \qquad (2-7)$$

Where x_K and y_K are the quantised values of the x(t) and y(t) sampled at intervals of $\Delta\tau$ and the correlation function is estimated at M equally spaced lag values with measurement time of $N\Delta\tau$.

To avoid loss of information the sampling rate of the input signals should not be less than the Nyquist sampling rate, which requires a minimum sampling rate of twice the highest frequency component of the input signals. The effect of quantisation of the input signals to be correlated have been considered by several authors, for example Watts (1962), Widrow (1956), (1961). It has been shown that the quantisation operation is equivalent to adding random unwanted noise to the signal with the mean value of the noise depending on the quantisation level. Therefore the variance of the correlation function estimate will increase if the input signals to the correlator are quantised. Finne (1965) has investigated the effect of quantisation on the variance of the correlation function estimate and he has shown that the variance of the correlation function estimate will

increases by a small factor, even for fairly coarse quantisation levels.

A significant reduction in implementation cost is achieved if quantisation is carried out to the extreme, resulting in two level signals, namely polarity signals. The polarity correlation algorithm is given by:-

$$R_{\rho yx}(j) = \frac{1}{N}\sum_{K=1}^{N} \mathrm{Sgn}\,(y_k) \cdot \mathrm{Sgn}\,(x_{K-j}) \qquad j=1,2,\ldots,M \qquad (2\text{-}8)$$

Where $\mathrm{Sgn}(x_K)$ and $\mathrm{Sgn}(y_K)$ are the polarity samples of x(t) and y(t) taken at intervals of $\Delta\tau$, and $R_{\rho yx}$, is the polarity correlation function estimate.

Van Vleck (1966) has shown that for a Gaussian random signal with zero mean the polarity correlation function ρ_p, is related to the normalised direct correlation function, ρ_d, by the expression:-

$$\rho_p = \frac{2}{\pi}\,\mathrm{Sin}^{-1}\rho_d \qquad (2\text{-}9)$$

Therefore the variance of the polarity correlation function will be increased compared with the variance of the direct function, but the peaks of the functions will coincide, as shown in figure 2-3. Hence the polarity correlation algorithm is ideal for applications such as correlation flow measurement, where the position of the peak of the correlation function is of great

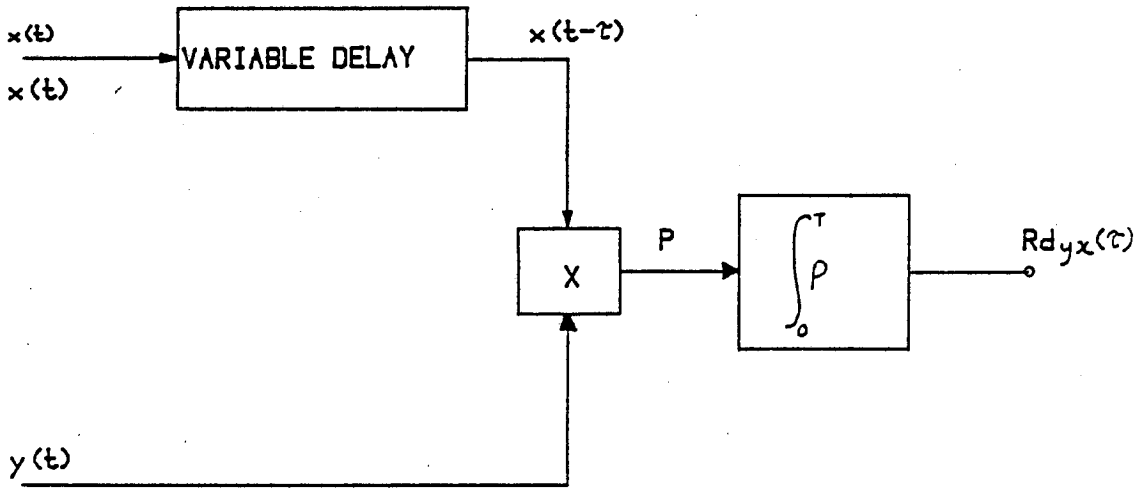

Fig. 2-1 IMPLEMENTATION OF THE CORRELATION FUNCTION INTEGRAL.

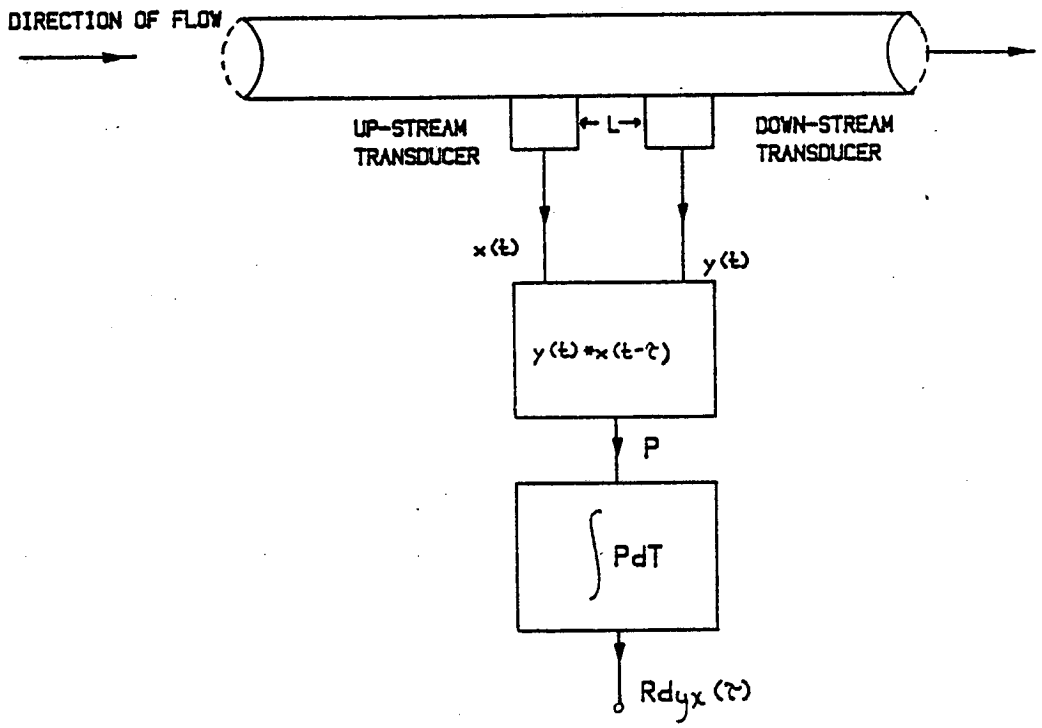

Fig. 2-2 CORRELATION FLOW MEASUREMENT.

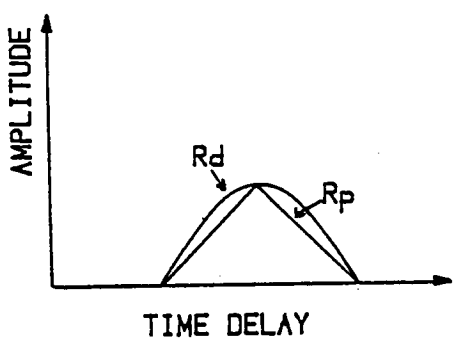

Fig. 2-3 POLARITY & DIRECT CORRELATION FUNCTIONS.

importance.

To further reduce the cost of the estimation of the polarity correlation function. Kam, Shore and Feher (1975) have described the slow sampling algorithm given by:-

$$R_{\rho yx}(j) = \frac{M}{N} \sum_{K=1,M+1,2M+1}^{N} Sgn(y_K) \cdot Sgn(x_{K-j}) \qquad j=1,2,\ldots,M \qquad (2\text{-}10)$$

The up-stream signal is slow sampled with a period of ΔT and the down-stream signal is sampled at a period of $\Delta\tau$, determined from the resolution required rather than the bandwidth of the signals being correlated, and M is given by:-

$$M = \frac{\Delta T}{\Delta \tau} \qquad (2\text{-}11)$$

Experimental results given by Thorn (1979) indicates that this simplification will have little effect on the accuracy of the correlation function estimate, however more work is required to investigate the variance of the correlation function estimate using the slow sampling technique.

2-2 Implementation of Correlators

In general the correlation function between two signals can be estimated using one of the three techniques given below:-

1) Hardware correlation using commercially available

digital circuits.

2) Customised single chip integrated circuit correlation.

3) Micro-computer based correlation.

2-2-1 Serial Correlator

The serial correlator has the simplest structure. It estimates the correlation function for a series of values of time delay taken in turn Korn (1966), Hayes and Musgrave (1973). This method is slow and is not suitable for real time operations and in particular it is not suitable for on line flow measurement applications.

2-2-2 Parallel Correlator

Due to the fast response of the parallel implementation method, shown in figure 2-4, this method can be used for real time estimation of the correlation function, Korn (1966), Hayes and Musgrave (1973). But it is not practical for industrial use due to its high cost and the complexity involved.

2-2-3 Serial Parallel Correlator

To reduce the complexity of the parallel correlators, the serial-parallel correlators shown in figure 2-5 can be used, Finne (1965), Korn (1970), Hayes and Musgrave (1973). This correlator still is relatively expensive to implement for industrial applications. Both the Hewlett-Packard HP3721A (1968), and the Honeywell Saicor (1970) correlators are based on the

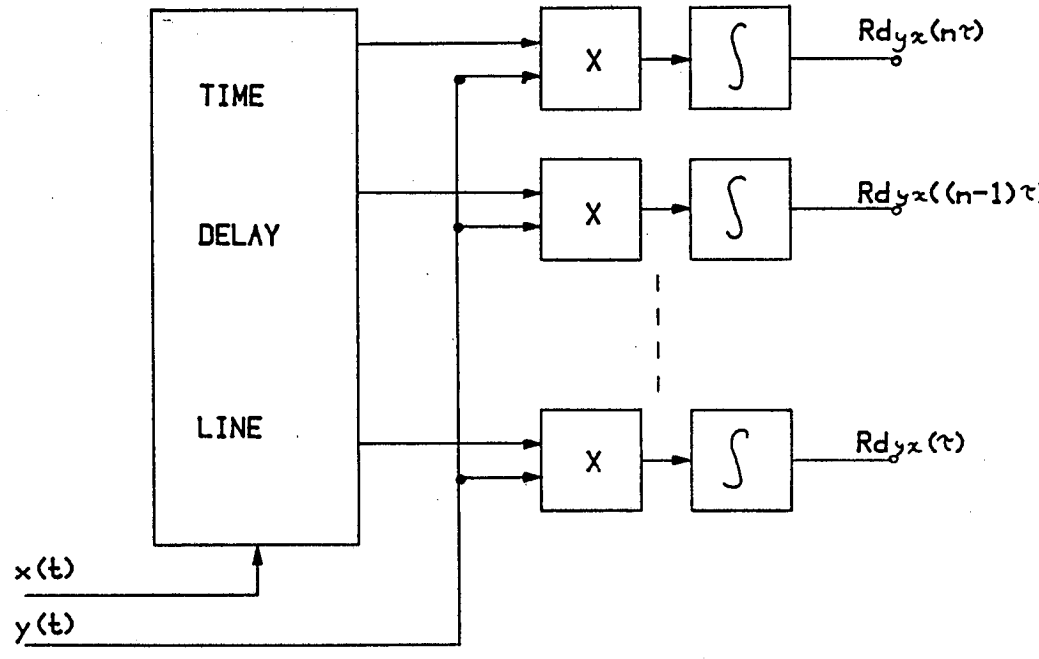

Fig. 2-4 PARALLEL CORRELATOR.

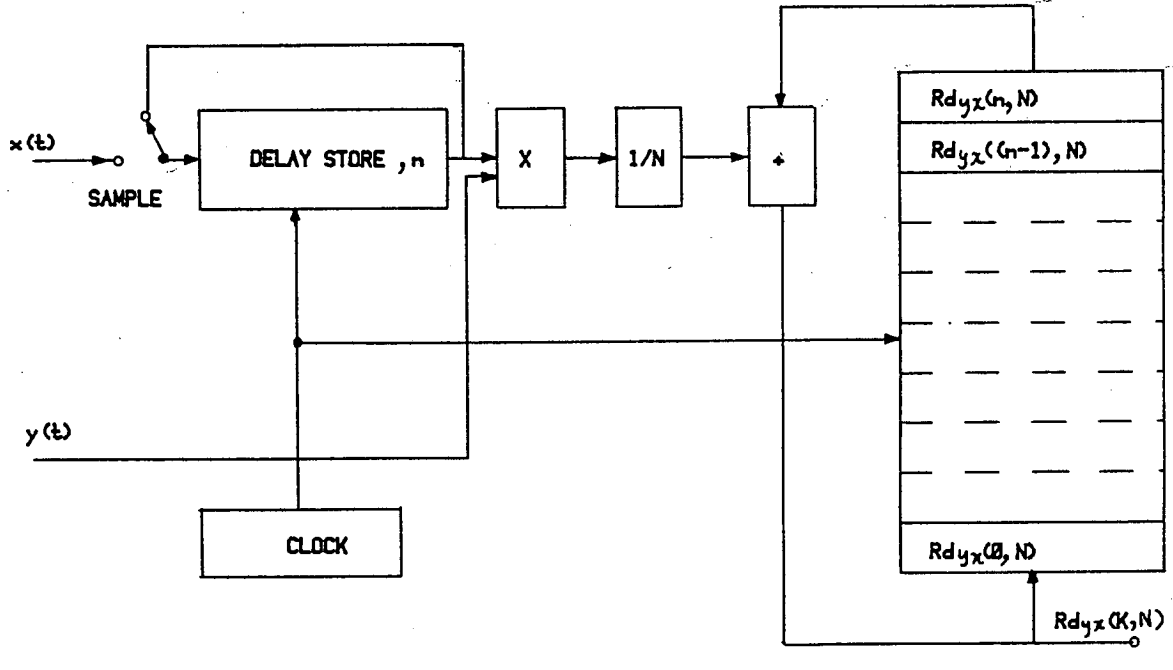

Fig. 2-5 SERIAL-PARALLEL CORRELATOR.

serial-parallel technique. Hewlett-Packard correlator quantises one channel to three bits and the other channel is quantised to seven bits. This quantisation technique is described by Finne (1965).

To find the position of the peak of the correlation function estimate Hayes and Musgrave (1973) have described a method where each value of the coefficient of the correlation function is compared with the highest already found value and the largest of the two is stored with the corresponding delay value. Therefore once the measurement time is completed the position of the peak of the correlation function is indicated by the stored delayed value.

2-2-4 Overloading Counter Correlator

A novel method for estimating the polarity correlation function and locating its peak position has been described by Jordan (1973). The overloading counter correlator is essentially a parallel correlator with both signals quantised to a single bit. The overloading counters that count the coincidences between up-stream and down-stream signals are arranged to indicate the position of the peak when a certain pre-set count is reached. Therefore the first counter to overload indicates the position of the peak of the polarity correlation function and hence no additional circuits are required.

The response time of the overloading counter correlators used for a flow measurement applications is not constant and

directly dependent on the input signal bandwidth (Taylor Instrument Ltd. 1976). Hayes (1975) developed an overloading counter correlator using standard available LSIC's. To maintain the complexity of the system to a reasonable limit he had to accept time delay resolution of +1.7%. The method described by Jordan is implemented on a single chip and is described in section 2-2-2. The single chip implementation of the overloading counters reduces the complexity involved with its hardware implementation.

Thorn (1979) developed a correlator with the available LSIC's using Jordan's method of peak detection. The correlator described by Thorn quantises both input signals to a single bit and the correlation function is estimated using the slow sampling technique. Using Jordan's method of peak detection and the slow sampling technique to estimate the correlation function, the complexity of the implementation of the correlator described by Thorn (1979) has been reduced significantly. To further reduce the cost and the complexity of the implementation of the correlators Browne , Deloughry, Green and Thorn (1982) have described a correlator based on Jordan's peak detection method where the polarity correlation function is estimated using a ROM as a sequence controller.

2-2-5 Tracking Correlators

In many applications of position measurement such as target tracking, radar, sonar, air and space navigation, it is necessary to measure the delay difference between two versions of the same signal, for example, the transmitted signal and the

returned signal reflected from the target. Spilker and Magill (1961) have described a method of determining the time difference between two signals using the delay lock discriminator as an optimum tracking device. Figure 2-6 describes the block diagram of the delay lock discriminator given by Spilker and Magill (1961). The delay lock discriminator is a non-linear feedback system comprising a multiplier, linear filter, and a controllable delay line. The error function of the delay lock discriminator can be defined as:-

$$e(t) = \tau_p(t) - \hat{\tau}_p(t) \qquad (2\text{-}12)$$

Where $\tau_p(t)$ is the actual input signal time delay and $\hat{\tau}_p(t)$ is the estimated time delay.

The expected value of the multipliers output, e(t), shown in figure 2-6 is given by:-

$$E[e(t)] \propto E\left[y(t) \cdot \frac{dx(t-\hat{\tau}_p(t))}{dt} \right] =$$

$$= \frac{d R_{dyx}(\tau_p - \hat{\tau}_p)}{d\tau} = KD(\tau_p - \hat{\tau}_p) \qquad (2\text{-}13)$$

Where KD is the slope of the differentiated correlation function in the region of the peak of the correlation function.

The delay-lock discriminator operates on a first order differentiation of the correlation function. The necessary condition to track the peak position of the cross -correlation function is given by:

$$\frac{d}{d\tau}\left[R_{dyx}(\tau) \right] \Big|_{\tau=\hat{\tau}_p} = 0 \qquad (2\text{-}14)$$

Therefore the differentiated correlation function must have a zero value at the peak position of the correlation function. Spilker and Magill (1961) have shown that the delay-lock discriminator will act as a negative feedback loop and can track time delay changes between two input signals.

One of the major problems associated with the tracking correlator described by Spilker and Magill (1961) is the possibility of tracking a spurious peak. For linear operation of the delay lock discriminator, a search operation should be performed by manually or automatically sweeping the delay line bias control to lock on to the target before the target can be tracked.

The operation and the model of the tracking correlators, as a negative feedback loop is similar to the model of the phase-locked loops, Gupta (1975). However, the tracking correlators error function ,e(t), is not periodical, whereas the phase-locked loops error function is expected to be periodical.

Different tracking correlators based on the tracking correlator described by Spilker and Magill (1961) and Spilker (1963) are reported by several authors for different applications. Haykim and Thorsteinson (1968) have described quantised tracking correlators to measure distance and velocity of the target in air and space navigation systems. Mesch, Fritsche and Kipphan (1974) have reported peak tracking correlators for flow measurement applications. Cernuschi-Frias and Rocha (1981) and Rocha (1982) have described a delay lock period estimator for the estimation of the time delay between two periodic signals. Fog (1982) has described coincidence tracker for wind-speed measurement systems. Non-contact speed measurement application of the peak tracking correlators have been described by Meyr (1976) and Bohmann, Meyr and Spies (1982).

The possibility that the peak tracking correlator could track a spurious peak has been considered by Meyr (1976) and the additional arrangement shown in figure 2-7 is suggested to indicate the out of lock condition of the peak tracking correlator, i.e. the condition where the peak tracking correlator is tracking a spurious peak. The serial correlator shown in figure 2-7 will indicate the out of lock condition if its output is below some pre-set value. Therefore when the out of lock condition is detected, the tracking correlator should be brought within the tracking region by sweeping the electronic delay line over a possible range of delays. Experimental results given in chapter 5 indicates that the output of the serial correlator can only be used to indicate the out of lock mode of the tracking correlator

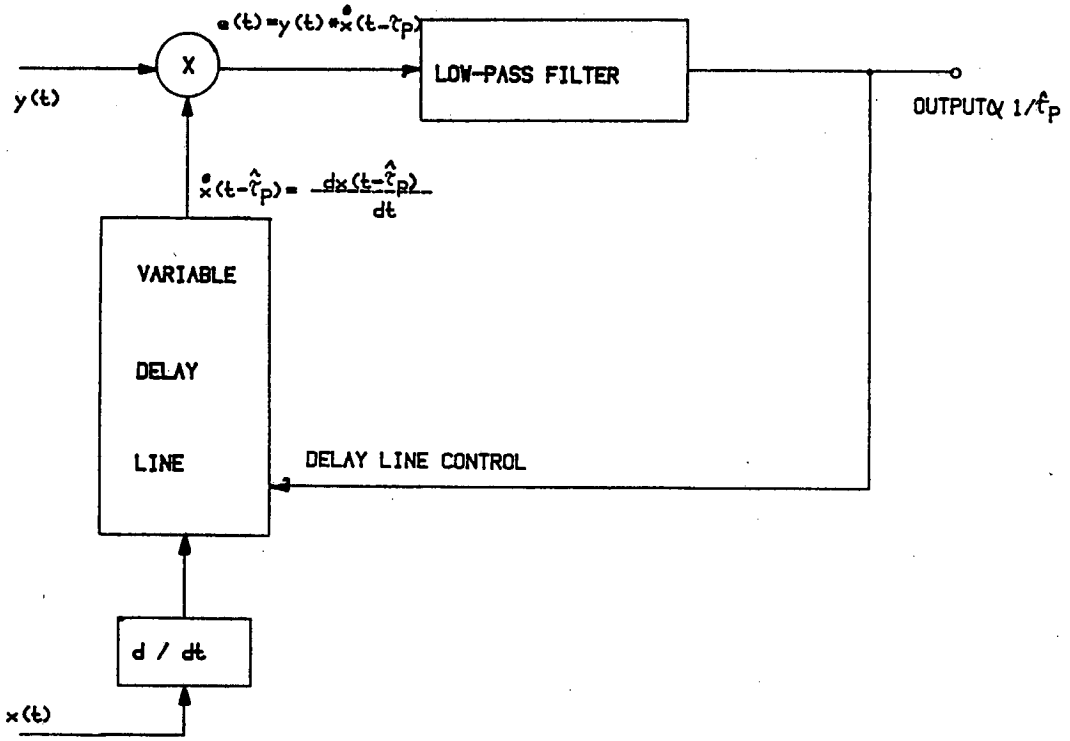

Fig. 2-6 DELAY LOCK DISCRIMINATOR.

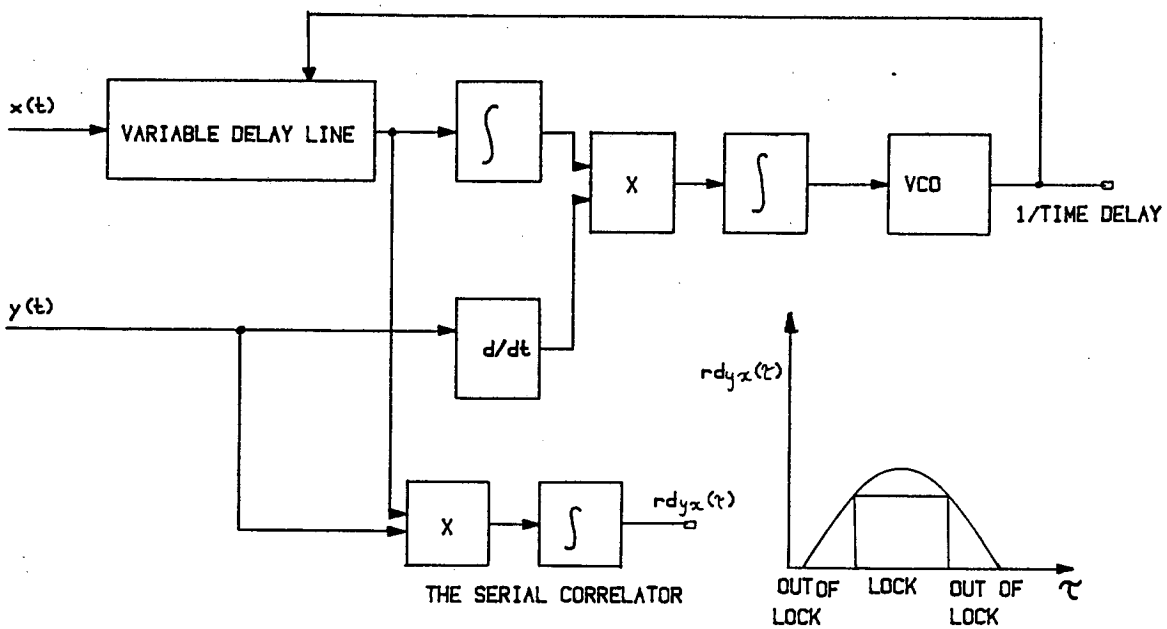

Fig. 2-7 TRACKING LOOP WITH ADDITIONAL SERIAL CORRELATOR.

and its output can not be used to ensure the linear operation of the tracking loop.

Jordan and Manook (1981) and Manook (1981) have described the constrained peak tracking correlator based on the tracking correlator described by Spilker and Magill (1961) for flow measurement applications. The tracking correlator is constrained to track the peak of the correlation function and its delay shift register length is set by the peak position estimate of the overloading counter correlator. A block diagram of the constrained peak tracking correlator described by Jordan and Manook (1981) and Manook (1981) is shown in figure 2-8.

Manook (1981) has reported that due to the quantised time delay axis of the overloading counter correlator the output response of the constrained peak tracking correlator is jittery. In addition since the delay shift register length of the loop is continuously being set by the peak position estimate of the overloading counter correlator, the accuracy of the tracking loop is directly dependent on the variance of the overloading counter correlators peak position estimate. Due to the problems mentioned above Manook (1981) has concluded that the system is not attractive for industrial flow measurement applications.

Another class of peak tracking correlators used to estimate time delays between two input signals is the "two point difference correlator". These have been described by several authors, for example Kashiwagi (1968), Hayes and Musgrave (1973),

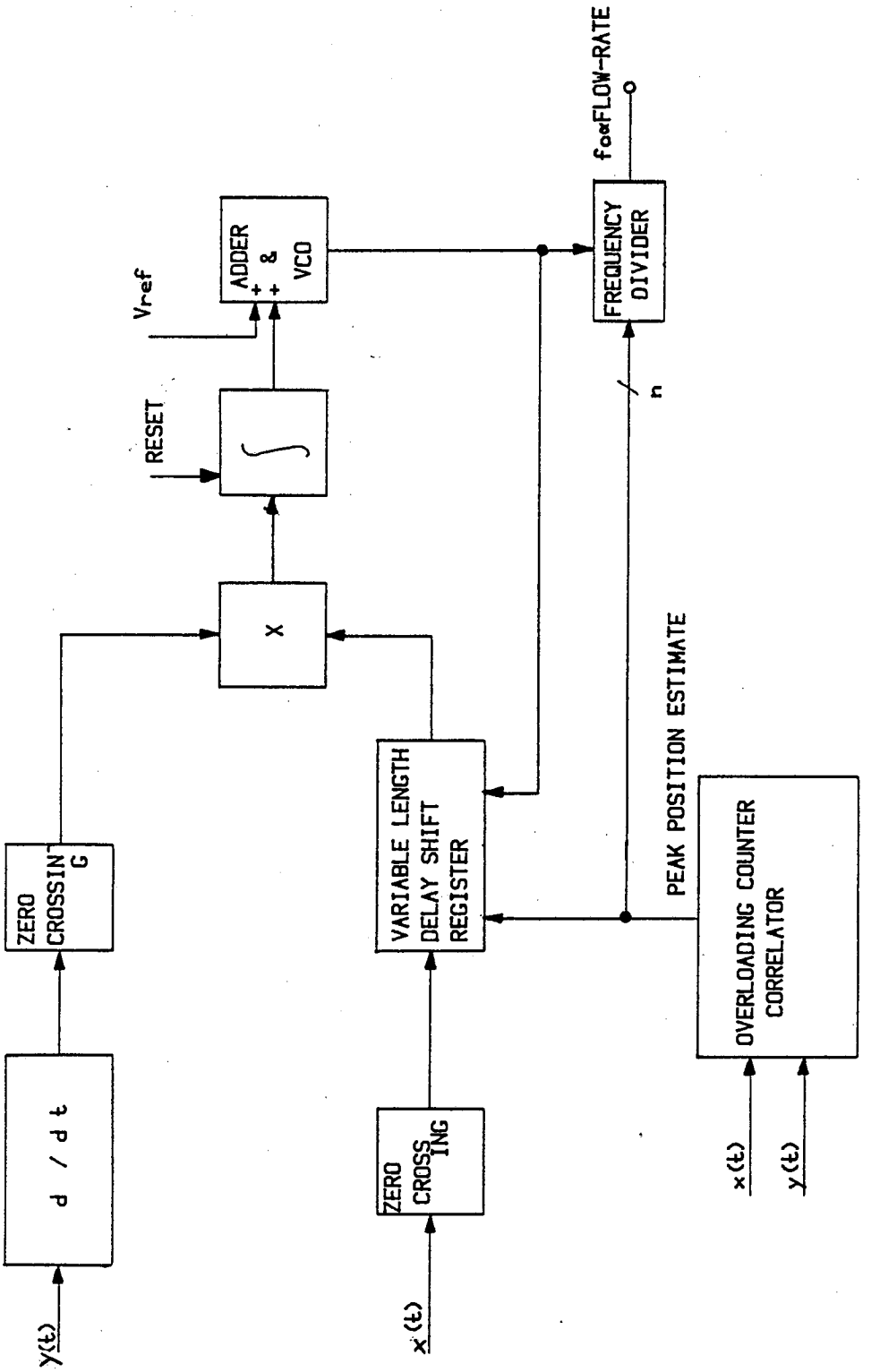

Fig. 2-8 CONSTRAINED PEAK TRACKING CORRELATOR.

Tompkins, Monti and Intaglietta (1974), Hayes (1975), Battye (1976) and Leitner (1979). The block diagram of two point difference correlators is shown in figure 2-9. The two point difference correlator estimates the correlation functions $R_{\rho yx}(\tau_1)$ and $R_{\rho yx}(\tau_2)$ at two different delay values τ_1 and τ_2. τ_1 and τ_2 can be moved to the balance position automatically by the control loop if the correlation function is symmetrical.

At the balance position the output of the voltage controlled oscillator is inversely proportional to the input signal time delay and in flow measurement application the output of the voltage controlled oscillator is proportional to the flow rate. Battye (1976) has used the two point difference correlator for flow measurement applications. Leitner (1979),(1980) has described a two point difference correlator for slurry flow measurement applications. To increase the tracking range of the two point difference correlator an additional micro-computer based correlator was used by Leitner. The microcomputer evaluates a coarse estimation of the correlation function peak position and an accurate estimate of the peak position is given by the two point difference correlator. Leitner has reported satisfactory results using the above arrangement for slurry flow measurement applications over a 6 to 1 time delay range.

The peak tracking correlators described in this section are not complex and expensive to implement and theoretically the input signal time delay can be estimated with infinite resolution. But the major obstacle for industrial application, and in

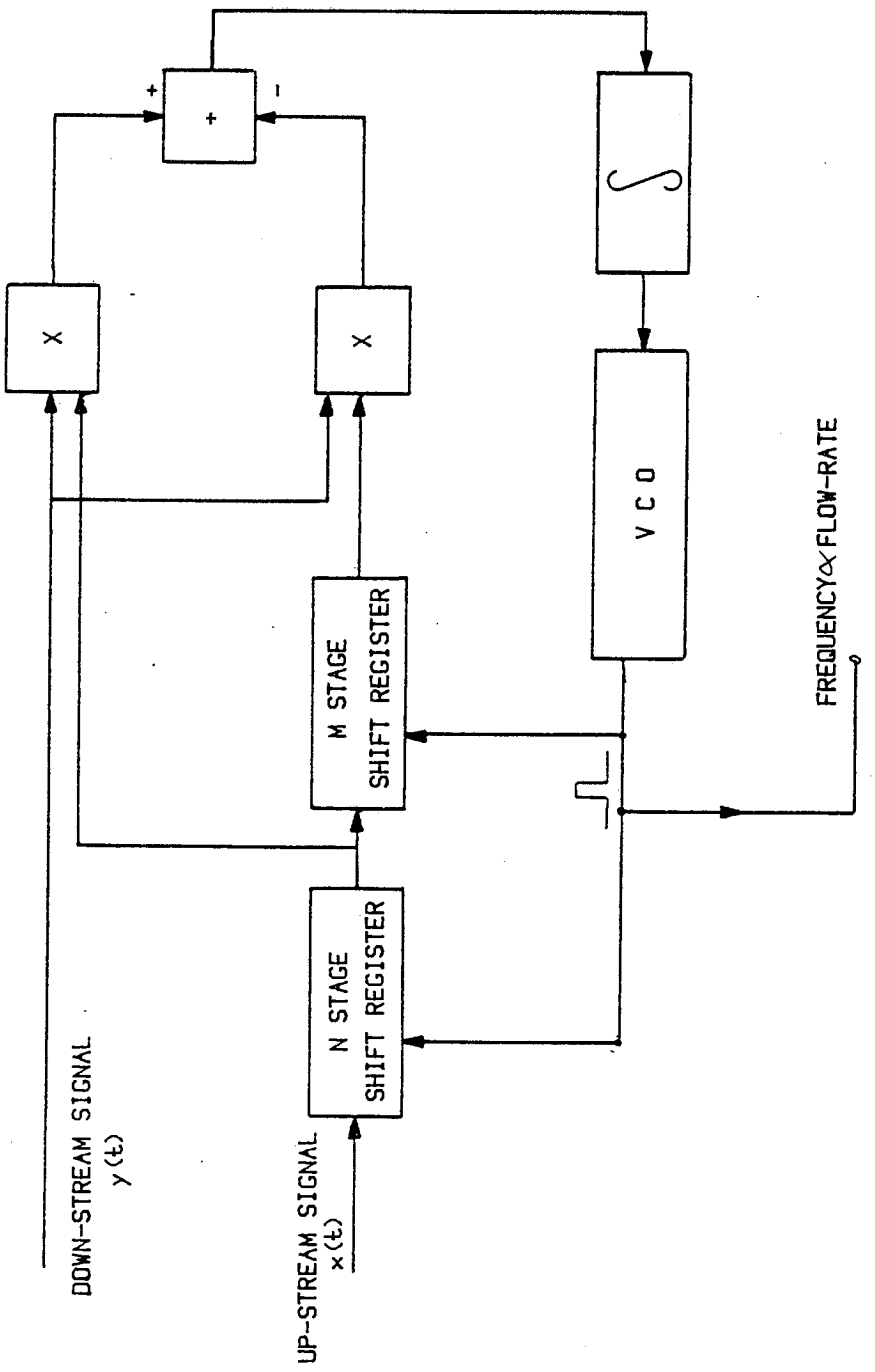

Fig.2-9 TWO POINT DIFFERENCE CORRELATOR.

particular for flow measurement applications is the possibility of tracking a spurious peak, which could lead to inaccurate estimation of time delays.

In this thesis a detailed investigation of the performance of an improved constrained peak tracking correlator is presented and solutions to the problems noted by Manook are given. The improved constrained peak tracking correlator described in chapter 4 is suitable for industrial applications and it can be designed to track the peak of the correlation function linearly with 0.6% resolution over a 32 to 1 time delay range.

2-2-6 Single Chip Customised Correlators

Recent advances in micro-electronic technology has lead to a dramatic improvement in the design of customised LSIC's. Correlator design on a single LSIC has lead to a significant improvement in the speed, power and reliability of correlation function estimation . The development of the single chip overloading counter correlator described by Jordan (1973) and Jordan and Kelly (1976) can be considered as the first serious attempt to implement the complex correlator circuit on a single customised chip. Each overloading counter correlator chip contains 12 channels of complete polarity coincidence detectors, integrating counters and the capability to indicate the overload pattern. The ease with which these correlator chips can be connected together to form a correlator with large time delay range being a particularly important feature. Taylor Instruments

Ltd. (1976) obtained a licence to use the 12 channel overloading counter correlators for flow measurement applications. They have developed a correlation flow-meter based on these chips which uses 12 chips connected in series to achieve the required delay range.

The original integrated circuit design for the overloading counter correlator is now ten years old. Fabrication technology and computer aided design has made significant advances during this period. Jordan and Blackley (1983) have indicated that the overloading counter correlator still is the most attractive circuit for use in measurement applications in comparison to a wide range of correlator circuits available. Initial study of CMOS circuit techniques has shown that a 512 stage overloading counter correlator can be realised on a single chip. Therefore a lower number of chips will be required for the large delay range and only one chip will be sufficient to provide the coarse peak position indication of the correlation function to the tracking correlator described in chapter 4.

Other reported developments are TRW's 64 stage correlator, Eldon (1981), which are commercially available. The TDC1004J will provide analogue output and the TDC1023J will provide digital output of the correlation function estimate. The block diagram of the TDC1004J is shown in figure 2-10 which provides current output proportional to the number of the correlated bits. The TDC1004J can be connected in series to cover a wide range of time delays. For applications where the position of the peak of the correlation function is of interest, additional

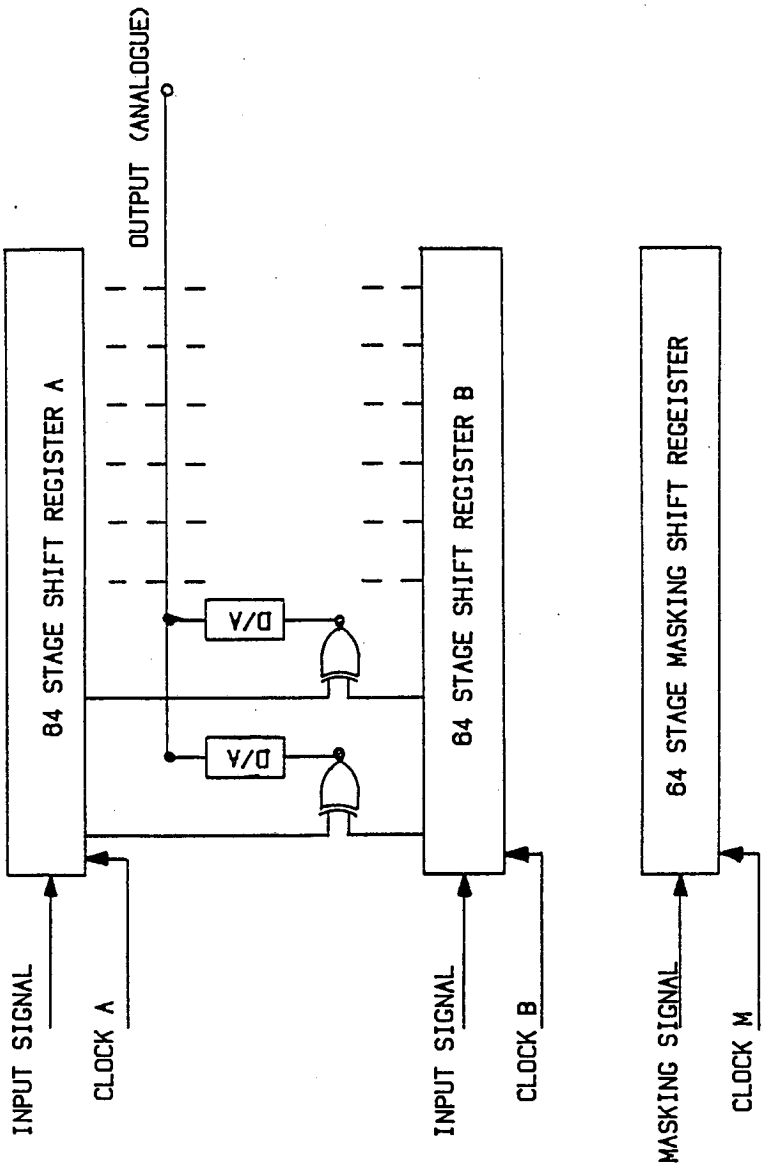

Fig.2-10 THE BLOCK DIAGRAM OF THE TRW TDC1004J CORRELATOR.

analogue to digital convertors and a peak detection circuit are required. Using the correlators designed by TRW a correlation function can only be estimated when the shift register B used to sample the polarity reference signal is filled with data. Note that the shift register A is continuously sampling the polarity delayed input signal.

To reduce the variance of the correlation function estimate of the single chip TRW TDC1004J correlators, Bendall (1980) has used a recirculating shift-store interface circuit described by Jordan (1979) for acoustic emission applications.

The all digital TRW TDC1023J correlator is similar in operation to the TDC1004J, where the correlation function is output as a serial sequence of digital words. Therefore if this version of the correlator is required to be connected in series, the correlation function estimate of each chip must be added digitally and hence this will create a great complexity due to the implementation of the digital adders.

Reticon (1978) have produced two versions of a 32 stage single chip correlators, the R5401 operates as a relay correlator and the R5403 performs direct estimation of the correlation function.

The currently SERC financed 256 stage relay correlator designed by Jordan at the Edinburgh University is directed towards investigating CCD relay correlator circuits for measurement system

applications. The 256 stage correlator offers short measurement time, easy to connect in series, and the estimated correlation function output can be readily displayed on an oscilloscope.

2-2-7 Micro-computer Based Correlators

Availability of 8 and 16 bit low cost micro-processors has lead to implementation of the correlation function algorithm on a micro-computer by several investigators. Micro-computer like any other single processor computer is a sequential device and can only execute one instruction at a time. Therefore unlike hardware and single chip correlators, sampling, multiplication and averaging can not be performed in parallel. Instruction cycle time of the majority of the commonly used micro-processors is of order of few μsecs. Due to the sequential operation, the micro-computer based correlator will have a slower response than the hardware and LSIC correlators.

To improve the efficiency and the response time of the micro-computer based correlator Henry and Alchalabi (1979) and Alchalabi (1980) have described the zero crossing algorithm to estimate the polarity correlation function. Where the zero crossing times of the polarity signals are read into the micro-computer and hence no redundant data are collected. A Z-80 based NASCOM II micro-computer used by Henry (1979) to implement the zero crossing algorithm for correlation flow measurement applications is capable of capturing data from two signal channels up to a maximum signal bandwidth of 3 KHz. It is important to

note that the measurement time of the zero crossing algorithm depends on the flow signal bandwidth. Therefore if the flow noise signal bandwidth is low, more time is required to capture the zero crossing data compared to the situation where the flow noise signal bandwidth is high.

Leitner (1979), (1980) has described a micro-computer based correlator using the SDK-80 evaluation kit based on the INTEL 8080A micro-processor. The micro-computer based polarity correlator described by Leitner is designed to operate in a serial- parallel mode, with a measurement time of a few seconds. The resolution of the correlation function estimate is poor and is used to indicate approximate peak position of the correlation function to the two point difference correlator described in section 2-2-5. Leitner has suggested that the micro-computer correlator is capable of estimating the correlation function within the delay range of 5 to 500 msecs. The polarity signals to the micro-computer are sampled at a frequency of 200 Hz, but no result to indicate the performance of the micro-computer correlator over the above range is given.

Fell (1982) has described the skip algorithm based on the slow sampling technique described by Kam, Shore and Feher (1975), for computing the correlation function using a micro-computer. Two different sampling frequencies are used for input signals, one being determined by the required time delay resolution and the other by the signal bandwidth. The reference signal sampling rate, should not be less than the Nyquist sampling

rate, otherwise some information will be lost and longer measurement time will be required. To estimate the correlation function over a delay range of 0 to K.ΔT, K samples of the reference signal with the sampling period of M$\Delta\tau$, should be correlated with M samples of the delay signal with the sampling period of $\Delta\tau$, where M is given by equation 2-11.

Figure 2-11 describes the sampling scheme used for a micro-computer to estimate the cross-correlation function over a time delay range of 0 to K.ΔT. From figure 2-11 it will be seen that only one sample of the down-stream signal, y(t), will result in K estimates of the cross-correlation coefficients and correlation function coefficients over a delay range of 0 to K.ΔT are estimated by M samples of the down-stream signal.

The skip algorithm can be used to compute direct, relay and polarity correlation functions, and a fast response time is obtained using polarity signals since the polarity multiplication operation is equivalent to the logical exclusive-NOR operation. A single exclusive-NOR instruction for an 8-bit micro-processor can evaluate 8 multiplications, if 8 samples of the up-stream signal are stored in one byte of the memory and one sample of the down-stream signal is packed in another byte. Using the polarity signal to compute the correlation function, Fell has reported the worst case multiply-add-store time of 6 μsecs on a 2 MHz MCS 6502 micro-processor.

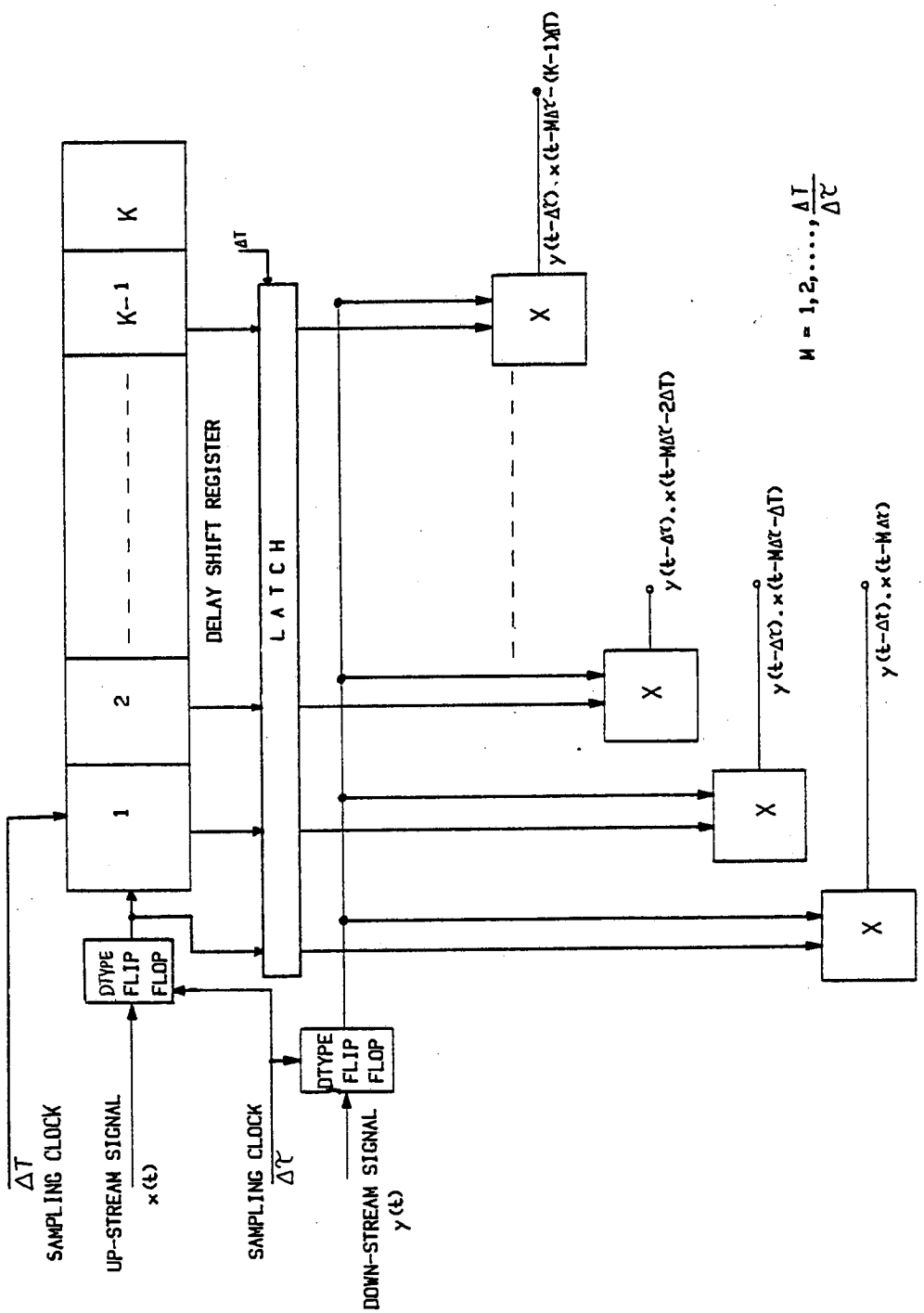

Fig.2-11 SKIP ALGORITHMS SAMPLING SCHEME.

This review of the micro-processor based correlators, indicates that any micro-computer used to compute the correlation function, must be capable of performing logical operations and capable of recognising more than one interrupt signal from external devices for synchronous operations. For example due to the sampling scheme of the algorithm described by Fell the micro-processor must have at least two hardware interrupts for efficient estimation of the correlation function.

2-3 Performance of The Correlators

From the discussion of application areas given in chapter 1, it can be concluded that a correlation based measurement system is required to be capable of determining the position and magnitude of the most significant peak of the correlation function. In a flow measurement applications the position of the peak of the correlation function is of great importance. Theoretically transit time can be derived from the peak position of the cross-correlation function of two flow noise signals, where flow noise signals are supplied by two transducers monitoring the flow noise at two points distance L apart in the flow stream.

Extreme care must be taken to ensure that the measurement method itself does not introduce any large errors. Due to fundamental and economic limitation imposed by the correlation function implementation, the problem requires greater care to achieve the possible accuracy from the data available. Although the performance of the correlation flow-meters under

static signal conditions have been carefully examined, Hayes (1975), Sykes (1975), Gray (1979) and Taylor Instrument Ltd. (1976), there is a second type of problem that has not received the same degree of attention. This second problem results from the assumption made in correlation function analysis that the data being analysed are generated by stationary processes. But not all the processes can be justified as stationary processes. Hence it can be expected that the above assumption will lead to inaccurate estimate of time delay, when the flow velocity is changing.

The variance of time delay estimates derived from the correlation function estimates under the assumption of stationary signal conditions have been discussed by several authors, for example Beck (1969), Jordan (1973), Hayes (1975), Sykes (1975), Taylor Instrument Ltd. (1976), Gray (1979), Manook (1981), and their general conclusion is the same and is given by:-

$$\text{Variance of the time delay estimate} = \frac{K}{B^3 . T . S/N} \qquad (2\text{-}15)$$

Where K is constant and different values of K based on data provided by Hayes (1975) and experiments carried out by Taylor Instrument Ltd. (1976) are given below:-

$$Kp = .066, \qquad Kr = .028, \qquad Kd = .026$$

where Kp = constant value for polarity correlation function.

Kr = constant value for relay correlation function.

Kd = constant value for direct correlation function.

and T = Integration time,

B = 3dB input signal bandwidth.

S = Signal mean square value.

N = Noise mean square value.

S/N = Signal to noise ratio.

Basically there are three major sources of errors which influences the accuracy of the correlation flow-meter. These sources of error are due to:-

1) The practical realisation of correlation flow-meter.
2) The physical nature of flow noise signal.
3) The transducer system.

The following sections will consider the above sources of errors individually. Since the study of the transducer system was not required in this research programme, the sources of errors due to the transducer system were not considered.

2-3-1 Errors Due to Practical Realization of the Correlation Flow-meter

The first group of errors are due to the constraints imposed by practical implementation of the correlation function, and are discussed under the following headings:-

a) Resolution

b) Range

c) Integration time

d) Quantisation error

a) Resolution

The sampled data, correlation based measurement system employs a coarsely quantised time delay axis. The quantisation of the time delay axis leads to an inaccurate estimation of time delay which becomes more serious the larger the range required. If the peak of the function is situated between two adjacent time delay increments, the estimated correlation function peak position can be in error by $0 < |E| < \Delta\tau$, where $\Delta\tau$ is the sample clock period and E is the error in the position of the peak. It should be noted that if the correlation function is symmetrical the worst case error will be $\pm$ E/2. Therefore percentage reading error is be given by:

$$\% \text{ READING ERROR} = \pm (1/2) \cdot \frac{\Delta\tau}{n.\Delta\tau} \times 100 = \pm \frac{100}{2n} \qquad (2\text{-}16)$$

Where n is quantised channel number and $\Delta\tau$ is the sampling period.

The sampling frequency is determined by the minimum time delay range, desired accuracy and response time. To achieve ±1% accuracy over a time delay range of 32 to 1, the number of delay stages required for a correlation flow-meter can be obtained using equation 2-16, and is equal to 1600 (50X32). Therefore the correlation flow-meter should have 1600 delay stages in order to operate over an input signal time delay of $50\Delta\tau$ to $1600\Delta\tau$ seconds, with ±1% resolution.

To reduce the cost and complexity of an implementation, Taylor Instrument Ltd.(1976) have used the variable frequency technique described by Jordan and Manook(1981A), Using the above method the resolution of the peak position estimate along the time delay axis is maintained approximately constant by reducing the clock frequency for the higher time delay segments of the delaying shift register. The prototype correlator designed by Taylor Instrument Ltd. uses 168 stages and has an accuracy of ±1% over a 10 to 1 range. To further improve the resolution of the above correlator , Taylor Instruments Ltd. (1976), have used the interpolated moment peak detection technique described by Jordan and Manook (1981A) and Manook (1981). It is important to note that the variance of the time delay measured using the interpolated moment is directly related to the variance of the correlation function estimate.

b) Range

This is defined as a ratio of the highest flow-rate to

the lowest flow-rate measured and is given by:-

$$\text{Range ratio} = \frac{\text{fastest flow-rate to be measured}}{\text{slowest flow-rate to be measured}} . \qquad (2\text{-}17)$$

The improved constrained peak tracking correlator described in chapter 4 is capable of tracking the peak of the correlation function with a resolution of 0.6% over an input signal bandwidth of 50 to 500 Hz and the time delay range of 32 to 1.

c) Integration Time

The finite integration time of the practical correlation function leads to uncertainty about the true value of a measured function. For a flow noise signal a sampling rate larger than the Nyquist rate is often required which is approximately 5 to 10 times larger than the flow noise signal bandwidth. Bandwidth of the flow noise signal can be related to the rate of transfer of information to the correlation flow-meter. Reduction of the bandwidth of the flow noise signal can be recovered by increase in the integration time and hence increase in the response time. Therefore response time of the correlation flow-meter is directly related to the integration time and the bandwidth of flow noise signal. Since the bandwidth of the flow noise signal is related to the response time of the correlation flow-meter, further discussion on the nature of the flow noise signal is given in the section 2-3-2.

d) Quantisation

Amplitude quantisation of the flow noise signal leads to a reduction in the cost and simpler implementation of the correlation flow-meter. In addition the effect of the quantisation is equivalent to a reduction of the information available to the correlation flow-meter, Widrow (1956). The two attractive cases of quantisation, polar and relay, are widely used for different applications and in particular for correlation flow measurement. The polarity correlator has received much attention, see for example Van Vleck (1966), Widrow (1956), (1961), Watts (1961), Korn (1966), and is the simplest form of the correlator to implement. The relay correlator is a compromise between simple polarity correlation and the complicated direct correlation. The relay correlator has been studied by several investigators for example Watts (1961), Veselova and Gribanov (1969), Greaves (1970), but more experimental work is required to describe the variance of the correlation function estimate using a relay correlator.

From the results given by Taylor Instrument Ltd. (1976) (using their own data and data given by Hayes (1975)) it has been shown that polarity correlator requires approximately 2.5 times longer integration time than direct correlation, whereas relay correlator requires approximately 1.7 times longer integration time, Jordan (1973). Since polarity correlation greatly simplifies the implementation of the correlation based measurement system, the penalty of an increased integration time can be acceptable.

2-3-2 Errors Due to the Physical Nature of the Flow Noise Signal

The second group of errors arises from the nature of the flow noise signal which is outside the influence of correlator design. This group of errors are divided into the following sub-groups:-

a) flow noise signal bandwidth

b) signal to noise ratio.

c) non-stationary signal condition.

a) Flow Noise Signal Bandwidth

From equation 2-15 it is clear that the bandwidth of the flow noise signal is one of the important parameters contributing to the error variance of the time delay estimate derived from the correlation function. Generally a flow noise signal is generated by the effect of both turbulent eddies and particles which are swept around by eddies, Hinze (1972), Ito (1977). In a fully developed flow there are a wide spectrum of eddies which generates different frequencies according to their size, Hinze (1972). In addition the eddy size is inversely proportional to the bandwidth of flow noise signal, the small eddies dissipate rapidly and large eddies persist, Hinze (1972), Ong (1975), Ito (1977).

Experiments carried out by Taylor Instrument Ltd. (1976), indicate that velocities in the range of 2 to 9 ft/sec (.61 to 2.74 meter/sec) generates flow noise signals which contain high frequencies up to 1000 Hz and low frequencies of about 5 Hz, (using 6 inch diameter pipe). This is due to the presence of

different eddy sizes where large low frequency eddies are generated near the centre of the pipe, and small high frequency eddies are generated near the pipe wall. In addition the bandwidth of the flow noise signal is proportional to the flow rate for a given pipe diameter, Manook (1981). Therefore the flow noise signal must be sampled in such a way that all the correlatable bandwidths within the flow range can be captured while maintaining the response time of the correlation flow-meter as small as possible.

b) Signal to Noise Ratio

The normalised cross-correlation function has a value of unity when the delay is zero and decreases as the transit time between upstream and down-stream transducers increases, Clinch (1969), Komiya (1966). Magnitude of the signal to noise ratio can be obtained using the relationship given by Boonstoppel, Veltman and Vergouwen (1968).

$$S / N = \frac{\rho^2(\tau_p)}{(1-\rho^2(\tau_p))} \qquad (2\text{-}18)$$

Where $\rho(\tau_p)$ is the peak value of the normalised correlation function and τ_p is the time delay of the peak position estimate.

Using Ong's (1975) data on 1 inch diameter pipe and data collected by Taylor Instrument Ltd.(1976), with 30 mm transducer spacing, it has been shown that the normalised correlation

function peak amplitude is directly related to the flow velocity, and is given by:-

$$\rho(\tau_p) = \exp\left\{ \frac{-9.5104.\tau_p}{(D/30)^{.8540}} \right\} \qquad (2\text{-}19)$$

Where D is the pipe diameter in cm, and τ_p is in seconds.

c) Nonstationary Signal Condition

Implementation of the correlation function integral is generally valid for stationary signal conditions. The term stationary refers to the class of signals having statistical properties which do not change with time, that is:-

$$f(X1,X2,\ldots Xn;t1,t2,\ldots,tn) = f(X1,X2,\ldots,Xn;t1+\xi,\ldots tn+\xi)$$

in particular:-

$$f(X,t) = f(X,t+\xi) \qquad (2\text{-}21)$$

Since a stationary process is independent of time it can be assumed that:-

$$f(X,t) = f(X) \qquad (2\text{-}22)$$

Therefore if the process is stationary the correlation function integral will allow an accurate estimation to be made, for

example, system time delay. Unfortunately not all processes are stationary and the conventional stationary estimation theory does not apply to the class of signals which have statistics which are changing with time, i.e. non-stationary signals.

A typical non-stationary flow noise signal is obtained from two phase flow (gas and liquid, two liquids with different viscosity, particles and liquid), where the bandwidth of the flow noise signal changes with time. It has been observed that under single phase flow situations it is also possible to obtain non-stationary signals (private communication Taylor Instrument Ltd. 1982). If the correlation function integral is used to analyse a non-stationary signal the function peak amplitude will be reduced and its width increases, compared with the function shape obtained under stationary signal conditions. In other words the non-stationary chracteristic of the input signals will be "smeared out" and this will lead to inaccurate time delay estimations.

The correlation and spectrum analysis of non-stationary signals is a topic of interest in different research areas, i.e. flow measurements, Leavell and Shahrokhi (1976), vibration analysis, Wirewille (1965), system identification, Sheppard and Mix, (1973). Unfortunately very few experimental results have been published to indicate the effect of non-stationary signals on the shape of correlation function integrals.

To obtain the power spectrum of non-stationary signals Page (1951) has introduced the term "instantaneous power spectrum"

in which a signal is divided into sections where the statistics of the signal within each section is considered to be stationary. Therefore the average power spectrum of all individual sections yields the estimate of the power spectrum of non-stationary signals. His technique is valid if each individual section of signal contains enough information, to estimate the power spectrum. Wirewille (1963) has discussed this method and he has indicated that the individual sections may not be of sufficient length to yield an accurate spectral information.

An approach to the spectral analysis of non-stationary processes based on an evolutionary power spectrum, has been given by Priestly (1965A, 1965B, 1970, 1971), where the evolutionary power spectrum is time dependent and describes the local power-frequency distribution at each instant of time. Hammond (1973) has used the evolutionary power spectrum method for vibration applications and satisfactory results are reported.

Papoulis (1965) introduced functions called average correlation and average spectrum functions, that is:-

$$\overline{R_{dyx}(\tau)} = \lim_{T\to\infty} \frac{1}{T} \int_0^T R_{dyx}(t,\tau)\, dt \qquad (2\text{-}23)$$

and

$$S(w) = F\{\overline{R(\tau)}\} \qquad (2\text{-}24)$$

Where $F\{\overline{R(\tau)}\}$ is the Fourier transform of the average correlation

function.

Use of Papoulis definition allows these signals to be treated as stationary functions. Papoulis states that these average functions have all the properties of the correlation or spectrum functions of the stationary process. Average correlation functions have been applied by Sheppard (1973) and, Mix and Sheppard (1973) for on line testing of linear electronic system and system identifications. Results obtained indicate that the average correlation function provides the information needed and confirms the validity of the Papoulis method. Note that the average correlation function has a smoothing effect on the correlation function this effect can be expected from the definition of the correlation function i.e.:-

$$R_{yx}(t,\tau) = E\,[\, y(t) \cdot x(t-\tau)\,]$$

Berndt (1963) and Berndt and Cooper (1965), (1966) have discussed multiplication of the integrand of a correlation function by a weighting function in order to approximate the best weighted time average of the correlation function. Approximation of optimum weighting coefficients from weighting function is complex and prior knowledge of the correlation function is required in order to obtain optimum weighting coefficients.

In an attempt to follow the variation of the correlation function with time, Wierwille (1965) has developed a method which

separates time smoothing for variation of delay from time smoothing for reducing variance of the correlation function, i.e. smoothing of $R(t,\tau)$ with respect to t and τ. This is given by:-

$$R_{dyx}(t,\tau) = \int_0^\infty \int_0^\infty h(\lambda)\, \ell(\gamma)\, y(t-\lambda)\, x(t-\gamma-\lambda-\tau)\, d\gamma d\lambda \qquad (2\text{-}25)$$

Where $h(\lambda)$ and $\ell(\gamma)$ are impulse responses of two one dimensional filters, and the correlation can be estimated accurately by the proper choice of the filters impulse response.

Larrowe (1966) reviews the method given by Wirewille (1965) and states that the analyser design is optimum only in terms of its response to signals having correlation function of the form used in specifying the filters impulse response. Therefore for other forms of time varying correlation functions other filter designs should be used.

Geranin and Kozlov and Shlyaktsu (1973) have reviewed methods suggested by Berndt (1963) and Wierwille (1965) and they agree with Larrowes (1966) assessment. Wierwille and Knight (1968),(1969) describes off-line correlation analysis of non-stationary signals based on the method given by Wierwille (1965). Discreet data non-stationary correlation function theory based on the non-stationary correlation function theory described by Wierwille (1965) is discussed by Greaves (1970).

Leavell and Shahrokhi (1977) have discussed tracking

non-stationary velocities in a two phase flow by an adaptive cross-correlation algorithm. Details of the adaptive algorithm is not given but briefly, the idea is based on the use of a variable integration time to track non-stationary delays.

Among other techniques which can be considered for the correlation function estimation of the non-stationary signal is the generalised cross-correlation approach described by Scarbrough, Ahmed and Carter (1981), Hassab and Boucher (1979), Knapp and Carter (1976), where:-

$$R^{G}_{dyx}(\tau) = \int_{-\infty}^{+\infty} W(f)\, G_{yx}(f)\, e^{j2\pi f \tau}\, df \qquad (2\text{-}26)$$

Where $R^{G}_{dyx}(\tau)$ is the generalised correlation function and $G_{yx}(f)$ is the cross power spectra and W(f) is the weighting function. It is important to note that due to the finite observation time, only an estimate of $G_{yx}(f)$ can be obtained. A block diagram representation of an implementation of the generalised cross-correlation function is shown in figure 2-12. The generalised correlation function is used for time delay estimation in boiling water reactor by Kostic (1981) and she has concluded that this method is more effective in producing well defined time delay estimation.

In this section, some of the approaches to the problems that arises under the non-stationary signal conditions and described by several investigators are high lighted, and it seems evident that averaged short term estimate of the correlation

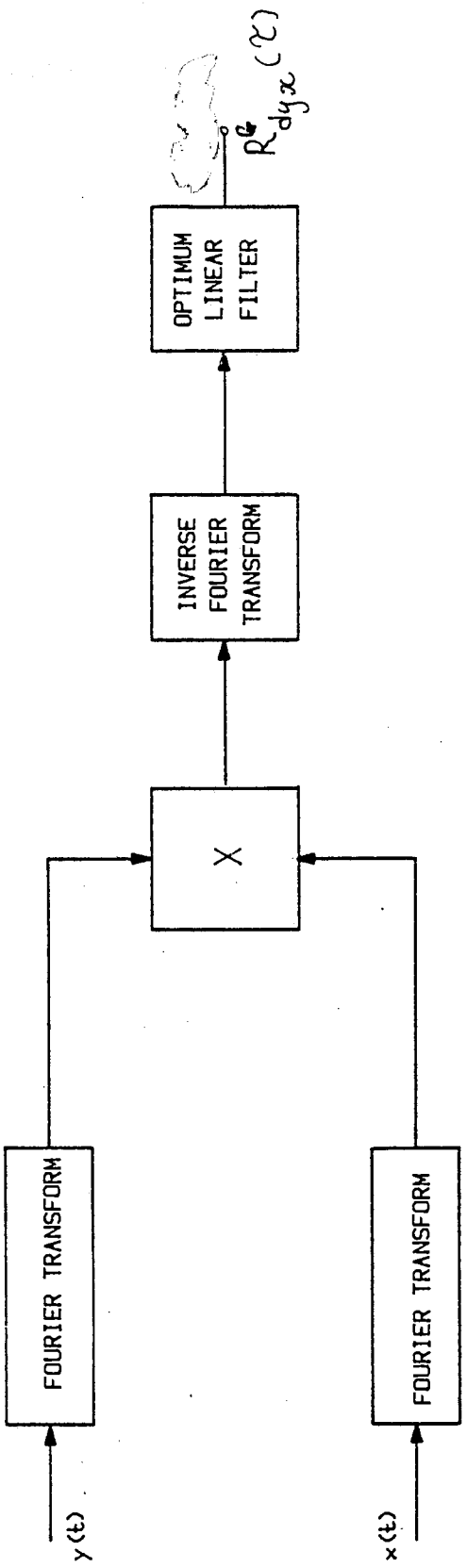

Fig. 2-12 GENERALISED CORRELATION FUNCTION IMPLEMENTATION.

function can yield more accurate information under changing signal conditions. But the above technique can not be applied if only one sample record of the correlation function is available, and the prior knowledge about the characteristic of the signal is required , in order to be able to multiply the correlation function integral by an optimum window function. The problems involved with the non-stationary signal analysis and in particular, correlation function estimation under the non-stationary signal conditions requires more research.

CHAPTER 3: THE NOISE SIMULATOR

3-1 Introduction

Noise simulation has been the subject of great interest by several investigators for different applications for example, radar (Wolf, 1963), telemetry (Spilker, 1965), system impulse response testing (Beck, 1974), vibration testing (Kramer 1965), navigation (Mitchell and McPherson 1981), system identification (Sheppard, 1973), communication (Schobi, 1981) and flow measurement (Elias, 1980). If experimentally derived noise is used as a test signal, the result of an experiment will be different each time it is repeated. Therefore a test signal is required which has the properties of a random noise and give reproducible and repeatable results when used in experimental investigations i.e. it should be random but its properties should be deterministic.

One method of generating an artificial random noise is to amplify the random emission of the electrons in a natural noise source such as a thyratron or a zenor diode, Korn (1966), Bell (1960). The disadvantage of a natural noise source is that the statistical characteristic of the signal generated is difficult to control and hold stable and is not reproducible.

An alternative method of generating artificial random noise is based on a digital waveform generator which produces a binary signal which switches randomly between two output levels

and is referred to as a pseudo random binary noise "PRBN" signal, Golomb (1964), and Korn (1965). The spectrum of the PRBN signals is related to the clock frequency used to generate the signal and is controllable, Newland (1976). However, the PRBN signals amplitude distribution is just a two level function and is very different from the Gaussian distribution common in naturally occurring environments.

A multilevel or continuous waveform with a Gaussian amplitude distribution can be generated by smoothing the two level digital PRBN signal through an analogue low-pass filter, Roberts and Davis (1966). A more attractive approach is to replace the analogue low-pass filter with a finite impulse response FIR filter.

The basic idea is to use an analogue tapped delay line filter Antoniou (1978) as a low-pass filter for the PRBN signal to obtain Gaussian amplitude distribution. The properties of the signals generated using the above method have been considered by Cumming (1967) and Davies (1971). The spectrum of the multilevel signals generated can be controlled by the clock frequency to the FIR filter. The Hewlett-Packard HP 3722A (1967) noise generator is based on this technique.

The two channel programmable flow noise simulator described in this chapter is based on the use of a PRBN generator and FIR filter to generate an analogue noise signal having characteristics similar to the flow generated noise signals.

Experimental results given in this chapter indicates that the characteristic of the signals generated by the flow noise simulator is very close to the flow generated noise signals. In addition the programmability of the noise generator has lead to an accurate evaluation of the performance of the improved constrained peak tracking (ICPT) correlator described in chapter 4 and 5.

3-2 The Flow Noise Simulator

Flow noise signals are characterised by random disturbances in the flow which are produced naturally by the fluid. To investigate the performance of a device which measures the correlation of these random disturbances requires that they can be simulated in a test laboratory. If a test rig is used to investigate the performance of a prototype correlator the experiments will not be reproducible and it will be difficult to optimise the design of the correlation flow measurement system.

The block diagram of the flow noise simulator used to investigate the performance of the improved constrained peak tracking correlator is shown in figure 3-1. The basic noise source of the flow noise simulator is a programmable PRBN signal generator. A FIR digital filter converts the output of the PRBN generator to a multilevel signal having characteristic very similar to the flow noise signal. A delayed version of the PRBN signal is generated using a programmable modulo-2 addition circuit and an FIR digital filter identical to the one used for the up-stream channel converts the delayed version of the PRBN signal to a multilevel signal.

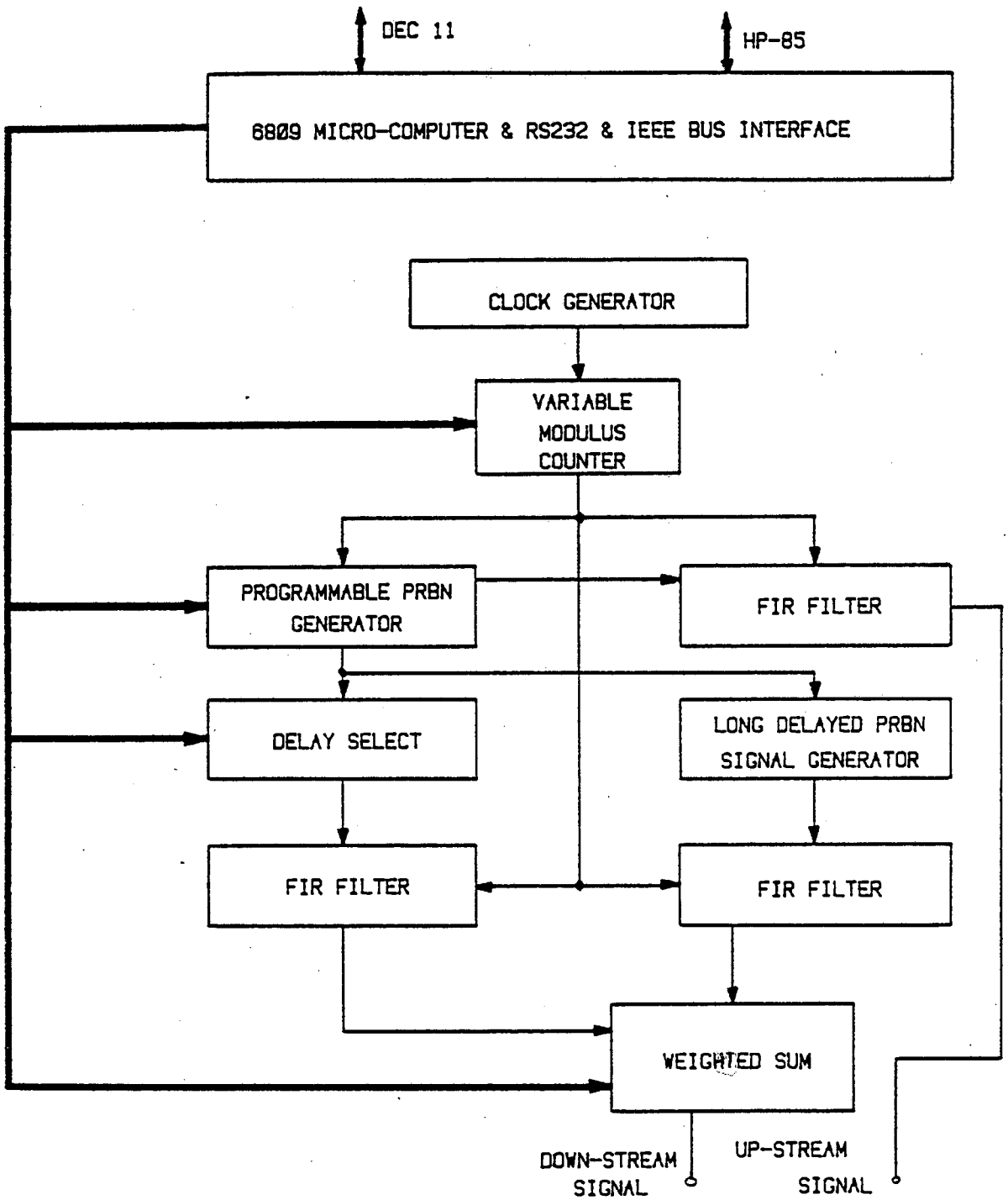

Fig. 3-1 THE BLOCK DIAGRAM OF THE FLOW NOISE SIMULATOR

The significance of the correlation function between the up-stream and down-stream signals is controlled by mixing a multilevel uncorrelated noise signal with the multilevel delayed output. The bandwidth of the up-stream and the down-stream signals are controlled by the output of the programmable frequency counter to the FIR filters and the PRBN generator.

3-2-1 Programmable PRBN Signal Generator

The PRBN signal is generated by means of a cascade of n-shift register stages connected in a feedback loop via an exclusive-OR gate, Hoffman (1971). The PRBN signals consist of completely defined patterns of selectable length and their statistics are controllable Korn (1967). In addition the PRBN sequences have an auto-correlation function which is constant for all defined points in one period, except at one point where it is unity, Korn (1967). Many different PRBN signals have been described in various mathematical treaties, for example Golomb (1967), Jordan and David (1973), Maritsas (1973A, 1973B), White (1967), and Lempel and Eastman (1971). The PRBN signals of most practical interest are those which can easily be generated with a small amount of electronic hardware.

The implementation of the programmable PRBN signal generator used as a basic noise source of the flow noise simulator is based on the method described by Greenshield and Jordan (1980). The block diagram of the programmable PRBN generator is shown in figure 3-2. The complete set of the feedback functions required to generate PRBN signals over a sequence length of (2^5-1) to

$(2^{24}-1)$ bits have been computed by means of a software routine written in PASCAL and are stored in two EPROMS shown in figure 3-2. Each output bit of the EPROMS corresponds to a complete feedback function of a particular sequence. A 6809 based micro-computer was used to select different sequences through 4 control lines as shown in figure 3-2. The EPROMS are addressed through the output stages of the shift register shown in figure 3-2. The address bus connections of each EPROMS to the output stages of the PRBN generators shift register are shown in table 3-1 and the functions implemented by each EPROM are given in table 3-2.

ROM address line	Shift Register Stages EPROM 1	EPROM 2
A0	1	2
A1	2	11
A2	3	12
A3	4	13
A4	5	14
A5	7	15
A6	8	16
A7	10	17
A8	11	18
A9	12	19
A10	24	20

Table 3-1 ROM Shift Register Connections.

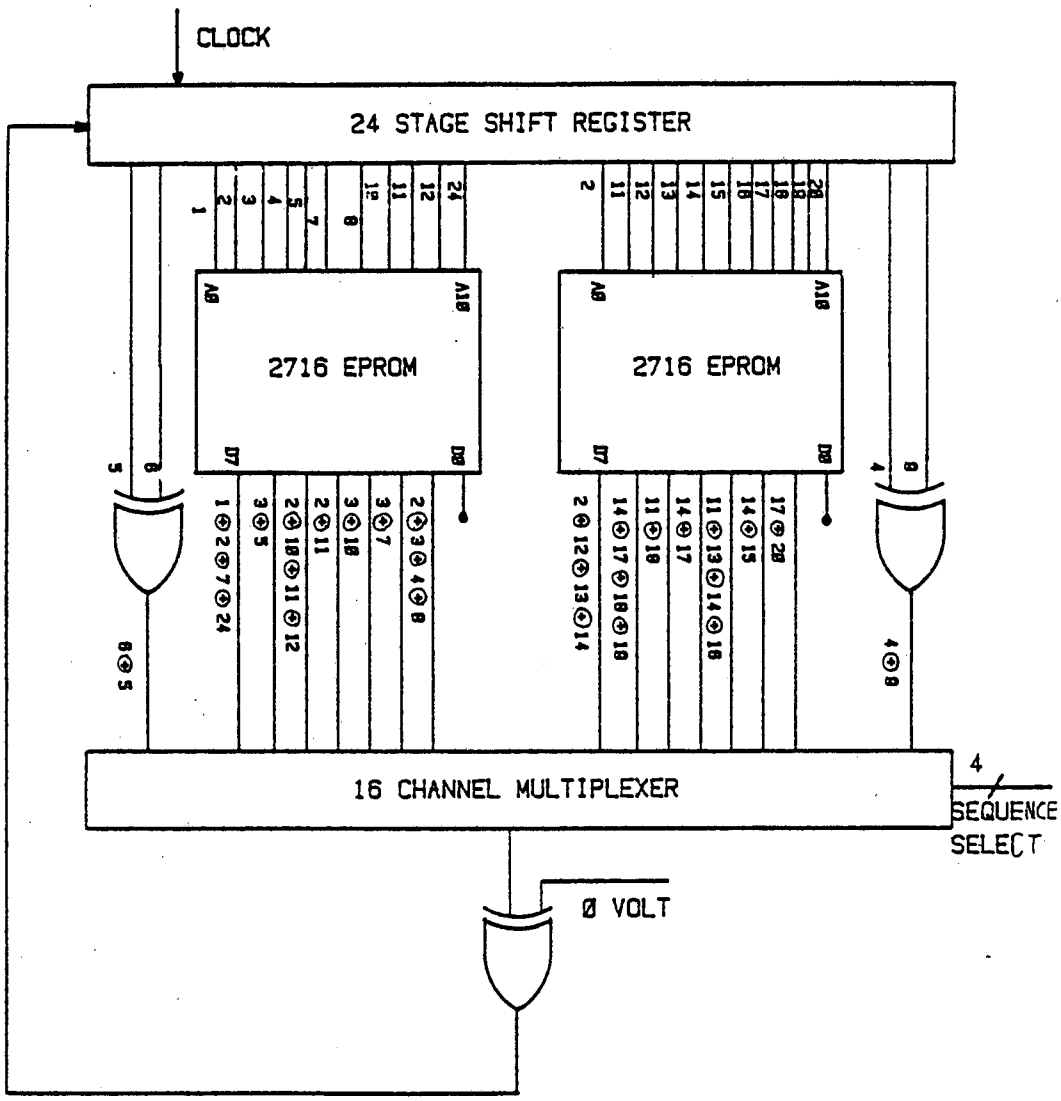

Fig. 3-2 THE BLOCK DIAGRAM OF THE PROGRAMMABLE PRBN GENERATOR.

ROM Output Line	Functions Implemented EPROM 1	EPROM 2
Do	-	-
D1	1⊕2⊕7⊕24	17⊕20
D2	3⊕5	14⊕17⊕18⊕19:
D3	2⊕10⊕11⊕12	11⊕18
D4	2⊕11	14⊕17
D5	3⊕10	11⊕13⊕14⊕16
D6	3⊕7	14⊕15
D7	2⊕3⊕4⊕8	2⊕12⊕13⊕14

Table 3-2 Functions Implemented for the EPROMS

Since the 8-stage shift register packages used in PRBN generators, are most conveniently designed to be reset to the all zero state, it is necessary to consider the use of exclusive -NOR feedback since the all zero state is the forbidden state for generators using exclusive-OR feedback. Therefore the feedback input to the shift register is inverted using a spare exclusive -OR gate shown in figure 3-2 in order to implement exclusive-NOR feedback. This allows the use of the reset line on the shift register to start and stop the sequence. The above arrangement to generate the PRBN sequences has been found to operate successfully under the control of the 6809 based micro-computer and is used as a basic noise source for the flow noise simulator.

3-2-2 Programmable Delayed PRBN Generator

The delayed version of the basic PRBN sequence is required to simulate the down-stream flow noise signal. Delayed version of the basic sequence can be generated using shift registers but this

approach would require large numbers of integrated circuit packages and is not practical. Therefore other methods described by several authors to generate delayed sequences from the PRBN signals using exclusive-OR feedback connections were considered, for example Gardiner (1965), Ireland and Marshall (1968A), (1968B), Douce (1968), and Hughes (1968). The matrix method described by Ireland and Marshall was found to be most suitable for implementation and requires a small amount of electronic hardware.

Therefore the method described by Ireland and Marshall was extended, Jordan and Kiani-Shabestari (1983), (see Appendix 1) to cover the case when the PRBN sequences are generated by exclusive-NOR feedback. The prototype micro-computer controlled delayed sequence generator has been constructed using available components and is used to generate the delayed version of the PRBN signals to simulate the down-stream flow noise channel.

3-2-3 The Digital Non-recursive FIR Filter

A multilevel Gaussian signal with the properties of random waveforms can be generated by low pass filtering of PRBN sequences, Roberts and Davies (1966). Since the signals to be smoothed are digital and single bit, a finite impulse response non-recursive filter, Antoniou (1978), offers the most convenient way to implement the low pass smoothing function. Statistical properties of the waveforms generated using FIR filters are described by Davies (1971).

A ROM based FIR filter, Jordan and Kiani-Shabestari (1982), (see Appendix 2) was used to generate a multilevel signal with a bell shaped amplitude distribution similar to the Gaussian amplitude distribution of flow generated noise signals. The Kaiser window was used to reduce the Gibbs oscillations caused by the truncation of the Fourier Series, Antoniou (1978). A design criteria for the window function was to find a window whose Fourier transform has relatively small side lobes with most of the energy concentrated in the centre lobe.

The FIR filter was designed such that the first null of the FIR filter impulse response occurred at nine clock periods i.e. cut off frequency was set to 1/18 of the clock frequency to the filter. It should be noted that the clock frequency applied to the ROM based filters and the PRBN generator are identical.

A 12-bit variable modulos counter was used to set the clock frequency to the PRBN generator as well as the ROM based FIR filters. It should be noted that the bandwidth of the simulated flow noise signal is determined by the design of the FIR filter as well as its clock frequency. Consequently time delay and bandwidth cannot be independently controlled. The method used to set the required time delay and the bandwidth of the simulated flow noise signal is described in section 3-3-2.

3-2-4 Uncorrelated Noise Generator

A practical flow noise signal has a normalised correlation function peak amplitude of unity when the input signal time delay

is zero and decreases as the transit time between the up-stream and down-stream transducers increases, Clinch (1969). In addition in a fully developed flow because the energy of the turbulent motion is constant, the auto-correlation function of the up-stream and down-stream signals are approximately equal (Taylor Instrument Ltd. 1976).

The significance of the correlation function can be controlled by performing a modulo-2 addition between the PRBN generators basic sequence and an uncorrelated binary sequence, Taylor Instrument Ltd. (1976), Manook (1981). Using this arrangement, the significance of the correlation function is controlled by the clock frequency applied to the uncorrelated PRBN generators shift register. Note that, the -3dB cut-off frequency of the PRBN sequences are equal to 0.45 x fs, Korn 1968, where, fs, is the clock frequency applied to the PRBN generator. Since the clock frequency to the uncorrelated PRBN generator is expected to be different from the basic sequence PRBN generators clock frequency, the -3dB cut-off frequency of the signals derived by mixing the basic sequence with the uncorrelated sequence is expected to be different from the -3dB cut-off frequency of the delayed basic sequences. Therefore the correlation function estimate is expected to be unsymmetrical. Massen (1982), has observed that the above approach is crude and will lead to unsymmetrical correlation function estimates.

To eliminate the above problem, the significance of the correlation function between two output signals of the flow noise

simulator was controlled by mixing an uncorrelated multilevel noise signal with the delayed multilevel noise signal. Initially the sequence length of the PRBN generator was set to $(2^{15}-1)$ bits, and this became a basic noise source for the flow noise generator to drive multilevel up-stream and down-stream signals. In addition a long delayed version of the basic sequence was derived by modulo-2 addition of the appropriate shift register output stages of the PRBN generator. The time delay between the basic sequence of the PRBN generator and its long delayed version was set to:-

Time delay=20000 x clock period of the PRBN generator

Note that the above time delay is well beyond the operating range of the ICPT correlator over the required input signal bandwidth of 50 to 500 Hz. The long time delayed version of the basic sequence is referred to as uncorrelated noise signal.

A ROM based FIR filter with identical characteristics to the ones used to generate a multilevel up-stream and its delayed signals was used to generate an uncorrelated multilevel signal. The block diagram of the arrangement used to control the significance of the correlation function by mixing a multilevel uncorrelated noise signal with a multilevel delayed output of the PRBN generator is shown in figure 3-3.

The output of the digital to analogue converter ,V_α, shown in figure 3-3 is used to control the significance of the

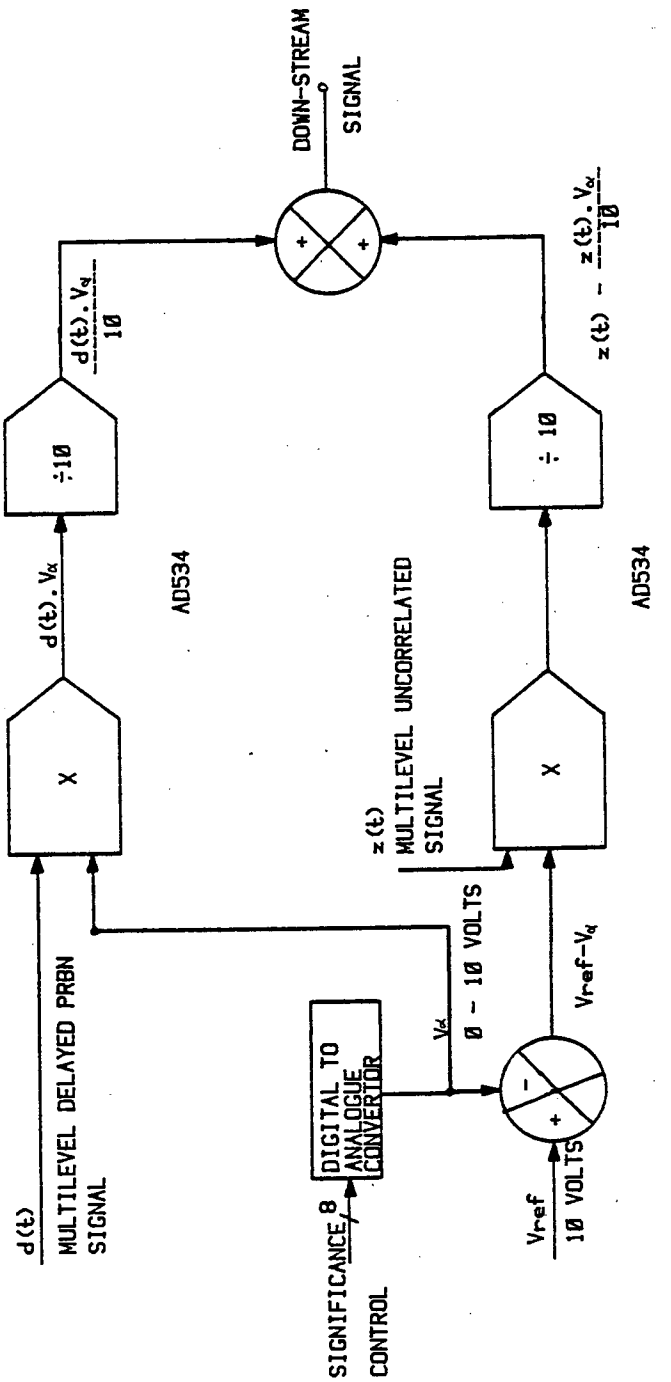

Fig.3-3 THE BLOCK DIAGRAM OF THE CIRCUIT USED TO CONTROL THE SIGNIFICANCE OF THE CORRELATION FUNCTION

correlation function relating the up-stream and down-stream signals derived from the flow noise simulator, through the 6809 based micro-computer. The summed output of the analogue multipliers, (AD534), shown in figure 3-3 is given by:-

$$y(t) = \{ z(t).[1-\theta] \} + \{ d(t).[\theta] \} \qquad (3\text{-}1)$$

and

$$\theta = \frac{V_\alpha}{10}$$

Where:-

$z(t)$ = Uncorrelated multilevel noise signal.

$d(t)$ = Delayed multilevel noise signal.

$y(t)$ = Down-stream signal derived from the flow noise simulator.

Using equation 3-1, the down-stream signal derived from the noise simulator, for θ equal to, 0 and 1 is given by:-

$y(t) = z(t)$ { for $\theta = 0$ }

and,

$y(t) = d(t)$ { for $\theta = 1$ }

Therefore, for $\theta = 0$, the significance of the cross-correlation function relating the signals derived from the noise simulator is equal to 0, and for $\theta = 1$, the normalised peak amplitude will be equal to 1. In addition from equation 3-1 it is clear that, as the magnitude of, θ, decreases the ratio of the uncorrelated multilevel signal, $z(t)$, to the delayed multilevel signal, $d(t)$,

increases and hence the significance of the correlation function between the signals derived from the noise simulator decreases.

It is important to note that, since the clock frequency to the FIR filters are identical, the -3dB cut-off frequency of the signals derived from the noise generator are expected to be of the same value regardless of the correlation function peak amplitude. In addition the auto-correlation functions of the up-stream and down-stream signals derived from the noise simulator are expected to be approximately equal, and independent of their normalised correlation function peak amplitude.

3-3 Flow Noise Simulation

To simulate the flow noise signals the following parameters of the noise simulator was set by the HP-85 computer through the IEEE bus interface circuit:-

1) Bandwidth of signals derived from the noise simulator.
2) Time delay difference between the signals derived.
3) Normalised correlation function peak amplitude.

3-3-1 Bandwidth of the simulated flow noise signal

The bandwidth of the signals derived from the flow noise simulator was set by the output clock frequency of the 12 bit variable modulus counter (VMC) which was supplied to the FIR filters as shown in figure 3-1. The bandwidth of the noise

signals is given by:-

$$\text{Bandwidth} = BW = \frac{fs}{18} \qquad (3\text{-}2)$$

where fs is equal to the output clock frequency of the VMC.

The output clock frequency of the VMC can be set through the IEEE bus interface by the HP-85 computer used as an experiment controller. The input clock frequency to the VMC is set to be equal to 1.2 MHz, and this can be divided by an integer number between 2 to 4096. Therefore the flow noise signal bandwidth can be set to vary over a range of 16 Hz to 33.5 KHz. Note that the above range is well beyond the flow noise signal bandwidth defined by Taylor Instrument Ltd. (1976).

A typical multilevel signals generated by the output of the FIR filters are shown in figure 3-4. An HP 3721A correlation computer (1968) were used to measure the probability density function of the multilevel signals derived from the flow noise simulator and is shown in figure 3-5. From figure 3-5 it will be seen that the amplitude distribution of the simulated flow noise signal is similar to the bell shaped Gaussian amplitude distribution of the signals derived from the real flow streams.

The auto-correlation function of the simulated flow noise signal with different bandwidths were measured using an HP 3721A correlation computer and are shown in figure 3-6. From figure 3-6 it will be seen that as the bandwidth of the simulated flow noise

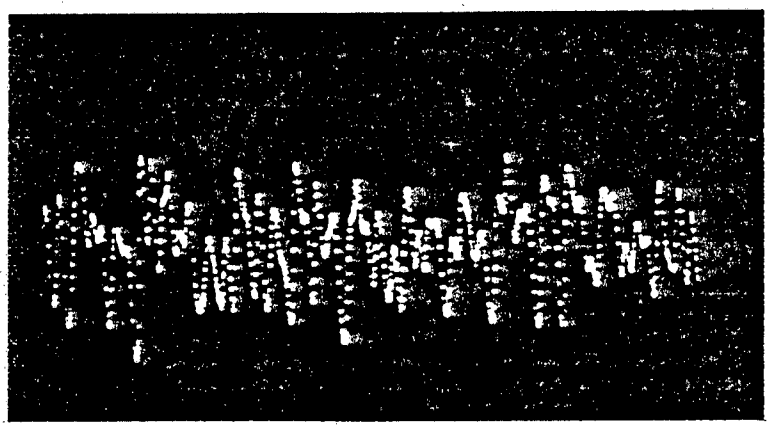

(a) Bandwidth = 500 Hz 20 μsecs

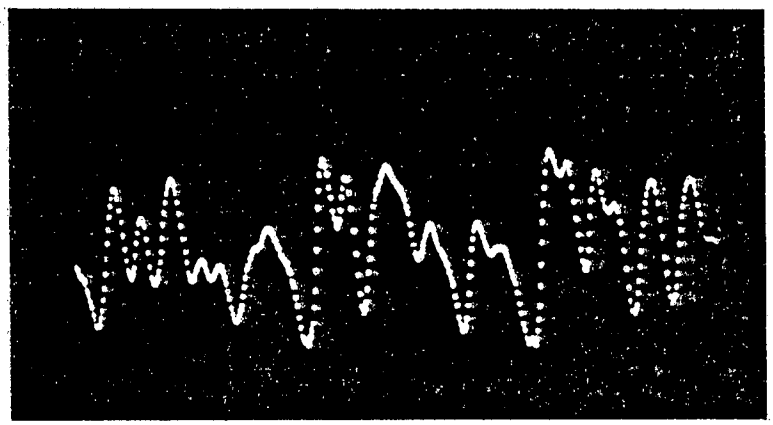

(b) Bandwidth = 250 Hz

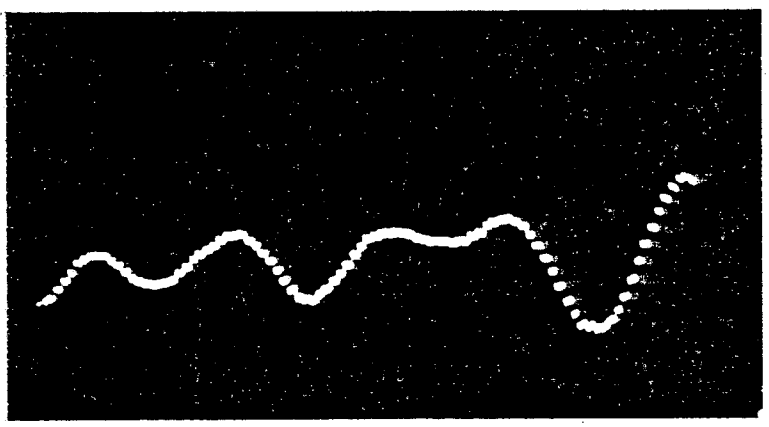

(c) Bandwidth = 50 Hz

Fig. 3-4 TYPICAL MULTILEVEL SIGNALS DERIVED FROM THE FLOW NOISE SIMULATOR.

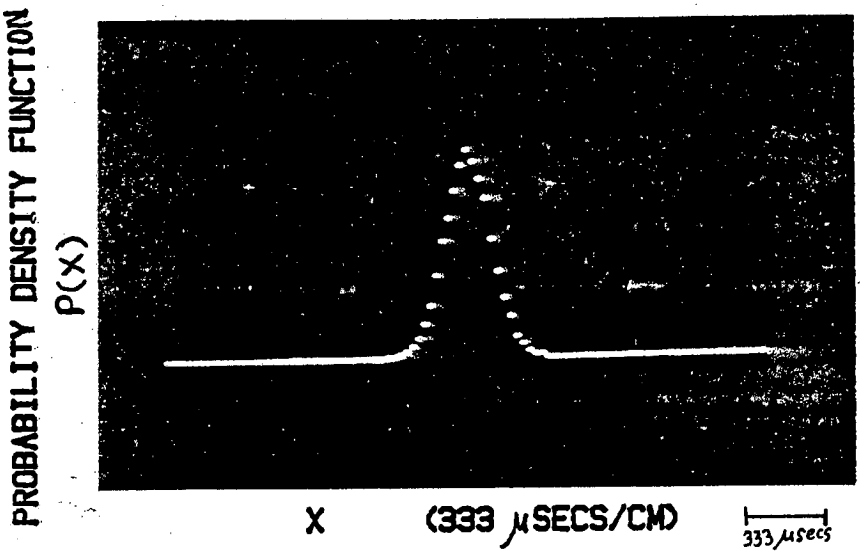

Fig. 3-5 PROBABILITY DENSITY FUNCTION OF THE UPSTREAM SIGNAL.

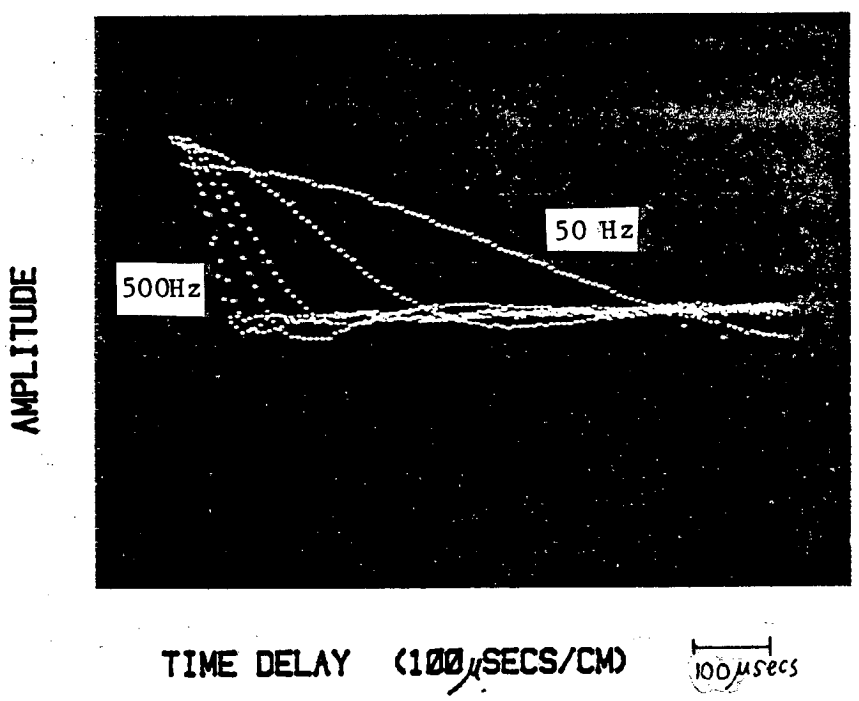

Fig. 3-6 AUTO-CORRELATION OF THE SIGNALS DERIVED OVER A A 50 TO 500 Hz BANDWIDTH.

signal increases, the width of the auto-correlation function decreases. Note that it has been shown that the first zero of the auto-correlation function is expected to occur at $\tau = 1/2BW$, Lange (1967), where t is equal to time delay.

3-3-2 Time Delay Setting

The simulated time delay of the flow noise signal is given by:-

$$\text{Time delay} = ns \cdot \tau s \qquad (3\text{-}3)$$

where:-

ns = the selected delay number using a modulo-2 addition of the appropriate output stages of the PRBN generators shift register.

and

$\tau s = 1/fs$ = the clock period to the PRBN generator and the FIR filters.

The bandwidth of the simulated flow noise signal is determined by the clock period applied to the FIR filters shown in figure 3-1 and is given by equation 3-2. Therefore the time delay and bandwidth of the signals derived from the flow noise simulator can not be controlled independently. Hence the following procedure is taken to set the time delay and the bandwidth of the signals derived from the flow noise simulator.

Consider a practical time delay of 6 msecs with a flow

noise signal bandwidth of 250 Hz arising from a flow velocity of 5 m/secs with a transducer spacing of 30 mm. To simulate the flow noise signals with the above characteristics, the required clock frequency to the FIR filters shown in figure 3-1 is estimated using equation 3-2 and is given by:-

$$fs = 18 \times 250 = 4500 \text{ Hz}.$$

Equation 3-3 is used to calculate the required delay setting, and is given by:-

$$ns = \frac{\text{Time delay}}{1/fs} = \frac{6 \times 10^{-3}}{1/4500} = 27$$

Hence the delay setting of 27 is required to simulate the flow noise signals with 250 Hz bandwidth and time delay of 6 msecs.

In addition we have:-

$$ns.\tau 2 = (ns + 1).\tau 1 \qquad (3-4)$$

where $\tau 1$ and $\tau 2$ are the clock periods to the FIR filters shift register.

Hence

$$\frac{\tau 2}{\tau 1} = \frac{ns+1}{ns} \qquad (3\text{-}5)$$

Or

$$\frac{f1}{f2} = \frac{BW1}{BW2} = \frac{ns+1}{ns} \qquad (3\text{-}6)$$

Therefore from equation 3-6 it is clear that a small change by the clock frequency will enable the flow noise signals time delay to be set between the discrete settings of the delay generator, without changing the bandwidth by a large amount.

For example to simulate flow noise signal with 250 Hz bandwidth and time delay of 6.05 msecs the following steps are taken:-

1) Time delay = $ns.\tau$ (from equation 3-3)

$ns = 6.05 \times 10^{-3} \times 4500 = 27.225$

Note that the flow noise signal time delay can only be set in discrete steps, therefore ns is required to be equal to 27.

2) To simulate flow noise signals with time delay of 6.05 msecs and bandwidth of 250 Hz, the actual bandwidth of the noise signal is estimated using equation 3-6 and is given by:-

$$BW2 = \frac{BW1 \times ns}{ns+1} = \frac{250 \times 27}{27.225} = 247.93 \text{ Hz}$$

Therefore to simulate time delay of 6.05 msecs, the actual

bandwidth of the flow noise signal is required to be approximately equal to 248 Hz.

3) The required setting for the 12-bit VMC is given by:-

$$\text{VMC setting} = \frac{\text{input clock frequency to VMC}}{\text{required clock frequency to FIR filters}}$$

$$= \frac{1.2 \times 10^6}{248 \times 18} = 268.8$$

Note that since the clock frequency to the VMC can only be divided by an integer number between 2 to 4096, the input clock frequency is divided by 268.

4) Therefore the actual flow noise signal bandwidth and time delay with the above settings are given by:-

$$fs = \frac{\text{input clock frequency to VMC}}{\text{VMC setting}}$$

$$fs = \frac{1.2 \times 10^6}{268} = 4460.9 \text{ Hz}$$

and

$$BW = \frac{fs}{18} = 247.8 \text{ Hz}$$

and

$$\text{Time delay} = \frac{27}{4460.9} = 6.052 \text{ msecs}$$

Therefore from above it is clear that the noise generator can be used to simulate the flow noise signal bandwidth and time delay very accurately between the discrete steps of the delay setting, without changing the bandwidth by a large amount. In addition the small difference between the required, and actual time delay and bandwidth of the signals derived from the noise simulator are computed by the HP-85 computer used as a experiment controller. It should be noted that the above procedure used to estimate the required time delay and bandwidth settings of the flow noise simulator are carried out and set by the HP-85 computer through the IEEE bus interface.

3-3-3 Correlation Function Significance

The significance of the correlation function relating the up-stream and down-stream signals can be changed by mixing an uncorrelated multilevel noise signal with the multilevel delayed signal. Figure 3-7 shows the probability density function of the multilevel uncorrelated noise signal, the probability density function of the multilevel delayed signal before mixing with an uncorrelated multilevel signal and the probability density function of the delayed signal mixed with the uncorrelated signal to yield a normalised correlation function peak amplitude of .5. From figure 3-7 it will be seen that, the bell shaped probability density function of the uncorrelated noise signal is similar to the probability density function of the delayed multilevel output signal. In addition from figure 3-7 it will be seen that the amplitude distribution of the mixed delayed signal is similar to the flow generated

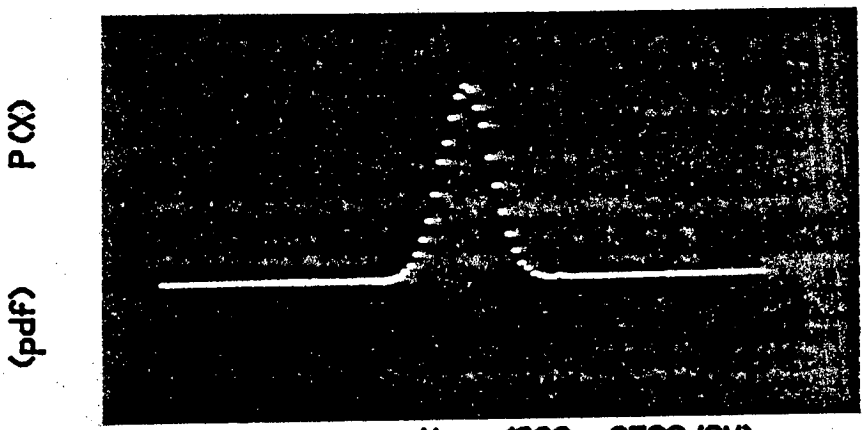

(a) DELAYED SIGNAL (pdf)

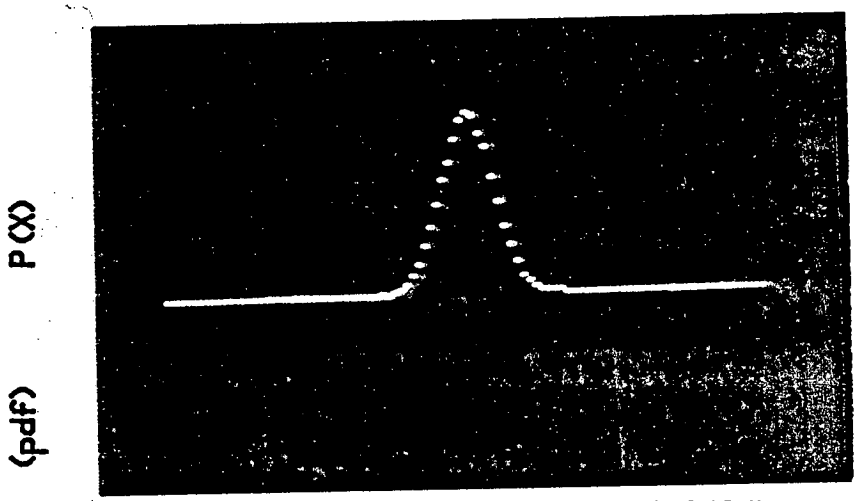

(b) UNCORRELATED SIGNAL (pdf)

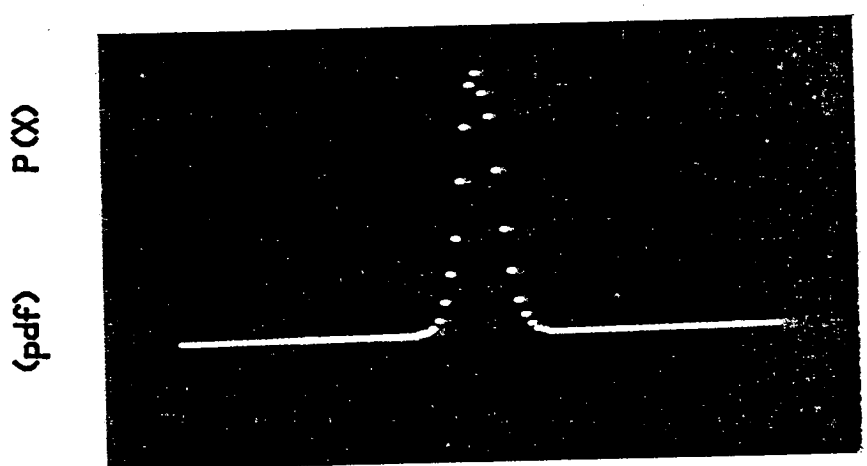

(c) UNCORRELATED & DELAYED SIGNAL MIXED (pdf)

Fig. 3-7 THE PROBABILITY DENSITY FUNCTION (pdf) OF DOWN-STREAM SIGNAL.

noise signals with the Gaussian amplitude distribution, but its standard deviation has decreased by approximately by factor of $2^{\frac{1}{2}}$, in comparison to the amplitude distribution of the multilevel delayed signal shown in figure 3-7. Mathematical derivation to estimate the standard deviation of the two mixed uncorrelated signals with a common mean and Gaussian amplitude distribution is given by Weatherburn (1952) and the experimental results shown in figure 3-7 confirms his mathematical prediction. It should be noted that an approximately identical probability density function to the up-stream channel can be obtained by adjusting the rms voltage amplitude of the uncorrelated multilevel signal before mixing with the delayed multilevel signal.

The auto-correlation function of the signals derived from the flow noise simulator over a simulated flow noise signal bandwidth of 50 to 250 Hz range with a normalised correlation function peak amplitude of 1,.5 and .2 is shown in figure 3-8. From figure 3-8 it will be seen that the amplitude of the auto-correlation function of the signals derived from the noise simulator at zero time delay are approximately equal. Note that a slight difference on the amplitude of the auto-correlation functions of the up-stream and down-stream signals at time delay of zero are due to the poor level adjustments of the HP 3721A correlation computer to capture multiple exposure photograph of the functions.

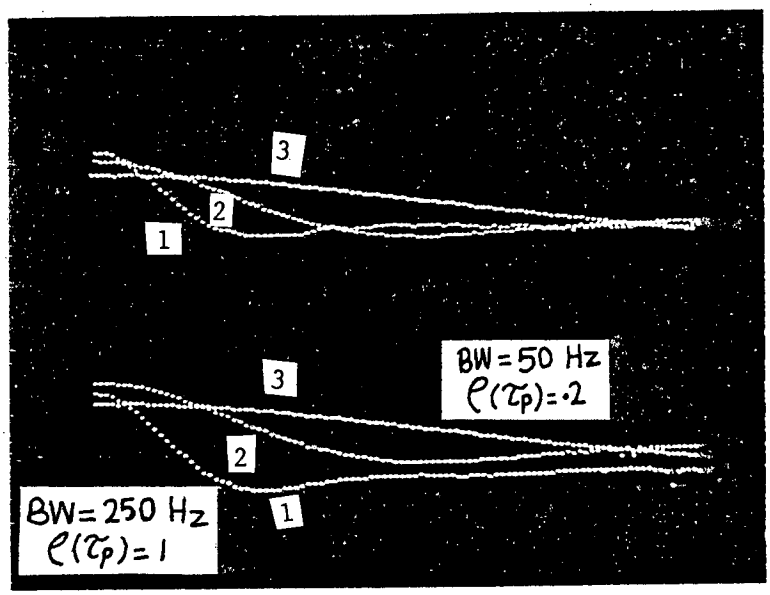

Fig. 3-8 THE AUTO-CORRELATION FUNCTIONS OF THE UP-STREAM AND DOWN-STREAM SIGNALS OVER A 50 TO 250 Hz BANDWIDTH.

1) Normalised correlation function peak amplitude = 1,
   Bandwidth = 250 Hz.
2) Normalised correlation function peak amplitude = .5,
   Bandwidth = 125 Hz.
3) Normalised correlation function peak amplitude = .2,
   Bandwidth = 50 Hz.

3-4 Calibration of the Flow Noise Simulator

The flow noise generator was calibrated to simulate the characteristic of the noise signals derived from the pipe size of 1 inch diameter using a pair of identical ultrasonic transducers with 30 mm spacing. The experimental data provided by Taylor Instrument Ltd. (1976) were used to simulate the flow noise signals bandwidth and time delay over a flow velocity range of 32 to 1. The flow noise signal bandwidth was calibrated to vary over a range of 50 to 500 Hz. The normalised peak amplitude of the correlation function was calculated using equation 2-19 of chapter 2, and is expected to vary between 0.2 and 0.9, over an input signal time delay range of 32 to 1. The typical flow generated noise signal bandwidth and its normalised correlation function peak amplitude over the time delay range of interest is given in table 3-3.

Time Delay msecs	Bandwidth Hz	Peak Amplitude Normalised
1.433	500	0.9
6.143	400	0.82
15.564	340	0.61
20.279	300	0.53
24.984	270	0.46
29.694	250	0.39
34.405	180	0.34
39.115	120	0.29
43.825	75	0.25
52.48	50	0.21

Table 3-3 Typical characteristics of the practical flow noise signals.

Data given in table 3-3 was used to simulate the signals derived from the flow noise generator and their typical correlation function estimates are shown in figure 3-9. Note that the 6809 based correlator was used to estimate the correlation functions shown in figure 3-9. From figure 3-9 it will be seen that the significance of the correlation function relating the signals derived from the noise simulator decreases along the time delay axis and the width of the correlation function around its peak position increases. The results given in this chapter indicates that the characteristics of the signals derived from the flow noise generator is similar to flow generated noise signals. Therefore the flow noise simulator can be used to realistically investigate the performance of the ICPT correlator.

3-5 Experimental system

The block diagram of the flow noise simulator used to investigate the performance of the ICPT correlator is shown in figure 3-1. The simulated flow noise signals bandwidth, sequence length, time delay and the correlation function peak amplitude were controlled by the 6809 based micro-computer board installed with the noise simulator circuits through the IEEE bus interface by the HP-85 computer. An RS232 interface circuit was designed to down load the software developed for the 6809 based micro-computer from a DEC11/60 main frame computer to the 6809 based micro-computer of the noise simulator. The final version of the software was stored in an EPROM.

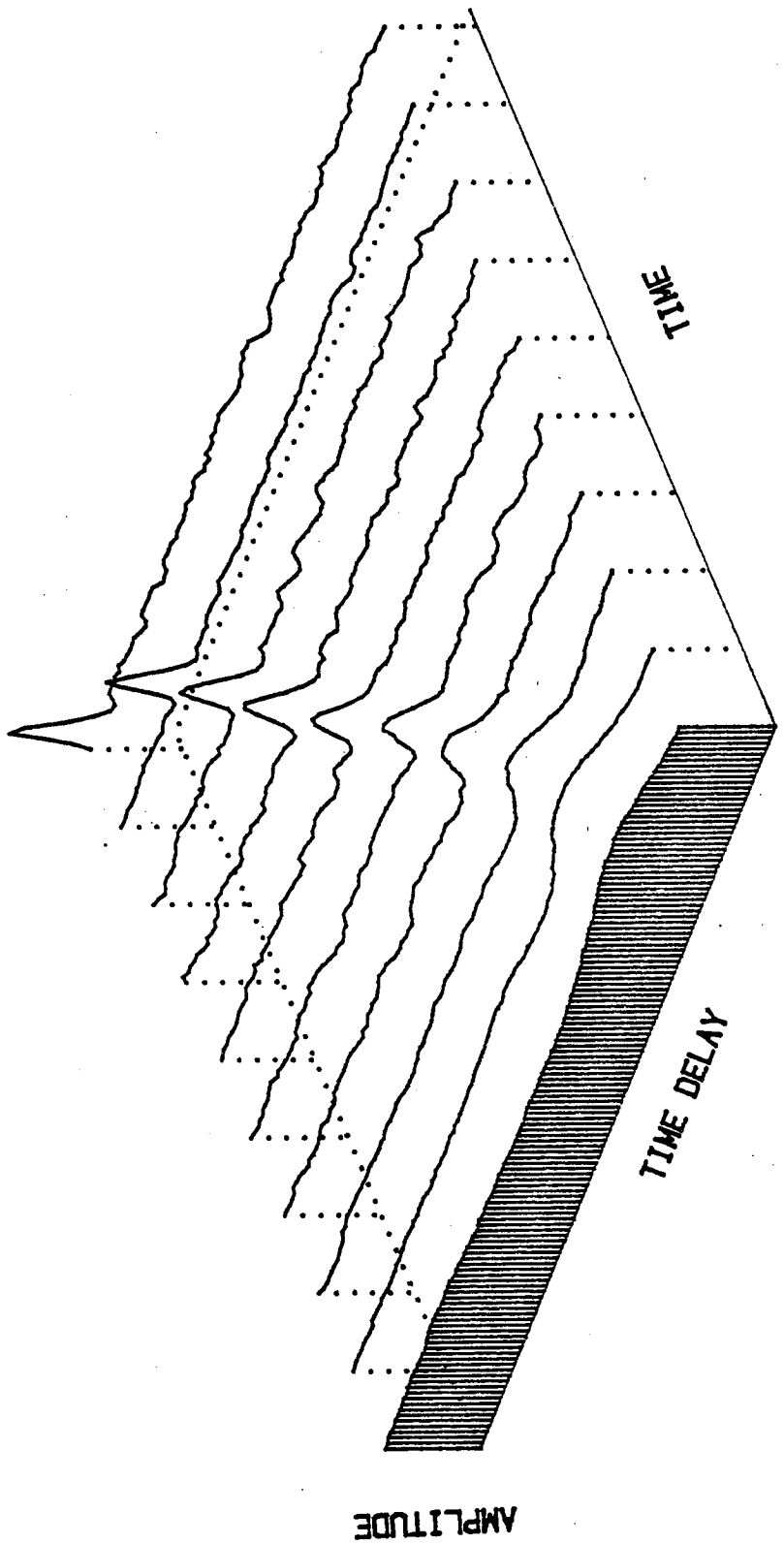

Fig. 3-9 TYPICAL CORRELATION FUNCTION ESTIMATES OF THE SIGNALS DERIVED FROM THE FLOW NOISE SIMULATOR.

An IEEE bus interface circuit has been designed and installed with the noise simulators 6809 based micro-computer to enable an HP-85 computer to act as an overall experiment controller. The IEEE bus implementation and the experimental system has lead to the collection of consistent results over long period of time. The software developed for the 6809 based micro-computer was designed in such a way that it can be expanded for further experimental investigations.

CHAPTER 4 IMPROVED CONSTRAINED PEAK TRACKING CORRELATOR

4-1 Introduction

The basic principle of the peak tracking correlators and their possible application areas have been described in Chapter 2. The improved constrained peak tracking ICPT correlator is most suitable for flow measurement applications, since it is simple to implement and reliably tracks the peak of the correlation function with high resolution defined by an analogue control loop. Jordan and Manook (1981B) and Manook (1981) have used the overloading counter correlator to constrain the tracking loop to track the peak of the function. No results are given to indicate the tracking performance of the peak tracking correlator on its own. The overloading counter correlator used to set the tracking loop can not by definition, give a steady indication of the peak position, typically deviations of $\pm 1\%$ about a peak position will be observed. Manook (1981) noticed that this leads to the tracking loop having an uncertain "jittery" response which leads to a flow rate display which jumps in discrete steps.

The ICPT correlator eliminates the possibility of losing the peak of the correlation function and tracking a spurious peak. The following sections describes techniques which can be used to solve the problem of the tracking loop jitter and optimise the performance of the constrained peak tracker. A detailed experimental investigation of the performance of the optimised tracking correlator has indicated that for flow measurement

applications a coarse correlator with approximate resolution of ±12.5% and measurement time of one second is sufficient to constrain the tracking correlator to track the peak of a correlation function over an input signal bandwidth of 50 to 500 Hz. It will be shown that only a small addition to the previous circuit is required to ensure that the improved constrained peak tracking correlator always tracks the peak of the correlation function linearly without output response jitter. A TRW TDC1004J based correlator and an on-line 6809 based correlator have been considered for coarse estimation of the peak position of the correlation function.

4-2 Improved Constrained Peak Tracking Correlator

The simplified block diagram of the improved constrained peak tracking (ICPT) correlator is shown in figure 4-1. Essentially it is comprised of three correlators operating in parallel:-

i) A digital correlator, providing a coarse indication of the peak position (this will be referred to as the coarse correlator).

ii) A peak tracking correlator, which is free to track the peak of the correlation function, once its delay shift register is set by the coarse correlators peak position estimate.

iii) A serial correlator, which is used to indicate the out of lock mode of the peak tracking correlator.

The basic principle of the ICPT correlator is similar to

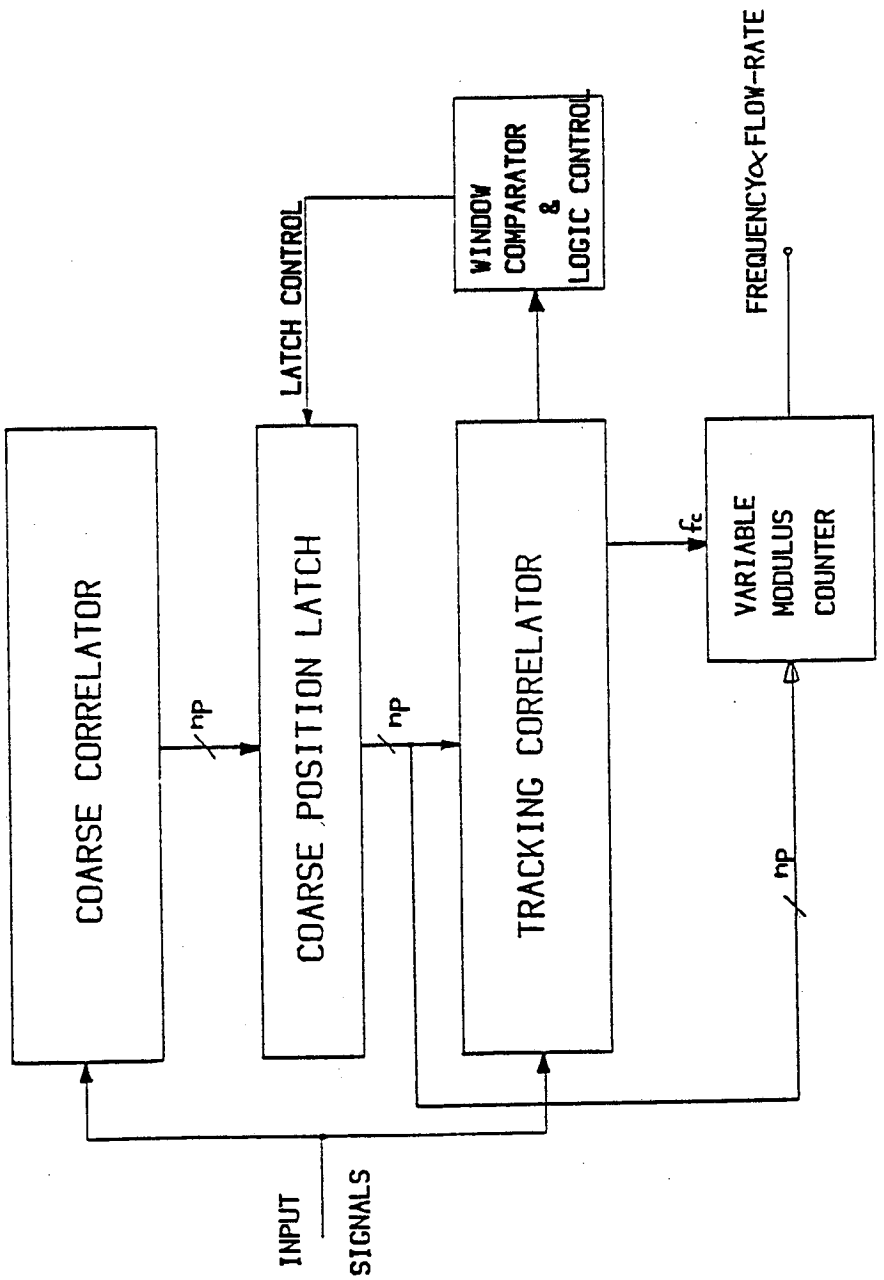

Fig. 4-1 THE BLOCK DIAGRAM OF THE "ICPT" CORRELATOR.

the constrained peak tracking correlator described by Jordan and Manook (1981B) and Manook (1981) and is shown in figure 4-2. The tracking correlator is a negative feedback loop operating on a first order differentiation of the correlation function. For linear operation, the tracking correlator is constrained to track the peak of the correlation function by a coarse correlator, setting the length of its time delay shift register by a coarse estimation of the peak position. The resolution of the coarse correlator is poor and approximately is of order of $\pm 12.5\%$. The theoretical resolution of the tracking correlator is infinite and in practice is defined by the analogue negative feedback loop circuit. The time delay range and the sample clock period of the coarse correlator is defined from the required flow velocity range to be measured by the ICPT correlator.

For accurate estimation of time delays the tracking correlator must be capable of tracking the peak of the correlation function with high resolution at least within the sample clock period of the coarse correlator. Hence the minimum tracking range of the negative feedback loop is defined by the resolution of the coarse correlator.

When the negative feedback loop is open its voltage controlled oscillator (VCO) operates at a pre-set frequency called the free-running frequency, fr. The choice of the free-running frequency,fr, depends on the required time delay range and the bandwidth of the signals to be correlated. To constrain the peak tracking correlator to track the peak of the correlation function

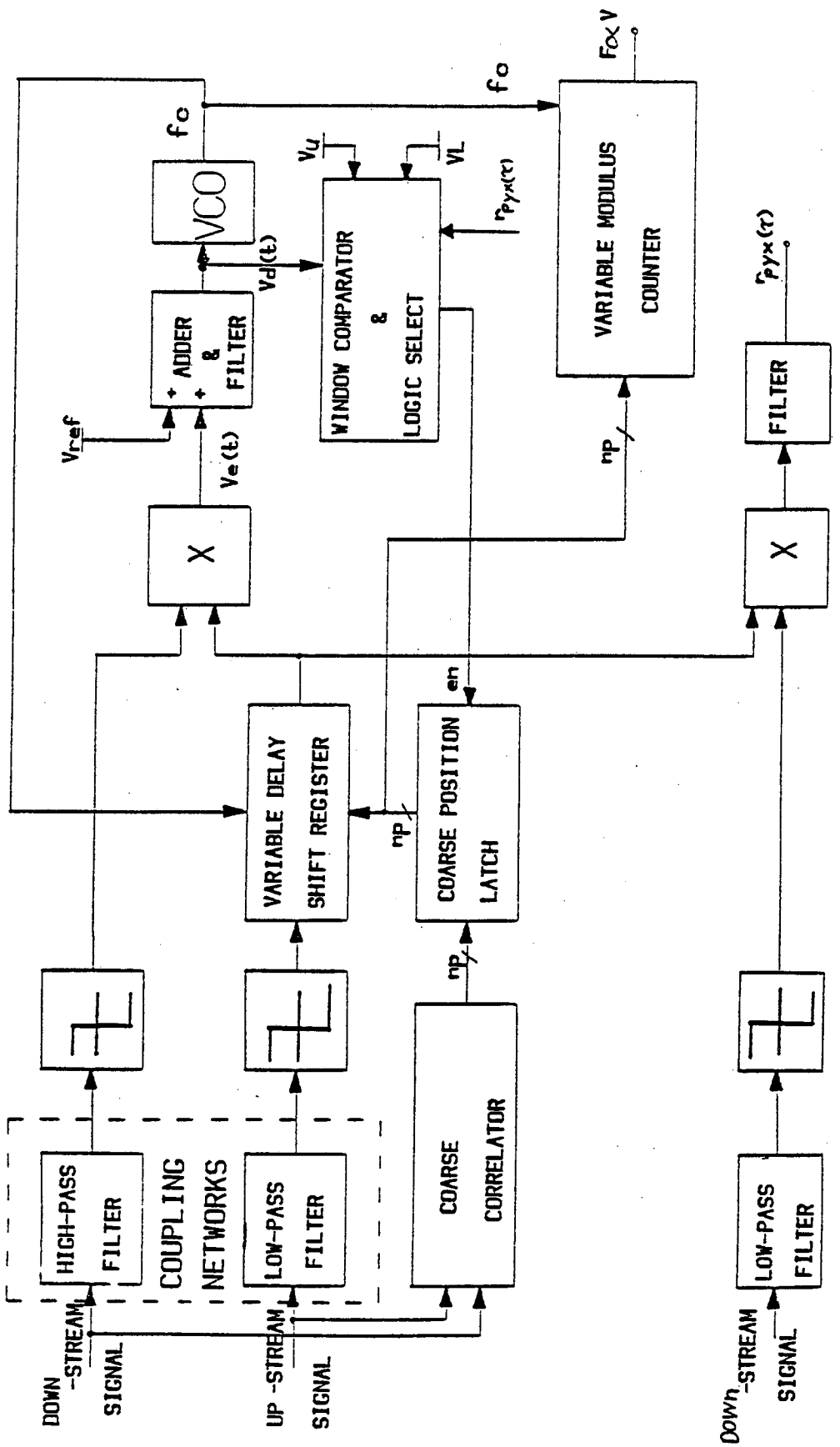

Fig. 4-2 THE BLOCK DIAGRAM OF THE " ICPT " CORRELATOR.

within the required time delay range, the coarse correlator and the tracking correlators time delay range must be identical. The free-running frequency of the tracking loop can be related to the sampling frequency of the coarse correlator and is given by:-

$$fr = \frac{Np}{Nc} \times fs \qquad (4\text{-}1)$$

Where:-

Np= The maximum length of the delay shift register of the tracking correlator.

Nc= The maximum delay range of the coarse correlator.

fs= Sampling frequency of the coarse correlator, and is derived from the required time delay range to be measured.

Hence, for example, if the maximum length of the delay shift register of the peak tracking correlator is equal to the coarse correlators maximum delay range, the free-running frequency of the tracking loop must be equal to the sampling period of the coarse correlator.

When the tracking loop is closed and the input signals are applied to the tracking system, the error signal Ve(t), shown in figure 4-2, will be generated on the output of the multiplier, and this is related to the multipliers input signals time delay difference. If the up-stream and down-stream input polarity signals are used, the required multiplication operation is equivalent to the exclusive-NOR operation. The error signal,

Ve(t) , together with, Vref, the free-running frequency reference voltage is filtered and applied to the input control terminal of the VCO. Due to the negative feedback action of the tracking loop, the output voltage of the smoothing filter, Vd(t), forces the VCO's output frequency to change the delay shift registers time delay in such a direction as to reduce the time delay difference between the two input signals of the multiplier. If the input signals time delay difference is sufficiently small the tracking correlator will track the peak of the correlation function. The tracking condition is defined by:-

$$\frac{d}{d\tau}\left[R_{pyx}(\tau) \right] \Big|_{\tau=\tau_p} = 0 \qquad (4\text{-}2)$$

Where τ_p is the position of the peak of the correlation function and it is given by:-

$$\tau_p = \frac{np}{fc}$$

Where:-

np = Length of the delay shift register set by the coarse correlator.

fc = Output frequency of the VCO.

The flow velocity, V, is given by:-

$$V = \frac{L}{\tau_p}$$

Therefore:-

$$V = L\left(\frac{fc}{np}\right) \qquad (4\text{-}4)$$

Hence the output frequency of the variable modulus counter shown in figure 4-2, having modulus set by the coarse correlators peak position estimate, np, and input frequency, fc, is proportional to the flow velocity.

The tracking correlator is a non-linear feedback system and it can be linearised by small signal analysis techniques. The tracking loop can be approximated as a linear system when the loop is in the lock mode and is tracking the peak of the correlation function. The simplified linearised model of the tracking loop as a negative feedback system is shown in figure 4-3.

Where:-

Kd is proportional to the slope of the differentiated correlation function, volts/secs.

Ko is the gain of the voltage controlled oscillator, Hz/volts.

Ka is the amplifier gain, volts/volts.

Kp refers to the gain control potentiometer settings ,volts/volts.

np is the delay shift register length set by a coarse correlator.

fc is the output frequency of the VCO, when the loop is in the look mode, Hz.

Δfc is small change in frequency, Hz.

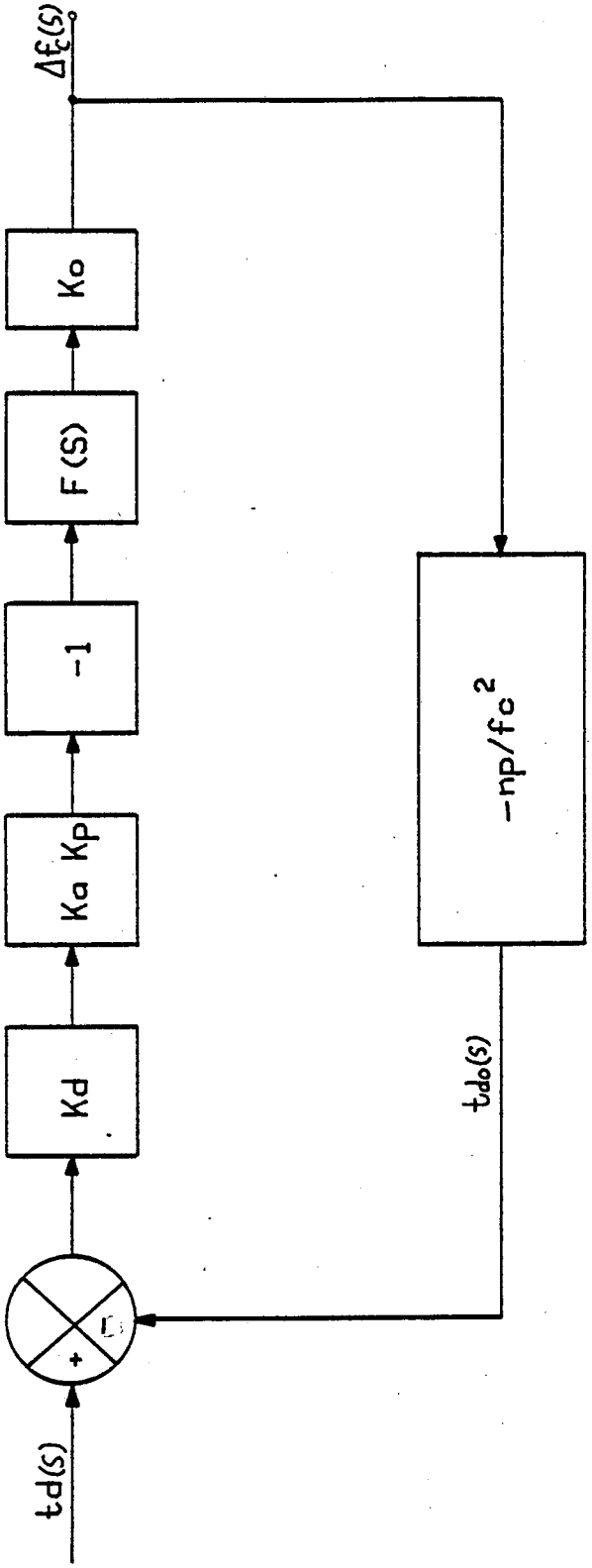

Fig. 4-3 THE LINEARISED BLOCK DIAGRAM OF THE LOOP.

td is the input signal time delay change, secs.

tdo is the estimated input signal time delay change, secs.

The small change in input signal time delay estimate, tdo, can be approximated by $\Delta\tau_p$, where:-

$$\tau_p = \frac{np}{fc}$$

and,

$$\frac{d\tau_p}{dfc} = np\left(\frac{-1}{fc^2}\right)$$

Hence small input signal time delay estimate is approximated by:-

$$tdo = \Delta\tau_p = np.\left(\frac{-1}{fc^2}\right).\Delta fc \qquad (4\text{-}5)$$

F(S) is the transfer function of the tracking loops smoothing filter and is given by:-

$$F(S) = \frac{1}{1 + S\tau}$$

Where τ is the smoothing filters time constant.

The closed loop transfer function of the tracking loop, H(S), is given by:-

$$H(S) = \frac{\frac{-KD.Ko}{\tau}}{S + \left(\frac{fc^2 + KD.Ko.np}{fc^2.\tau}\right)} \qquad (4\text{-}6)$$

Where:- KD = Ka.Kd.Kp volts/secs.

An experimental system has demonstrated the expected first order response to the step changes.

The impulse response characteristic of the tracking loop, h(t), is derived by taking the inverse Laplace transform of the equation 4-6, and is given by:-

$$h(t) = \frac{-KD.Ko}{\tau} \exp\left\{-\left(\frac{fc^2 + KD.Ko.np}{fc^2\,\tau}\right) t\right\} \qquad (4\text{-}7)$$

From equation (4-6) and (4-7) it is clear that, if the length of the delay shift register of the tracking correlator, np ,for a given KD,Ko and τ is increased, the time constant of the tracking correlator will be decreased. Therefore if the length of the delay shift register is large, the transient response of the tracking correlator to a step change is fast relative to the situation, when the length of the delay shift register is small. Hence the position of the peak of the correlation function can be tracked with a faster response for longer time delays. Under changing signal conditions, this is of great importance, since the statistics of the input signals are changing with time, and a correlation functions peak position can be estimated more accurately if the closed loop time constant of the tracking correlator is small.

The range over which the negative feedback loop can

track the peak of the correlation function linearly and stay in the lock mode, regardless of the direction of the input signal time delay change, is called the linear lock range of the tracking correlator. This range is a function of the input signal bandwidth, and is less than the tracking range of the loop. It is important to note that the linear lock range refers to the range over which the negative feedback loop can track the peak of the correlation function linearly with a fixed delay shift register length, np.

The tracking range of the negative feedback loop with a fixed delay shift register length, input signal bandwidth, and signal to noise ratio, is directly dependent on the direction of the input signal time delay change. This can be explained with reference to figure 4-4, where the delay shift register length ,np, is set to be equal to N, and the input signal bandwidth ,signal to noise ratio are independent of the input signal time delay change. Initially the input signal time delay is set to its maximum value and gradually swept backward and forward. The response of the error voltage ,Vd(t), to a decreasing input signal time delay is shown in figure 4-4(a). From figure 4-4(a) it will be seen that the loop does not respond to the input signal time delay change until its input signal time delay difference is equal to τ_1 . At τ_1 ,the loop suddenly locks on to the peak of the correlation function, as the output voltage of the tracking loops filter Vd(t), jumps to the value of Vdl(t) shown in figure 4-4(a). The loop continues to track the peak of the correlation function, until the input signal time delay is equal to τ_2 , shown in figure

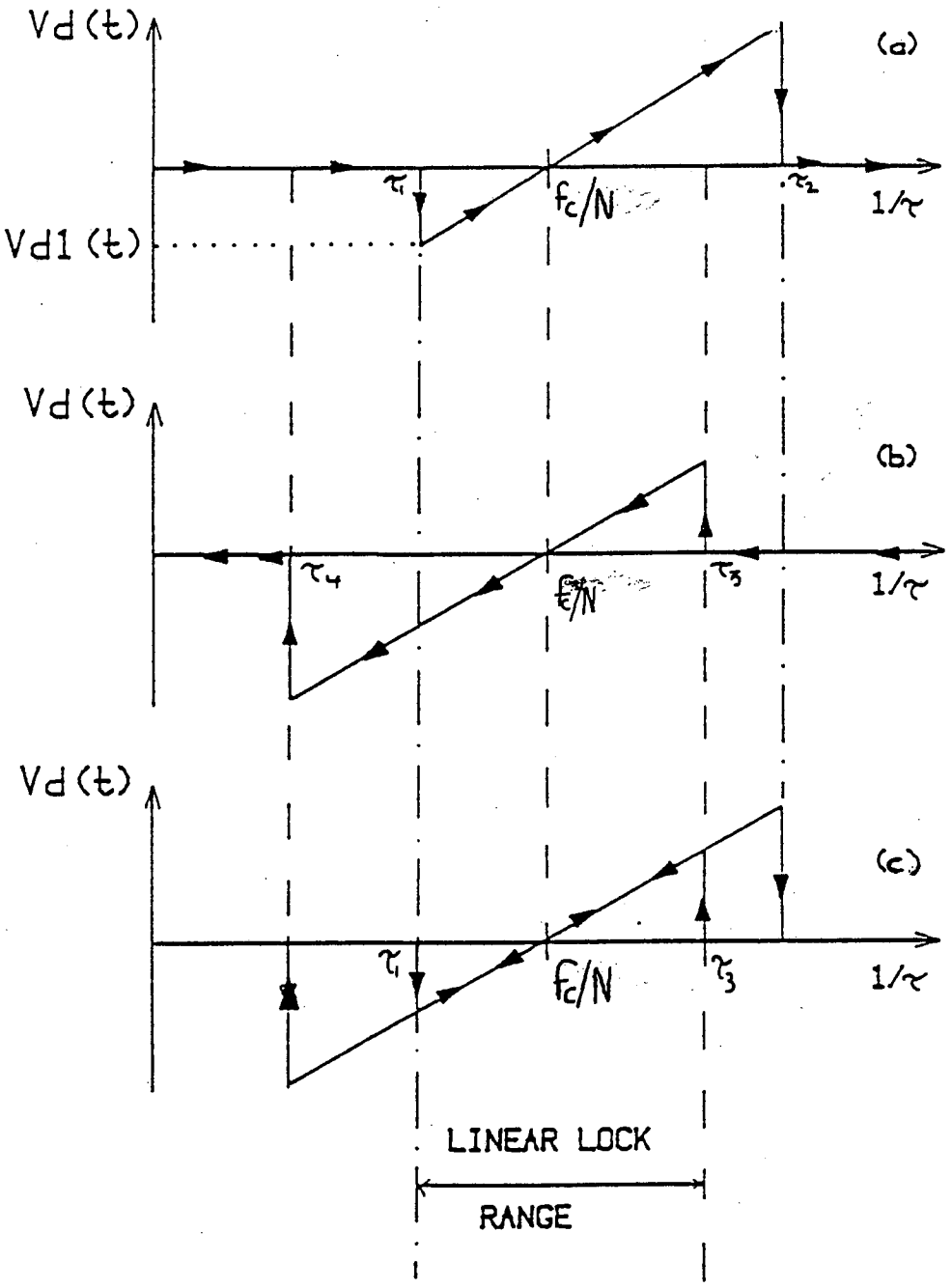

(a) The tracking range of the loop when the flow-rate is swept from left to right.

(b) The tracking range of the loop when the flow-rate is swept from right to left.

(c) The linear lock range of the loop.

Fig. 4-4 THE LINEAR LOCK RANGE OF THE LOOP.

4-4(a). Then the tracking loop loses the peak and remains in the out of lock mode. If the input signal time delay is increased slowly, the loop re-captures the peak of the correlation function, at τ_3 , and stays in the lock mode down to τ_4, as shown in figure 4-4(b). The linear lock range of the tracking loop is shown in figure 4-4(c). Experimentally it has been found that this range is smaller than the tracking range of the loop, and the peak of the correlation function can only be tracked linearly within this range, regardless of direction of the input signal time delay change.

The tracking loop operates by adjusting the delay shift register clock frequency to satisfy the condition given by:-

$$\left.\frac{dR_{yx}(\tau)}{d\tau}\right|_{\tau=\tau_p} = 0$$

When the tracking correlator is in the lock mode the output of the serial correlator shown in figure 4-2 is expected to indicate the amplitude of the peak of the correlation function. Hence the output of the serial correlator may be used as a test point to indicate the out of lock mode of the tracking correlator. In flow measurement situations the normalised peak amplitude of the correlation function is expected to reduce from 1 to .2 as the input signal time delay increases (Taylor Instrument Ltd. 1976). Therefore once the normalised output of the serial correlator is below .2, the tracking correlator is likely to be tracking a spurious peak, or indicating the no-flow situation.

If the length of the delay shift register of the tracking correlator is continuously being up-dated by the coarse correlators peak position estimates, the output of the tracking correlator is expected to exhibit a random fluctuation or jitter. This jitter will be exacerbated by the poor resolution of the coarse correlator. The output response jitter can be avoided by setting the length of the delay shift register through a coarse position latch operated by the logic control as shown in figure 4-2. The coarse position latch is disabled once the tracking correlator is in the lock mode and is tracking the peak of the correlation function. The coarse position latch is expected to be enabled only if the input signal time delay change is beyond the linear lock range of the negative feedback loop, and is large enough to cause the tracking loop to track a spurious peak, or to track the peak of the correlation function inaccurately.

The output of the serial correlator, shown in figure 4-2, may be used to control the coarse position latch, for example the coarse position latch can be enabled only if the output of the serial correlator is below some pre-set value. In flow measurement situations the output of the serial correlator is compared with the minimum expected normalised amplitude of the correlation function, e.g. if its normalised output is below .2 the coarse position latch is expected to be enabled. The block diagram of this arrangement is shown in figure 4-5.

To reduce the variance of the correlation function estimate by the serial correlator over an input signal bandwidth

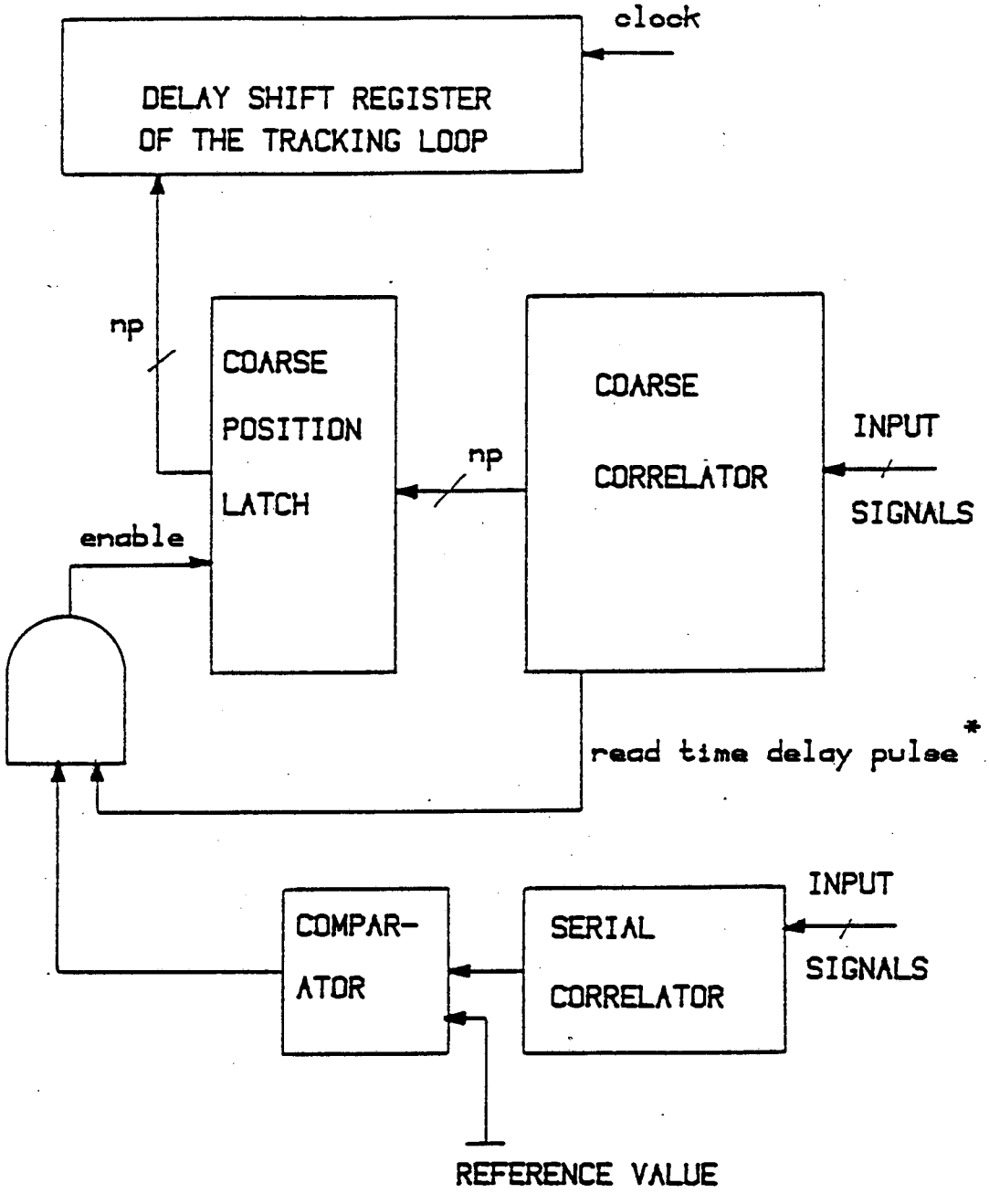

* The read time delay pulse is generated after a coarse estimate of the peak position of the correlation function.

Fig. 4-5THE BLOCK DIAGRAM OF THE ARRANGEMENT TO CONTROL THE COARSE POSITION LATCH BY THE SERIAL CORRELATORS OUTPUT.

of 50 to 500 Hz, its smoothing filters time constant is set to be equal to 10 seconds. The out of lock mode of the tracking correlator can be detected by the serial correlator after ts seconds. In the case of the simple exponential smoothing this time will be equal to 5 time constants if a settling bound of $\pm 1\%$ of the steady state value is accepted. Therefore if the serial correlator is used to control the coarse position latch its smoothing filters time constant will increase the total response time of the ICPT correlator. In the worst case an additional time must be allowed for the coarse correlator to find the new peak position.

Since the tracking and the linear lock range of the loop are not identical it is possible that the serial correlator used to control the coarse position latch could give a false indication of the amplitude of the correlation function being tracked by the negative feedback loop. Consider the situation when the negative feedback loop is tracking the peak of the correlation function at position ,τ_1,with a linear lock range of τ_A to τ_B , as shown in figure 4-6. If the input signal time delay is increased at a rate slower than the transient response of the tracking correlator, the peak of the correlation function will jump to the positions τ_2, , τ_3 and ,τ_4,from position ,τ_1, as shown in figure 4-6. As the correlation function peak position changes from τ_1 to τ_4, the normalised output of the serial correlator is expected to be above .2. For the situation described above and illustrated by figure 4-6 the coarse position latch will remain disabled and the tracking correlator will continue to track the peak of the

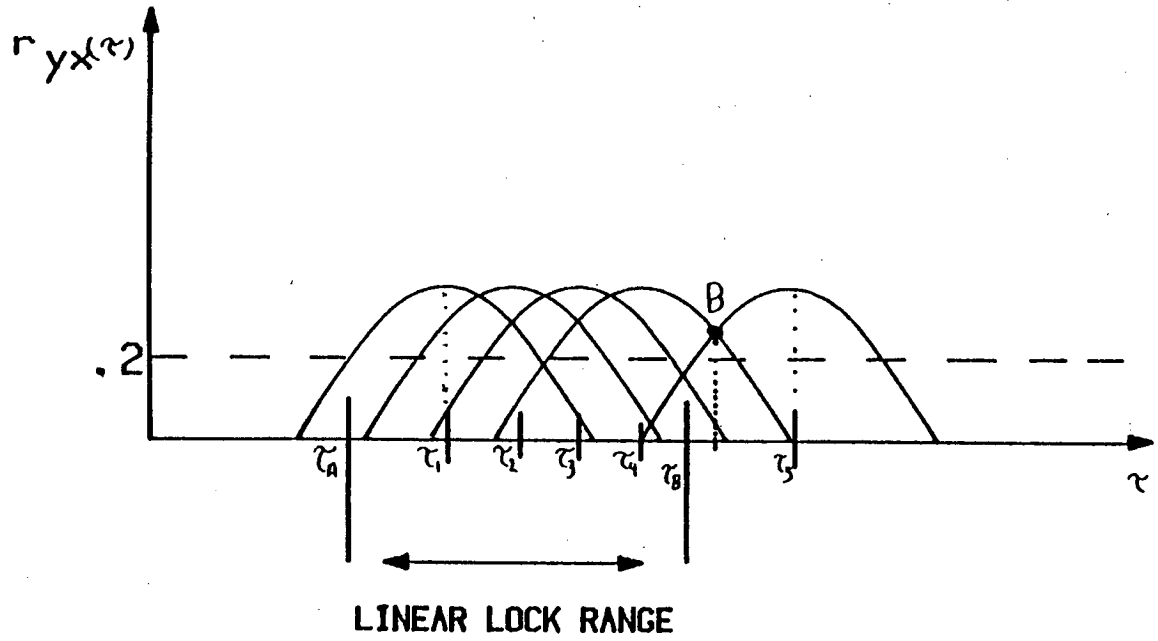

B=The output of the serial correlator when the peak of the function is at 5.

Fig. 4-6 The performance of the serial correlator.

correlation function.

For the linear operation of the ICPT correlator the coarse position latch is expected to be enabled if the peak of the correlation function jumps from position τ_4 to τ_5, i.e. where τ_5, shown in figure 4-6 is beyond the linear lock range of the negative feedback loop. But from figure 4-6 it is clear that when the position of the peak of the correlation function jumps from τ_4 to τ_5, the normalised output of the serial correlator will be above .2. Therefore the coarse position latch will remain disabled and the tracking correlators time delay estimate will be inaccurate.

Two serious problems associated with the use of the serial correlator to control the coarse position latch are summarised as below:-

1) The coarse position latch can not be controlled accurately by the serial correlators output.

2) The smoothing time constant of the serial correlator will increase the total response time of the ICPT correlator.

Therefore the penalty of using the output of the serial correlator to control the coarse position latch is high and this could lead to inaccurate estimation of time delays by the tracking correlator. Note that, the output of the serial correlator can be

used to indicate the out of lock mode of the negative feedback loop. In addition the serial correlators output can be used to indicate no-flow conditions.

The output of the window comparator shown in figure 4-2, has been used to control the coarse position latch, and experimentally it has been shown that this approach will eliminate the problems associated with the use of the output of the serial correlator for the same purpose. For the linear operation of the tracking loop over an input signal bandwidth of 50 to 500 Hz, the output voltage of its smoothing filter ,Vd(t), can only vary within a certain range, and this range is directly proportional to the linear lock range of the negative feedback loop. The upper and lower voltage limits of the window comparator ,Vh and Vl, are set to be equal to the maximum and minimum output voltage swing of the tracking loops smoothing filter,Vd(t), within its linear lock range, over an input signal bandwidth of 50 to 500 Hz. Therefore once the output of the tracking correlators smoothing filter,Vd(t), is beyond the given limits, the coarse position latch is expected to be enabled. The window comparators upper and lower limits, which is equal to the linear lock range of the loop is found experimentally in chapter 5. In addition, it has been shown that the upper and the lower limits of the window comparator can be predicted using the first order transfer function of the loop given by equation 4-6. Note that the upper and lower limits of the window comparator must be set in such a way that the tracking correlator can track at least the position of the peak of the correlation function, within the sample clock period of the

coarse correlator.

The performance of the ICPT correlator when the input signal time delay suddenly changes beyond the linear lock range of the loop, with the window comparator used to control the coarse position latch is explained with reference to figure 4-7. Consider the situation that the tracking correlator is tracking the peak of the correlation function at position τ_1, shown in figure 4-7 with a linear lock range of ($\tau_A - \tau_B$) over an input signal bandwidth of 50 to 500 Hz, and τ_1 is given by:-

$$\tau_1 = \frac{\tau_B - \tau_A}{2} \qquad (4-8)$$

If the position of the peak of the correlation function suddenly changes to ,τ_2, due to the negative feedback action of the loop, the smoothing filters output ,Vd(t), will be reduced in order to increase the delay line shift registers time delay, and to track the peak of the correlation function at ,τ_2, shown in figure 4-7. But, when the output of the tracking loops smoothing filter,Vd(t), is beyond the lower limit of the window comparator, which corresponds to τ_B shown in figure 4-7, the coarse position latch will be enabled and the new peak estimate of the correlation function will re-adjust the length of the time delay shift register. Therefore while the tracking correlator was increasing its delay line shift registers time delay, the new shift register length, will increases the input signal time delay of the tracking correlators multiplier further than the actual input signal time delay of the loop. The input signal time delay difference to the

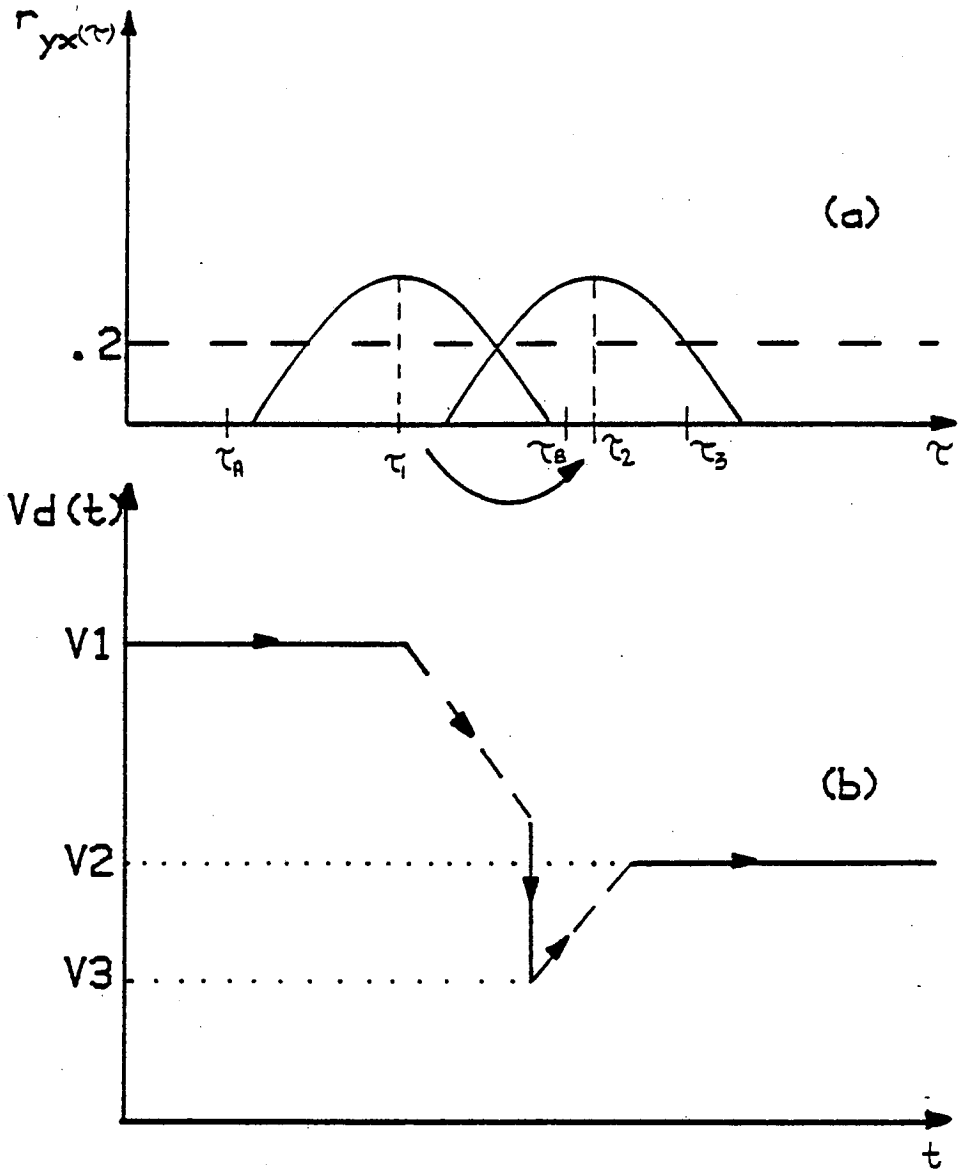

(a) The peak of the function at τ_1 and τ_2.

(b) The response of the error voltage Vd(t).
V1=The error voltage output at τ_1.
V2=The error voltage output at τ_2.
V3=The error voltage output at τ_3.

Fig. 4-7 THE STEP RESPONSE OF THE LOOP TO A NEW SHIFT REGISTER LENGTH.

multiplier of the loop will be equal to ,τ_3, as shown in figure 4-7. Hence due to the negative feedback action of the loop, the output of its smoothing filter ,Vd(t), will be increased, as shown in figure 4-7, in order to track the peak of the correlation function at ,τ_2.

If the input signal time delay suddenly changes within a large range (say larger than 10 to 1 range), the error voltage may remain within the upper and lower limits of the window comparator. Hence the coarse position latch will remain disabled and the loop will track a spurious peak. To avoid the above problem the output of the serial correlator shown in figure 4-2 is compared with a reference value equal to the normalised correlation function peak amplitude of .2, and if the normalised output of the serial correlator is below .2, the coarse position latch will be enabled. The block diagram of the arrangement used, is shown in figure 4-8. Note that when the tracking loop is tracking a spurious peak the normalised output of the serial correlator is below .2,and the coarse position latch can only be enabled by the output of the serial correlators comparator if the serial correlators output is below .2.

Therefore to avoid any possibility of tracking a spurious peak and to estimate the position of the peak of the correlation function linearly, the output of the window comparator together with the output of the serial correlators comparator are used to control the coarse position latch through a logic control shown in figure 4-8. The truth table of the logic control shown in

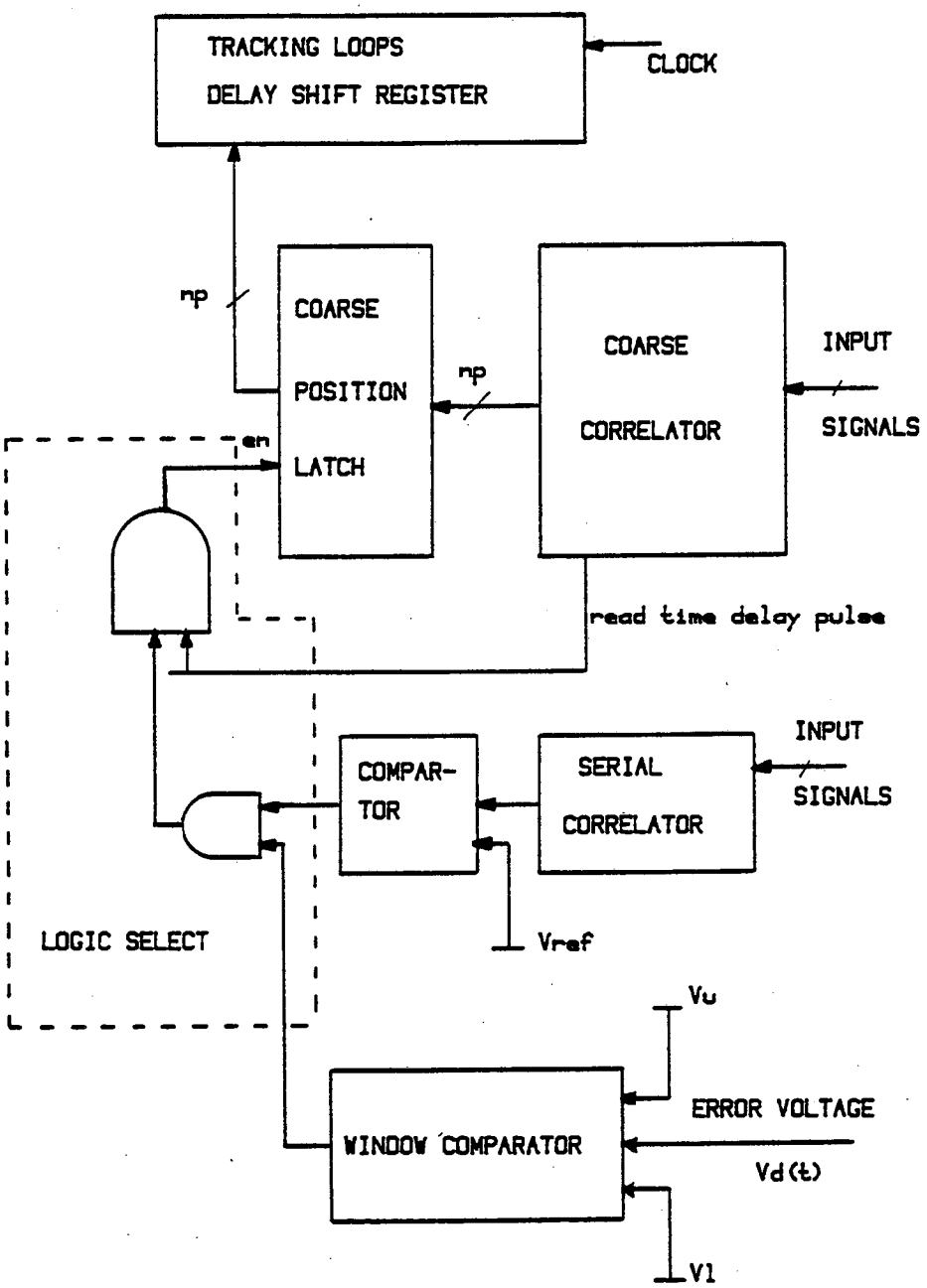

Fig. 4-8 THE BLOCK DIAGRAM OF THE COARSE POSITION LATCH CONTROL.

figure 4-8 is given in table 4-1. From table 4-1 it will be seen that the output of the serial correlators comparator can only enable the coarse position latch if the tracking loop is tracking a spurious peak.

WINDOW COMPARATORS OUTPUT	SERIAL CORRELATOR COMPARATORS OUTPUT	ENABLE PULSE TO THE COARSE POSITION LATCH
1 (lock mode)	1 (above .2)	0 (disabled)
0 (beyond its linear lock range)	1 (above .2)	1 (enabled)
1 (within its linear lock range)	0 (below .2)	1 (enabled)
0 (beyond its linear lock range)	0 (below .2)	1 (enabled)

Table 4-1 The truth table of the logic control.

It should be noted that the upper and lower limits of the window comparator is required to be set only once for a given flow velocity range,and the 6809 based coarse correlator can be programmed to estimate and to set the upper and lower limits of the window comparator for a range of flow rates to be measured using the first order transfer function of the loop given by equation 4-6. In addition the 6809 micro-processor based correlator can be programmed to enable the coarse position latch if a large input signal time delay change is detected, and this approach will eliminate the use of the serial correlators comparator output to control the coarse position latch.

4-3 ICPT Correlators Circuit Design

The circuit diagram of the peak tracking correlator is shown in figure 4-9. To obtain a first order differentiated correlation function with respect to delay time, the down-stream input signal to the tracking correlator is differentiated with respect to time, t. The coupling networks shown in figure 4-9, suggested by Jordan (1973), is used to obtain a first order differentiated correlation function with respect to delay time. The coupling networks shown in figure 4-9 are essentially formed from a high-pass and a low-pass filters with a transfer functions of Hd and Hu respectively and given by:-

$$Hd = \frac{S\tau_F}{1 + S\tau_F} \qquad (4\text{-}9)$$

and

$$Hu = \frac{1}{1 + S\tau_F} \qquad (4\text{-}10)$$

Where τ_F is the time constant of the high-pass and low-pass filters. Symmetrical differentiated correlation function with respect to delay time is obtained, if the coupling networks cut-off frequencies are set to be equal.

Experimentally the optimum performance of the tracking correlator over an input signal bandwidth of 50 to 500 Hz was obtained when the -3dB cut-off frequency of both filters are set to 49.7 Hz, with a buffer amplifier bandwidth of 100 KHz. An HP

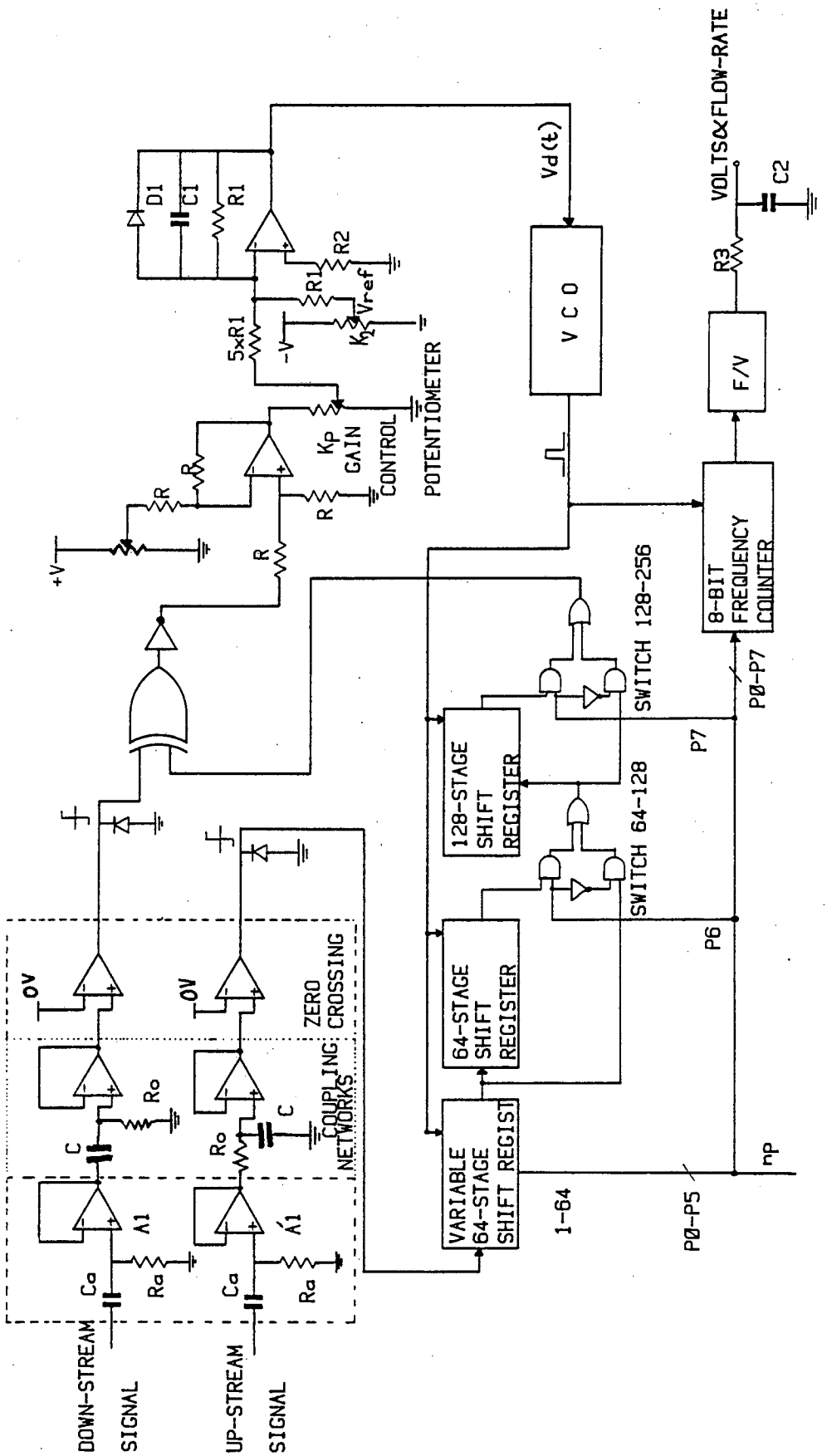

Fig. 4-9 THE CIRCUIT DIAGRAM OF THE TRACKING CORRELATOR.

3721A correlation computer (1968) was used to measure the first order differentiated correlation function shown in figure 4-10. If the time constants of the coupling networks are not identical, the differentiated correlation function will be unsymmetrical as shown in figure 4-11. The 3dB cut-off frequency of the AC-coupling unity gain amplifiers A1,A'1, shown in figure 4-9, are set to be equal to 1 Hz.

A 256 stage digital shift register is used as a controllable delay line for the up-stream input signal channel. The length of the variable delay shift register shown in figure 4-9 can be varied from 0 to 255 by eight control lines.

The TTL logic levels of the exclusive-NOR gate are converted to ± 2 volts using the level shifter shown in figure 4-9. The gain control potentiometer shown in figure 4-9 is used to control the voltage levels of the error signal, Ve(t). The output of the gain control potentiometer with the reference voltage, Vref, used to set the free-running frequency of the VCO, is fed into the input terminal of the smoothing filter shown in figure 4-9.

The output of the VCO shown in figure 4-9 is calibrated to operate over a frequency range of .1 to 25 KHz, with a full scale input voltage of 0 to 10 volts. Since the operating input voltage of the VCO is within 0 to 10 volts the smoothing filters output is limited to operated over a range of -.7 to + 9.8 volts ,using a zener diode shown in figure 4-9 across the capacitor C1.

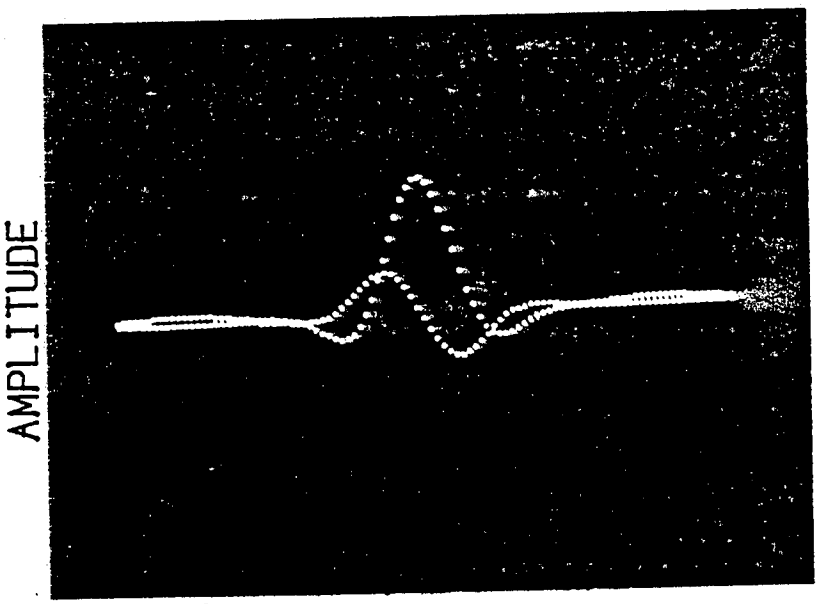

Fig. 4-10 CORRELATION AND ITS DIFFERENTIATED FUNCTION.

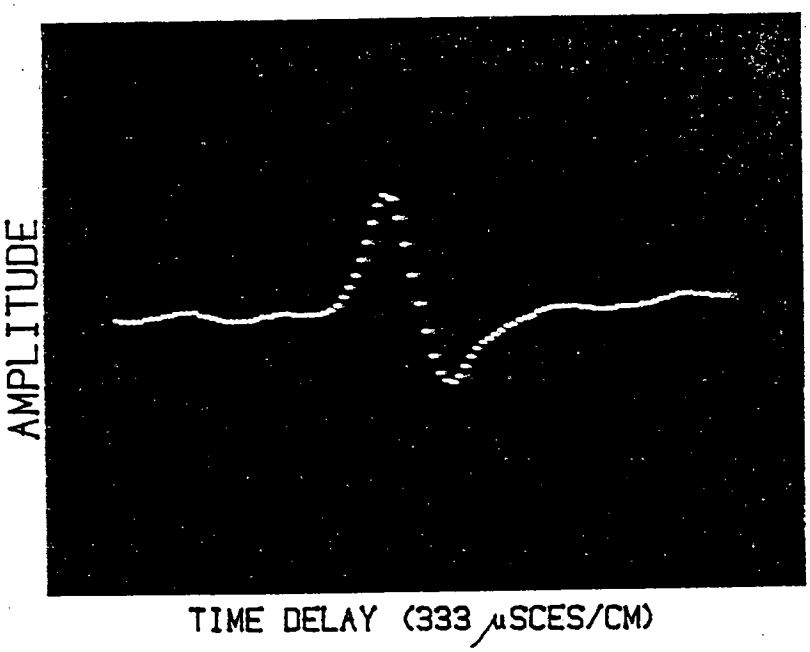

Fig. 4-11 UNSYMMETRICAL DIFFERENTIATED CORRELATION FUNCTION.

Therefore once the ICPT correlator is switched on the output of the smoothing filter will not rise to a large negative voltage.

The free-running VCO frequency can be adjusted through the potentiometer, K2, shown in figure 4-9. The reference voltage, Vref, is set to be equal to approximately -2 volts, with the free-running frequency of 4882 Hz. Therefore the smoothing filters output, Vd(t), can swing the output frequency of the VCO over a 5 to 1 range in either direction, with reference to the free-running frequency. It is important to note that, the free-running frequency of the VCO was estimated using equation 4-1, and the sampling frequency of the coarse correlators are determined from the required time delay range of the ICPT correlator, (i.e 1.64 to 52.48 msecs).

An 8 bit variable modulus counter shown in figure 4-9 is used to divide the output frequency of the VCO by the tracking correlators delay shift register length, np. The output frequency of the variable modulus counter is proportional to the flow velocity, and was converted to an equivalent voltage by using the frequency to voltage convertor shown in figure 4-9. A smoothing filter of 2 seconds time constant is used on the output of the frequency to voltage convertor shown in figure 4-9.

The circuit diagram of the serial correlator together with the window comparator and the logic control, described in section 4-2 are shown in figure 4-12. Note that the output of the tracking loops smoothing filter, Vd(t), is fed to the input

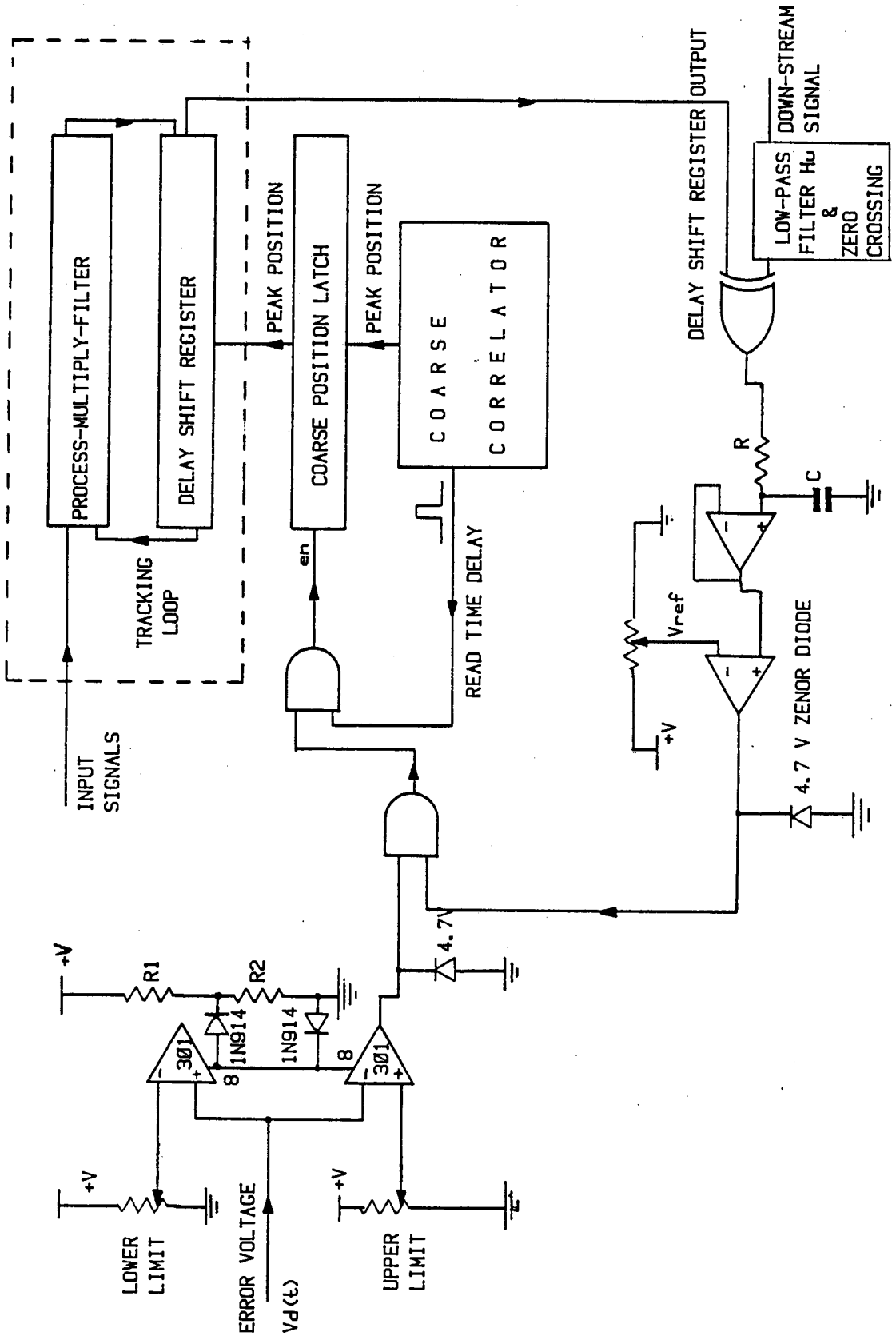

Fig. 4-12 THE CIRCUIT DIAGRAM OF THE COARSE POSITION LATCH CONTROL.

terminal of the window comparator. The upper and lower limits of the window comparator are set to be equal to the linear lock range of the tracking correlator over an input signal bandwidth of 50 to 500 Hz, and experimentally , they have been found to be equal to 2.50 and 1.75 volts respectively.

4-4 Coarse Correlators

A digital correlator which provides a coarse estimate of the peak position to constrain the tracking loop to track the peak of the correlation function will be referred to as a coarse correlator. The resolution of the coarse correlator is poor and its sample clock period must be equal or less than the linear lock range of the tracking correlator over a specified input signal bandwidth range. Although the resolution of the coarse correlator is poor, the variance of its peak position estimate is required to be low.

Two digital coarse correlators have been considered for use with the tracking correlator described in section 4-2. The coarse correlators considered are:-

i) A TRW TDC1004J based polarity correlator. (The TRW device is a 64 stage polarity correlator).

ii) A 6809 based polarity correlator.

A single chip TDC1004J based correlator requires additional peak finding circuitry and an analogue to digital convertor. Four TRW TDC1004J correlators were connected in series in order to estimate 256 correlation coefficients over an input signal time delay range of 32 to 1, with ±6.25% resolution. From the required time delay range to be measured by the ICPT correlator, (i.e. 1.64 to 52.48 msecs), the sampling frequency of the TDC1004J based coarse correlator was set to 4882 Hz. When the normalised peak amplitude of the correlation function is about .2, with the input signal bandwidth of 50 Hz the percentage repeatability of the peak position estimate is approximately equal to 100%. Hence due to its short measurement time (52.4 ms) the variance of the peak position estimate is high.

The micro-computer based correlator can estimate 128 correlation coefficients to cover a 32 to 1 time delay range with a worst case resolution of ±12.5%, over an input signal bandwidth of 50 to 500 Hz. From the required time delay range to be measured by the ICPT correlator the sampling frequency of the micro-computer correlator was set to be equal to 2441 Hz. The variance of the peak position estimate can be reduced by increasing its measurement time. The maximum percentage repeatability of the micro-computer based correlator with measurement time of one second is approximately equal to 30% .

4-4-1 The TRW TDC1004J Based Correlator

The basic principle of operation of the TRW TDC1004J

correlator is described in section 2-2-6 of chapter 2. When the polarity input signals are serially shifted into the two independently clocked shift registers A and B, the current output of the TDC1004J correlator is proportional to the estimate of the correlation function coefficients. The block diagram of the coarse correlator based on the single chip TDC1004J correlator is shown in figure 4-13. To achieve $\pm$6.25% resolution over a 32 to 1 range, four TDC1004J correlators are connected in series and their current outputs are summed together.

The method chosen to achieve the necessary delay is to periodically stop the shift register B while data is continuously being clocked to the shift register A. With register B stopped the sum of the current outputs of the four serially connected correlators with each successive clock pulses to register A represents the degree of correlation between the down-stream signal $y(t)$ and the increasingly delayed up-stream signal $x(t-\tau)$ held in register B. for example with register B stopped the first clock pulse to register A estimates the degree of correlation between $x(t-1)$ and $y(t)$.

Since the correlation function can only be estimated when the register B is filled with the polarity up-stream data, another four packages of the TDC1004J correlators are connected in series to estimate the correlation function while the register B of the other correlators are being filled. The analogue multiplexer shown in figure 4-13 is used to select the summed output of the correlators which are estimating the coefficients of

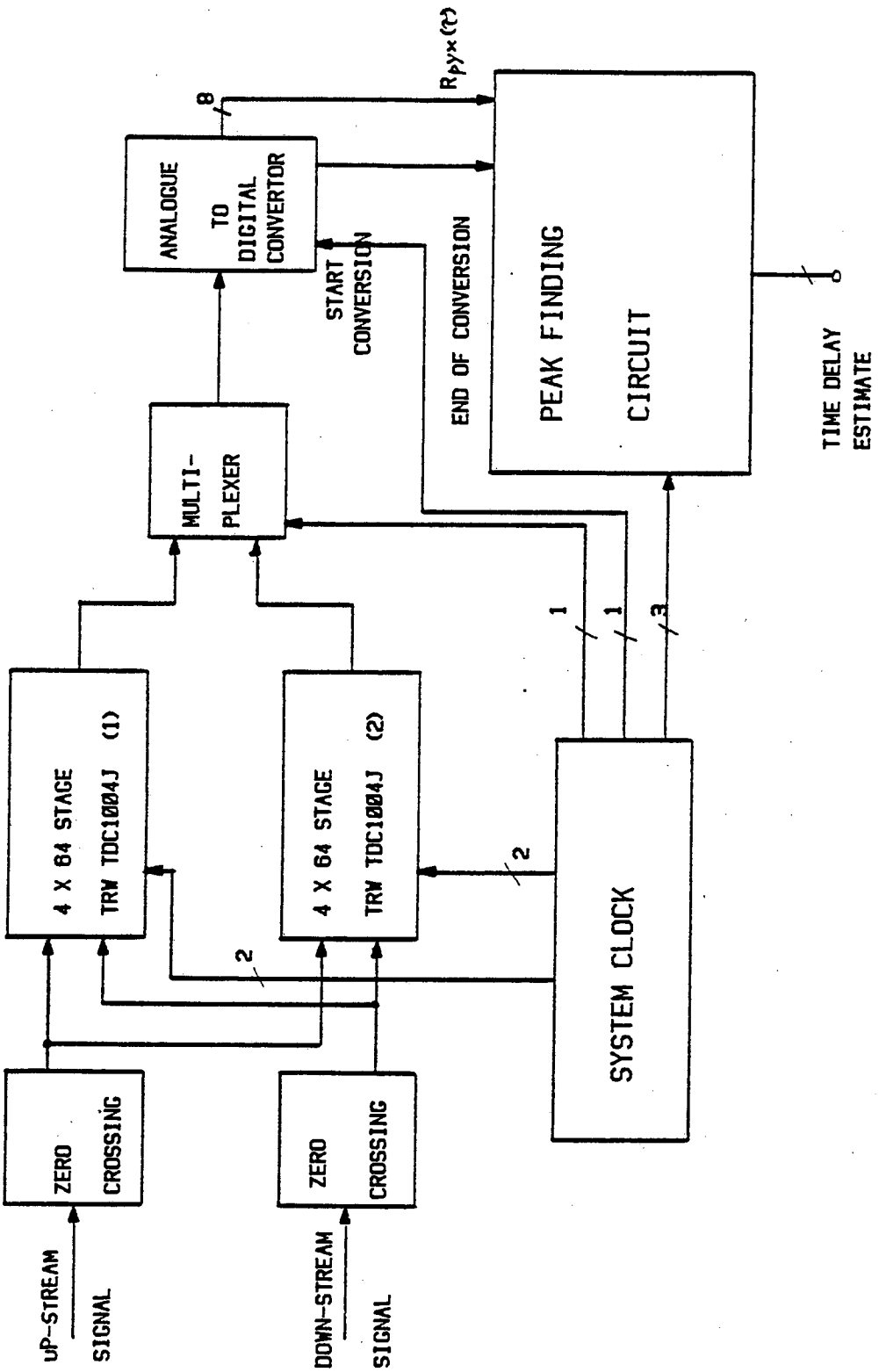

Fig. 4-13 THE BLOCK DIAGRAM OF THE TRW TDC1004J CORRELATOR.

the correlation function. The timing diagram of the TRW TDC1004J based coarse correlator is shown in Figure 4-14. From the requiered time delay range to be measured by the ICPT correlator, (1.64 to 52.48 msecs), the sampling frequency of the TDC1004J based correlator is set to 4882 Hz.

The block diagram of the peak finding circuitry based on the method described by Hayes and Musgrave (1973) is shown in figure 4-15. Each 8-bit digital value of the correlation function coefficients is compared with the highest already found value in buffer-store A, shown in figure 4-15, and the largest of two is stored in buffer-store A. At the same time the corresponding delay value is read into the buffer-store B shown in figure 4-15. To synchronise the peak finding circuit with the sample clock period of the correlators an "end of conversion" pulse generated by the analogue to digital convertor together with the comparator output are used to enable the buffer-stores A and B, shown in figure 4-15. The "read time delay" pulse shown in figure 4-14 is used to transfer the content of the buffer-store B into the buffer-store C. An 8-bit digital word stored in buffer-store C represents the position of the peak of the correlation function. The read time delay pulse is followed by the "counter clear" pulse, shown in figure 4-14, was used to clear the content of the counter for the next estimate of the correlation function peak position.

The output of the buffer-store C which represents the position of the peak of the correlation function is used to set

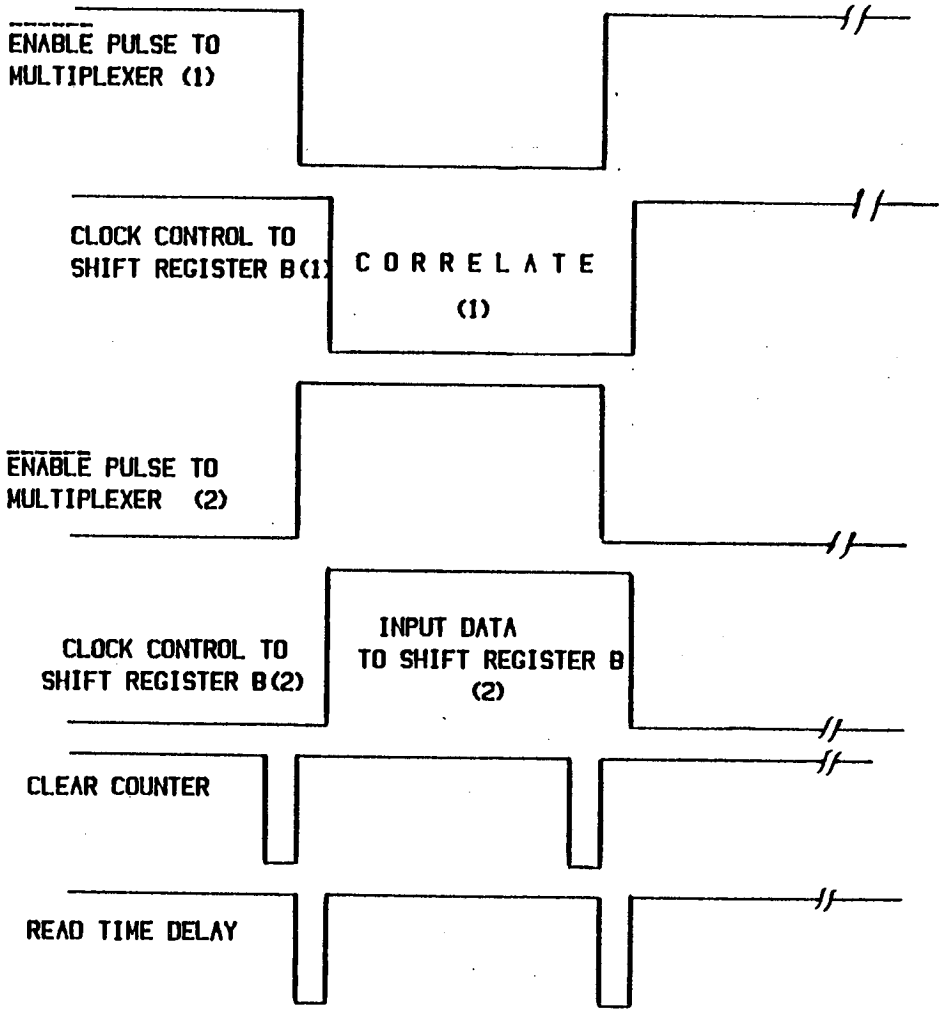

Fig. 4-14 TIMMING DIAGRAM OF THE TRW TDC1004J BASED CORRELATOR.

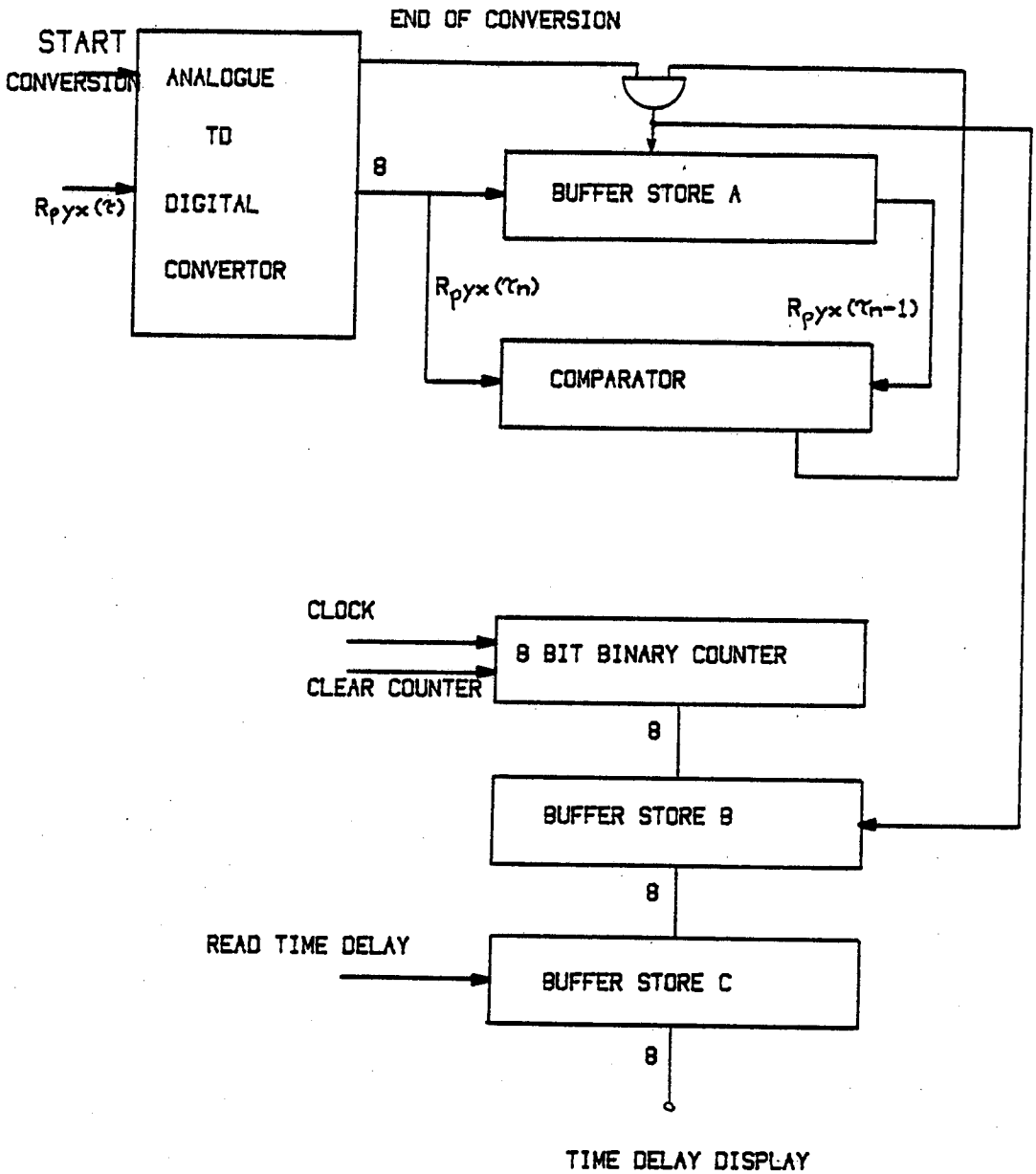

Fig. 4-15 THE BLOCK DIAGRAM OF THE PEAK POSITION DISPLAY.

the length of the delay shift register of the tracking correlator through the coarse position latch.

4-4-2 Micro-computer Based Correlator

A block diagram of the 6809 micro-computer based correlator is shown in figure 4-16. The polarity correlation function is computed, using the skip algorithm described by Fell (1982), over a 32 to 1 time delay range with $\pm$12.5% resolution and with a maximum measurement time of 1 second. The main function of the micro-computer is the computation of the correlation function coefficients using equation 2-10 of chapter 2, and indication of the peak position of the correlation function.

Additional hardware used for the micro-computer based coarse correlator are, two packages of 8 stage shift register, two packages of mono-stables, one package of 4-bit binary counter and one package of D Type flip-flop. The polarity signals generated for the TRW TDC1004J based correlator are used for the 6809 based correlator. The delayed version of the up-stream input signal is obtained using a 16 stage serial input, parallel output shift register shown in figure 4-16. To synchronise the micro-computers computation cycle with the polarity input signals sampling rate, two hardware interrupts of the 6809 micro-processor, IRQ and FIRQ are used. The mono-stables shown in figure 4-16 are used to generate interrupt pulses IRQ and FIRQ, and are triggered by the sampling clock period of the up-stream and down-stream input signals respectively. Using the above arrangement the polarity of the down-stream signal is read into the micro-computer at its

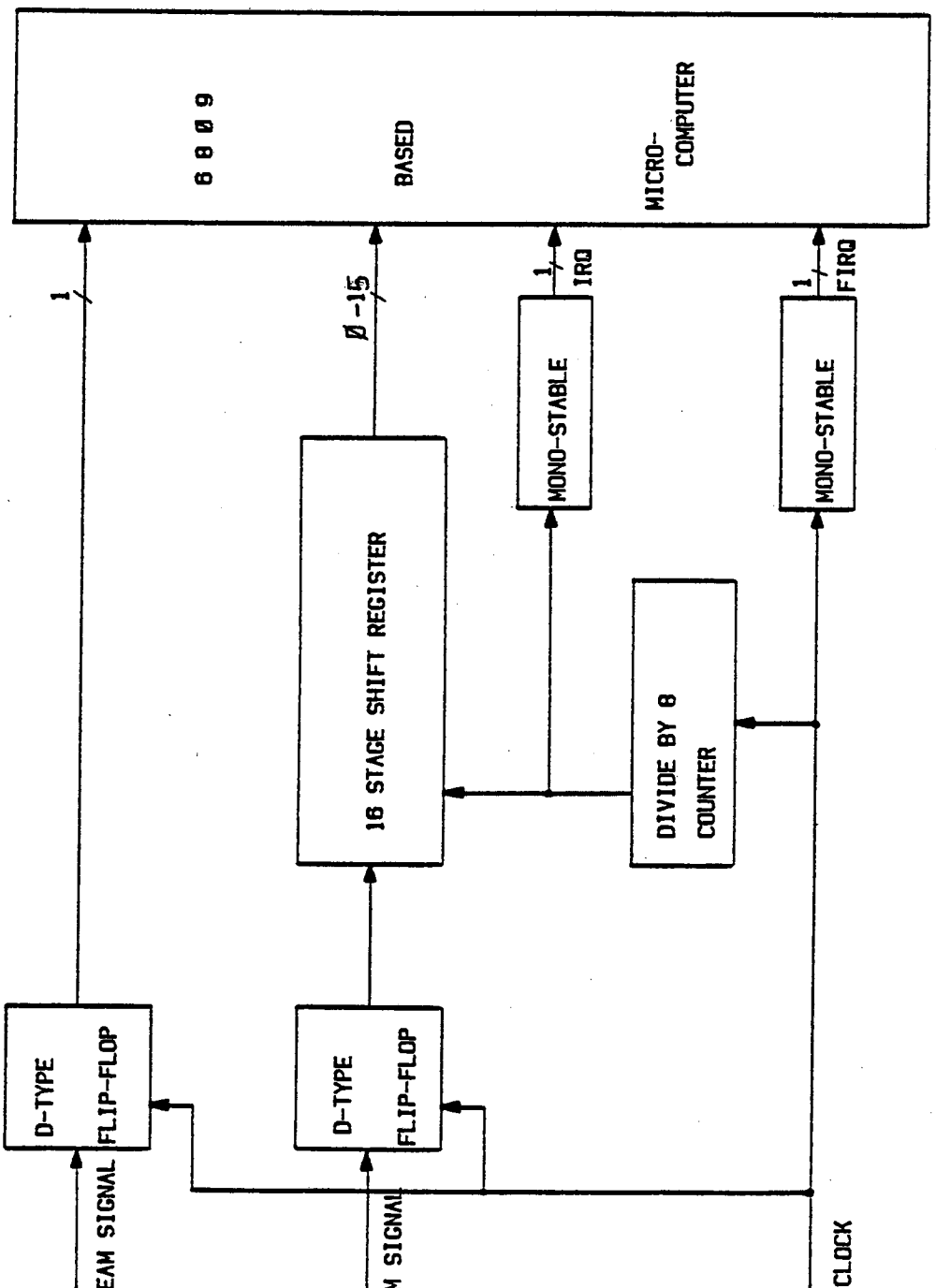

Fig. 4-16 THE BLOCK DIAGRAM OF THE 6809 BASED CORRELATOR.

sampling rate, and the content of the 16 stage shift register is read by the 6809 micro-computer at the sampling rate of the up-stream signal to the shift register.

The time delay range over which the correlation function coefficients are estimated is given by:-

$$0 \leqslant \text{Time delay range} \leqslant K\Delta T \qquad (4\text{-}11)$$

where:-

K is equal to the length of the shift register stages used, i.e. 16.

and

ΔT is the sample clock period of the up-stream polarity signal.

ΔT is related to the sample clock period of the down-stream signal $\Delta\tau$, and is given by:-

$$\Delta T = M\Delta\tau \qquad (4\text{-}12)$$

Where $\Delta\tau$ is set to be equal to the down-stream input signal sampling rate, and from the required time delay range, M determines the ratio of the input signals sampling periods. Substituting equation 4-12 into the equation 4-11 we have:-

$$0 \leqslant \text{Time delay range} \leqslant K.M.\Delta\tau \qquad (4\text{-}13)$$

To compute 128 correlation function coefficients with K equal to 16, from equation 4-13, M is found to be equal to 8. Hence 128 lagged values of the correlation function coefficients are computed by multiplying 8 samples of the polarity down-stream input signal with the 16 samples of the up-stream input signal.

Since the coarse estimate of the correlation function peak position was used to set the delay shift register length of the tracking correlator, from the required time delay range of the ICPT correlator, (i.e. 1.64 to 52.48 msecs), the sampling period of the down stream signal , $\Delta\tau$, was set to be equal to 2441 Hz. The flowchart of the program developed to compute 128 coefficients of the correlation function is shown in figure 4-17. It is important to note that, regardless of the normalised correlation function peak amplitude the correlation function coefficients are estimated over a 256 coincidences, and each coefficient is stored in an 8-bit RAM. The maximum measurement time of the 6809 based coarse correlator with the above settings is found to be equal to .85 seconds.

The peak estimate of the micro-computer correlator is multiplied by 2 to allow the delay shift register length of the tracking correlator to be set with any even number between 2 to 256. The worst case computation time to find the peak of the correlation function and multiply by 2 is equal to .05 seconds. Hence the maximum total measurement time of the 6809 based correlator is equal to .90 seconds. An assembled listing of the program used to estimate and find the peak of the correlation

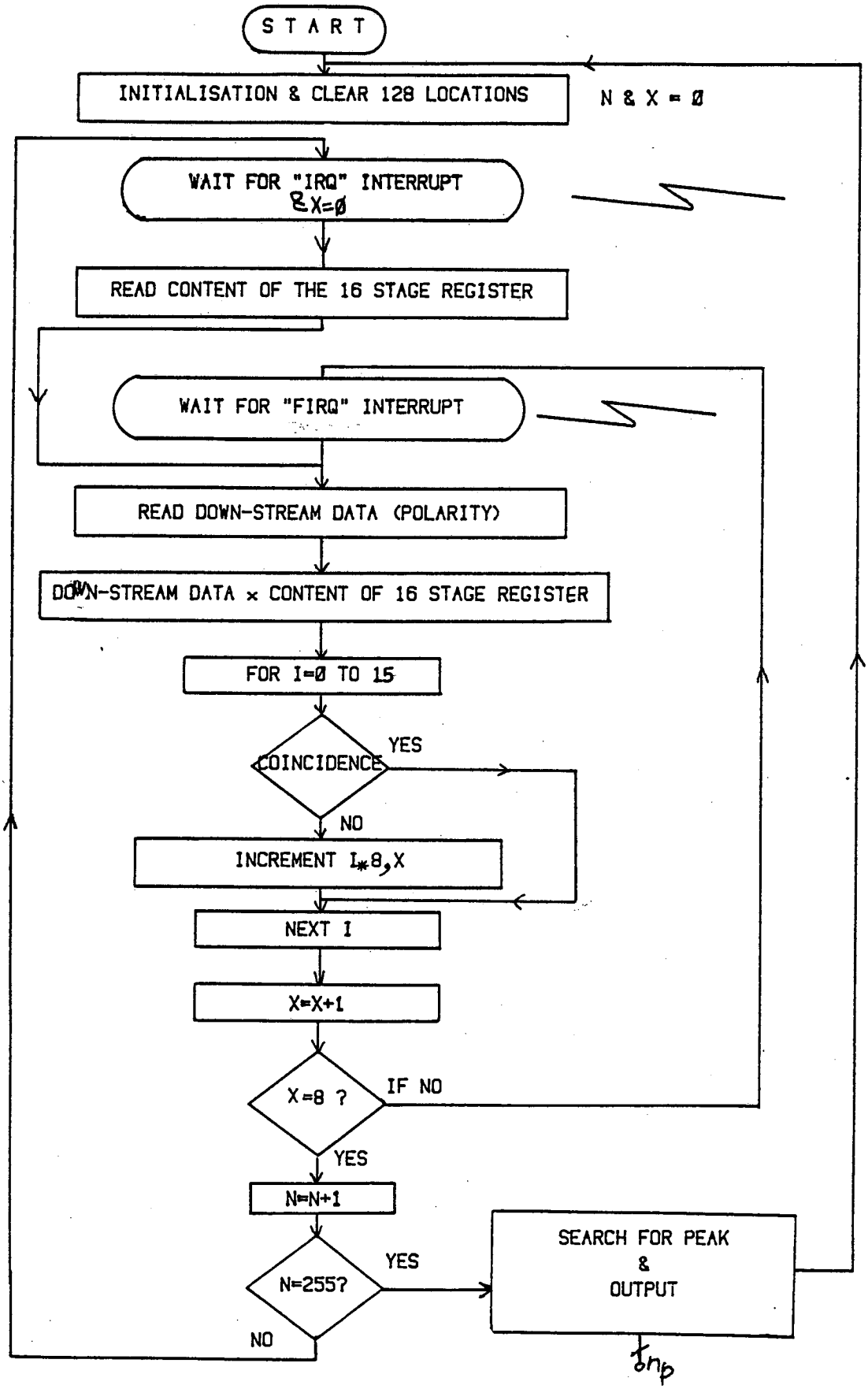

Fig. 4-17 THE FLOWCHART OF THE 6809 BASED CORRELATOR.

function is given in Appendix 3. Since the measurement time and the variance of the correlation function estimate was found to be adequate for coarse indication of the peak position to the tracking correlator, the program was not optimised any further.

4-5 Experimental System

The block diagram of the experimental system designed to explore the performance of the ICPT correlator and the coarse correlators is shown in figure 4-18. The 6809 based micro-computer with 8 K-byte of RAM and 16 K-byte of ROM is used to compute a coarse estimation of the correlation function as well as controlling the communication of the experimental system through the IEEE bus interface with the experiment controller (HP-85 computer) . The IEEE bus interface circuit design is based on the MC68488 general purpose adapter.

2 K-byte of software in machine code was developed to perform all the required communications through the IEEE bus interface between the HP-85 computer and the experimental system. Therefore all the parameters of the coarse correlators for example, sampling rate, integration time are set by a HP-85 computer. In addition the estimated correlation function coefficients by the coarse correlators are sent by the experimental system through the IEEE bus interface to the HP-85 computer for further investigations. Note that additional 1K byte of RAM shown in figure 4-18 was used as a buffer to store the estimated correlation function coefficients of the TRW TDC1004J

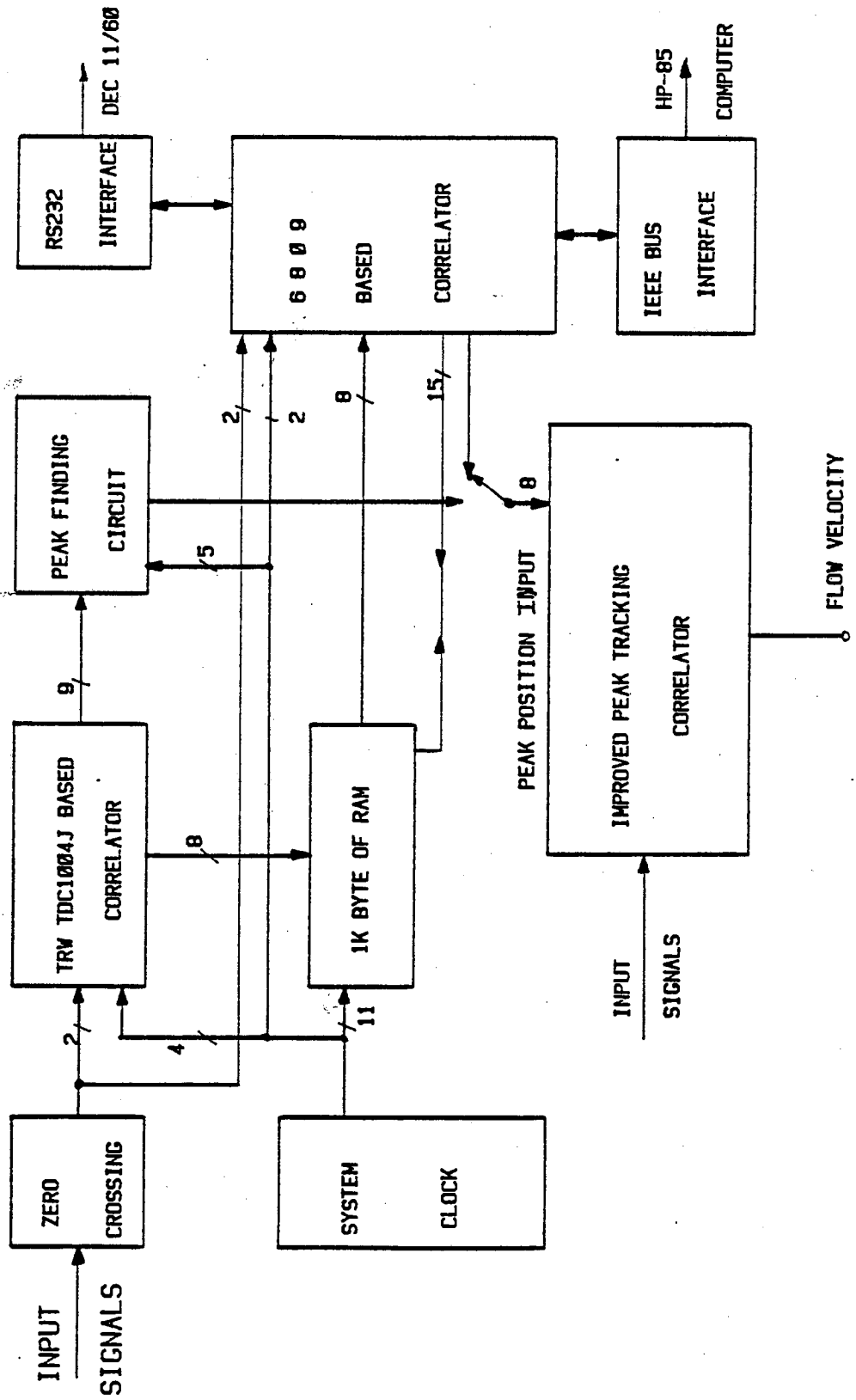

Fig. 4-18 THE BLOCK DIAGRAM OF THE EXPERIMENTAL SYSTEM.

based coarse correlator at its sample clock period before sending them to the HP-85 computer.

The assembled software developed for the 6809 based micro-computer is down loaded from the main frame DEC 11 computer through the RS232 interface circuit shown in figure 4-18. The final version of the software was stored in an EPROM.

CHAPTER 5: PERFORMANCE OF THE "ICPT" CORRELATOR.

5-1 Introduction

The performance of the ICPT correlator was investigated using signals derived from the flow noise simulator described in Chapter 3. The major sources of errors which influences the accuracy of the correlation flow-meter have been discussed in Section 2-3 and the experimental performance of the ICPT correlator is described in this chapter. Since the flow noise simulator was used to investigate the performance of the ICPT correlator the errors due to flow noise transducer systems will not be considered.

Experiments to illustrate the performance of the ICPT correlator have been divided into two categories:-

i) Dynamic tests

ii) Static tests

The dynamic tests, for example small signal step response and linear lock range, were carried out over an input signal bandwidth of 50 to 500 Hz, and a time delay range of 32 to 1. Industrial experience (Taylor Instrument Ltd. 1976), has shown that in order to achieve $\pm 1\%$ accuracy the measurement time of the coarsely quantised time delay axis correlation flow-meters, is required to be of the order of 2 to 20 seconds over an input signal bandwidth of 50 to 500 Hz.

The dynamic performance of the correlation flow-meter under changing (i.e. non-stationary) signal condition is of great importance and although this is one of the major factors which affects the accuracy of the correlation flow-meter it has received very little attention. A detailed experimental investigation of the performance of the improved constrained peak tracking correlator under changing input signal conditions indicates that this correlator can be designed to offer an industrially acceptable performance.

The repeatability and the resolution of the ICPT correlator has been obtained under static signal conditions. The scatter of the measurements around an average value is described by the repeatability function and is given by:-

$$\% \text{ Repeatability} = \frac{2 \times \text{Standard Deviation}}{\text{Mean Value}} \times 100 \quad (5\text{-}1)$$

The ICPT correlator described in chapter 4 and shown in block diagram from in figure 5-1, is essentially made up of three correlators operating in parallel:-

a) A digital correlator, providing a coarse indication of the peak position (this will be referred to as the coarse correlator).

and

b) A peak tracking correlator, which is free to track the peak of the correlation function, once its delay shift register length is being set by the coarse correlators peak

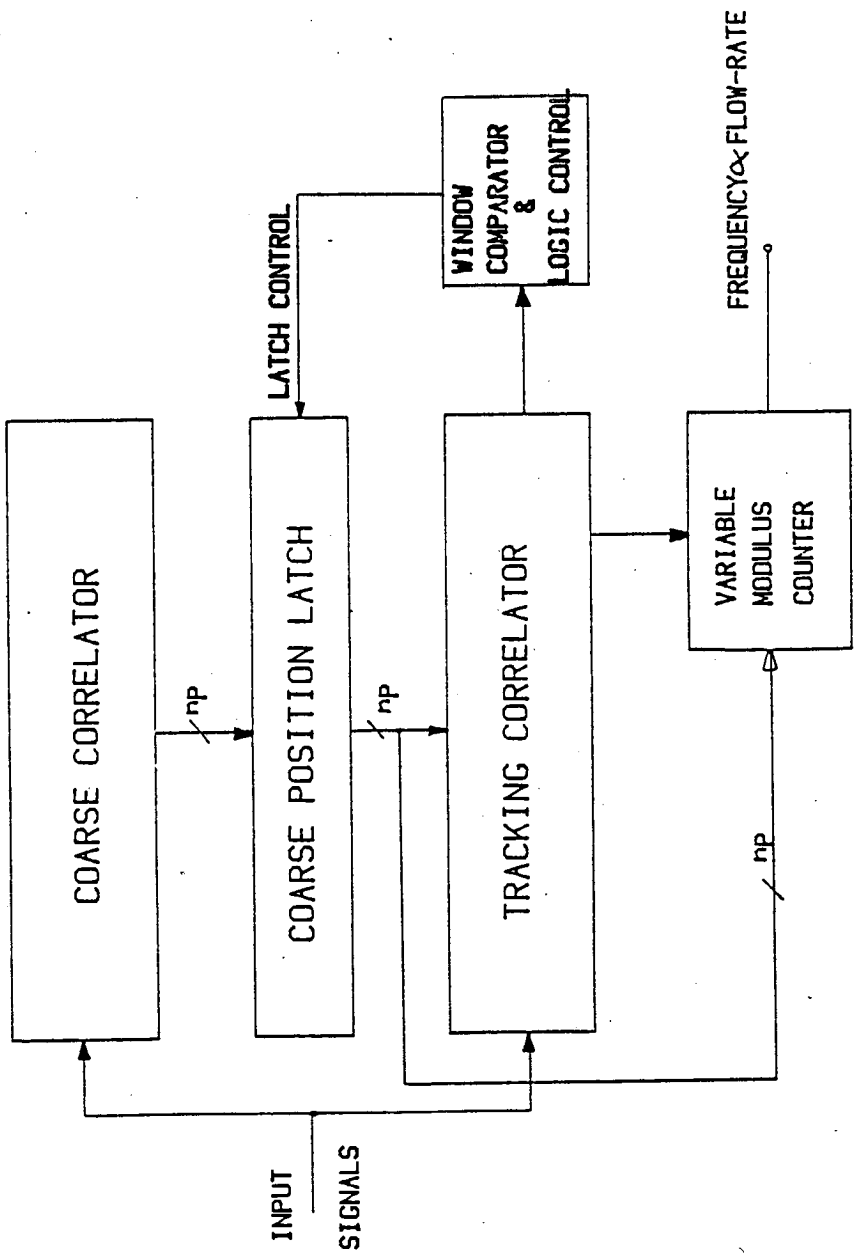

Fig. 5-1 THE BLOCK DIAGRAM OF THE "ICPT" CORRELATOR.

position estimate.

c) A serial correlator, which is used to indicate the out of lock mode of the tracking loop.

In addition to the overall performance of the ICPT correlator, the performance of the tracking correlator as well as the coarse correlators are given individually.

A simplified block diagram of the experimental set-up is shown in figure 5-2. The majority of the equipment used is connected through the IEEE bus interface to an HP-85 computer, which operates as the master experiment controller. Extensive software in BASIC (i.e for the HP-85 computer) and in assembly language for the 6809 based micro-computer of the noise simulator and the correlators has been developed to enable the experiments to be operated under the control of the HP-85 computer. Hence different parameters of the noise simulator, and coarse correlators are set through the IEEE bus interface by the HP-85 computer. In addition results from the correlators, transient recorder, digital voltmeters and the logic analyser shown in figure 5-2 are collected and stored in magnetic tape by the HP-85 computer. It should be noted that the programmability of the noise simulator has lead to the collection of repeatable results, and in addition repetitive and time consuming experiments have been carried out automatically and accurately under the complete control of the HP-85 computer.

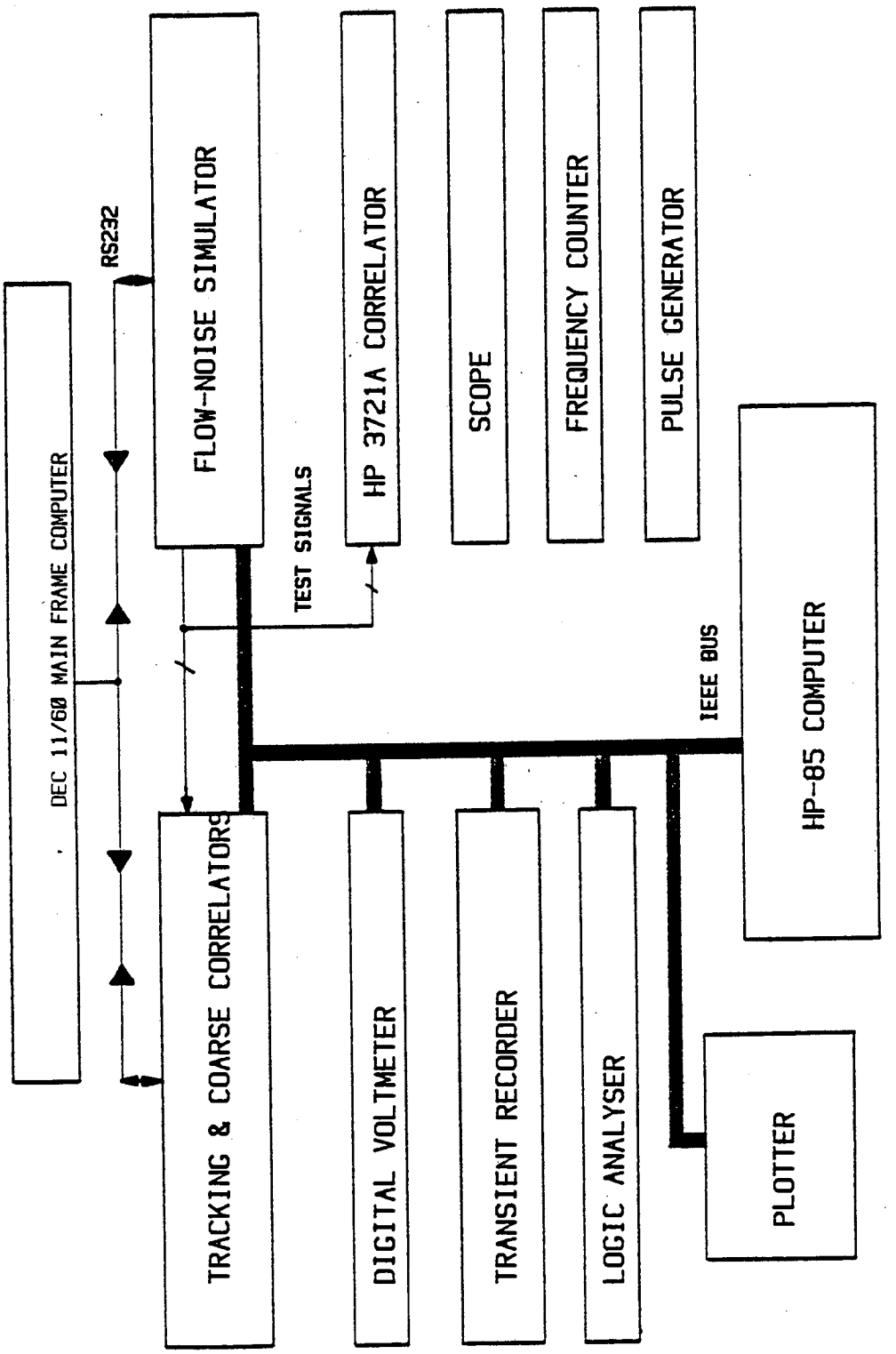

Fig.5-2 THE BLOCK DIAGRAM OF THE MEASUREMENT SYSTEM.

5-2 Performance of the Tracking Correlator

The principle of operation and detailed circuit diagram of the tracking correlator has been given in chapter 4. To determine the performance of the tracking loop, tests have been carried out using simulated noise signals with a symmetrical Gaussian shaped correlation function over a input signal bandwidth of 50 to 500 Hz. The coarse position latch shown in figure 5-1 is permanently disabled and the length of the delay shift register is set manually. To ensure the accurate setting of the delay shift register length, the logic analyser shown in figure 5-2 is used to read the delay shift register length of the tracking correlator at the sample clock period of the tracking correlator.

A block diagram of the tracking correlator and the test points used to monitor the dynamic and the static performance of the tracking correlator is shown in figure 5-3(a). A Burr-Brown VFC-32 voltage to frequency convertor is used in the tracking loop. The calibrated operating range of the VCO is shown in figure 5-3(b). The output of the serial correlator described in chapter 4 is used as an additional test point and its performance when the negative feedback loop is in the lock and un-lock mode is given.

To optimise the dynamic performance of the tracking loop experiments have been carried out to indicate its linear lock range over an input signal bandwidth of 50 to 500 Hz, with different negative feedback loop parameters. In addition static tests have been carried out to indicate the resolution of the

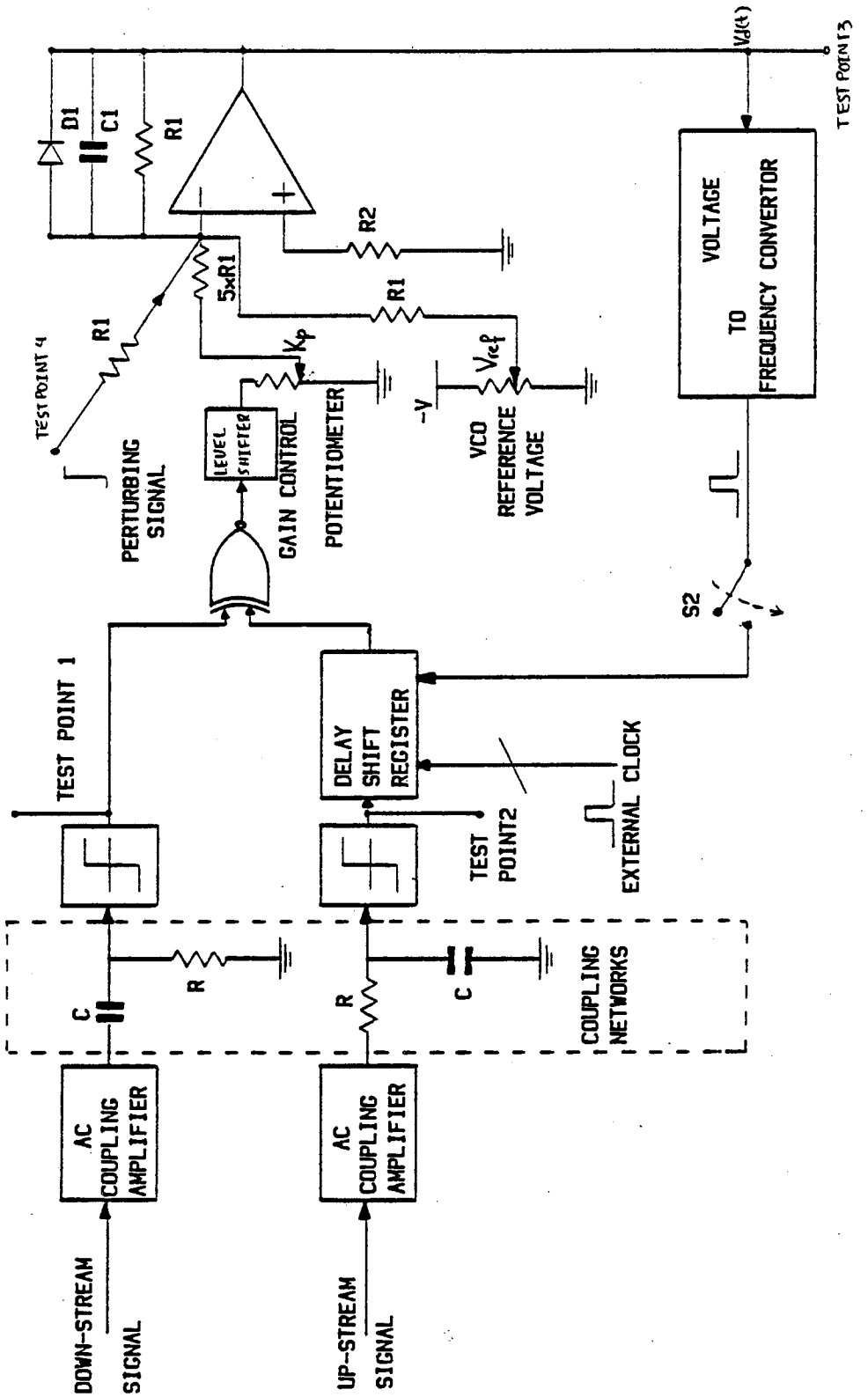

Fig. 5-3(a) EXPERIMENTAL TRACKING LOOP

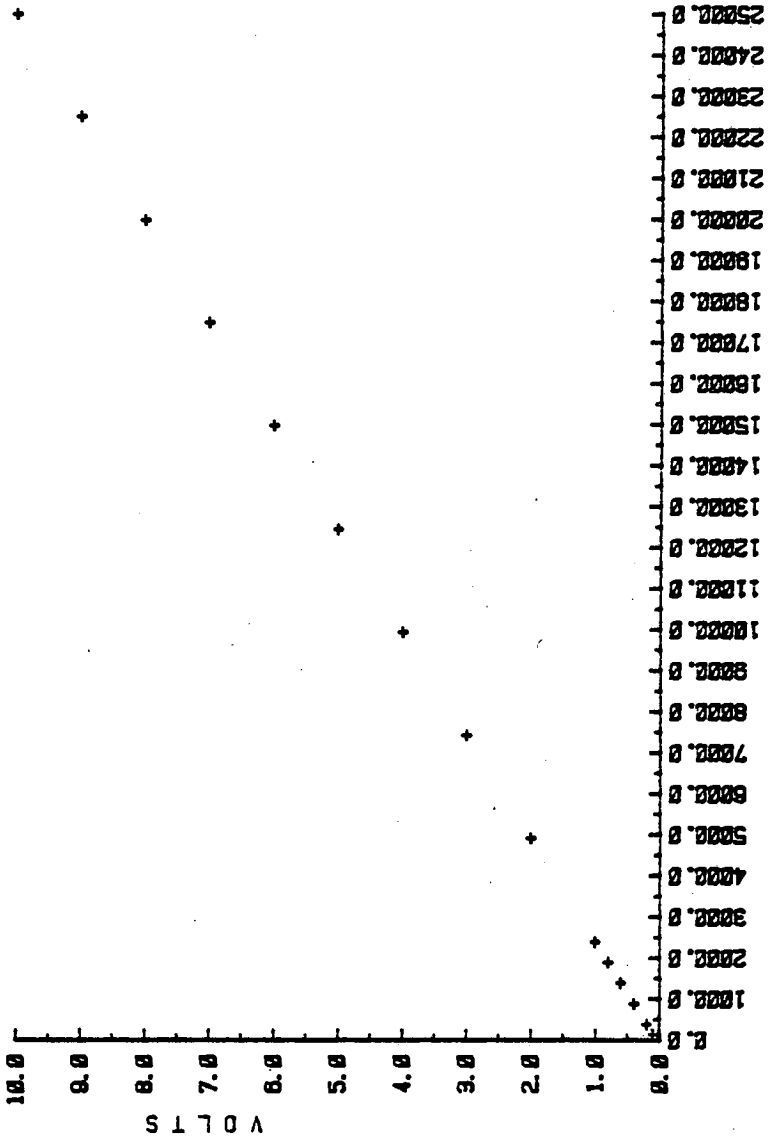

5-3b) CALIBRATED RANGE OF THE FREQUENCY TO VOLTAGE CONVERTOR.

tracking correlator.

5-2-1 Dynamic Performance of the Tracking Correlator

Various measurement techniques have been used to monitor the dynamic performance of the negative feedback loop controlling the tracking error. This is achieved by monitoring the output of the smoothing filter, Vd(t), shown in figure 5-3(a). Note that the output of the smoothing filter, Vd(t) (error voltage), is directly proportional to the output frequency of the VCO.

To determine the optimum performance of the tracking correlator, experiments have been designed to illustrate the effect of constraints imposed by the practical realisation of the tracking correlator as well as the physical nature of the flow noise signal. It should be remembered that the delay shift register length is kept constant during the tracking loop experiments.

The experimental programme is divided into three parts. First the step response characteristic of the tracking loop as defined by its first order transfer function and given by the equation 4-6 is considered. Second the computed and recorded step response characteristic of the loop to input signal time delay change is compared. Finally , the dynamic performance of the loop under changing signal condition is described by sweeping the input signal time delay beyond the linear lock range of the tracking loop.

From the closed loop transfer function, H(S), of the tracking correlator described in chapter 4 and given by the equation 4-6 , it is clear that the closed loop time constant of the tracking correlator to an input signal step change, is inversely proportional to the slope of the differentiated correlation function (polarity), Kd, overall gain of the tracking correlator, the delay shift register length, np, and is directly proportional to the time constant of the smoothing filter, τ.

A Hewlett-Packard HP-3721A correlation computer (1968), was used to investigate the slope of the differentiated correlation function (polarity) around the operating region of the loop, by cross-correlating the output signals taken from test points 1 and 2 shown in figure 5-3(a). The input signal bandwidth was set to be equal to 250 Hz with the normalised correlation function peak amplitude of 1. Figure 5-4 describes how the slope of the differentiated correlation function (polarity) changes with different coupling networks cut-off frequencies. From figure 5-4 it will be seen that as the coupling networks cut-off frequency reduces, the slope of the differentiated correlation function (polarity) decreases. From the equation 4-6 of chapter 4 the closed loop time constant of the tracking loop is inversely proportional to the slope of the differentiated correlation function (polarity), Kd. Therefore the closed loop time constant of the tracking correlator is expected to increase as the coupling network cut-off frequency decreases.

On the other hand for a coupling networks cut-off

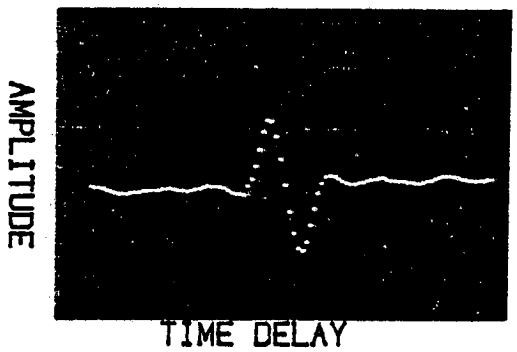

(a) COUPLING NETWORKS CUT-OFF FREQUENCY OF 723 Hz.

TIME SCALE .333 ms/cm.

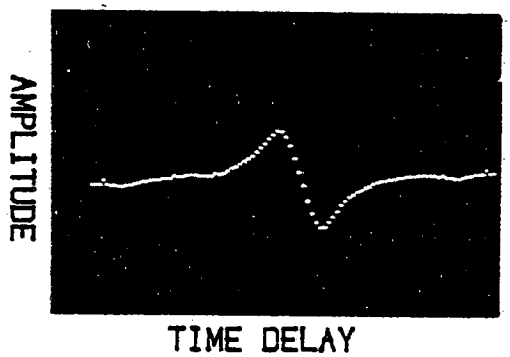

(b) COUPLING NETWORKS CUT-OFF FREQUENCY OF 49.7 Hz.

TIME SCALE .333 ms/cm.

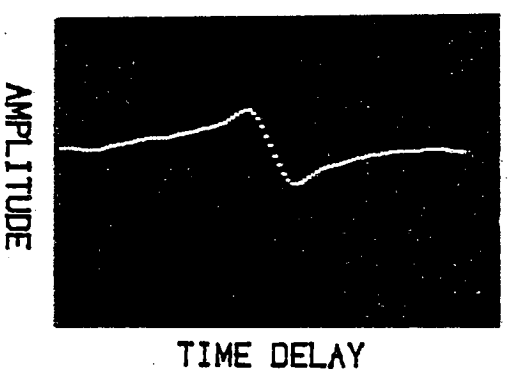

(c) COUPLING NETWORKS CUT-OFF FREQUENCY OF 10 Hz.

TIME SCALE .333 ms/cm.

Fig.5-4 First order differentiated correlation function (polarity) with the input signal bandwidth of 250 Hz.

frequency of 49.7 Hz, the slope of the differentiated correlation function (polarity) decreases as the input signal bandwidth decreases as shown in figure 5-5. Hence from equation 4-6 of chapter 4 the closed loop time constant of the tracking correlator is expected to increase as the input signal bandwidth decreases.

Additional experiments have been designed to investigate the step response characteristic of the tracking correlator over an input signal bandwidth of 50 to 500 Hz with different slopes of the differentiated correlation function (polarity), Kd, as well as different delay shift register length, np, and gain control potentiometer settings, Kp. To indicate the effect of the above parameters on the performance of the tracking correlator the switch S2 is closed and a external square wave signal is applied to the input terminal of the smoothing filter through a test point 4 shown in figure 5-3(a). Since the output frequency of the VCO is directly proportional to the flow-velocity, the effect of the square wave signal applied to the test point 4 when the loop is in the lock mode, is equivalent to perturbing the error voltage, Vd(t), or the flow velocity over a certain range, i.e. this forces the loop away from its lock mode. Therefore the negative feedback loop will track the peak of the correlation function only if it is capable of cancelling the effect of the external voltage applied to it by the voltage levels of the perturbing square wave signal. The period of the perturbing square wave signal is chosen to be above the time that is required by the tracking correlator to settle within the tolerance band of $\pm 1\%$, and its amplitude is set to perturbe the error voltage, Vd(t), within its linear lock

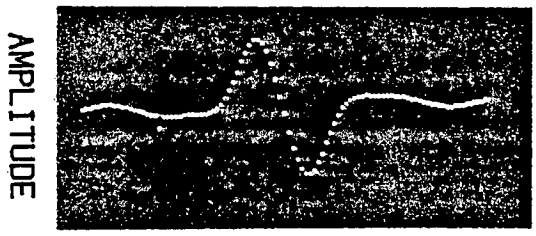

(a) INPUT SIGNAL BANDWIDTH OF 50 Hz.
TIME SCALE 1 ms/cm.

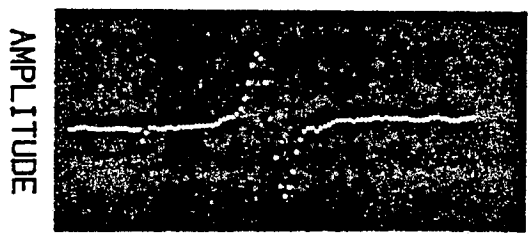

(b) INPUT SIGNAL BANDWIDTH OF 125 Hz.
TIME SCALE 1 ms/cm.

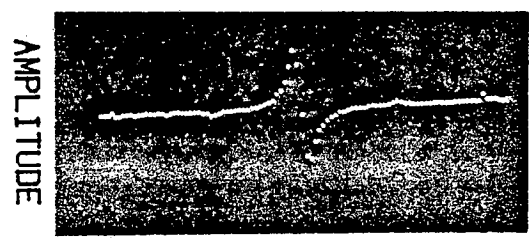

(c) INPUT SIGNAL BANDWIDTH OF 250 Hz.
TIME SCALE 1 ms/cm.

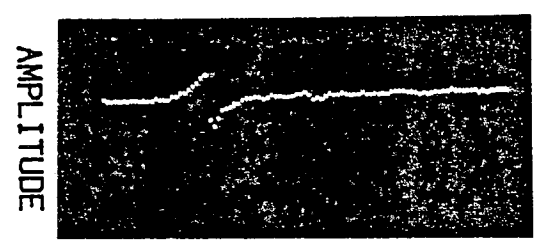

(d) INPUT SIGNAL BANDWIDTH OF 500 Hz.
TIME SCALE 1 ms/cm.

Fig.5-5 First order differentiated correlation function (polarity) with the coupling networks cut-off frequency of 49.7 Hz.

range. The two channel transient recorder with 4K byte memory space shown in figure 5-2 was used to sample and store the output of the error voltage, Vd(t), together with the perturbing square wave signal at a sample clock period of 50 msecs, to give a sampling window of 50x2048 (102.4) seconds for each channel. Note that for the results shown in this section, the amplitude of the perturbing square wave signal is not scaled.

The simplified linearised model of the tracking loop with the external perturbing square wave signal is shown in figure 5-6. The system shown in figure 5-6 is considered to be linear, when the tracking loop is in the lock mode, the amplitude of the external signal ,D1, is small and is perturbing the error voltage Vd(t) within its linear lock range. Therefore with the above assumptions the transfer function of the system between the external perturbing signal ,D1, and the output of the smoothing filter, and the transfer function of the system between the input signal time delay and the smoothing filters output was derived.
From figure 5-6, we have:-

$$E1(S)=td(S) + \Delta Vd(S).(Ko.np/fc^2) \qquad (5\text{-}2)$$

Where E1=The error signal, and ΔVd is equal to small error voltage change.

and,

$$\Delta Vd(s)= - F(S).E2(S) \qquad (5\text{-}3)$$

Where:-

$$\Delta Vd(S) = - F(S) [KD.E1(S) + D1(S)] \qquad (5\text{-}4)$$

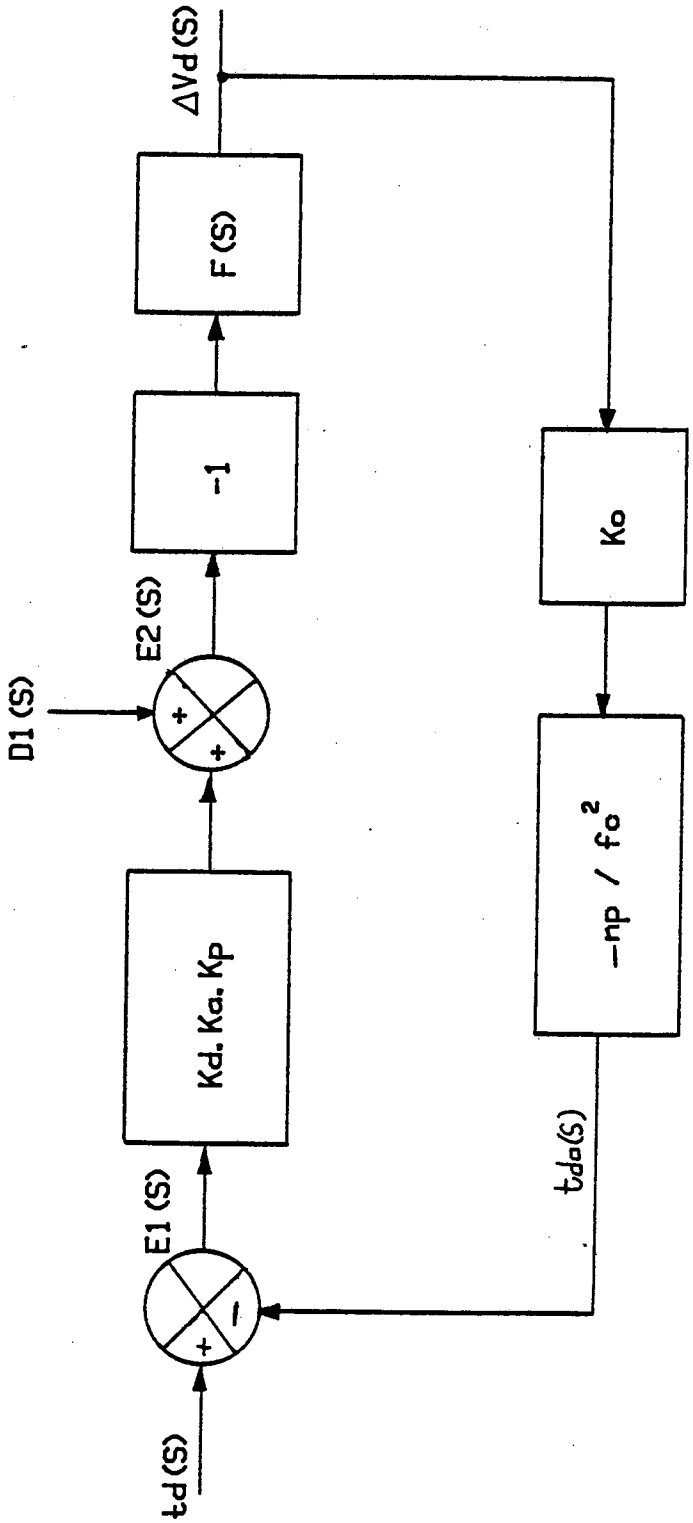

Fig. 5-6 THE LINEARISED MODEL OF THE LOOP WITH THE EXTERNAL PERTURBING SIGNAL.

Where:-

$$KD = Kd.Ka.Kp \qquad \text{volts/secs} \qquad (5\text{-}5)$$

Therefore:-

$$\Delta Vd(S) = -F(S)\ \{\ KD\ [td(S) + \frac{\Delta Vd(S).Ko.np}{fc^2}\ ] + D1(S)\}\quad (5\text{-}6)$$

Hence:-

$$\Delta Vd(S) = \frac{-F(S).KD.td(S)}{1+\frac{F(S).KD.Ko.np}{fc^2}} - \frac{F(S).D1(S)}{1+\frac{F(S).KD.Ko.np}{fc^2}} \qquad (5\text{-}7)$$

From equation 5-7 the transfer function of the system ,H´(S), between the external perturbing square wave signal ,D1, and the output of the smoothing filter, ΔVd, is given by:-

$$H'(S) = \frac{\Delta Vd(S)}{D1(S)} = \frac{-F(S)}{1 + \frac{F(S).KD.Ko.np}{fc^2}} \qquad (5\text{-}8)$$

By applying the final value theorem for the case when the input is unit step function, steady state error is given by:-

$$\text{Steady state error} = \lim_{t\to\infty} \Delta Vd(t) = \frac{-fc^2.D1}{fc^2 + KD.Ko.np} \qquad (5\text{-}9)$$

Where D1 is equal to the peak to peak voltage amplitude of the perturbing square wave signal.

Equation (5-8) and (5-9) are used to compute the step response characteristic of the loop as well as the output voltage variation, (i.e. steady state error), of the smoothing filter. The computed results are compared with the experimental results, when the external perturbing square wave signal is applied to the tracking loop shown in figure 5-6. The peak to peak amplitude of the perturbing square wave signal is set to 1.5 volts,with the signal amplitude of +1 to -.5 volts. The magnitude of the KD term around the operating point of the tracking correlator was found from the open loop slope of the differentiated correlation function (polarity) at the output of the smoothing filter for a given input signal bandwidth and coupling networks cut-off frequency. The gain of the VCO ,Ko, is estimated from the slope of the VCO within its operating range shown in figure 3(b), and fc is is equal to the output frequency of the VCO when the loop is in the lock mode.

To plot and estimate the open loop slope of the differentiated correlation function (polarity) shown in figure 5-7 and 5-8, the switch, S2, shown in figure 5-2 is opened and the clock frequency of the delay shift register is set to be equal to the free-running frequency of the VCO (i.e. 4882 Hz) using an external clock generator, with a fixed delay shift register length, np. The HP-85 computer is programmed to increment the input signal time delay to the tracking correlator at equal steps. After each time delay increment the output of the smoothing filter is taken from the digital voltmeter (DVM) by the HP-85 computer and is plotted against the time delay increments of the noise

simulator. Time interval between each increment was equal to 120 seconds. For the results shown in figure 5-7 and 5-8, the smoothing filters time constant is 11.4 seconds, and the error signal Ve(t) amplitude is set by the gain control potentiometer to its maximum value (i.e. ± 2 volts). Figure 5-7 describes the differentiated correlation function (polarity) with coupling networks cut-off frequencies of 49.7 and 10 Hz, and input signal bandwidth of 250 Hz. The differentiated correlation function (polarity) with input signal bandwidth of 50 and 500 Hz, and coupling networks cut-off frequency of 49.7 Hz is shown in figure 5-8. From figure 5-7 and 5-8 the slopes of the differentiated correlation function (polarity) around the operating point of the tracking loop is computed using the auto-regression standard package of the HP-85 computer (1981) and the results are given in table 5-1.

Slope V/secs	Input signal bandwidth,Hz	Coupling networks cut-off frequency,Hz	From figure
-7837.86	500	49.7	5-8(a)
-4929.63	250	49.7	5-7(b)
-3388.47	250	10.0	5-7(a)
-2118.04	50	49.7	5-8(b)

Table 5-1: The slope of the differentiated correlation function (polarity) with different input signal bandwidth.

To plot the output of the serial correlator, shown in figure 5-9, the above procedure is repeated but instead the output of the serial correlator with a time constant of 10 seconds is monitored and plotted by the HP-85 computer.

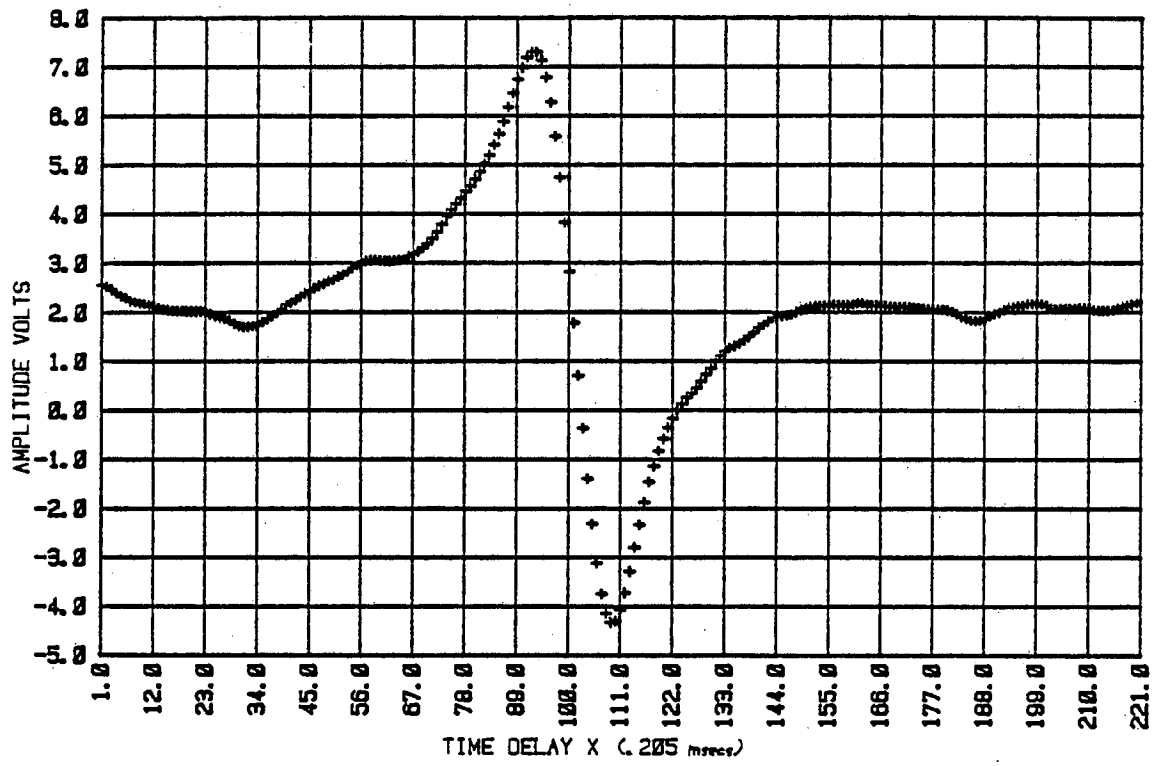

(a) THE COUPLING NETWORKS CUT-OFF FREQUENCY=49.7 Hz.
INPUT SIGNAL BANDWIDTH=250Hz

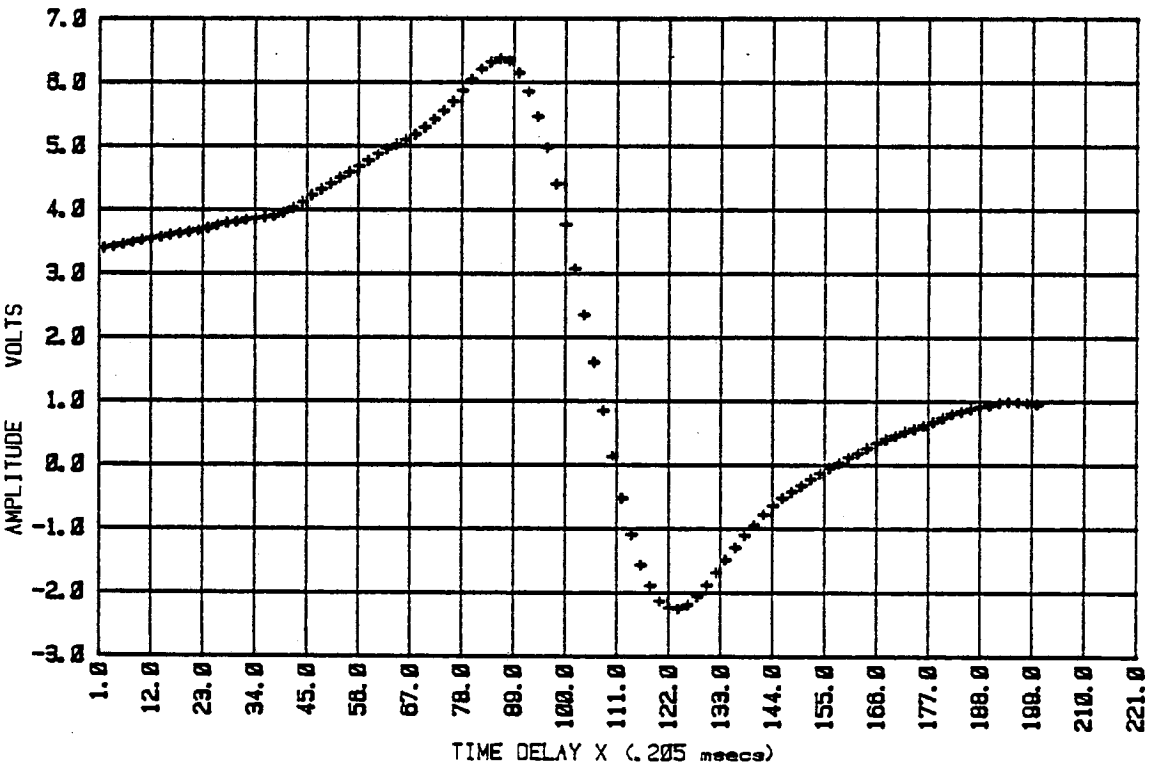

(b) THE COUPLING NETWORKS CUT-OFF FREQUENCY=10 Hz
INPUT SIGNAL BANDWIDTH = 250 Hz.

Fig. 5-7 SLOPE OF THE DIFFERENTIATED CORRELATION FUNCTION (POLARITY).

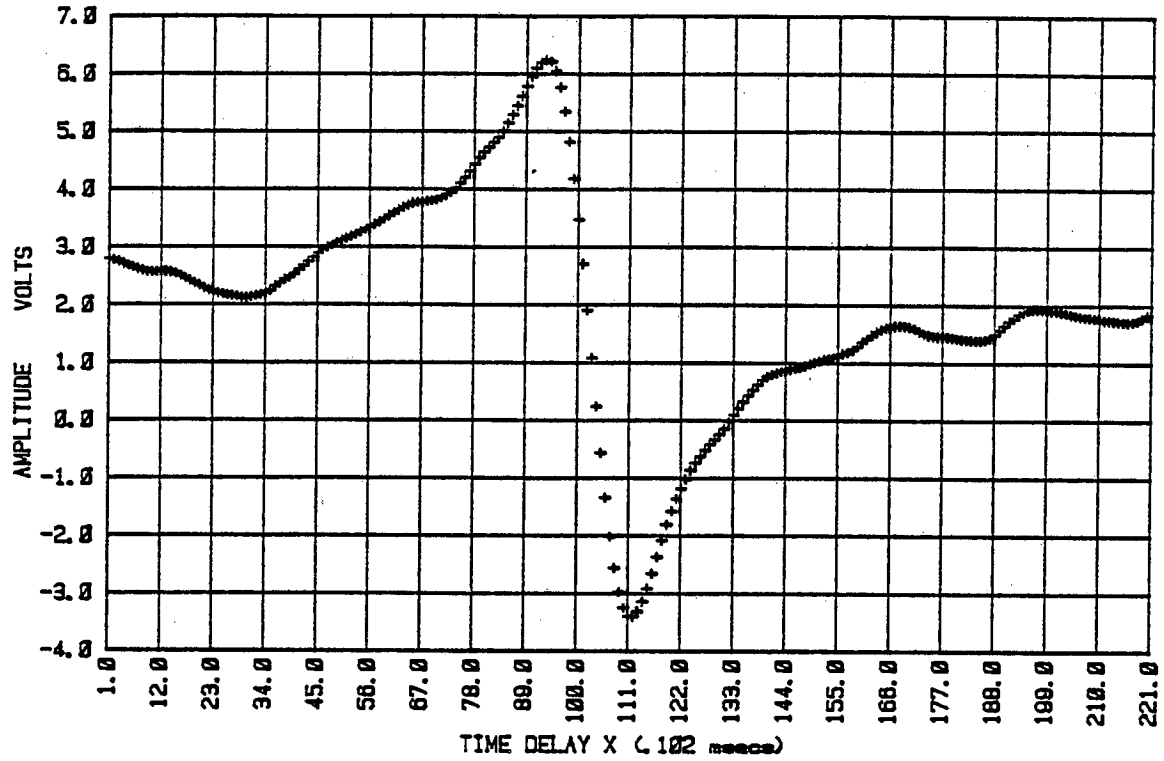

(a) THE COUPLING NETWORKS CUT-OFF FREQUENCY=49.7 Hz.
INPUT SIGNAL BANDWIDTH= 500 Hz.

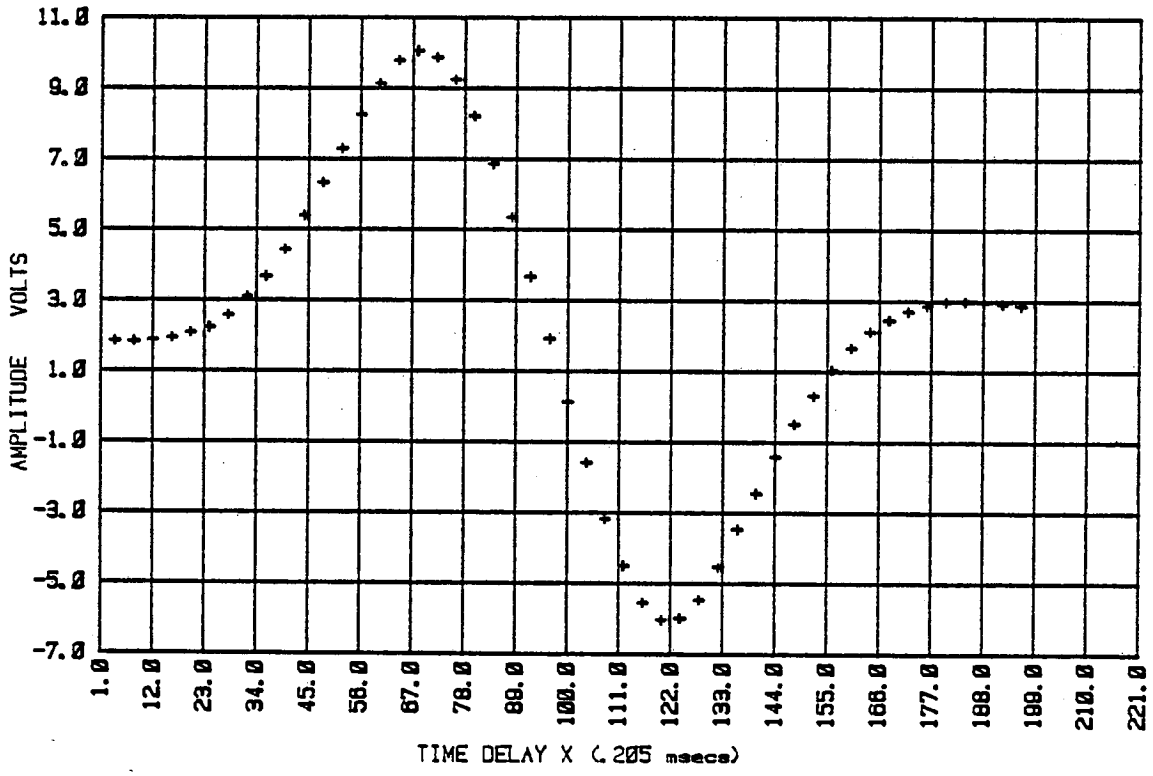

(b) THE COUPLING NETWORKS CUT-OFF FREQUENCY = 49.7 Hz.
INPUT SIGNAL BANDWIDTH= 50 Hz.

Fig. 5-8 SLOPE OF THE DIFFERENTIATED CORRELATION FUNCTION (POLARITY).

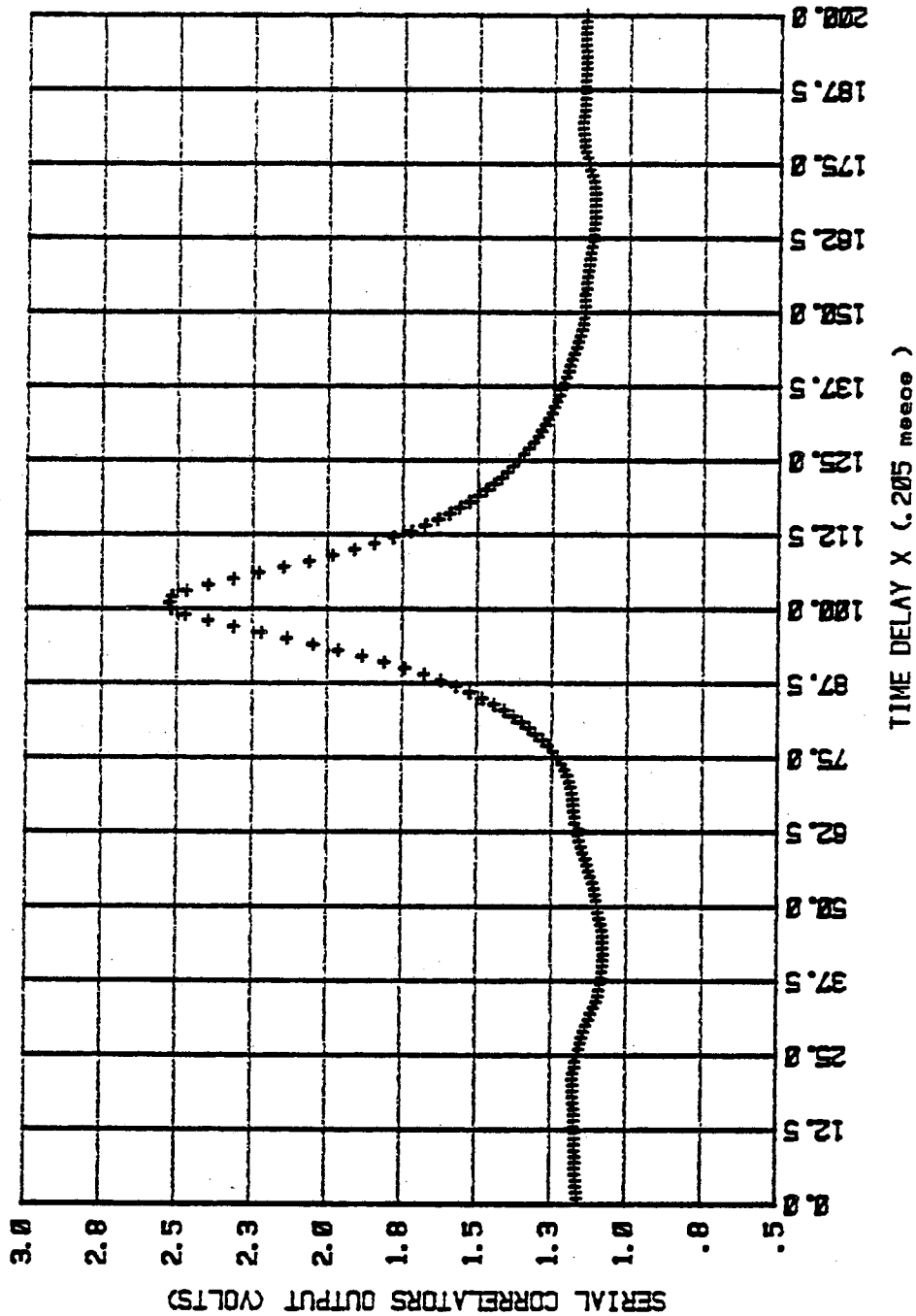

Fig.5-9 THE ESTIMATED CORRELATION FUNCTION BY THE SERIAL CORRELATOR

To investigate the performance of the tracking loop with different slops of the differentiated correlation function (polarity), two sets of experiments were carried out by applying the perturbing square wave signal to the tracking loop. The length of the delay shift register, np, held at a constant value of 20, smoothing filter time constant of 11.4 seconds, a free running VCO frequency of 4882 Hz, and the error signal, Ve(t), amplitude is set by the gain control potentiometer to its maximum value. First, the step response of the tracking correlator to a perturbing square wave signal, with an input signal bandwidth of 250 Hz and normalised correlation function amplitude of 1, with different coupling networks cut-off frequencies, together with their computed step response characteristics are shown in figure 5-10. It is important to note that the input signal time delay derived from the noise simulator was to be equal to the tracking correlators delay shift registers time delay, (i.e. 4.09 msecs) at its open loop mode. Figure 5-10 shows that the closed loop time constant of the tracking correlator increases as the slope of the differentiated correlation function (polarity) is decreased by reducing the coupling networks cut-off frequency. From figure 5-10 the closed loop time constant of the tracking loop with the coupling networks cut-off frequency of 10 and 49.7 Hz is found to be of order of 1.25 and 1 seconds respectively.

Second, the step response characteristic of the tracking correlator to the perturbing square wave signal having the same settings as above, but with a coupling networks cut-off frequency of 49.7 Hz and different input signal bandwidth was investigated.

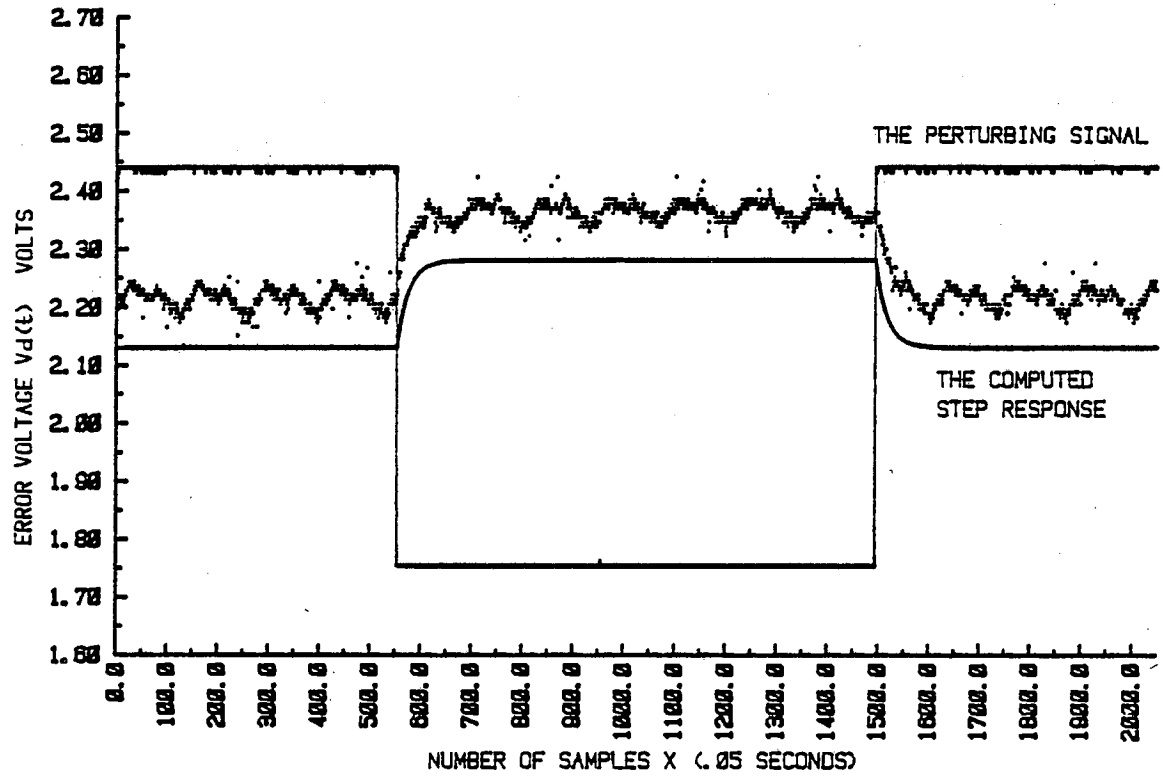

(a) THE COUPLING NETWORKS CUT-OFF FREQUENCY = 49.7 Hz.
INPUT SIGNAL BANDWIDTH = 250 Hz.

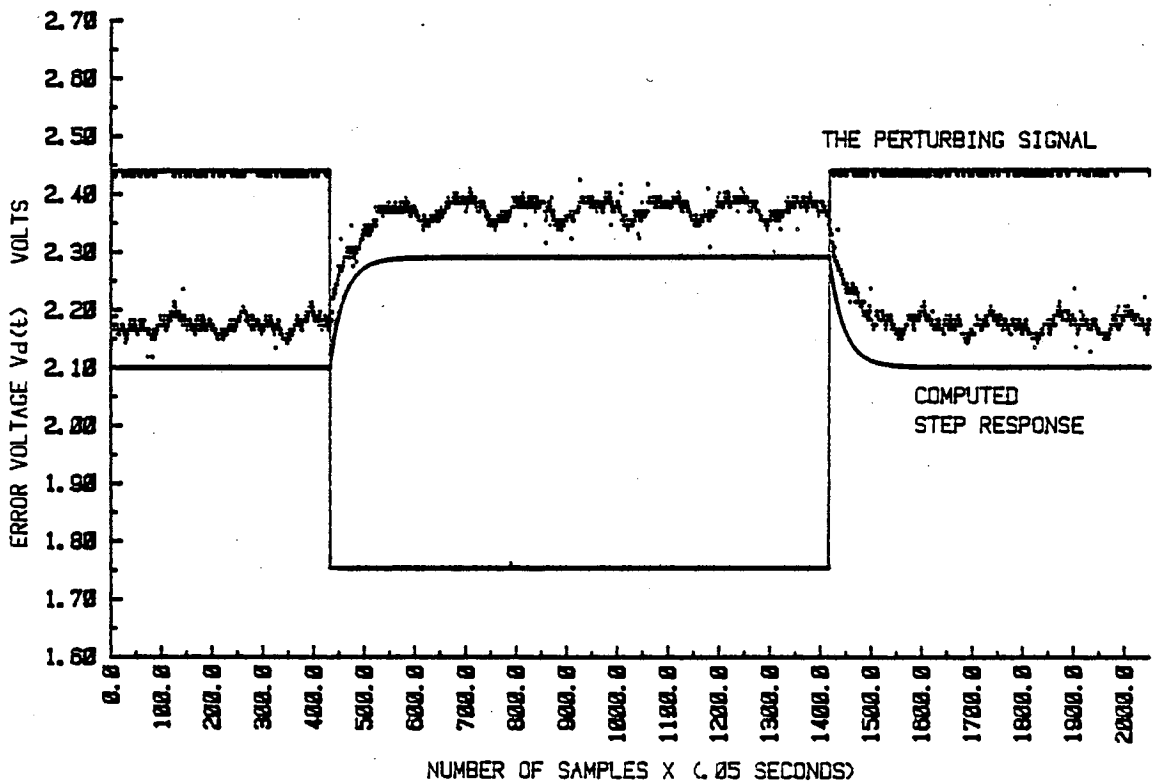

(b) THE COUPLING NETWORKS CUT-OFF FREQUENCY = 10 Hz.
INPUT SIGNAL BANDWIDTH = 250 Hz.

Fig. 5-10 STEP RESPONSE OF THE LOOP WITH DIFFERENT COUPLING NETWORKS CUT-OFF FREQUENCY.

The recorded and the computed step response characteristic of the loop with the input signal bandwidth of 50 and 500 Hz is shown in figure 5-11. It is important to note that, the time delay of the input signal with normalised correlation function peak amplitude of 1, was kept equal to 4.09 msecs, over an input signal bandwidth of 50 to 500 Hz. From figure 5-11 it will be seen that the closed loop time constant of the tracking correlator increases as the slope of the differentiated correlation function (polarity) decreases. The closed loop time constant of the tracking correlator with the input signal bandwidth of 50 and 500Hz shown in figure 5-11 is found to be of order of 2.3 and .8 seconds respectively.

The step response of the tracking correlator to the perturbing square wave signal with a different setting of the gain control potentiometer,Kp, together with their computed step response characteristics are shown in figure 5-12. The input signal bandwidth is 250 Hz, normalised correlation function amplitude is 1, VCO free running frequency is 4882 Hz, delay shift register length is 20, and the coupling networks cut-off frequency is set to 49.7 Hz. From figure 5-12 it will be seen that the closed loop time constant of the tracking correlator increases as the peak to peak amplitude of the error signal, Ve(t), is reduced by reducing the percentage setting of the gain control potentiometer. The closed loop time constant of the tracking loop with different settings of the gain control potentiometer is given in table 5-2.

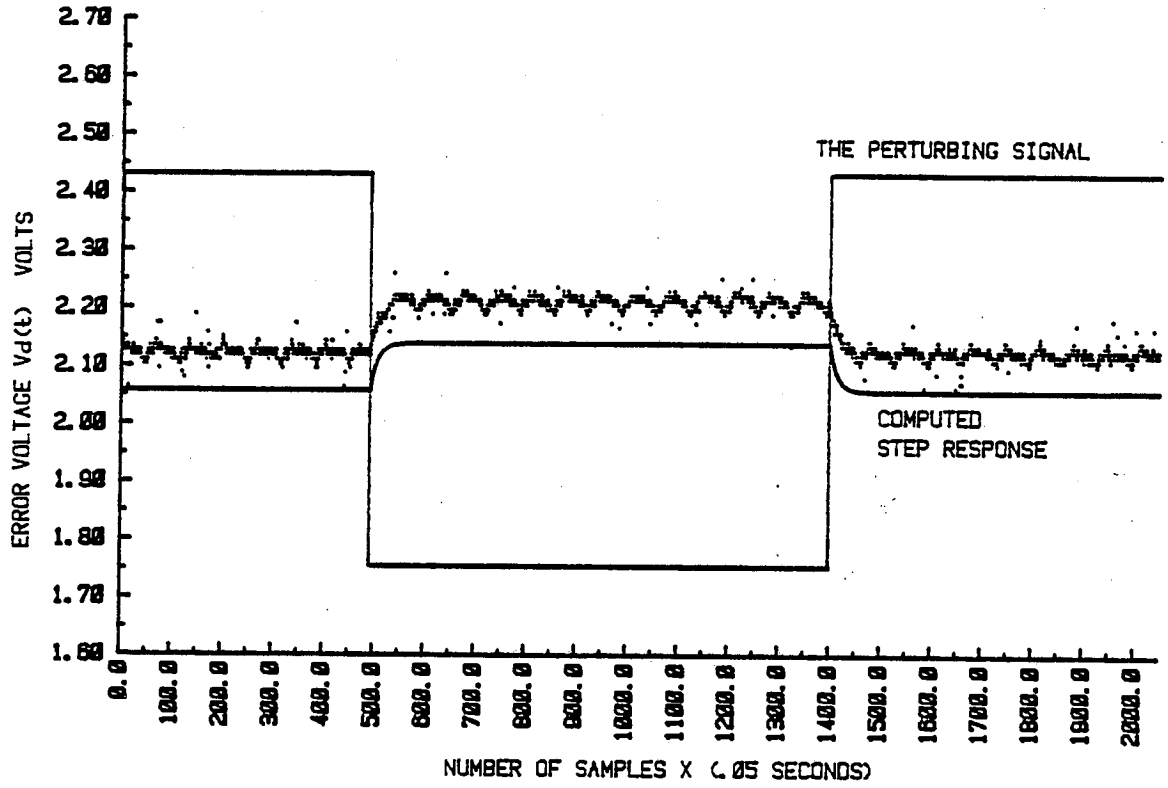

(a) THE COUPLING NETWORKS CUT-OFF FREQUENCY = 49.7 Hz
INPUT SIGNAL BANDWIDTH = 500 Hz.

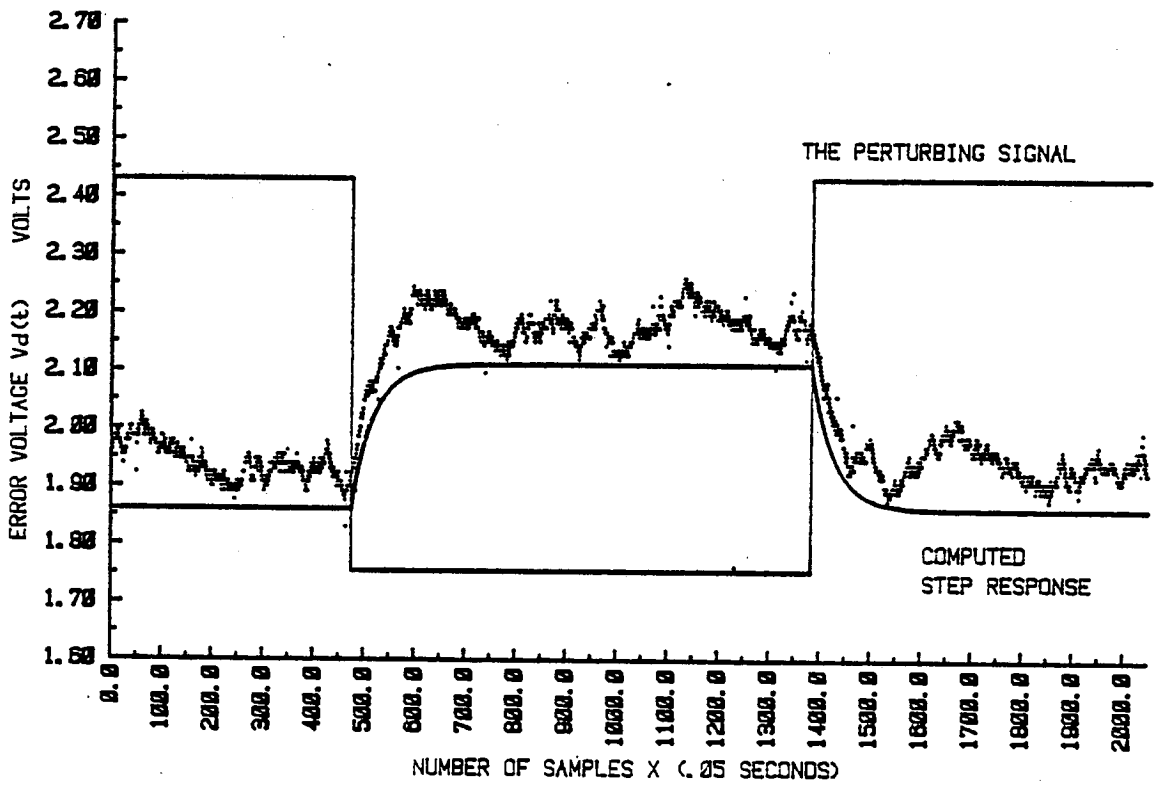

(b) THE COUPLING NETWORKS CUT-OFF FREQUENCY = 49.7 Hz.
INPUT SIGNAL BANDWIDTH = 50 Hz.

Fig. 5-11 STEP RESPONSE OF THE LOOP WITH INPUT SIGNAL BANDWIDTH OF 50 AND 500 Hz.

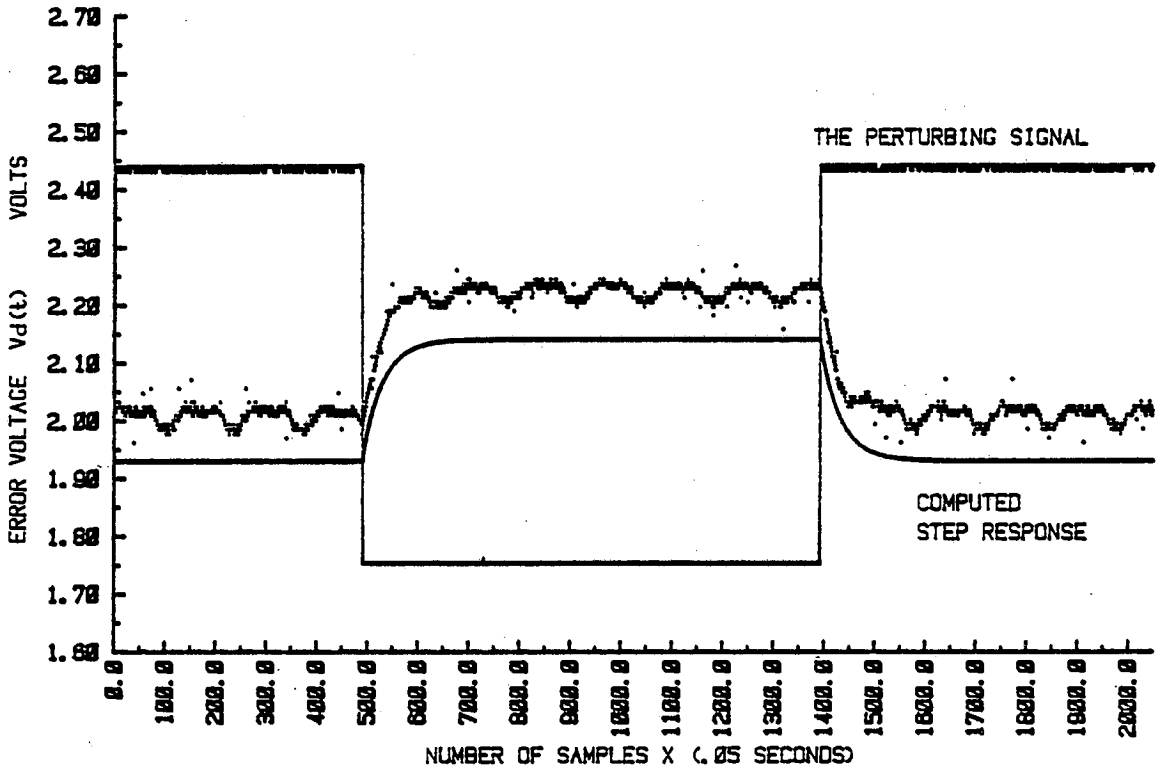

(a) % SETTING OF THE GAIN CONTROL POTENTIOMETER = 50% .
THE COUPLING NETWORKS CUT-OFF FREQUENCY = 49.7 Hz.
INPUT SIGNAL BANDWIDTH = 250 Hz.

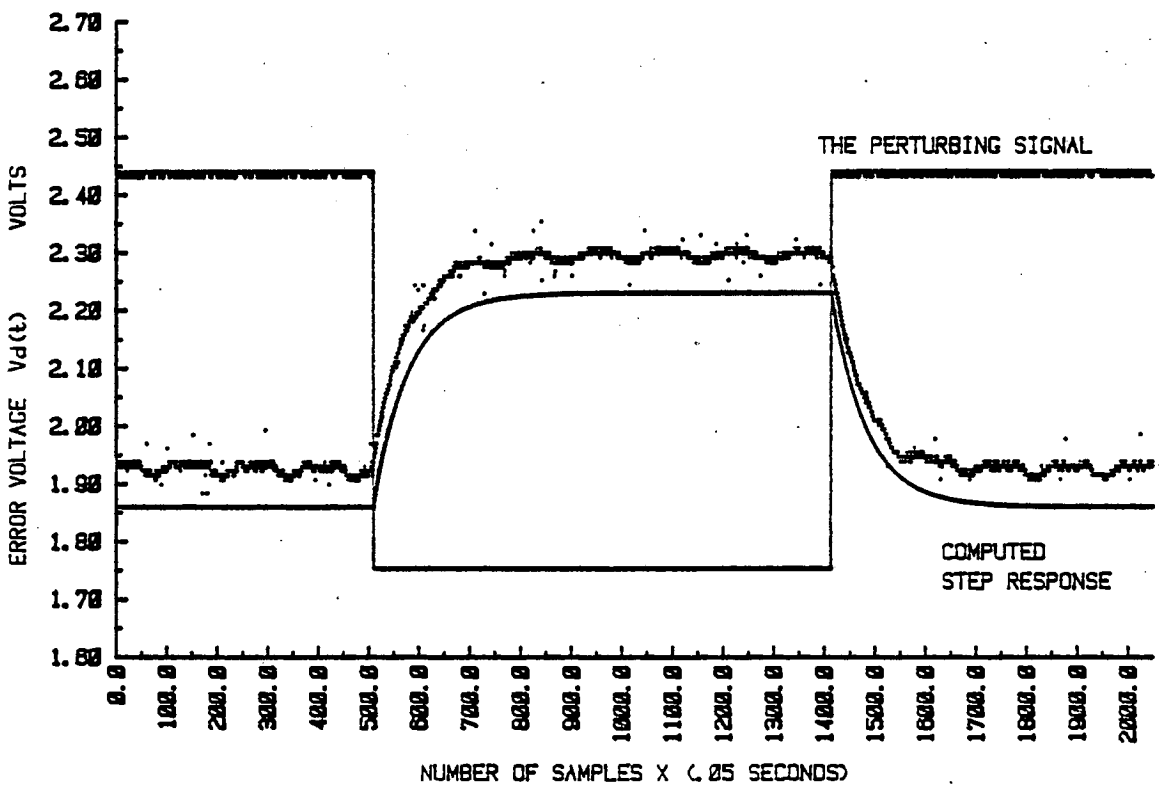

(b) % SETTING OF THE GAIN CONTROL POTENTIOMETER = 25% .
THE COUPLING NETWORKS CUT-OFF FREQUENCY = 49.7 Hz.
INPUT SIGNAL BANDWIDTH = 250 Hz .

Fig. 5-12 STEP RESPONSE OF THE LOOP WITH DIFFERENT GAIN CONTROL POTENTIOMETER SETTINGS.

% setting of the gain control potentiometer	Error signal Ve(t),Volts	Time constant Seconds	From figure
100%	±2	1	10(a)
50%	±1	1.6	12(a)
25%	±.5	2.5	12(b)

Table 5-2: The closed loop time constant of the tracking loop with different setting of the gain control potentiometer.

The step response characteristic of the tracking loop with a different delay shift register length,np, were investigated by applying the perturbing square wave signal through the test point 4 shown in figure 5-3(a). The input signal bandwidth was set to 250 Hz with the normalised correlation function peak amplitude of 1, coupling networks cut-off frequency of 49.7 Hz, and with the gain control potentiometer at 100% of its maximum setting (i.e. Ve(t) = ±2 volts). For simplicity the clock frequency to the PRBN generator and the FIR filters of the noise simulator is set to be equal to the free-running frequency of the VCO, (i.e. 4882 Hz). Therefore if the input signal time delay is set to be equal to ns/4882 seconds the tracking correlator will track the peak of the correlation function if its delay shift register length, np, is equal to the noise simulators delay setting, ns.

The step response of the tracking correlator to the perturbing square wave signal together with its computed step response characteristic, for a different delay shift register length,np, is shown in figure 5-13. From figure 5-13 it will be

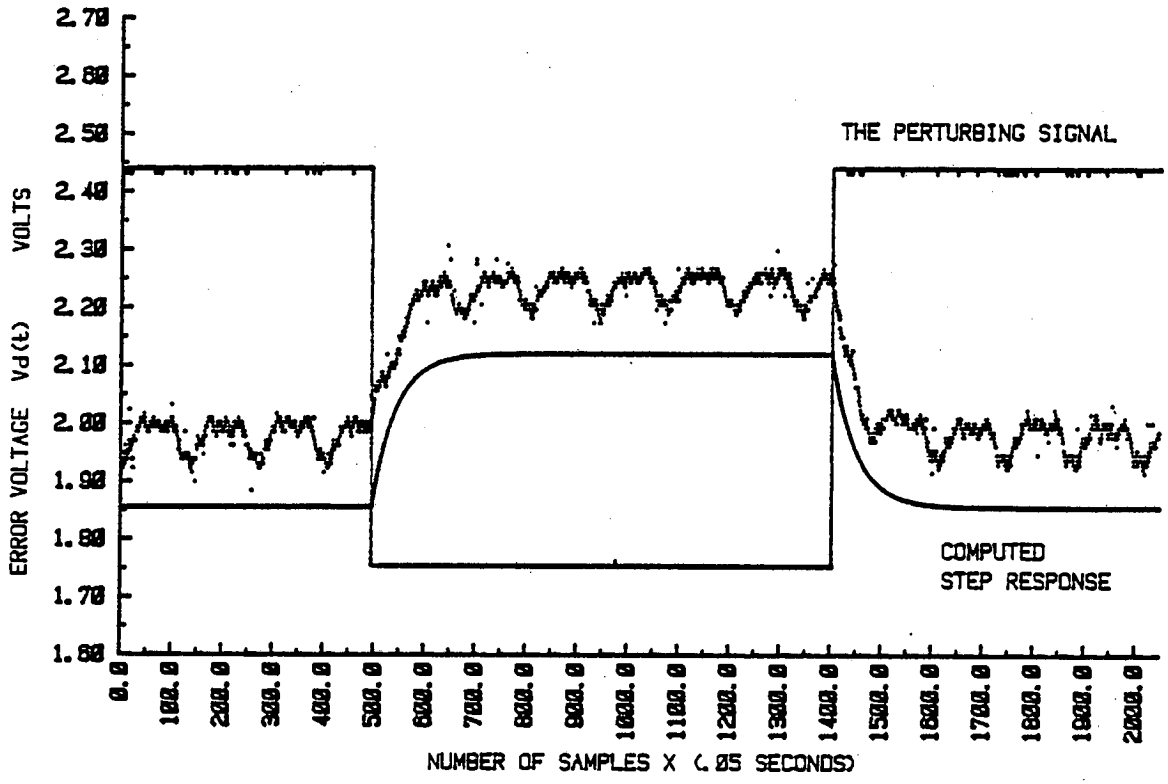

(a) THE COUPLING NETWORKS CUT-OFF FREQUENCY = 49.7 Hz.
INPUT SIGNAL BANDWIDTH = 250 Hz.
DELAY SHIFT REGISTER LENGTH = 8 .

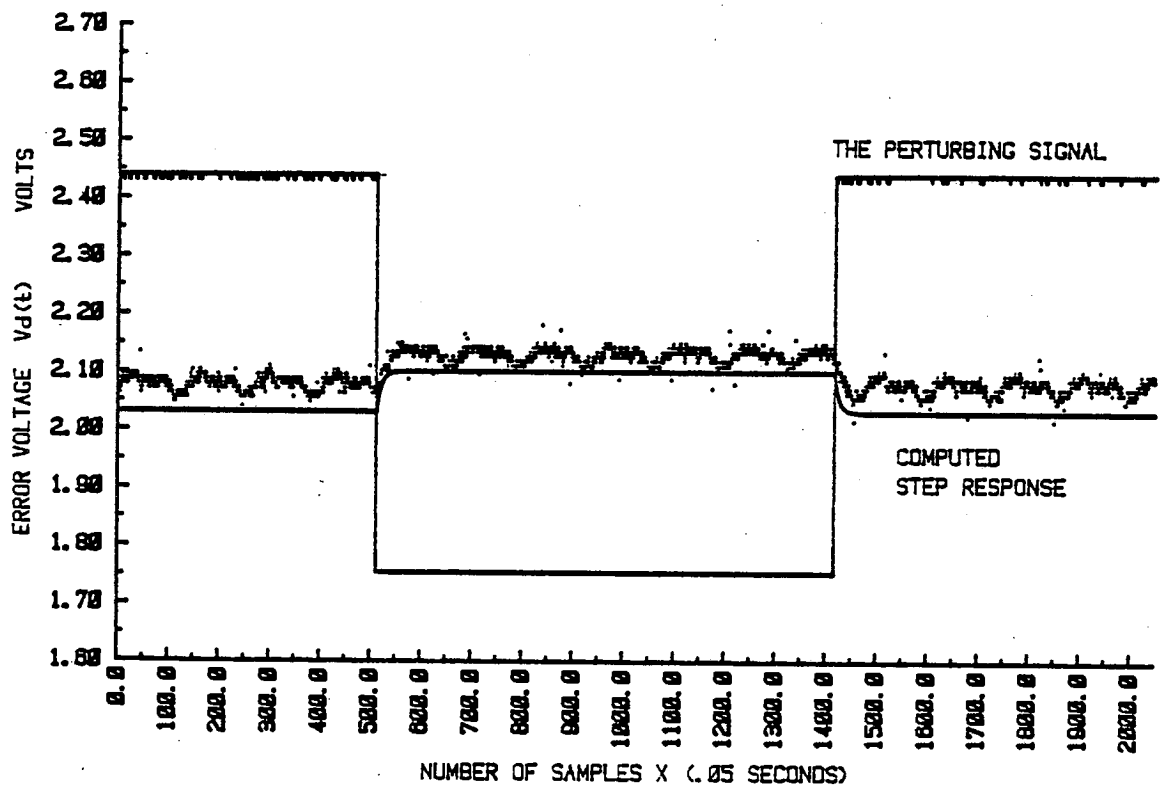

(b) THE COUPLING NETWORKS CUT-OFF FREQUENCY = 49.7 Hz.
INPUT SIGNAL BANDWIDTH = 250 Hz.
DELAY SHIFT REGISTER LENGTH = 50 .

Fig. 5-13 STEP RESPONSE OF THE LOOP WITH DIFFERENT DELAY SHIFT REGISTER LENGTH.

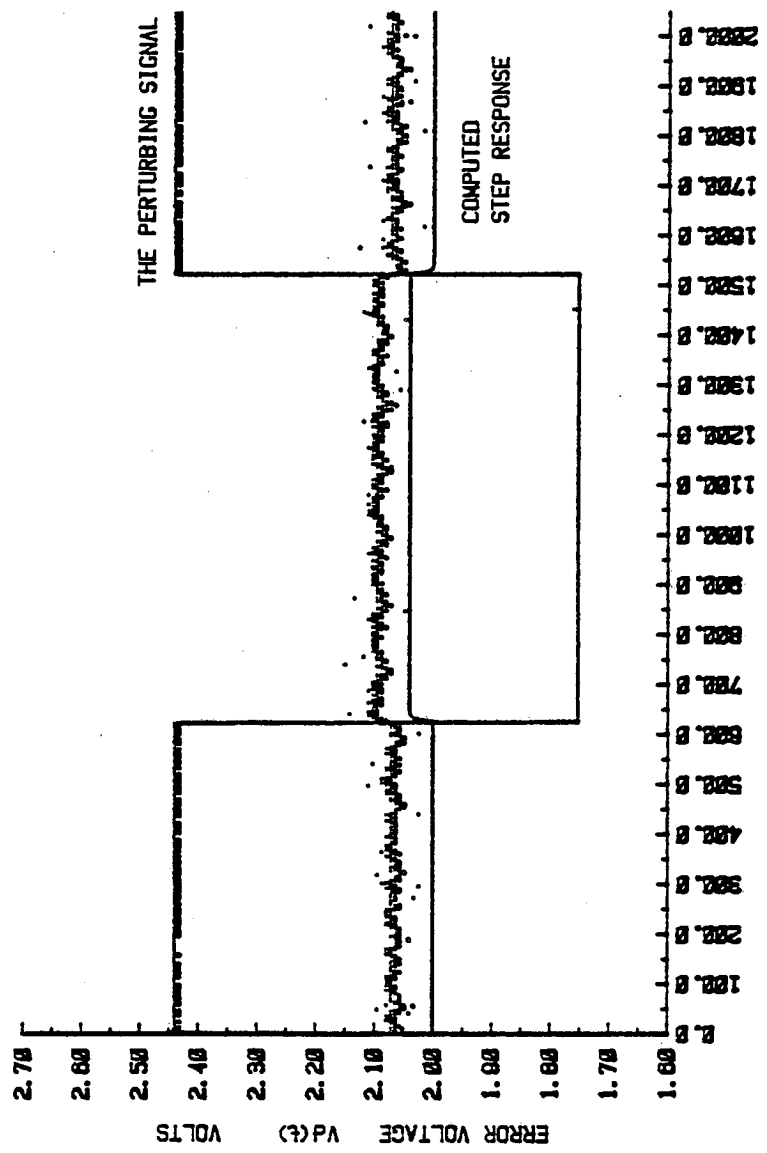

Fig.5-13(c) STEP RESPONSE OF THE LOOP WITH DELAY SHIFT REGISTER LENGTH OF 100.

seen that the closed loop time constant of the tracking correlator increases as the delay shift register length,np, decreases. The closed loop time constant of the tracking loop with different delay shift register length is given in table 5-3.

Delay shift register length ,np,	Time constant Seconds	From figure
8	2.35	13(a)
50	.9	13(b)
100	.5	13(c)

Table 5-3: Closed loop time constant of the tracking loop with different delay shift register length, np.

The expected output voltage variation of the tracking loops smoothing filter, $\Delta Vd(t)$, (steady state error), due to the perturbing square wave signal is calculated using the equation 5-9. The calculated output voltage variation of the smoothing filter with different slope of the differentiated correlation function (polarity) are compared with the experimental results obtained from figure 5-10,5-11,5-12,5-13 and is given in table 5-4. From comparison of the results given in table 5-4, it will be seen that, the first order transfer function of the system can be used to predict the output voltage variation ,(steady state error), of the smoothing filter when the external perturbing square wave signal is applied to the loop. In addition the computed and the recorded step response characteristic of the loop

shown in figure 5-10,5-11,5-12 and 5-13 indicates that the first order transfer function of the system can be used to predict the step response characteristic of the loop.

Slope* V/secs	% gain control setting	Operating frequency fc,Hz	np†	Steady state computed Volts	|error| recorded Volts	From figure
-3388.47	100%	4931	20	.187	.19	5-10(b)
-4929.63	100%	5100	20	.142	.15	5-10(a)
-7837.86	100%	5120	20	.093	.08	5-11(a)
-2118.03	100%	4996	20	.284	.25	5-11(b)
-2464.8	50%	5030	20	.245	.21	5-12(a)
-1232.4	25%	5015	20	.432	.37	5-12(b)
-4929.63	100%	5075	8	.309	.26	5-13(a)
-4929.63	100%	5100	50	.060	.07	5-13(b)
-4929.63	100%	5100	100	.031	.04	5-13(c)

Table 5-4: The comparison of the computed and recorded output voltage variation of the smoothing filter ,Vd(t).

* Slopes derived from table 5-1 .

† np = delay shift register length.

Two sets of experiments were carried out to investigate the step response characteristic of the tracking loop to the simulated flow noise signal time delay change. First the step response characteristic of the loop to the input signal time delay change with the normalised correlation function peak amplitude of

.82 and bandwidth of 400 Hz was recorded. The input signal time delay was initially set to 6.11 msecs, and the step response of the loop to the time delay change from 6.11 msecs to 6.49 msecs, and back to 6.11 msecs was recorded. Figure 5-14(a) describes the computed and the recorded step response characteristic of the tracking loop. Note that equation 5-7 was used to compute the step response characteristic of the loop, and the slope of the differentiated correlation function (polarity) around the operating region of the loop is estimated from figure 5-15(a).

Second, the step response of the loop to the input signal time delay change with the normalised correlation function peak amplitude of .32 and bandwidth of 180 Hz was recorded. The input signal time delay was initially set to 34.40 msecs, and the step response characteristic of the loop to time delay change from 34.40 msecs to 37.68 msecs and back to 34.40 msec was recorded. The computed and the recorded step response of the loop is shown in figure 5-14(b). The slope of the differentiated correlation function (polarity) is estimated from figure 5-15(b).

For the above two experiments the expected output voltage variation of the smoothing filter, (steady state error), as well as the time constant of the loop was estimated using the first order transfer function of the loop given by the equation 5-7. The equations used to estimate the output voltage variation, (steady state error), $\Delta Vd(t)$, and the closed loop time constant of the tracking correlator

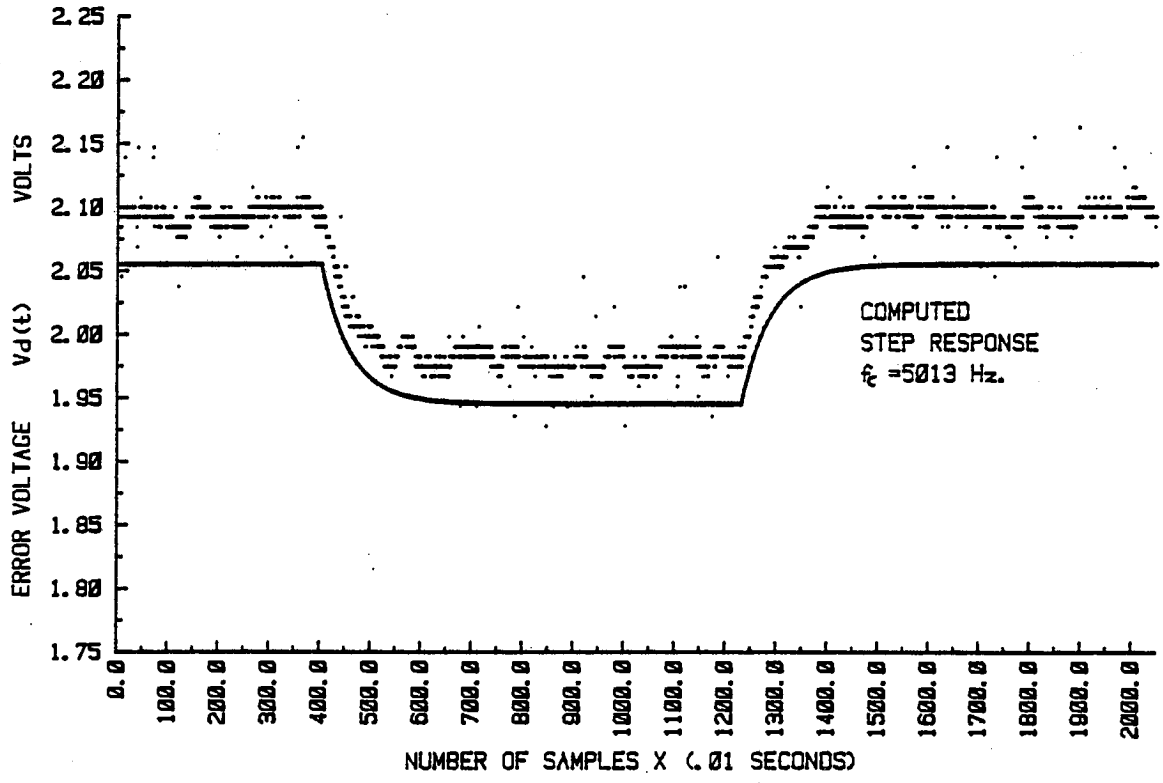

(a) THE COUPLING NETWORKS CUT-OFF FREQUENCY = 49.7 Hz.
INPUT SIGNAL BANDWIDTH = 400 Hz.
NORMALISED CORRELATION FUNCTION PEAK AMPLITUDE = .82 .
DELAY SHIFT REGISTER LENGTH = 30 .

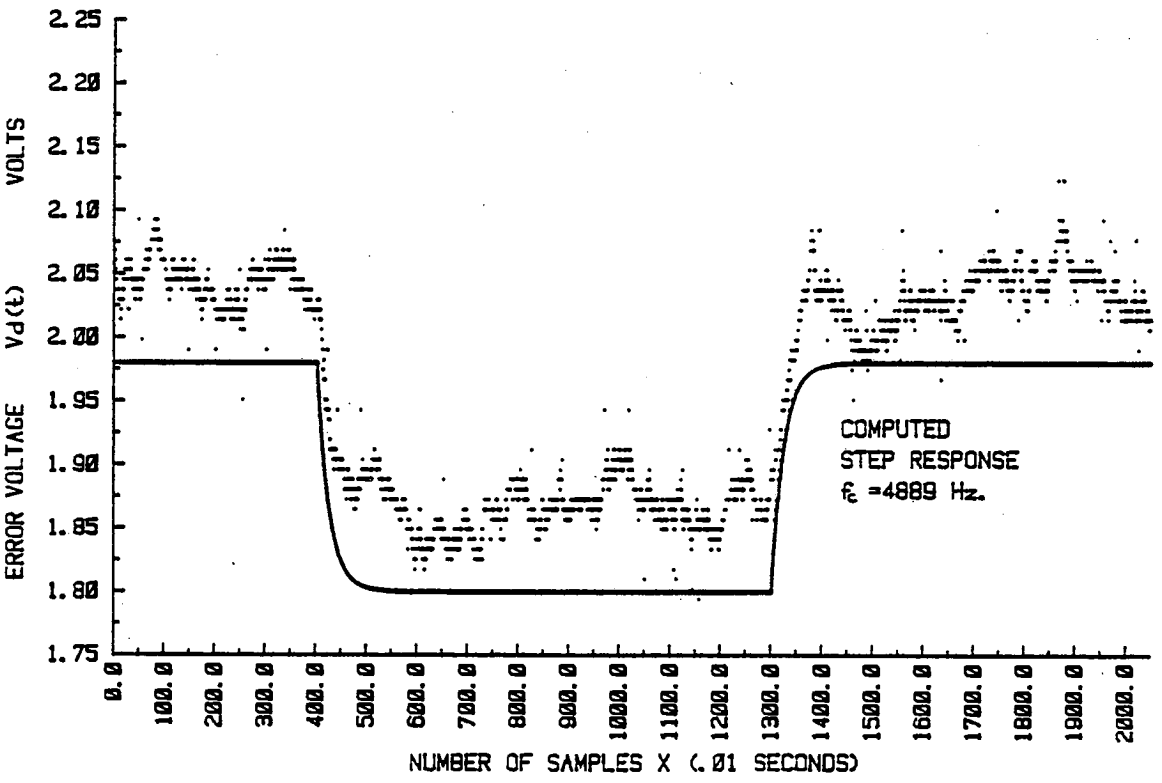

(b) THE COUPLING NETWORKS CUT-OFF FREQUENCY = 49.7 Hz .
INPUT SIGNAL BANDWIDTH = 180 Hz .
NORMALISED CORRELATION FUNCTION PEAK AMPLITUDE = .32 .
DELAY SHIFT REGISTER LENGTH = 167 .

Fig. 5-14 STEP RESPONSE OF THE LOOP.

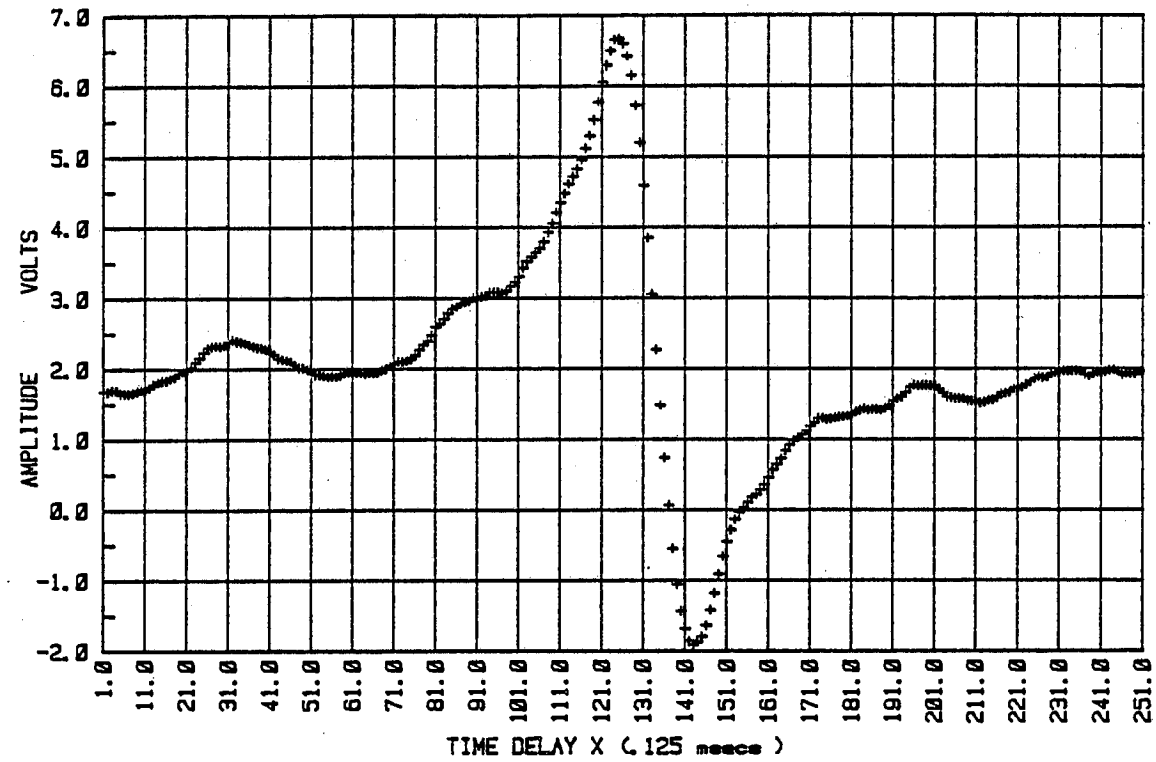

(a) THE COUPLING NETWORKS CUT-OFF FREQUENCY = 49.7 Hz.
INPUT SIGNAL BANDWIDTH = 400 Hz.
NORMALISED CORRELATION FUNCTION PEAK AMPLITUDE=.82 .

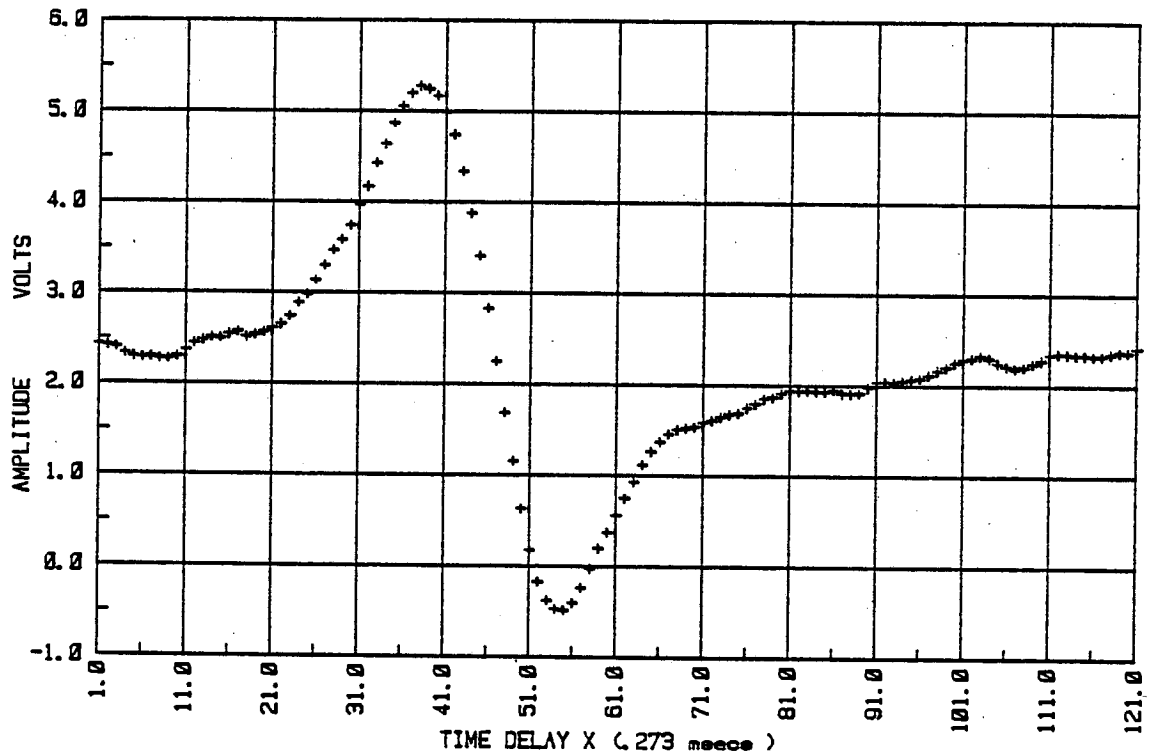

(b) THE COUPLING NETWORKS CUT-OFF FREQUENCY = 49.7 Hz.
INPUT SIGNAL BANDWIDTH = 180 Hz .
NORMALISED CORRELATION FUNCTION PEAK AMPLITUDE = .32 .

Fig. 5-15 SLOPE OF THE DIFFERENTIATED CORRELATION FUNCTION (POLARITY).

(due to the input signal time delay change) are given by:-

$$\text{Steady State Error} = \lim_{t\to\infty} \Delta Vd(t) = \frac{-fc^2.KD.td}{fc^2 + KD.Ko.np} \qquad (5\text{-}10)$$

and

$$\text{Tracking loops time constant} = \frac{\tau}{1 + \dfrac{KD.Ko.np}{fc^2}} \qquad (5\text{-}11)$$

The recorded results from figure 5-14 are compared with the computed results in table 5-5. From the results given in table 5-5 it will be seen that for small simulated flow noise signal time delay change the first order transfer function of the loop can be used to predict the closed loop time constant of loop as well as the smoothing filters output voltage variation, (steady state error).

Slope* V/secs	Time constant computed seconds	Time constant recorded seconds	Steady state computed volts	|error| recorded volts	From figure
-6240.12	.58	.50	.11	.11	5-14(a)
-2627.10	.27	.22	.18	.18	5-14(b)

Table 5-5: Computed and recorded time constant and output voltage variation of the loop.

* Slopes are estimated from figure 5-15.

Further experiments were carried out to investigate the linear lock range of the tracking correlator over an input signal

bandwidth of 50 to 500 Hz. This was achieved by sweeping the flow noise signal over a 25-1 range with the length of the delay shift register set to give a time delay of 10.24 msecs, (np=50 and fr=4882 Hz). This time delay was chosen so that a 5 to 1 range from either side of this delay is equivalent to the 25 to 1 sweep range set by the noise simulator. Since the error voltage, Vd(t), to the input terminal of the VCO is directly proportional to the flow velocity, the HP-85 computer was programmed to sweep the input signal time delay at 100 equally spaced flow rates over a 25 to 1 range, with the approximately constant input signal bandwidth. Due to the constraints imposed on developing the software to sweep the input signal time delay over a 25 to 1 range it was necessary to allow the clock frequency to the PRBN generator and the FIR filters of the noise simulator to vary by a small factor in order to simulate 100 equally spaced flow velocities. The input signal time delay was swept over a 25 to 1 range at different rates, bandwidths and normalised correlation function amplitudes. In addition these experiments were repeated for different coupling networks cut-off frequencies, smoothing filter time constant, and different gain control potentiometer settings.

Initially the smoothing filter time constant was set to 50 seconds, the coupling networks cut-off frequency to 49.7 Hz, and the gain control potentiometer was set to 25% of its maximum setting (i.e. Ve(t)=$\pm$.5 volts). To determine the minimum sweep time which will allow the tracking correlator to stay in its lock mode, regardless of the direction of the flow velocity change the

input signal time delay was swept over a 25 to 1 range in both directions with an input signal bandwidth of 250 Hz and normalised correlation function amplitude of 1. After each time delay setting, the error voltage Vd(t), is read and stored through a DVM by the HP-85 computer. The response of the error voltage, Vd(t), to the input signal time delay being swept at 100 equally spaced points within 707 seconds in each direction is shown in figure 5-16(a). Since the flow velocity is being swept at a much faster rate than the closed loop time constant of the tracking loop the error voltage, Vd(t), response curves shown in figure 5-16(a) for increasing and decreasing time delays do not overlap. This error is eliminated by increasing the sweep time to 1900 seconds, with the result shown in figure 5-16(b).

From figure 5-16(b) it will be seen that the tracking region of the negative feedback loop as described in chapter 4, depends on the direction of the input signal time delay sweep and this is not linear over a 25 to 1 sweep range. In addition from figure 5-16(b) it will be seen that the linear lock range of the tracking correlator (i.e. the tracking region over which the loop can track the peak of the correlation function linearly regardless of direction of time delay sweep) is less than its tracking range. Therefore for linear operation of the ICPT correlator the upper and lower limits of the window comparator is required to be equal to the linear lock range of the negative feedback loop.

To investigate the effect of the overall gain of the

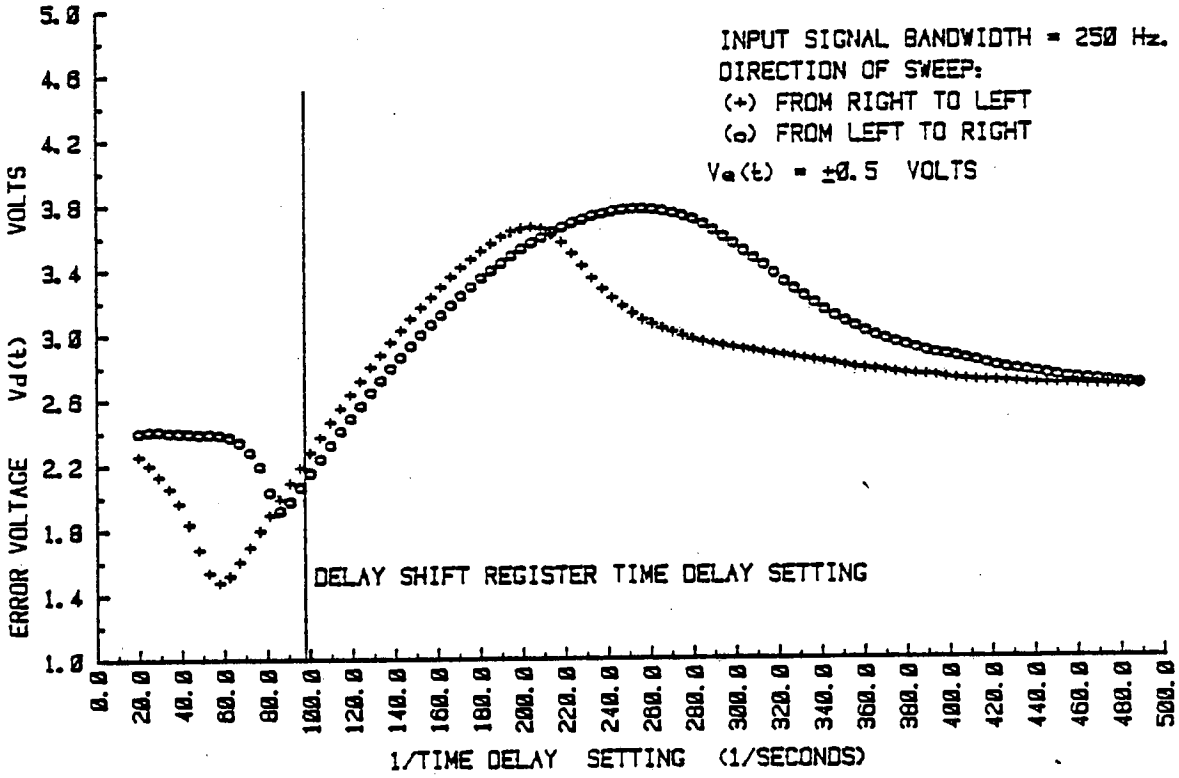

(a) THE COUPLING NETWORKS CUT-OFF FREQUENCY = 49.7 Hz
SMOOTHING FILTERS TIME CONSTANT = 50 SECONDS
TIME DELAY SETTING PERIOD = 7 SECONDS (707/100).

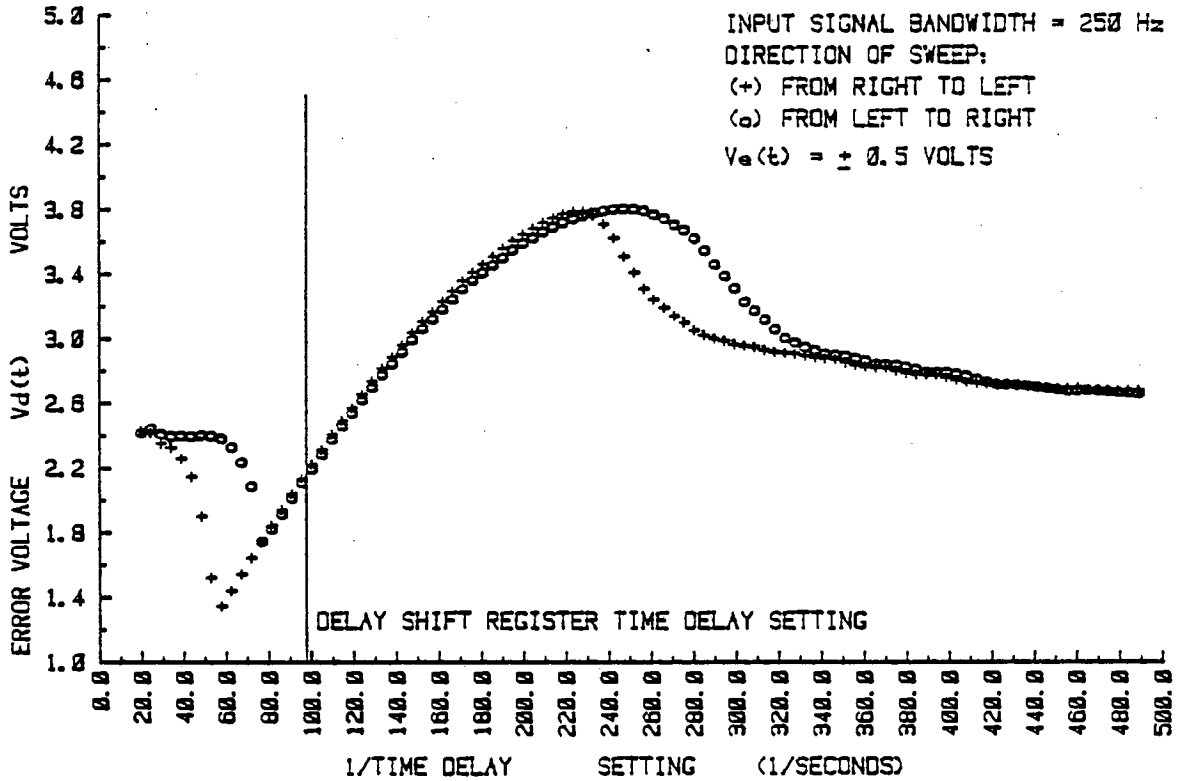

(b) THE COUPLING NETWORKS CUT-OFF FREQUENCY = 49.7 Hz.
SMOOTHING FILTERS TIME CONSTANT = 50 SECONDS .
TIME DELAY SETTING PERIOD = 19 SECONDS (1900/100).

Fig. 5-16 ERROR VOLTAGE RESPONSE TO THE INPUT SIGNAL TIME DELAY SWEEP.

negative feedback loop on its tracking range, the gain control potentiometer is set to 100% of its maximum value, , (i.e. Ve(t)= ±2 volts) and the above experiment is repeated. The response of the error voltage to an input signal time delay sweep in each direction, with a sweep time of 707 and 1900 seconds is shown in figure 5-17. These results indicates that when the overall gain of the loop is increased the negative feedback action of the loop can swing the error voltage, Vd(t), further and this will increase the tracking and its linear lock range.

The tracking performance of the negative feedback loop may be studied using the output of the serial correlator described in chapter 4. The output of the serial correlator is expected to be proportional to the peak amplitude of the correlation function when the tracking correlator is in the lock mode. The output response of the serial correlator to the input signal time delay sweep of the tracking correlator is shown in figure 5-18. The output response of the serial correlator shown in figure 5-18 corresponds to the tracking loops error voltage response given in figure 5-17(b).

For the linear operation of the ICPT correlator, the coarse position latch is required to be disabled only within the linear lock range of the tracking correlator. Therefore, if the output of the serial correlators comparator is used to control the coarse position latch on its own, in addition to the problems described in chapter 4, from figure 5-18 it is clear that the output of the serial correlator can not be used to indicate

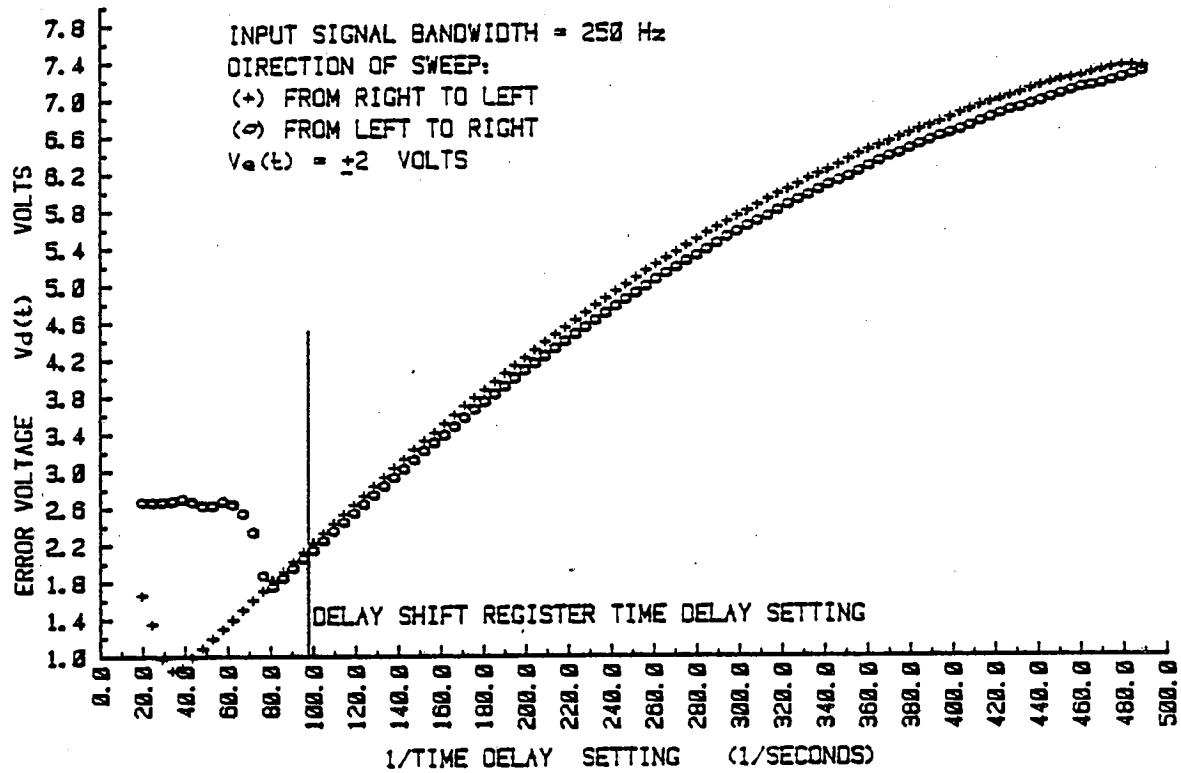

(a) THE COUPLING NETWORKS CUT-OFF FREQUENCY = 49.7 Hz .
SMOOTHING FILTERS TIME CONSTANT = 50 SECONDS .
TIME DELAY SETTING PERIOD = 7 SECONDS (707/100).

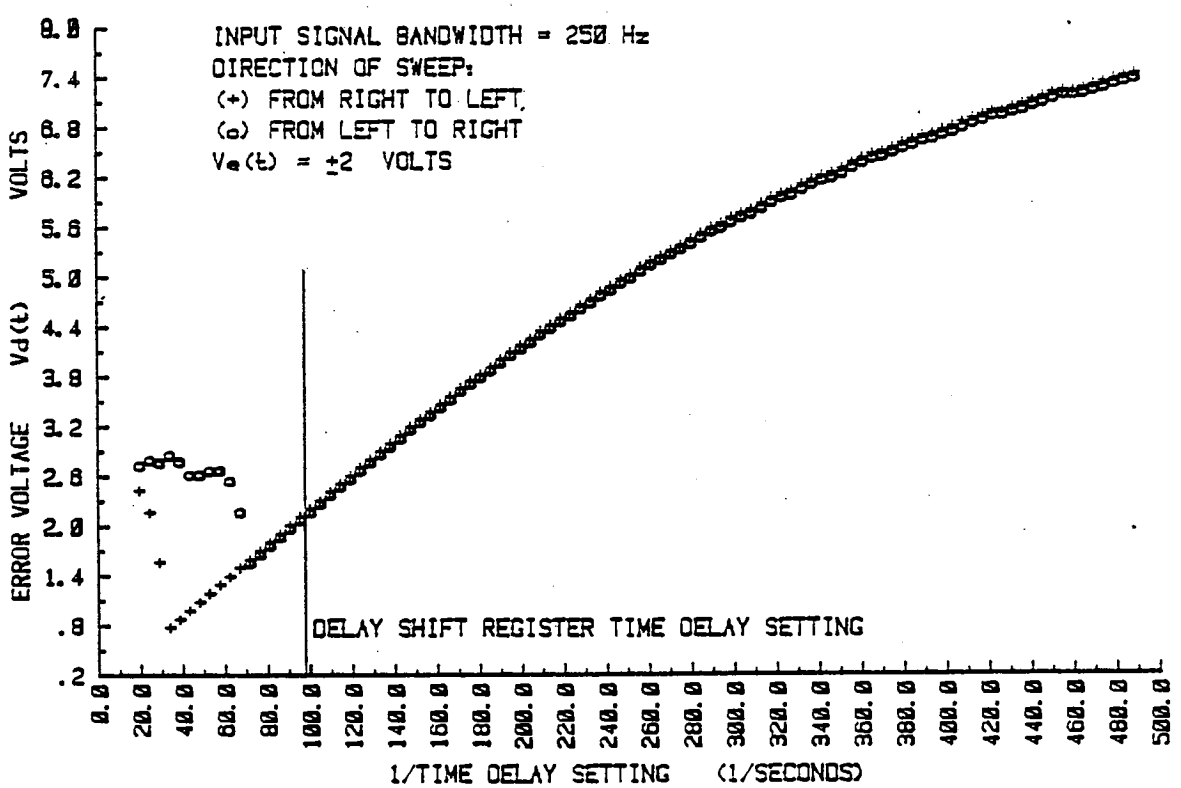

(b) THE COUPLING NETWORKS CUT-OFF FREQUENCY = 49.7 Hz.
SMOOTHING FILTERS TIME CONSTANT = 50 SECONDS.
TIME DELAY SETTING PERIOD = 19 SECONDS (1900/100).

Fig. 5-17 ERROR VOLTAGE RESPONSE TO THE INPUT SIGNAL TIME DELAY SWEEP.

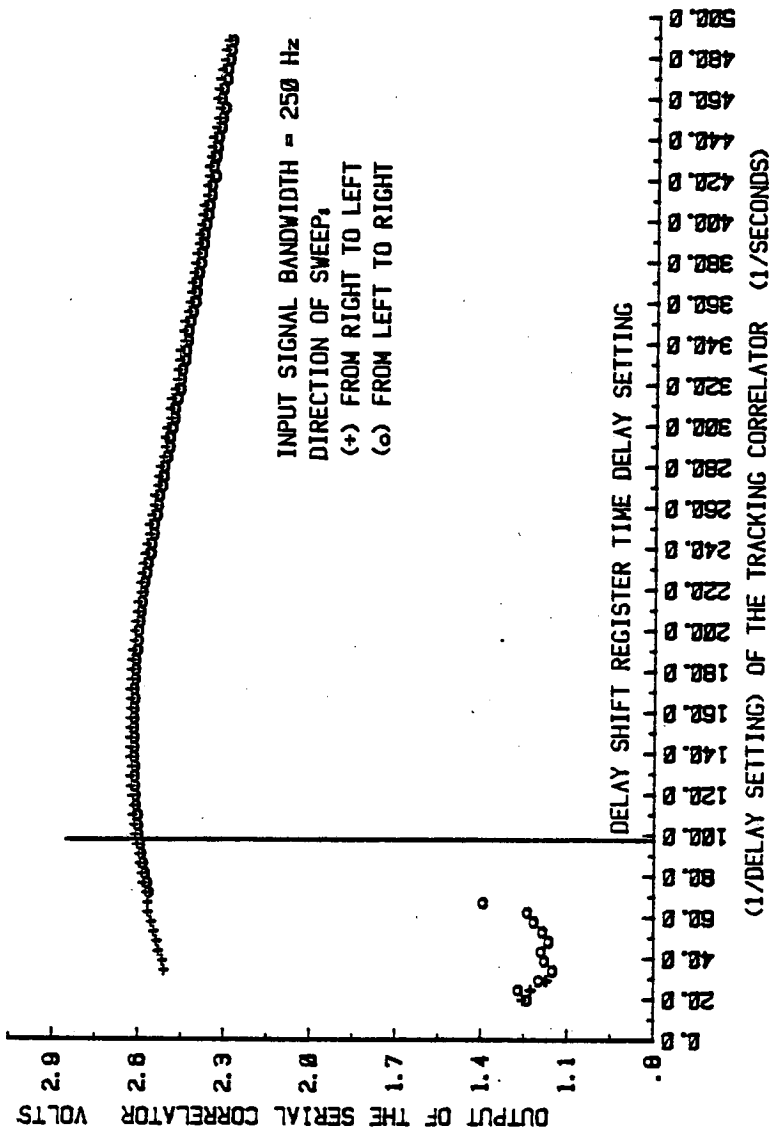

FIGURE 5-18 OUTPUT RESPONSE OF THE SERIAL CORRELATOR TO THE INPUT SIGNAL TIME DELAY SWEEP OF LOOP.

significantly the difference between the linear lock and tracking range of the negative feedback loop, and its output stays approximately the same value within the tracking range of the loop. Hence if only the output of the serial correlators comparator is used to control the coarse position latch, the ICPT correlator may not be tracking the peak of the correlation function linearly.

To reduce the variance of the error signal, Ve(t), the time constant of the smoothing filter was initially set to 50 seconds. To decrease the closed loop time constant of the tracking correlator, the smoothing filters time constant was reduced to 11.4 seconds and the gain control potentiometer setting was maintained at 100% of its maximum setting (i.e. Ve(t)=$\pm$2 volts). To investigate the performance of the tracking loop with the smoothing filter time constant of 11.4 seconds, the input signal time delay was swept over a 25 to 1 range within 707 seconds in each direction. The error voltage, Vd(t), response with the above settings and the input signal bandwidth of 250 Hz is shown in figure 5-19. From figure 5-19 it will be seen that the variance of the error voltage is not affected significantly by decreasing the closed loop time constant of the negative feedback loop in comparison to the situation shown in figure 5-17.

In flow measurement situations the normalised peak amplitude of the correlation function is expected to vary over a .2 to 1 range (Taylor Instrument Ltd. 1976). Therefore the above experiment was repeated, with the normalised peak amplitude

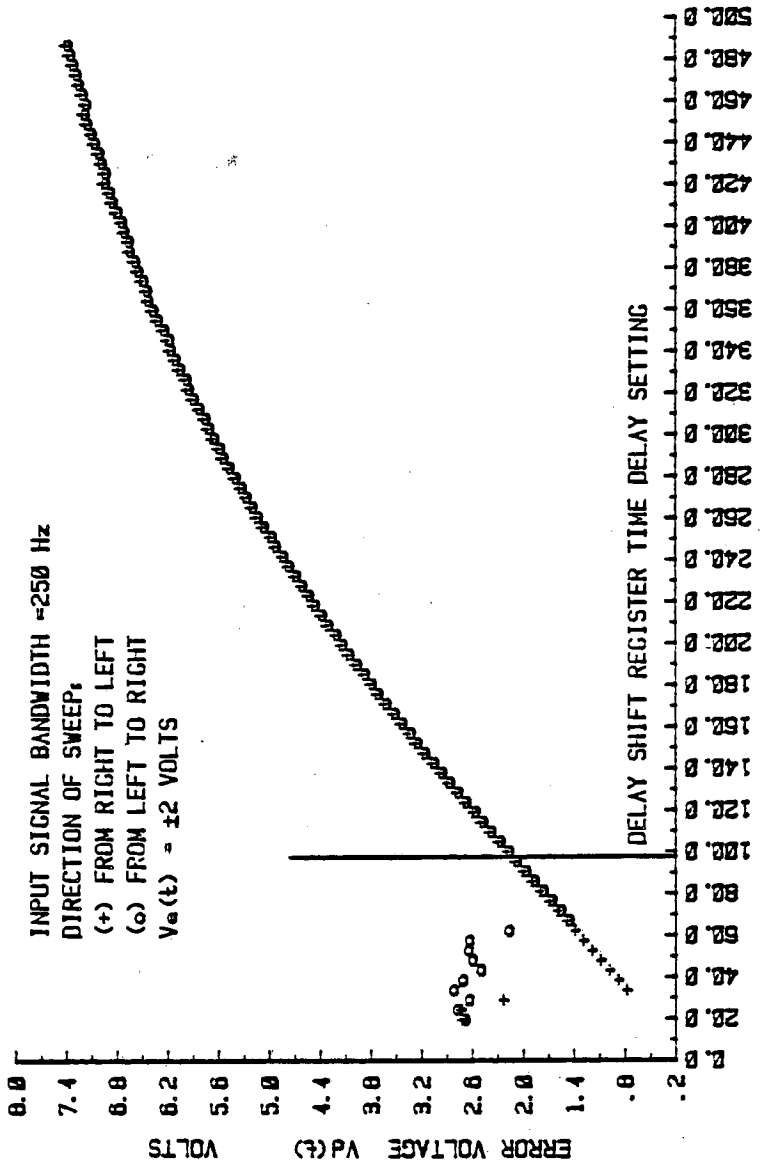

Fig.5-19 ERROR VOLTAGE RESPONSE TO THE INPUT SIGNAL TIME DELAY SWEEP.

of .2 and the response of the error voltage is shown in figure 5-20(a). From figure 5-20(a) it will be seen that the variance of the error voltage has not been significantly affected by this change. For the purpose of comparison figure 5-20(b) has been included to show the response of the error voltage when the time constant of the smoothing filter was set to 50 seconds.

The results given in figure 5-16 to 5-20 are summarised as below:-

i) As the overall gain of the tracking correlator increases, the tracking and the linear lock range of the loop increases.

ii) If the tracking loops smoothing filters time constant is reduced from 50 seconds to 11.4 seconds, the transient response of the tracking correlator will become faster and the variance of the error signal Ve(t) will remain low for normalised correlation function peak amplitudes of 1 and .2.

iii) The tracking region of the negative feedback loop depends on the direction of the input signal time delay change as well as the peak amplitude of the correlation function.

iv) The linear lock range of the tracking correlator is independent of the direction of the input signal time delay change and is less than its tracking range.

One of the major factors controlling the response characteristic of the tracking loop is the slope of the

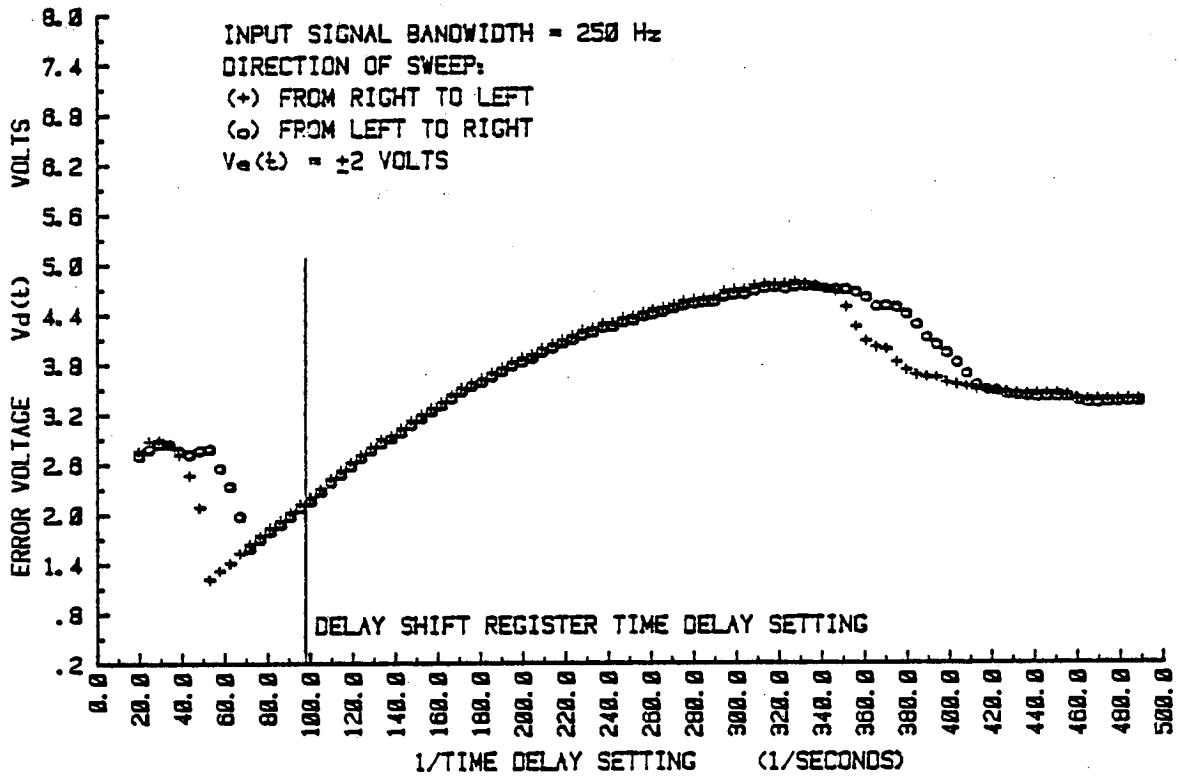

(a) THE COUPLING NETWORKS CUT-OFF FREQUENCY = 49.7 Hz.
SMOOTHING FILTERS TIME CONSTANT = 11.4 SECONDS.
TIME DELAY SETTING PERIOD = 7 SECONDS (707/100).
NORMALISED CORRELATION FUNCTION PEAK AMPLITUDE = 0.2 .

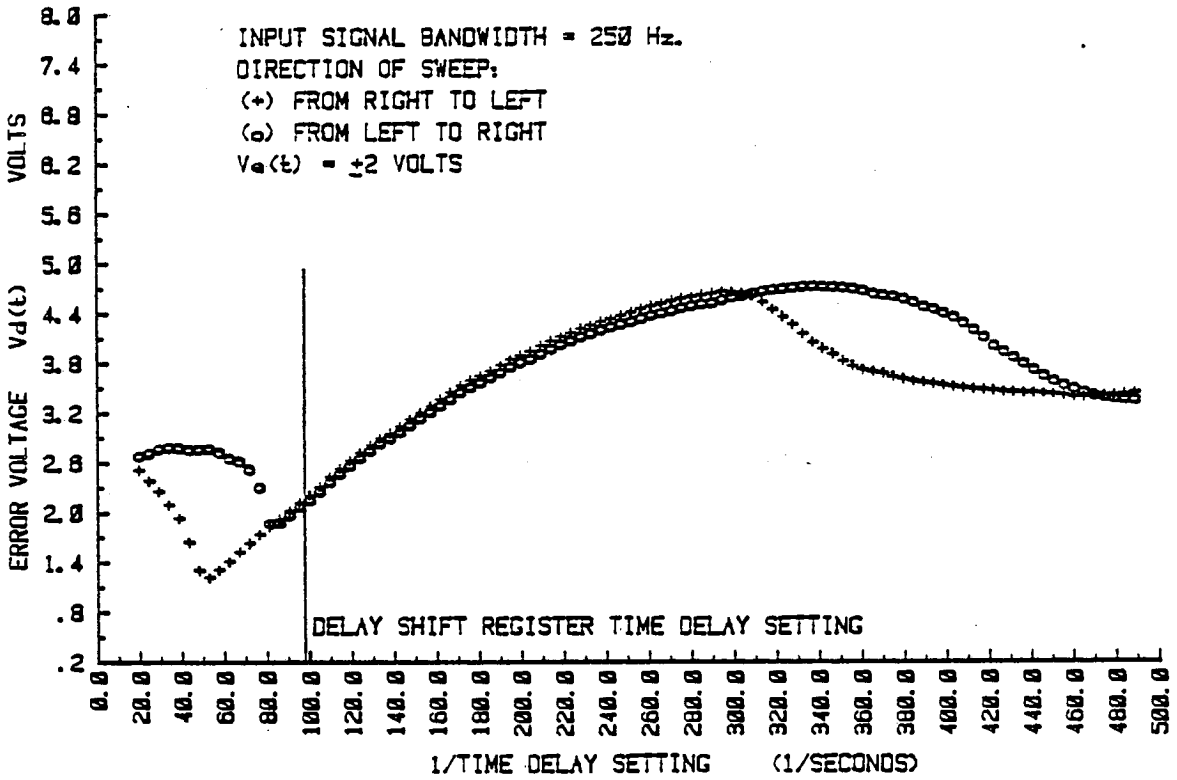

(b) THE COUPLING NETWORKS CUT-OFF FREQUENCY = 49.7 Hz.
SMOOTHING FILTERS TIME CONSTANT = 50 SECONDS.
TIME DELAY SETTING PERIOD = 19 SECONDS (1900/100).
NORMALISED CORRELATION FUNCTION PEAK AMPLITUDE = 0.2 .

Fig. 5-20 ERROR VOLTAGE RESPONSE TO THE INPUT SIGNAL TIME DELAY SWEEP.

differentiated correlation function (polarity), Kd. This slope, Kd, is being determined by the coupling networks cut-off frequency as well as the input signal bandwidth. The performance of the tracking loop with different slopes was investigated by sweeping the input signal time delay over a 25 to 1 range with sweep time of 707 seconds in either direction. Since figure 5-19 and 5-20 describes the response of the error voltage, Vd(t), with the coupling networks cut off frequency of 49.7 Hz, for the purpose of comparison the performance of the tracking loop with the coupling networks cut-off frequency of 10 Hz was investigated and is given in figure 5-21.

From figure 5-21 it will be seen that the tracking correlator with the coupling networks cut-off frequency of 10 Hz is capable of tracking the peak of the correlation function within its linear lock range accurately. In addition from figure 5-21 it is clear that the tracking range of the loop is reduced in comparison to the situation shown in figure 5-19 and 5-20(a), where the coupling networks cut-off frequency was set to 49.7 Hz. Therefore for a given input signal bandwidth, the tracking range of the loop decreases as the coupling networks cut-off frequency reduces.

Since the flow noise signal is expected to vary over a 50 to 500 Hz bandwidth range, the performance of the loop at the top and the bottom of this range, with the coupling networks cut-off frequency of 49.7 Hz was investigated. The response of the error voltage to the input signal time delay sweep with the bandwidth of

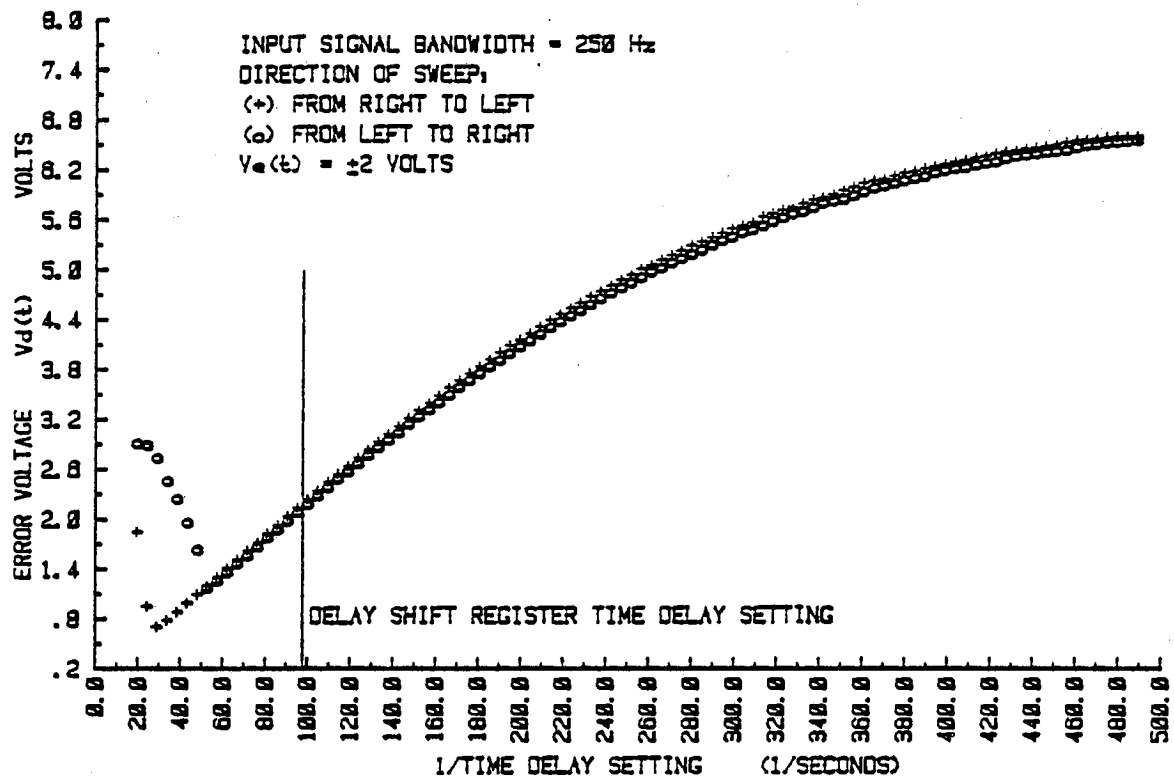

(a) THE COUPLING NETWORKS CUT-OFF FREQUENCY = 10 Hz.
SMOOTHING FILTERS TIME CONSTANT = 11.4 SECONDS.
TIME DELAY SETTING PERIOD = 7 SECONDS (707/100).
NORMALISED CORRELATION FUNCTION PEAK AMPLITUDE = 1 .

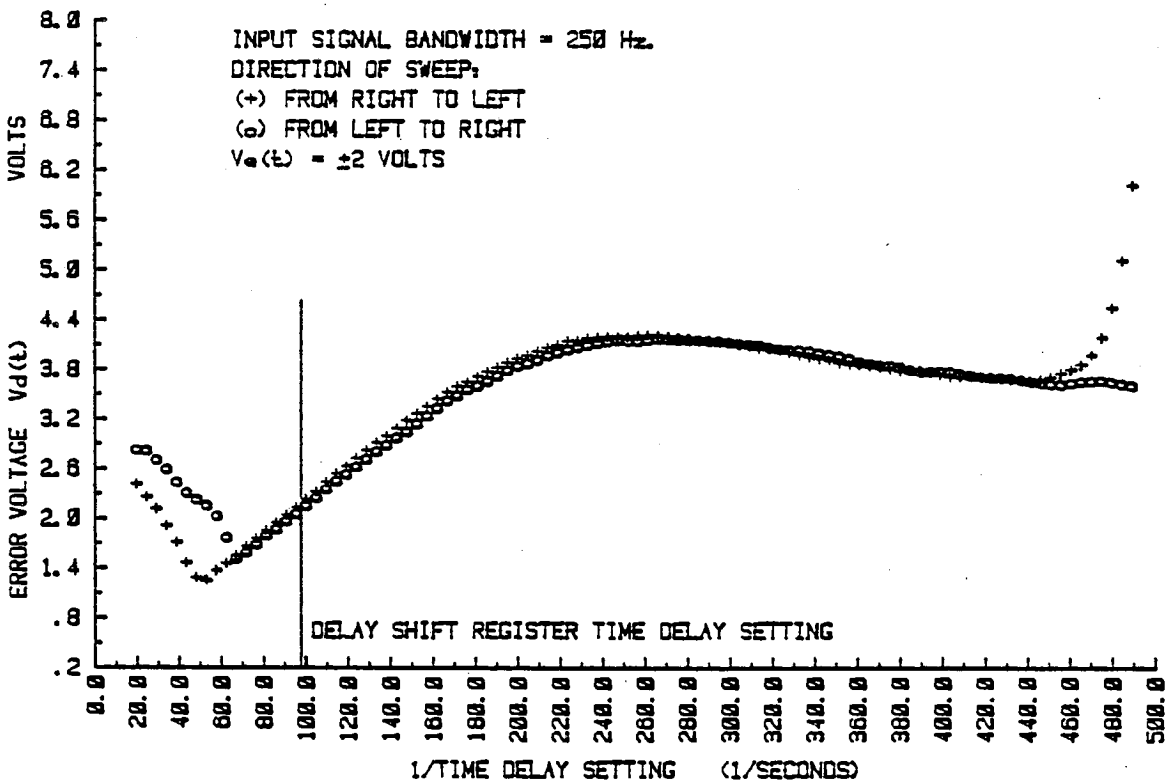

(b) THE COUPLING NETWORKS CUT-OFF FREQUENCY = 10 Hz.
SMOOTHING FILTERS TIME CONSTANT = 11.4 SECONDS.
TIME DELAY SETTING PERIOD = 7 SECONDS (707/100).
NORMALISED CORRELATION FUNCTION PEAK AMPLITUDE = 0.2 .

Fig. 5-21 ERROR VOLTAGE RESPONSE TO THE INPUT SIGNAL TIME DELAY SWEEP.

500 Hz and the normalised correlation function peak amplitude of 1 is shown in figure 5-22. From figure 5-22 it will be seen that the loop is capable of tracking the peak of the correlation function within its linear lock range. The response of the error voltage to the input signal time delay sweep of 50 Hz bandwidth and the normalised correlation function peak amplitude of 1 and .2 is shown in figure 5-23. From the results shown in figure 5-23(b) it will be seen that the loop is capable of tracking the peak even under the worst case input signal condition, (i.e. when the input signal bandwidth is approximately equal to 50 Hz with the normalised correlation function peak amplitude is .2).

Under the worst case input signal condition, the error voltage response to the input signal time delay sweep, shown in figure 5-23(b), is fluctuating about its mean value within its tracking range. An additional experiment was performed to investigate the performance of the tracking loop, with the coupling networks cut-off frequency of 49.7 Hz, but the smoothing filters time constant was increased to 20 seconds. From the results given in figure 5-24 it will be seen that although the time constant of the smoothing filter has increased to 20 seconds, the variance of the error signal has not been improved significantly and the error signal is still fluctuating about its mean value.

It has been found that an additional external smoothing filter having a time constant of 2 seconds, will reduce the error voltage, Vd(t), fluctuations, and the closed loop time constant of

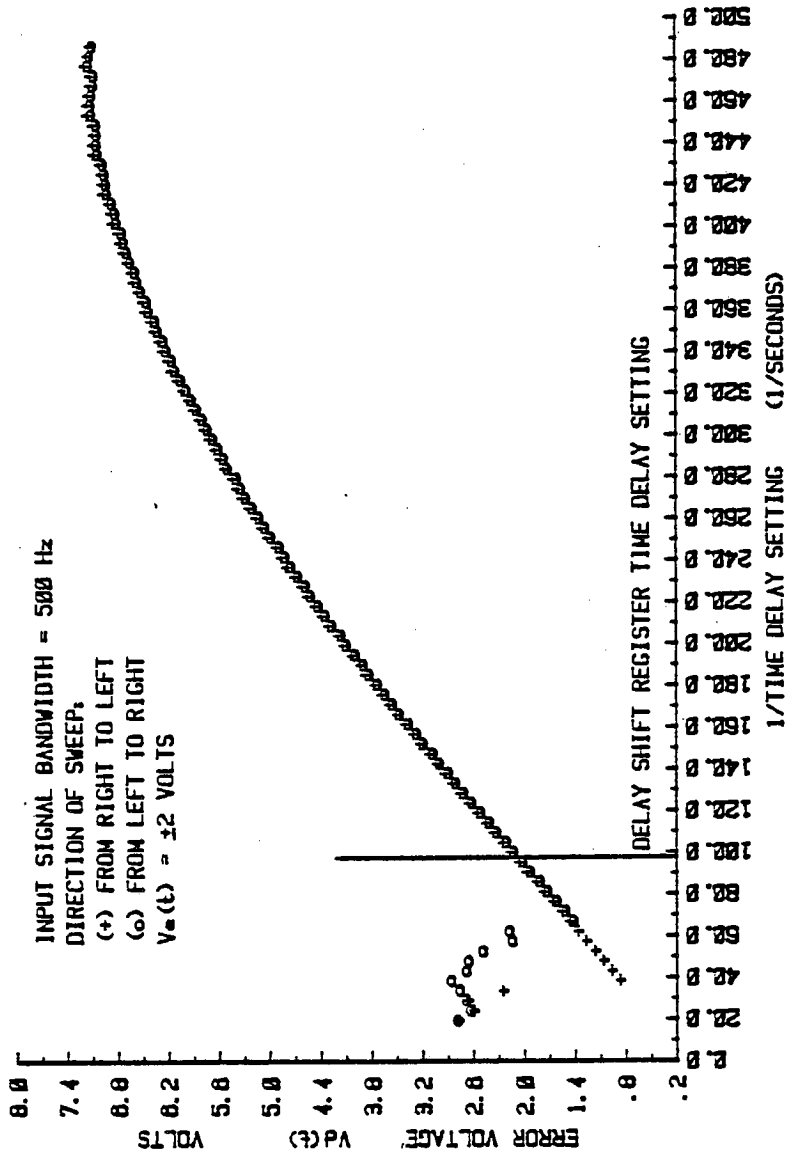

Fig. 5-22 ERROR VOLTAGE RESPONSE TO THE INPUT SIGNAL TIME DELAY SWEEP.

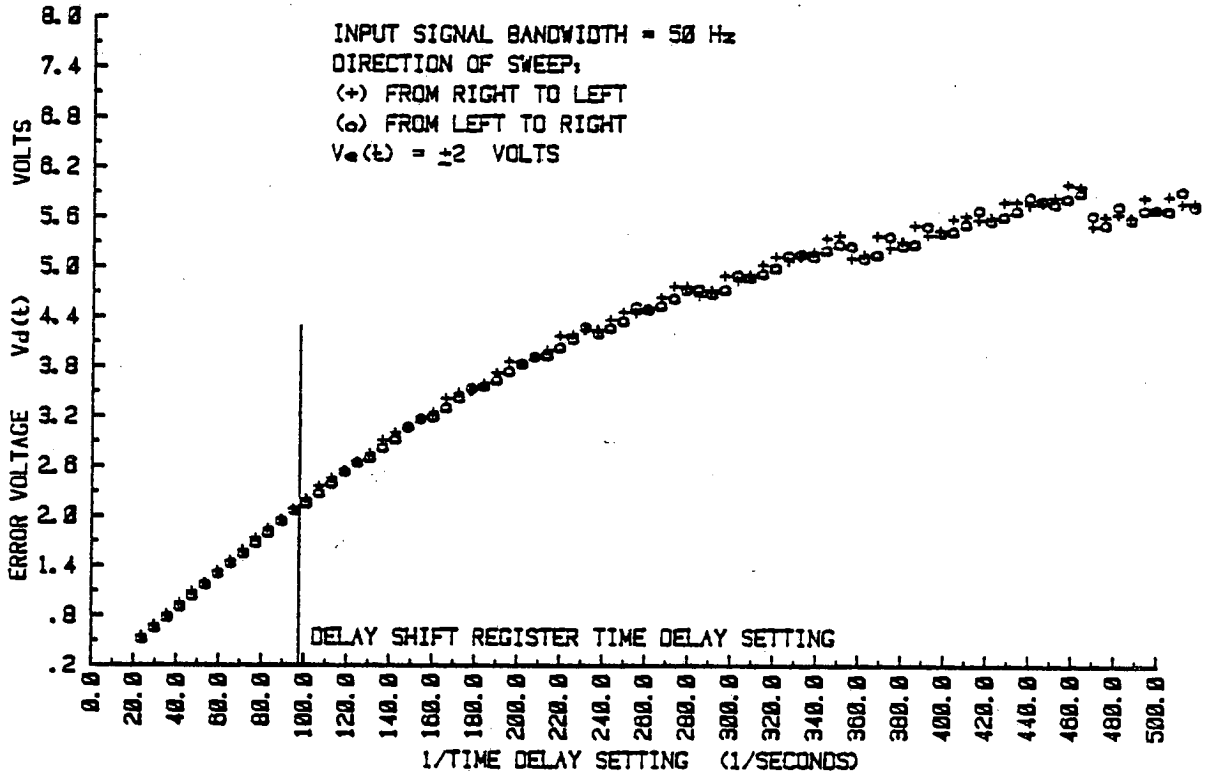

(a) THE COUPLING NETWORKS CUT-OFF FREQUENCY = 49.7 Hz.
SMOOTHING FILTERS TIME CONSTANT = 11.4 SECONDS.
TIME DELAY SETTING PERIOD = 7 SECONDS (707/100).
NORMALISED CORRELATION FUNCTION PEAK AMPLITUDE = 1 .

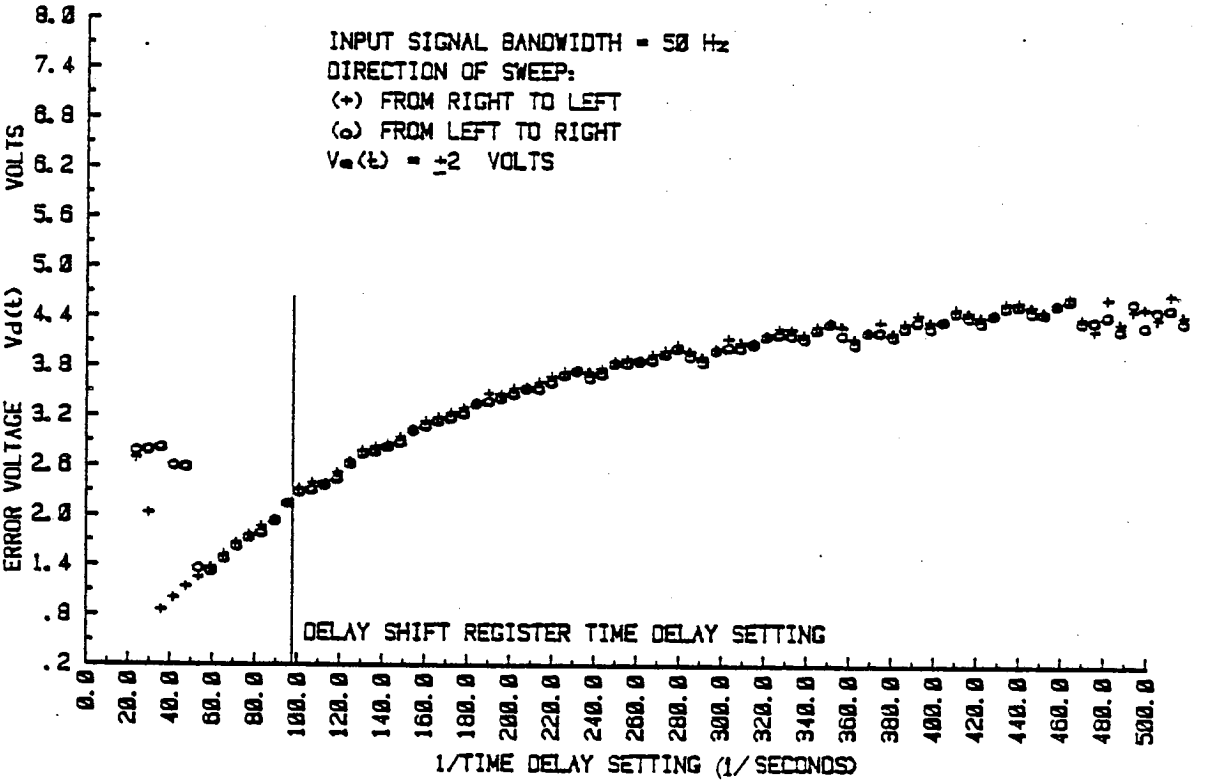

(b) THE COUPLING NETWORKS CUT-OFF FREQUENCY = 49.7 Hz.
SMOOTHING FILTERS TIME CONSTANT = 11.4 SECONDS.
TIME DELAY SETTING PERIOD = 7 SECONDS (707/100).
NORMALISED CORRELATION FUNCTION PEAK AMPLITUDE = 0.2 .

Fig. 5-23 ERROR VOLTAGE RESPONSE TO THE INPUT SIGNAL TIME DELAY SWEEP.

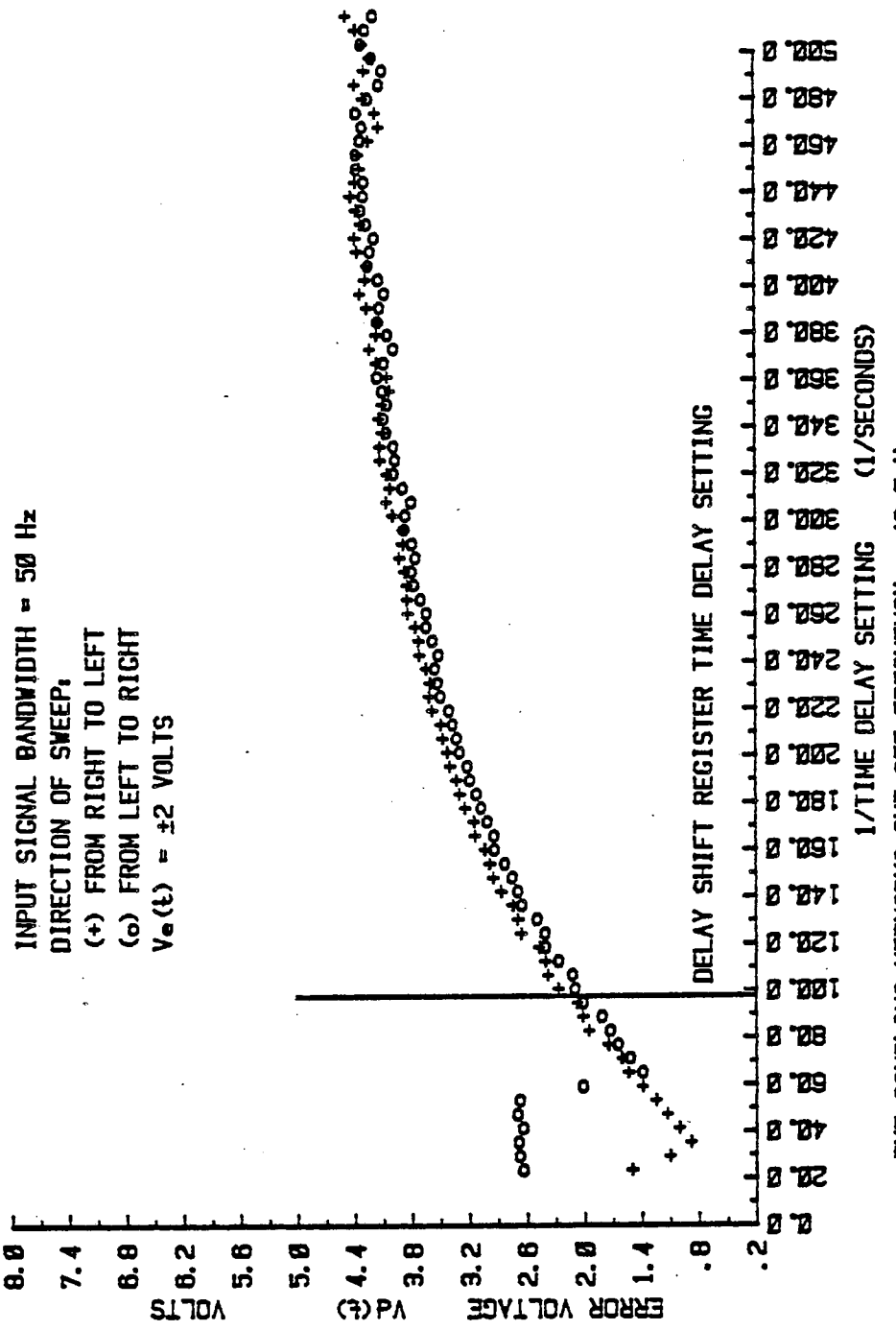

Fig. 5-24 ERROR VOLTAGE RESPONSE TO THE INPUT SIGNAL TIME DELAY SWEEP.

the tracking loops smoothing filter can be maintained at 11.4 seconds. Figure 5-25 describes the response of the error voltage to the input signal time delay sweep with the external smoothing filter time constant of 2 seconds. Note that the error voltage, Vd(t), is directly proportional to the output frequency of the VCO as well as the output voltage of the frequency to voltage convertor of the ICPT correlator shown in figure 5-1. Therefore the external smoothing filter used to reduce the error voltage fluctuations can be placed at the output terminal of the frequency to voltage convertor. From figure 5-25 it will be seen that although the error voltage fluctuation is reduced, the tracking loops linear lock range is poor.

Industrial experience has shown that the input signal bandwidth and its correlation function peak amplitude reduces as the flow velocity reduces, and the worst case situation is likely to happen when the input signal time delay is large (Taylor Instrument Ltd. 1976). Since the tracking loops overall gain increases as its delay shift register length increases, the gain of the loop is expected to be high at the worst case input signal condition (i.e. input signal bandwidth of 50 Hz and the normalised correlation function amplitude of .2). Therefore to observe the linear lock range of the tracking correlator the shift register length, np, is increased from 50 to 167 (i.e 34.21 msecs) and the input signal time delay is being swept over a range of 28.60 to 42.55 msecs, corresponding to 15 equally spaced flow velocities. The response of the error voltage, Vd(t), to input signal time delay sweep in both directions is shown in figure 5-26.

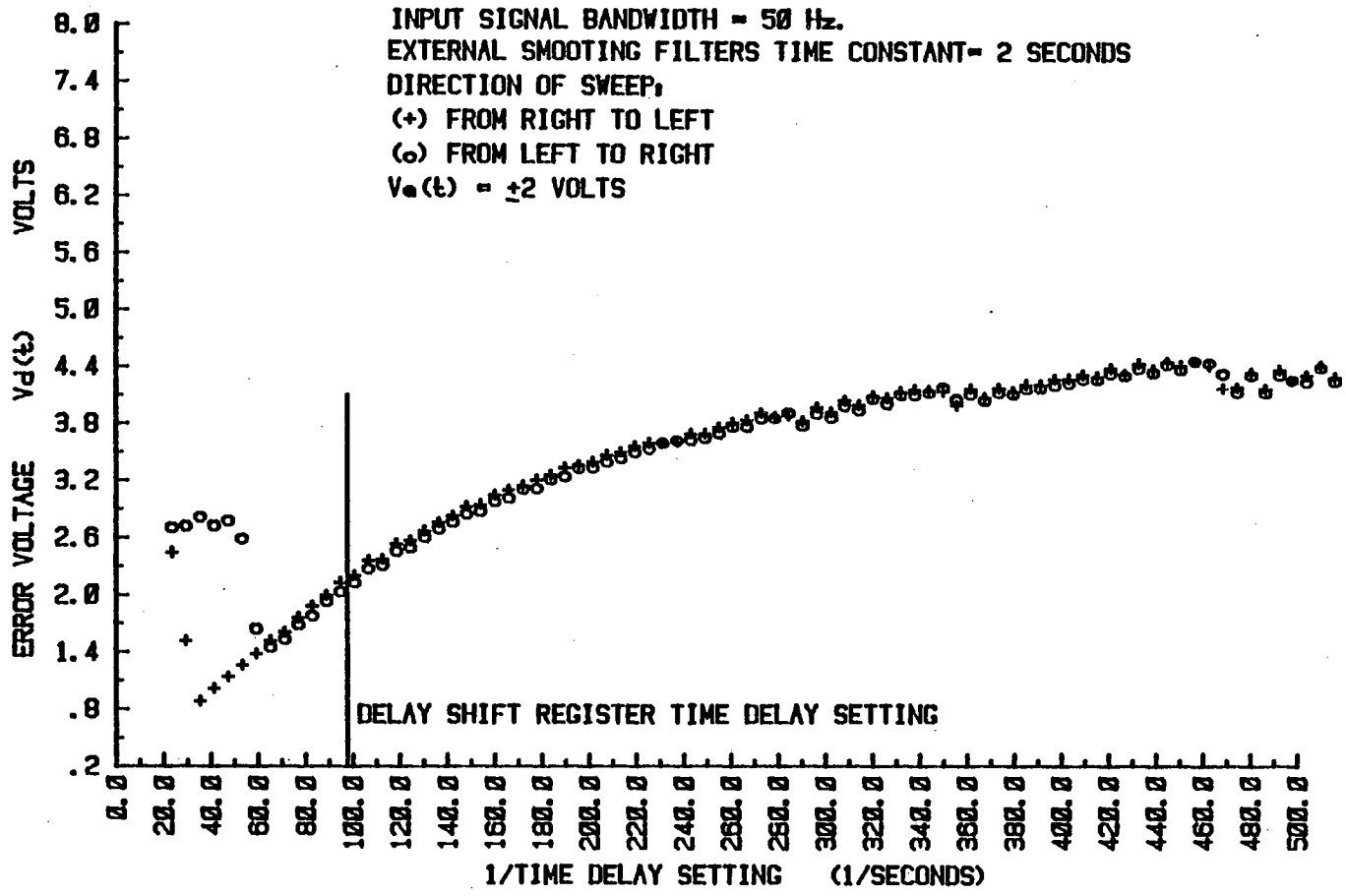

THE COUPLING NETWORKS CUT-OFF FREQUENCY = 49.7 Hz.
SMOOTHING FILTERS TIME CONSTANT = 11.4 SECONDS
TIME DELAY SETTING PERIOD = 14.5 SECONDS (1450/100).
NORMALISED CORRELATION FUNCTION PEAK AMPLITUDE = 0.2 .

Fig. 5-25 ERROR VOLTAGE RESPONSE TO THE INPUT SIGNAL TIME DELAY SWEEP.

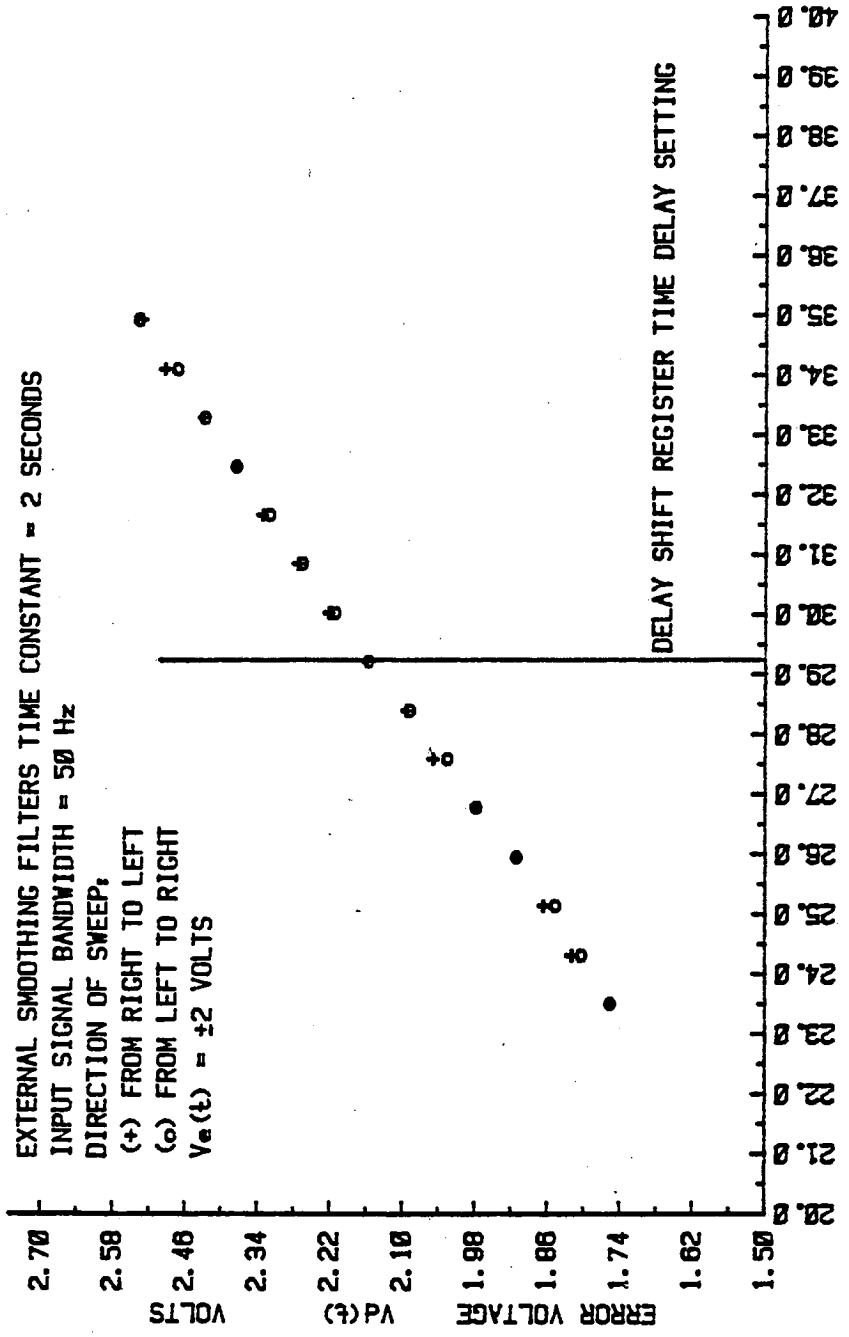

Fig. 5-26 ERROR VOLTAGE RESPONSE TO THE INPUT SIGNAL TIME DELAY SWEEP.

From figure 5-26 it will be seen that since the input signal time delay is being swept over a small range with the shift register length of 167, and the external smoothing filter time constant of 2 seconds, the error voltage fluctuation is reduced and its linear lock range is observable.

Leitner (1979) has suggested that in order to maintain the two point difference correlator in the lock mode, the micro-computer based correlator can be programmed in such a way that if a change in the peak position is detected, the two point difference correlator is required to be set by the micro-computers new peak position estimate. To observe the performance of the tracking correlator with the suggestion made by Leitner the coarse position latch is permanently enabled and the micro-computer correlator is programmed as suggested, and the above experiment with the worst case input signal condition is repeated. Figure 5-27 describes the response of the tracking correlator to input signal time delay sweep in both directions. Note that since the coarse position latch is permanently enabled the output of the frequency to voltage convertor with the external smoothing filter time constant of 2 seconds, is plotted against the flow-rate sweep. From figure 5-27 it will be seen that at the worst case input signal condition, due to the high percentage repeatability of the 6809 based coarse correlator (i.e. approximately 30%) the output response of the tracking correlator is jittery. Therefore by comparison of the results given in figure 5-26 and 5-27 it is clear that even at the worst case input signal condition, the tracking correlator can track the peak of the correlation function

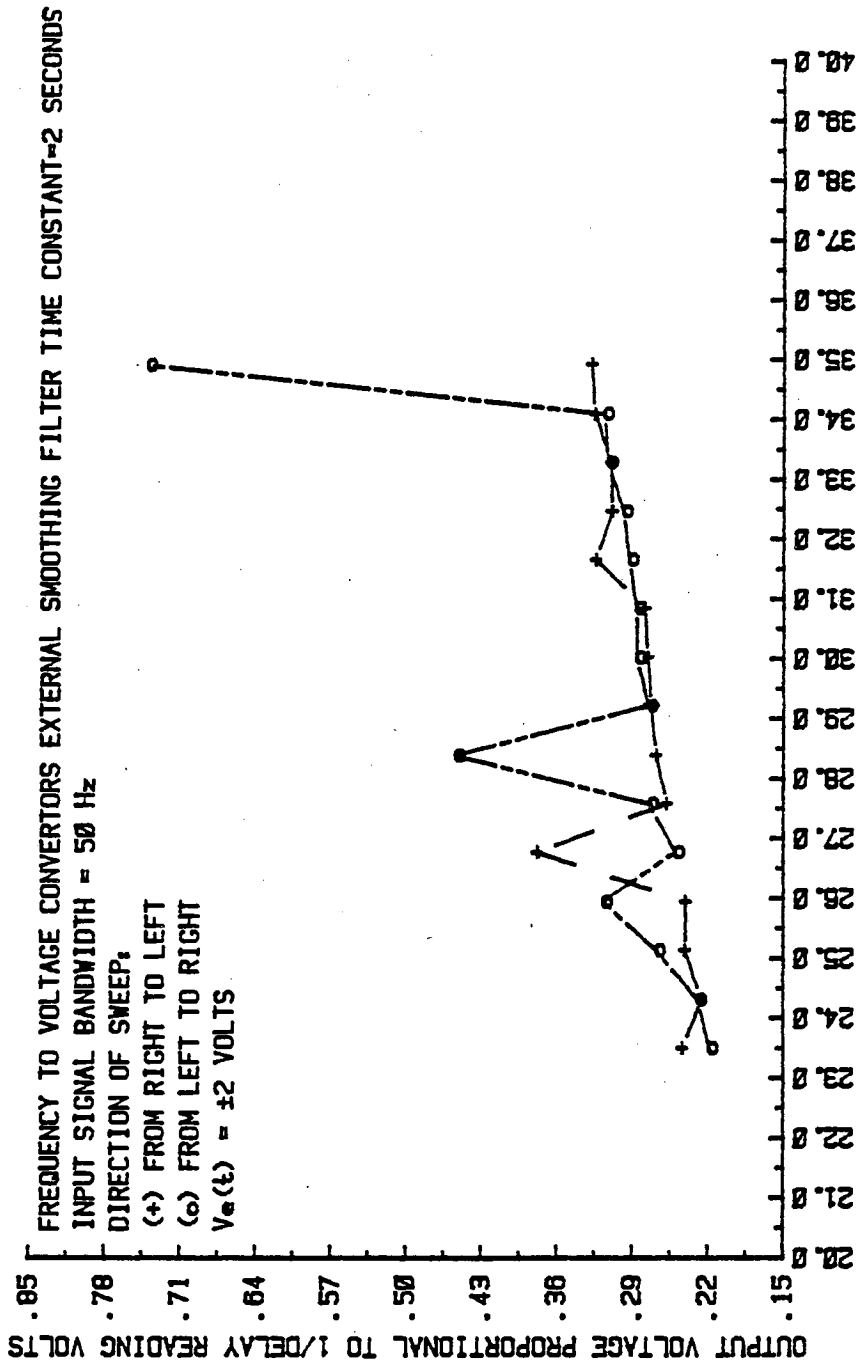

Fig.5-27 PERFORMANCE OF THE MICRO-COMPUTER CONTROLLED LOOP.

more linearly when the coarse position latch is maintained disabled within its linear lock range.

From the experimental results obtained in this section the optimum settings for the tracking correlator, over an input signal bandwidth of 50 Hz to 500 Hz, with the normalised correlation function of 1 to .2 is given below:-

i) Coupling networks cut-off frequency = 49.7 Hz.

ii) Tracking correlators smoothing filters time constant = 11.4 seconds.

iii) Percentage setting of the gain control potentiometer = 100 % (i.e. Ve(t)= $\pm$ 2 volts.).

iv) Shift register length = 256.

v) Free-running frequency of the VCO = 4882 Hz, (from the required time delay range to be measured by the ICPT correlator).

vi) External smoothing filter time constant at the output of the frequency to voltage convertor = 2 seconds.

For linear operation of the ICPT correlator the upper and lower limits of the window comparator is required to be equal to the linear lock range of the tracking loop over an input signal bandwidth of 50 to 500 Hz. The results given in figure 5-19, 5-20(a), 5-22, and 5-26 are used by the HP-85 auto-regression package (1981) to estimate the linear lock range of the tracking correlator, over an input signal bandwidth of 50 Hz to 500 Hz. Note that the upper and the lower limits of the linear curves refers to the upper and lower limits of the window comparator. In

addition the expected output voltage variation of the tracking correlators smoothing filter (error voltage) within its linear lock range is computed using the equation (5-10), by setting the input signal time delay variation, td , to be equal to the tracking loops time delay swing within its linear lock range. The computed and experimental results are compared in table 5-6. The slope of the differentiated correlation function (polarity) around the operating region of the tracking loop with the input signal bandwidth of 50 and 250 Hz, normalised correlation function peak amplitude of .2 are estimated from figure 5-28.

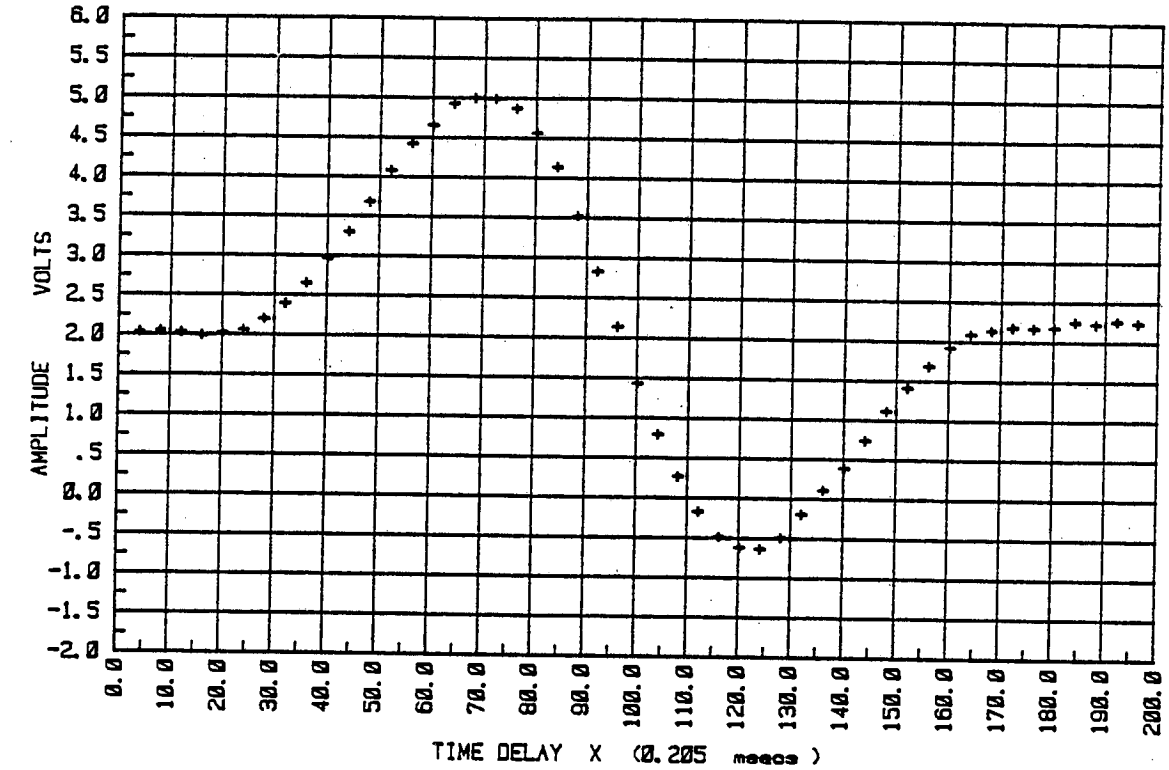

(a) THE COUPLING NETWORKS CUT-OFF FREQUENCY = 49.7 Hz.
INPUT SIGNAL BANDWIDTH = 50 Hz.
NORMALISED CORRELATION FUNCTION PEAK AMPLITUDE = 0.2 .

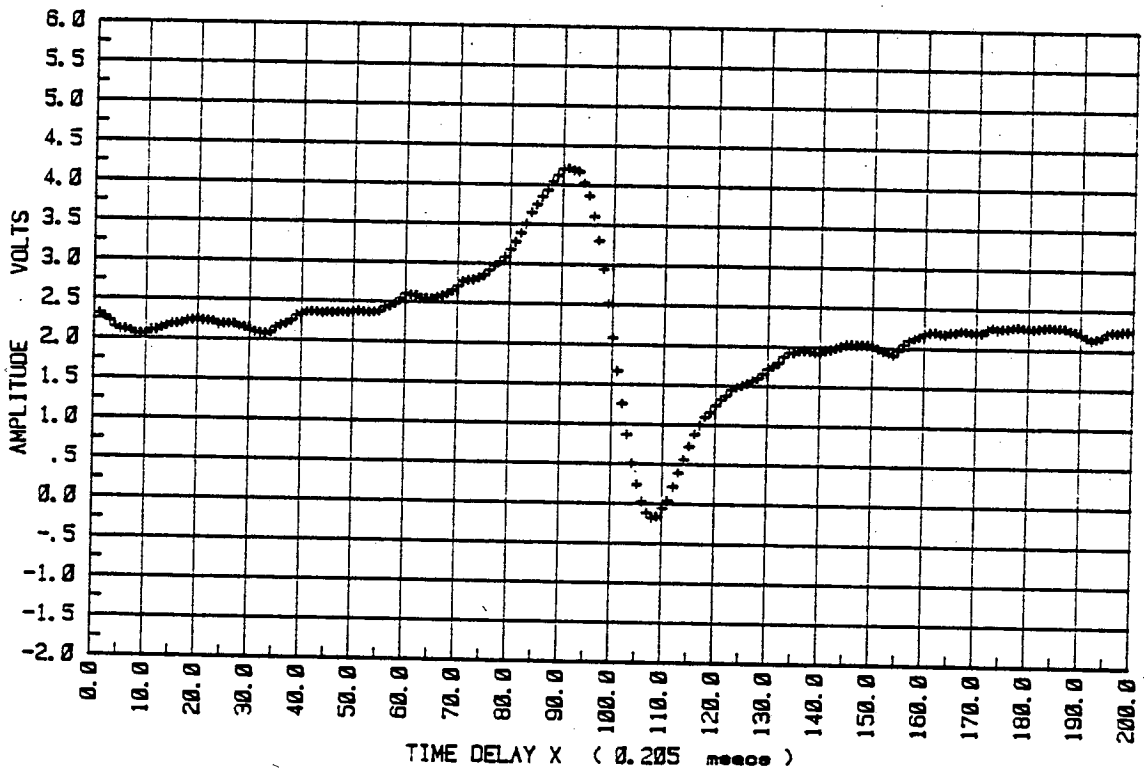

(b) THE COUPLING NETWORKS CUT-OFF FREQUENCY = 49.7 Hz.
INPUT SIGNAL BANDWIDTH = 250 Hz.
NORMALISED CORRELATION FUNCTION PEAK AMPLITUDE = 0.2 .

Fig. 5-28 DIFFERNTIATED CORRELATION FUNCTION (POLARITY).

INPUT SIGNAL BANDWIDTH Hz	500	250	250	50
NORMALISED PEAK AMPLITUDE	1	1	0.2	0.2
SLOPE V/SECS	−7837.86 (Fig.5-8)	-4929.63 (Fig.5-7)	-1998.12 (Fig.5-28)	-833.77 (Fig.5-28)
OPERATING FREQUENCY,Hz	5082	5050	5010	4950
RECORDED UPPER LIMIT, VOLTS	3.0	2.95	2.50	2.53
RECORDED LOWER LIMIT,VOLTS	1.45	1.6	1.70	1.75
RECORDED WINDOW VOLTAGE VOLTS	1.55	1.39	0.8	0.78
FROM FIGURE	5-22	5-19	5-20(a)	5-26
COMPUTED WINDOW VOLTAGE VOLTS	1.57	1.33	0.76	0.75

Table 5-6: The comparison of the recorded and computed window voltage over a input signal bandwidth of 50 to 500 Hz.

From comparison of the results given in table 5-6 it will be seen that, for a given slope of the differentiated correlation function (polarity), the upper and lower limits of the window comparator can be computed using equation (5-10). For example the upper and

the lower limits of the window comparator with the input signal bandwidth of 50 Hz, normalised correlation function peak amplitude of .2, and the linear lock range shown in figure 5-26 is computed as follows:-

i) The time delay difference,tDl and tDh, between the delay shift register time delay (at its operating point ,i.e tD = 167/4950 secs, fc = 4950 Hz, Vd(t)=2.16 volts) and the highest and the lowest time delay swing of the loop within its linear lock range is estimated from figure 5-26, and is given by:-

$$tDl=(1/23.5 - 167/4882) = 8.34 \text{ msecs}$$

and,

$$tDh=(167/4882 - 1/34.8) = 5.47 \text{ msecs}$$

ii) The error voltage variation ,Vd(t), is computed by substituting,td, of equation (5-10) with tDh and tDl respectively. Therefore the modulus of the highest error voltage difference with reference to the error voltage at the operating point of the loop is computed to be equal to .298 volts, and replacing td with tDl the modulus of the lowest error voltage difference is computed to be equal to .459 volts. Hence:-

Upper limit of the window comparator = 2.16+.298 = 2.458 volts

Lower limit of the window comparator = 2.16-.459 = 1.701 volts

Note that the computed upper and lower limits of the window comparator under the worst case input signal condition are in agreement with the experimental results given in table 5-6.

For linear operation of the ICPT correlator over an input signal bandwidth of 50 to 500 Hz from the results given in table 5-6, the upper and lower limits of the window comparator are set to be equal to 2.50 and 1.75 volts respectively. The performance of the ICPT correlator with the above window comparator settings is given in section 5-4.

5-2-2 Static Performance of the Tracking Correlator

The static performance of the tracking correlator with its optimum settings and a fixed delay shift register length was investigated using signals derived from the flow noise simulator described in chapter 3. The percentage repeatability of the tracking loops output was computed using equation 5-1 and taking 200 readings at each flow rate settings. Note that the percentage repeatability of the loop depends upon the bandwidth and signal to noise ratio of the input signal as well as the overall gain and the smoothing filter time constant of the tracking correlator. In addition the percentage output error of the tracking loop (Taylor Instrument Ltd. 1976) was computed using :-

$$\%\text{output error} = \frac{\%\text{output} - \%\text{input}}{\%\text{input}} \qquad (5\text{-}12)$$

Two set of experiments were carried out to investigate the static performance of the tracking loop within its linear lock range, over an input signal bandwidth of 50 to 500 Hz. It is important to note that initially, the length of the delay shift register ,np, was set by the peak position estimate of the 6809 based coarse correlator and the coarse position latch was disabled during the experiments.

First the static performance of the tracking loop over an input signal time delay range of 1.896 to 1.638 msecs was recorded. The above time delay range is approximately equal to the smallest time delay required to be measured by the ICPT correlator. The HP-85 micro-computer was programmed to divide the above time delay range to 21 equally spaced flow velocities, and the output of the frequency to voltage convertor of the tracking loop with the smoothing filter time constant of 2 seconds was recorded after each time delay settings. The measurement time by the HP-85 computer for each setting was set to be equal to 30 seconds.

Figure 5-29 describes the linear relationship between the input signal time delay and the output of the tracking loops frequency to voltage convertor at 21 equally spaced flow velocities. The time delay range shown in figure 5-29 is approximately equal to one sample clock period of the micro-computer based correlator. From figure 5-29 it will be seen that the smallest time delay range to be measured by the tracking loop is equal to 12.28 μ secs.

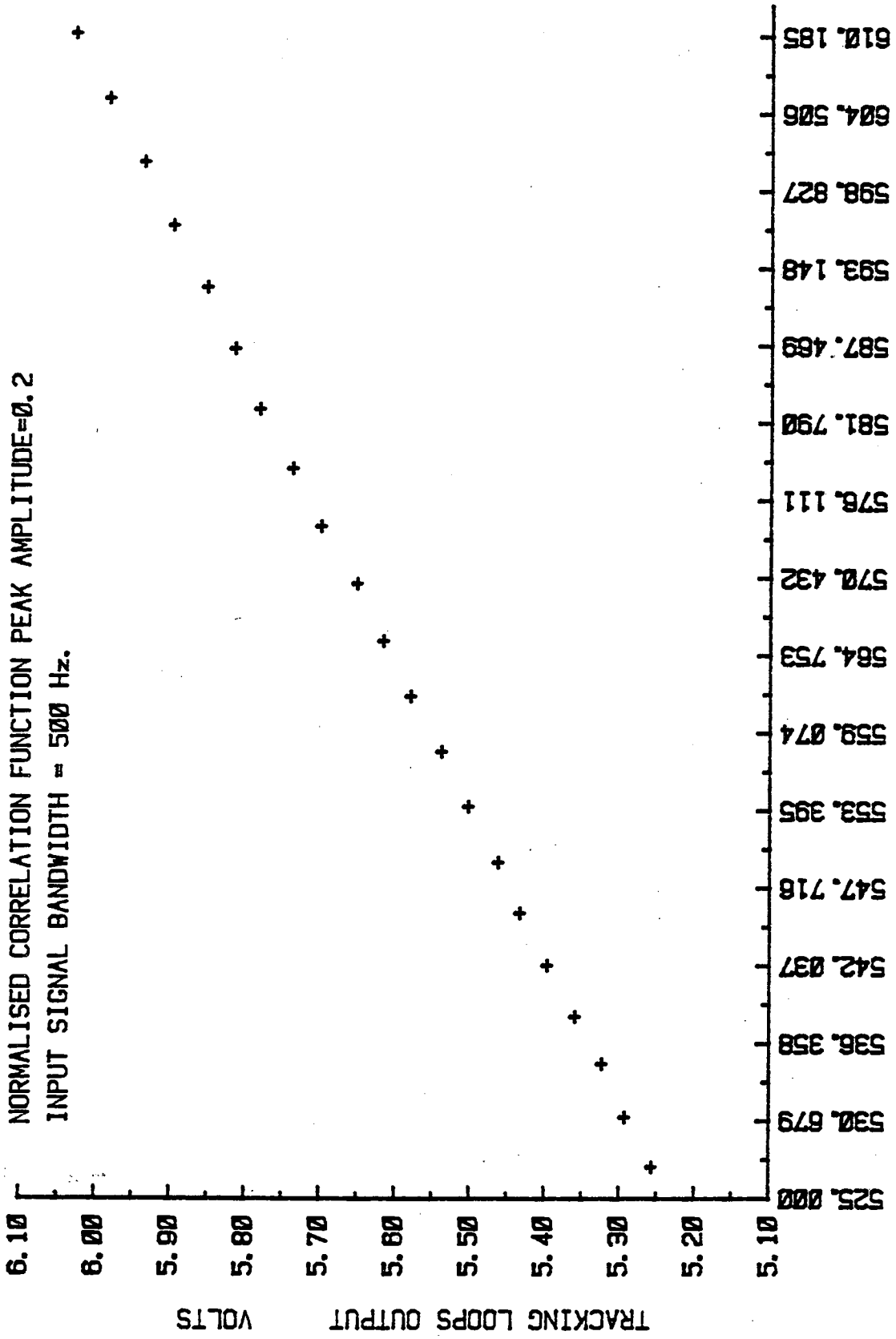

Fig. 5-29 STATIC PERFORMANCE OF THE LOOP.

The percentage output error of the tracking loop over the above input signal time delay range is shown in figure 5-30, and approximately is of order of +1.1%. Figure 5-31 describes the tracking loops percentage repeatability over an input signal time delay range of 1.896 to 1.638 msecs and is found to be of order of 0.3%.

The static performance of the tracking loop over an input signal time delay range of 51.153 to 43.371 msecs was investigated using the flow noise signal with bandwidth of 50 Hz and normalised correlation function amplitude of .2. The above time delay range is approximately equal to the largest time delay required to be measured by the ICPT correlator over an input signal time delay range of 32 to 1. The HP-85 computer was programmed to divide the above time delay range to 47 equally spaced flow velocities and the required settings for the flow noise simulator was computed. The measurement time between each input signal time delay setting was equal to 30 seconds. Figure 5-32 describes the linear relationship between the input signal time delay of the tracking loop and its frequency to voltage convertors output with the smoothing filter time constant of 2 seconds.

From figure 5-32 it will be seen that the tracking loop is capable of tracking the input signal time delay change with high resolution at the worst case input signal condition. The smallest time delay range being measured by the loop is equal to .17 msecs. The percentage output error of the tracking loop over the above

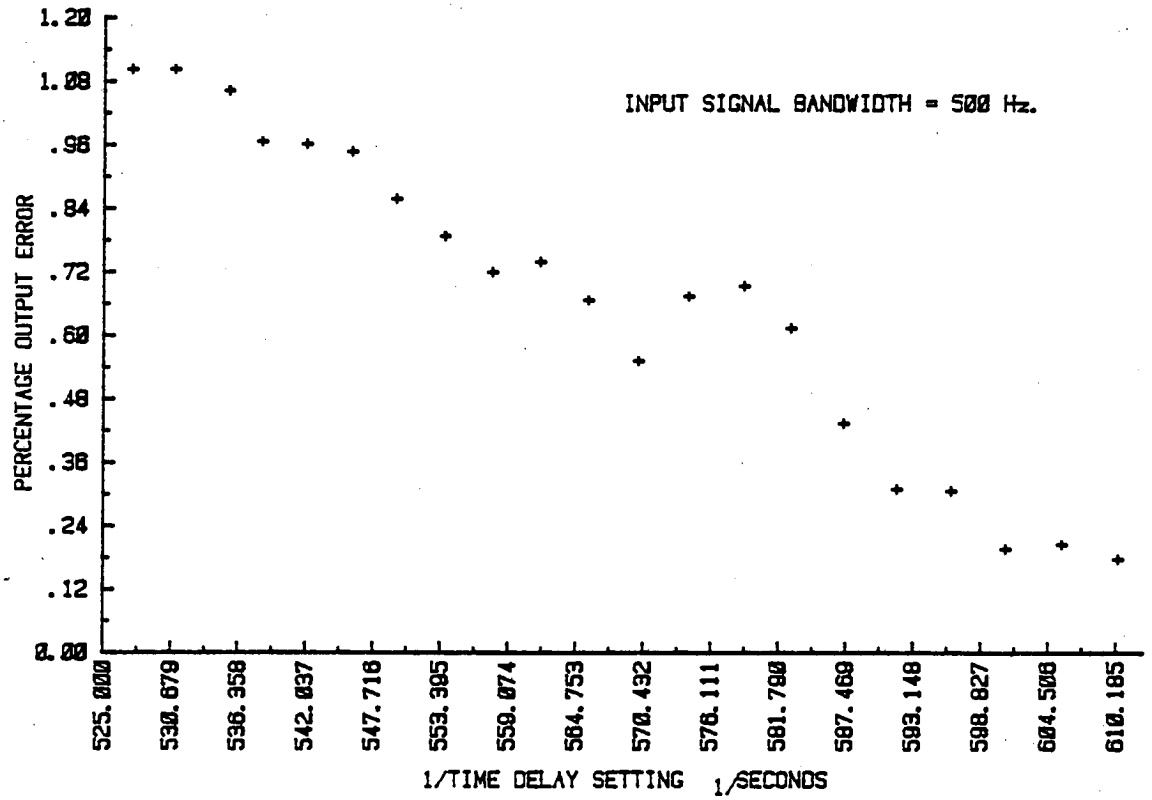

Fig. 5-30 PERCENTAGE OUTPUT ERROR OF THE LOOP

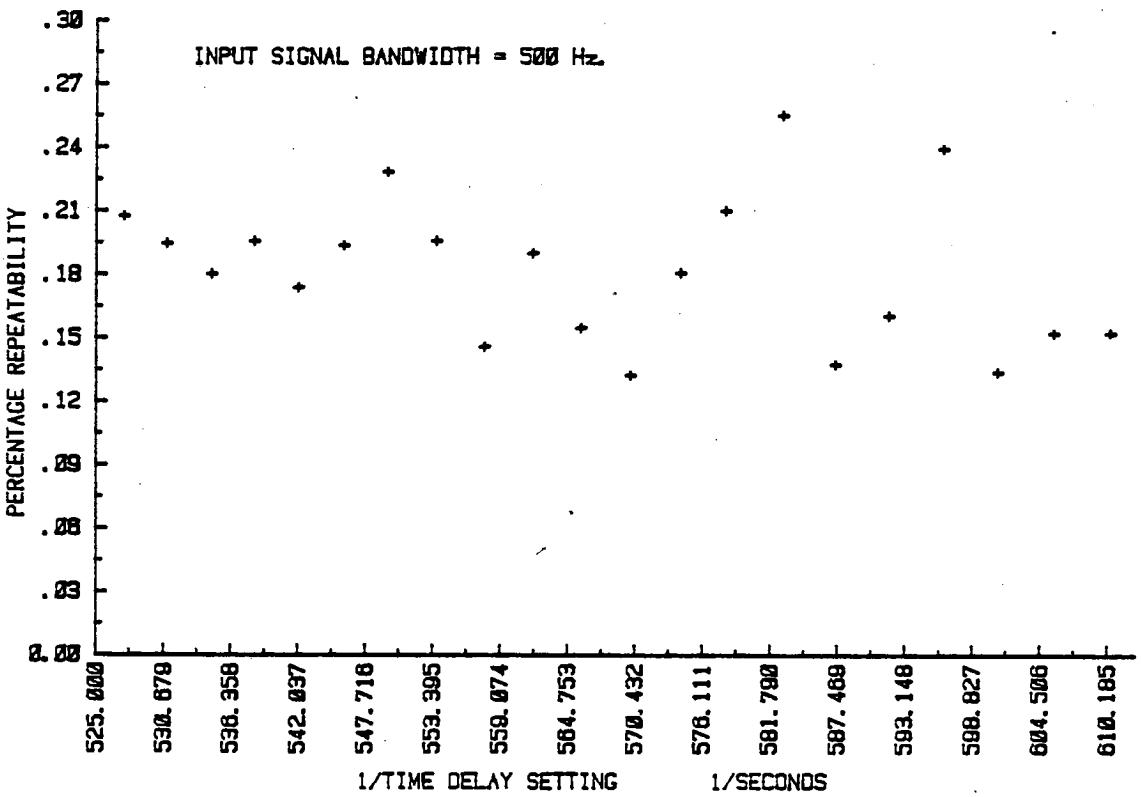

Fig. 5-31 PERCENTAGE REPEATABILITY OF THE LOOP.

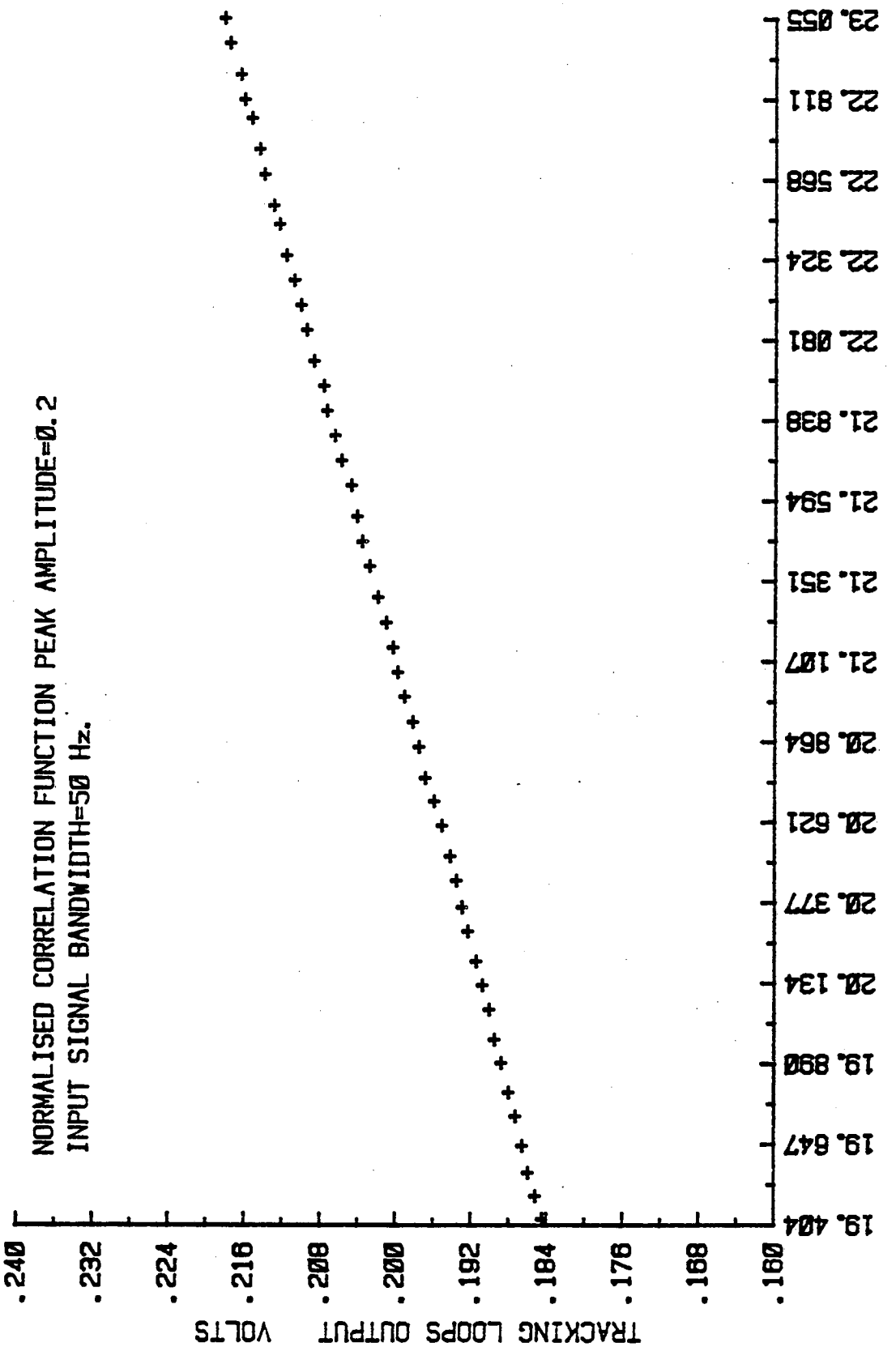

Fig.5-32 STATIC PERFORMANCE OF THE LOOP.

input signal time delay range is found to be less than -0.85% and is shown in figure 5-33. In addition the percentage repeatability of the tracking loops output shown in figure 5-34, is approximately of order of +1.7% .

From the results given in this section the resolution of the tracking loop with its optimum settings over an input signal time delay range of 32 to 1 was found to be equal to .6%. In addition the tracking loop is capable of tracking the input signal time delay with approximately ±1% output reading error and maximum repatability of 1.7%.

5-3 Performance of the Coarse Correlators

The performance of the coarse correlators was investigated using the noise signals derived from the flow noise simulator described in chapter 3. Equation 5-1 was used to compute the percentage repeatability of the coarse correlators time delay estimate over an input signal bandwidth of 50 to 500 Hz at 10 different settings. The percentage repeatability of the coarse correlators was computed by taking 200 readings from each input signal time delay settings.

The percentage repeatability function of the TRW TDC 1004J based coarse correlator with sampling clock frequency of 4882 Hz was computed using equation 5-1. To investigate the effect of averaging on the repeatability of the correlation function peak position estimate, the HP-85 computer was programmed to average 2,

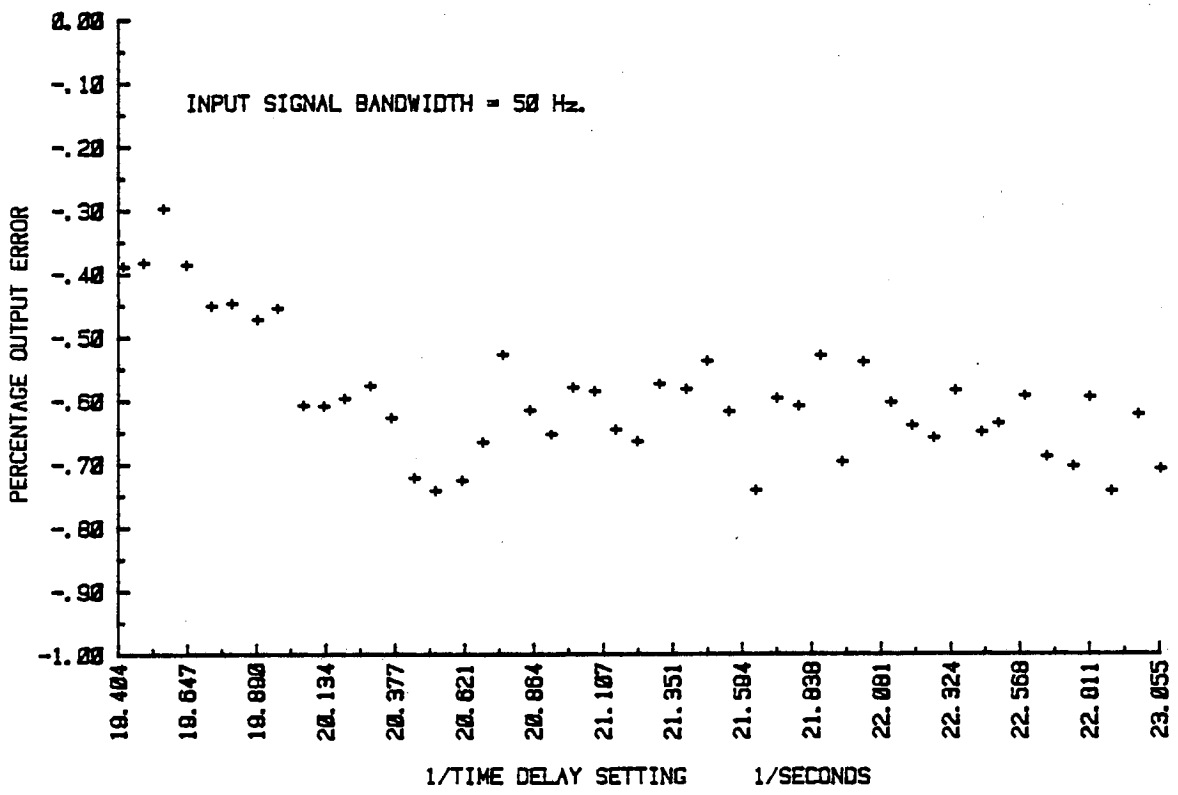

Fig. 5-33 PERCENTAGE OUTPUT ERROR OF THE LOOP.

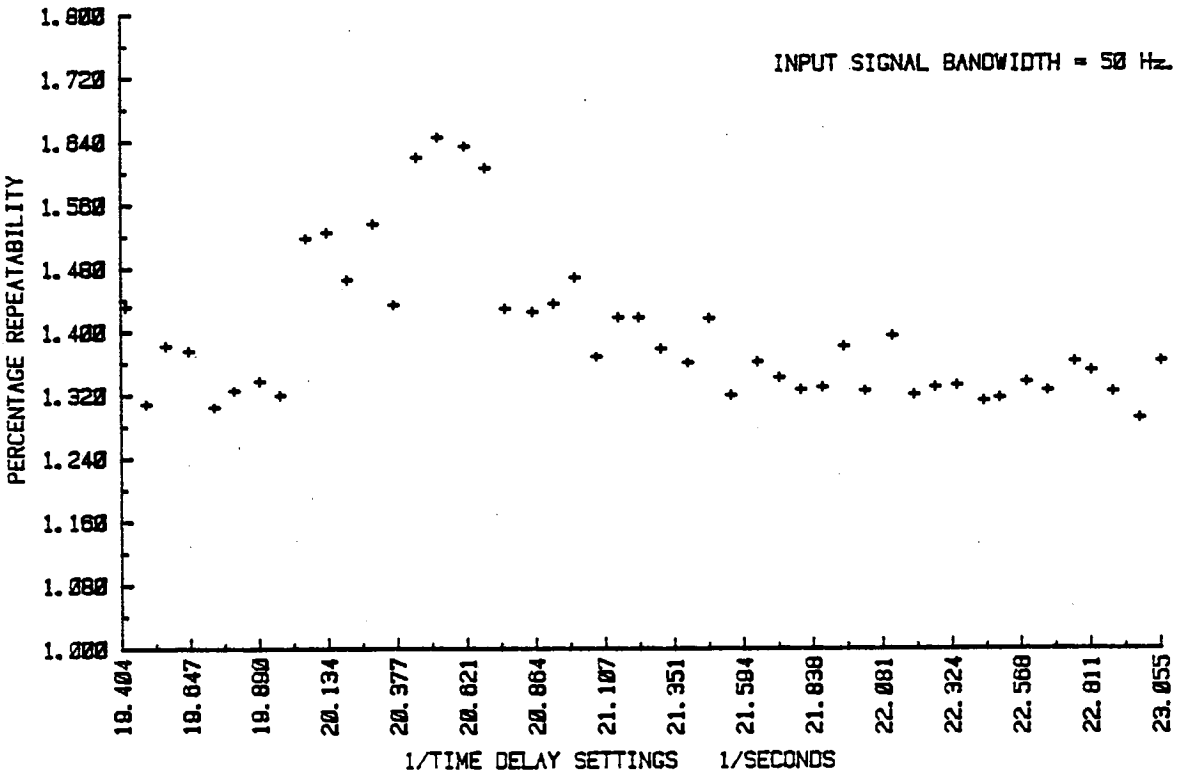

Fig. 5-34 PERCENTAGE REAPEATABILITY OF THE LOOP.

3 and 4 estimates of the correlation function before computing their percentage repeatability.

Figure 5-35 describes how the percentage repeatability of the TRW TDC1004J based coarse correlator varies over an input signal bandwidth of 50 to 500 Hz, and time delay range of 32 to 1. From figure 5-35 it will be seen that the percentage repeatability of the TRW TDC1004J based coarse correlator reduces as the number of the averaged correlation function estimates increases. In addition from the results given in figure 5-35 it will be seen that when the input signal bandwidth and its normalised correlation function peak amplitude is relatively low, due to its short measurement time, the percentage repeatability the TRW TDC1004J based coarse correlator is too high to be used as a coarse correlator. Therefore the TRW TDC 1004J based coarse correlator cannot be used to constrain the tracking loop to track the peak of the correlation function within its linear lock range over an input signal bandwidth of 50 to 500 Hz.

The above experiment was repeated to investigate the percentage repeatability of the micro-computer based coarse correlator with a measurement time of 1 second. The percentage repeatability of the micro-computer based coarse correlator with a sampling clock period of 2441 Hz is shown in figure 5-36. From figure 5-36 it will be seen that the maximum percentage repeatability of the micro-computer based coarse correlator is of the order of 30% and hence the position of the peak of the correlation function can be estimated more accurately using the

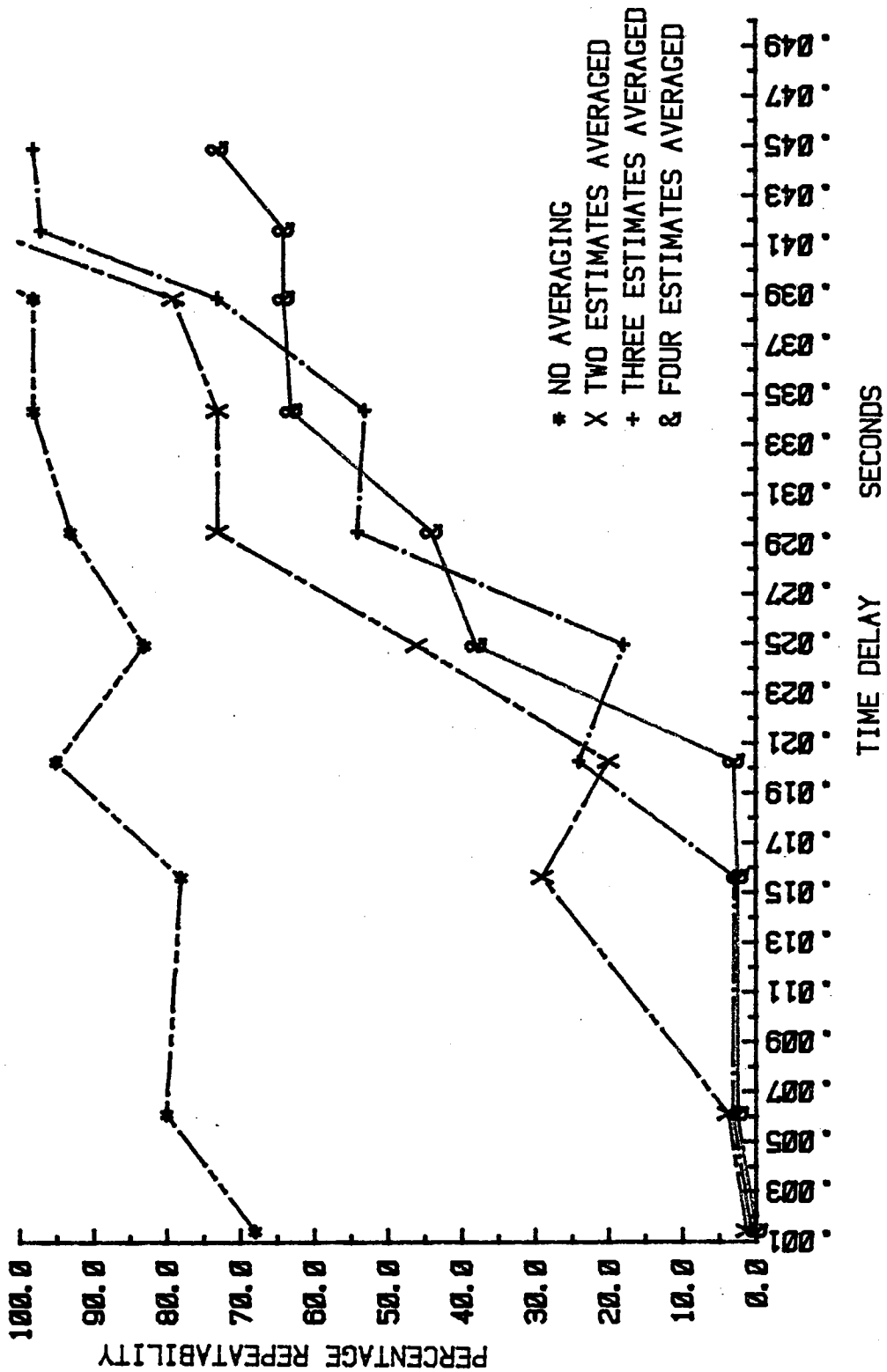

Fig. 5-35 PERCENTAGE REPEATABILITY OF THE TRW TDC1004J BASED CORRELATOR.

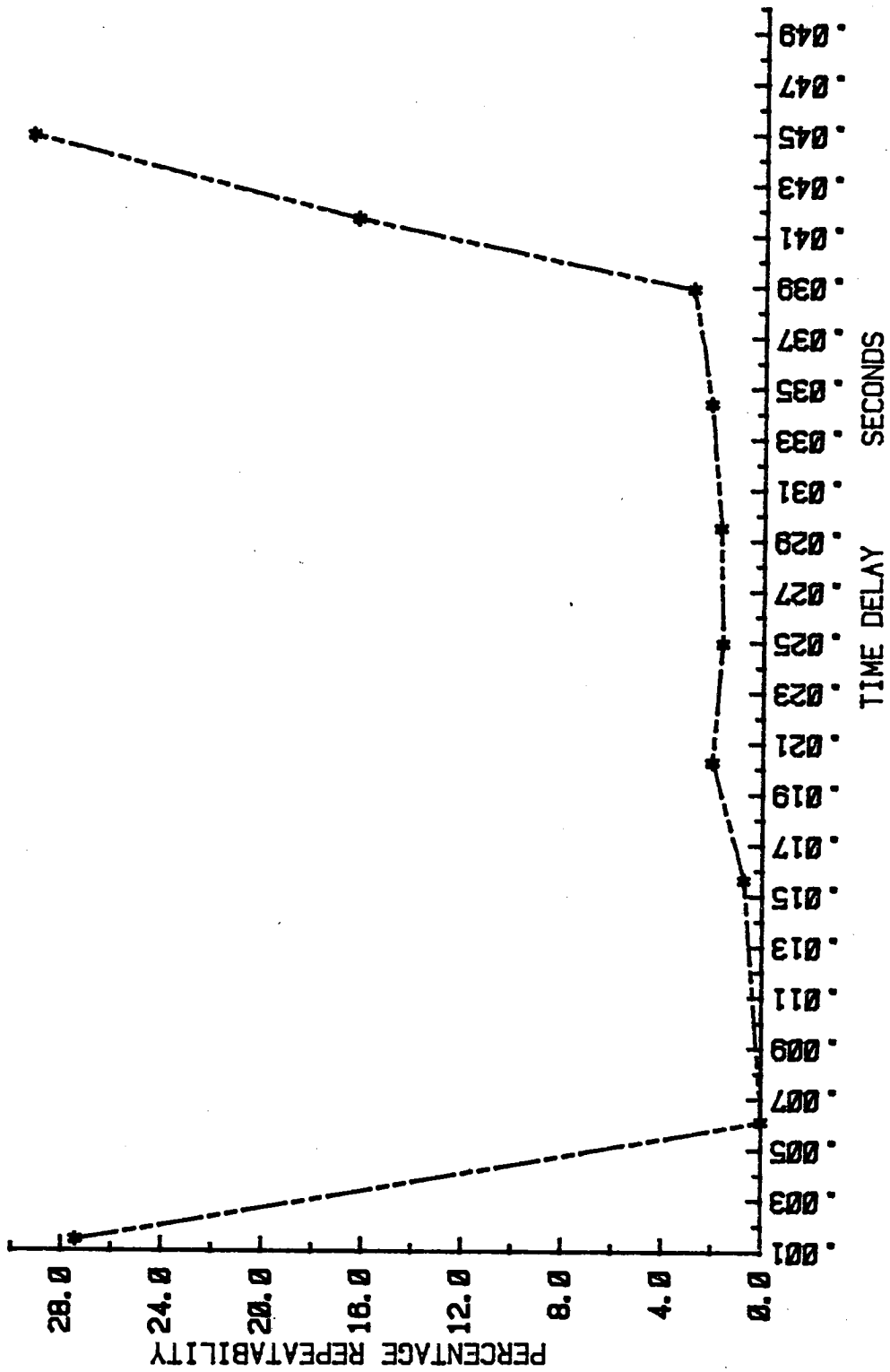

Fig. 5-36 PERCENTAGE REPEATABILITY OF THE 6809 BASED CORRELATOR.

micro-computer based coarse correlator.

5-4 Performance of the ICPT Correlator

The performance of the ICPT correlator over an input signal time delay range of 32 to 1, was investigated using the simulated flow noise signals derived from the noise simulator described in chapter 3. The 6809 based coarse correlator with maximum response time of 1 second was used to constrain the tracking loop to track the peak of the correlation function. From the results given in table 5-6, the upper and lower limits of the window comparator were set to be equal to the linear lock range of the tracking correlator over an input signal bandwidth of 50 to 500 Hz, (i.e. Vh = 2.50 volts, Vl = 1.75 volts). Therefore the coarse position latch is expected to be enabled only if the tracking loops error voltage is beyond the linear lock range of the tracking correlator.

The experimental programme to investigate the performance of the ICPT correlator was divided into two parts:-

i) Dynamic performance

ii) Static performance

The dynamic performance, for example the step response characteristic of the tracking loop when the shift register length is re-set by the new peak position estimate as well as the performance of the ICPT correlator under changing signal conditions are given. The percentage output error and repeatability of the ICPT correlator over an input signal time

delay range of 32 to 1 are given under static signal conditions.

5-4-1 Dynamic Performance of the ICPT Correlator

The output of the frequency to voltage convertor of the tracking correlator with 2 seconds smoothing filter time constant together with the error voltage, Vd(t), of the tracking loop was used to monitor the dynamic performance of the ICPT correlator. Note that the output of the window comparator together with the serial correlators comparator output was used to control the coarse position latch through the logic control with a truth table given in table 4-1 of chapter 4. The micro-computer based coarse correlator was used to estimate the peak of the correlation function continuously and the coarse position latch is expected to be enabled when the tracking loop is beyond its linear lock range.

The step response characteristic of the tracking loop when the error voltage is beyond its linear lock range was recorded using the two channel transient recorder shown in figure 5-2. The sample clock period of the transient recorder was set to 10 msecs and the output of the serial correlator together with the tracking loops smoothing filter output, Vd(t), were recorded. Initially the tracking loop was tracking the peak of the correlation function within its linear lock range with the delay shift register length of 14, and the input signal time delay of 3.07 msecs. The response characteristic of the error voltage, Vd(t), together with the output of the serial correlator when the input signal time delay suddenly changes to 4.6 msecs is shown in figure 5-37. Note that the above time delay change is beyond the

tracking loops linear lock range.

From figure 5-37 it will be seen that as the input signal time delay suddenly changes to 4.6 msecs the negative feedback action of the loop reduces the error voltage, Vd(t), in order to track the new peak of the correlation function. But the input signal time delay change is beyond the tracking loops linear lock range. Therefore once the error voltage is beyond the lower limit of the window comparator the output of the window comparator enables the coarse position latch and the delay shift register length is set by a new peak position estimate of the coarse correlator. The new delay shift register length of the loop increases, the input signal time delay of the tracking correlators multiplier further than the actual input signal time delay of the loop. Hence, as described in chapter 4, the negative feedback action of the loop increases the error voltage, Vd(t) in order to track the peak of the correlation function within its linear lock range as shown in figure 5-37.

From figure 5-37 the total transient response time of the loop to settle within the tolerance band of $\pm 1\%$, when the input signal time delay change is beyond its linear lock range is approximately equal to 1.57 seconds. The experimental results shown in figure 5-40 indicates that the step response of the loop to the sudden change of the delay shift register length is not significant on the output of the frequency to voltage convertor when a smoothing filter time constant of 2 seconds is used. Note that the above step response characteristic of the loop on the

output of the frequency to voltage convertor can be eliminated by programming the 6809 based coarse correlator to disable the output of the frequency to voltage convertor once the delay shift register length is up-dated and instead its coarse peak estimate can be used for a period of approximately 2 seconds.

In addition from figure 5-37 it will be seen that for a given input signal time delay change the output of the serial correlator with a time constant of 10 seconds was not changed significantly. Hence the serial correlators output can not be used to indicate the situations when the loop is tracking the peak of the function inaccurately.

From the truth table of the logic control given in chapter 4 , table 4-1, it will be seen that the serial correlators comparator output can only enable the coarse position latch if the input signal time delay suddenly changes over a large range. Figure 5-38 describes the output of the serial correlator together with the error voltage, Vd(t), when the input signal time delay suddenly changes over a 32 to 1 range. Initially the tracking loop was in the lock mode with input signal time delay of 1.433 msecs and the input signal time delay suddenly has changed to 51.2 msecs. From figure 5-38 it will be seen that the negative feedback action of the loop is forcing the error voltage to move away from the peak position of the correlation function. Therefore the output of the serial correlator falls below a normalised correlation function peak amplitude of .2 as shown in figure 5-38, and the coarse position latch will be enabled. From

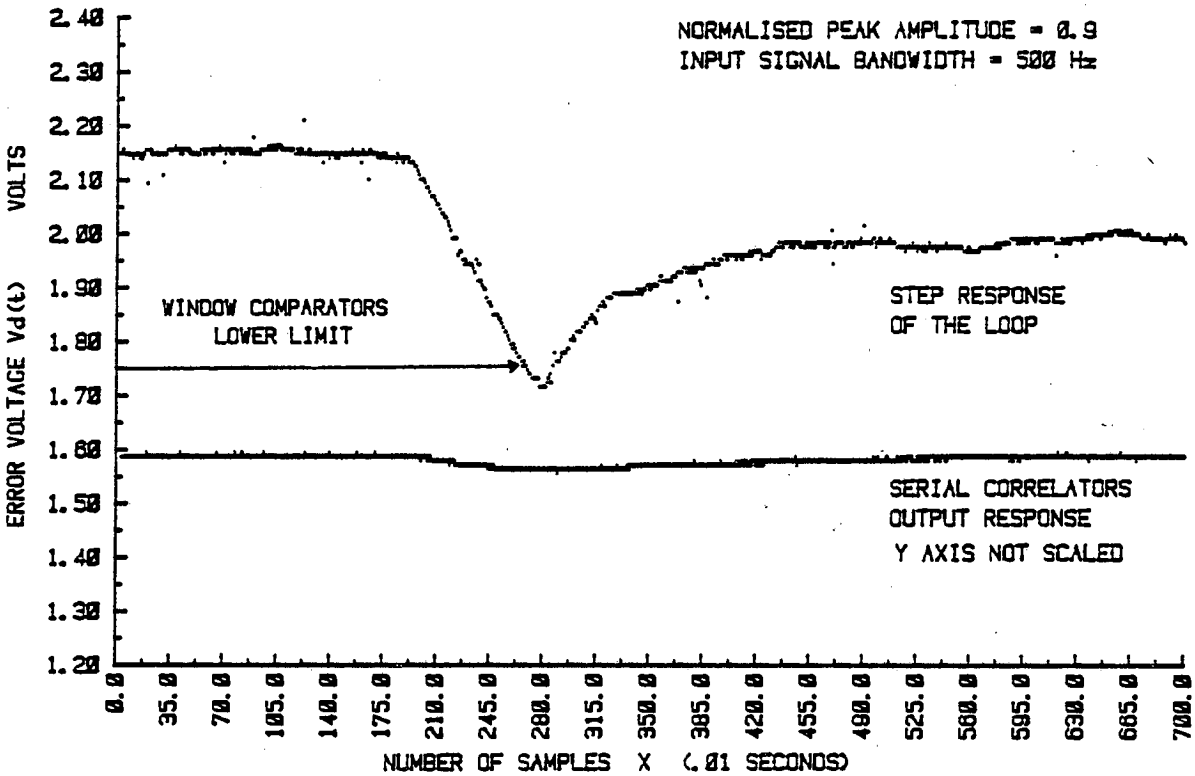

Fig. 5-37 STEP RESPONSE CHARACTERISTIC OF THE "ICPT" CORRELATOR.

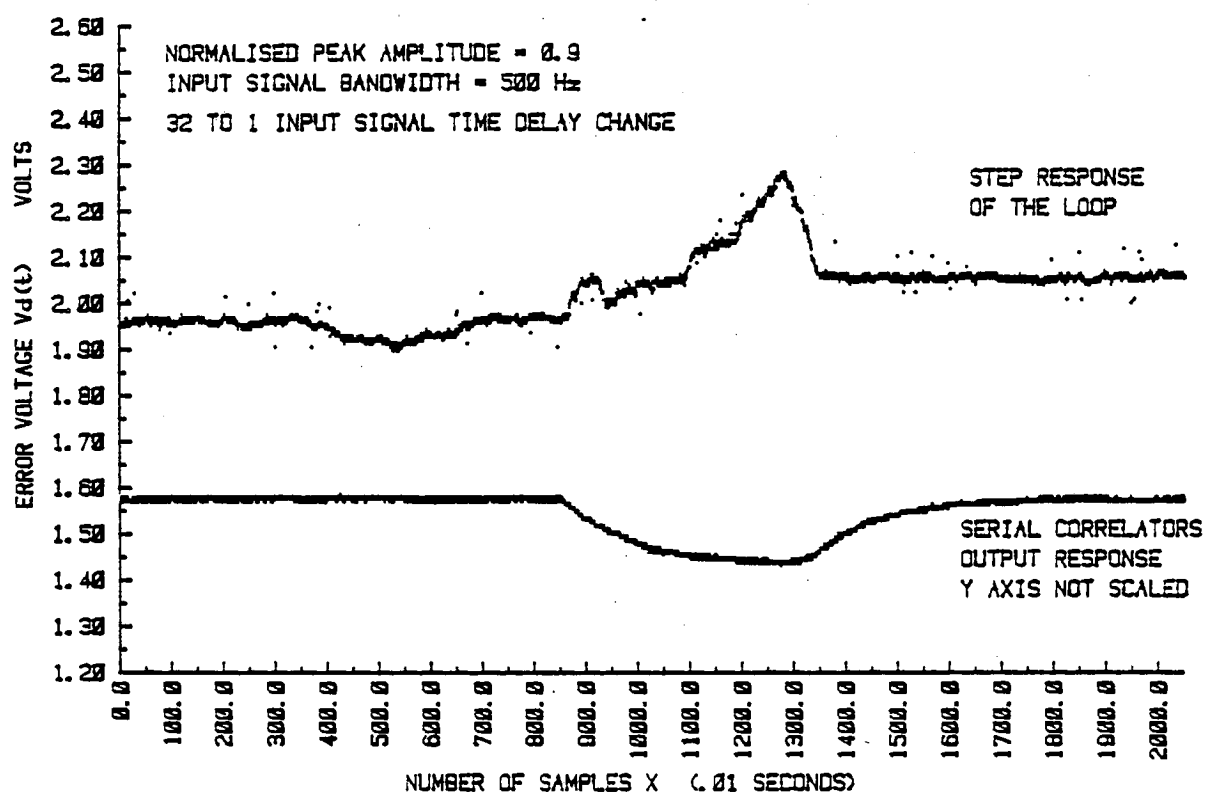

Fig. 5-38 STEP RESPONSE CHARACTERISTIC OF THE "ICPT" CORRELATOR.

figure 5-38 the total transient response time of the loop to settle within the tolerance band of $\pm 1\%$ is equal to 4.9 seconds.

The performance of the tracking correlator under changing signal conditions was investigated by sweeping the input signal time delay over a 24 to 1 range in both directions, at a different rates. The input signal time delay settings was computed to correspond to 100 equally spaced flow rates over an input signal bandwidth of 50 to 400 Hz. Therefore by sweeping the 100 equally spaced flow noise signal settings in both directions the output of the ICPT correlator (flow velocity) is expected to vary as a ramp function.

The expected normalised peak amplitude of the correlation function at 100 equally spaced flow velocities was computed using the equation 2-19 given in section 2-3-2 of chapter 2. Therefore the normalised peak amplitude and the input signal bandwidth is expected to reduce as the input signal time delay is increasing.

Figure 5-39 describes how the normalised peak amplitude and the bandwidth of the correlation function changes along the time delay axis. For simplicity only 8 different settings for each direction are shown.

The computed settings for the noise simulator were stored in an EPROM and were used as a look-up table by the 6809 based micro-computer of the noise simulator. The internal timer of the noise simulators micro-computer (Rockwell 6522 (VIA)) were used

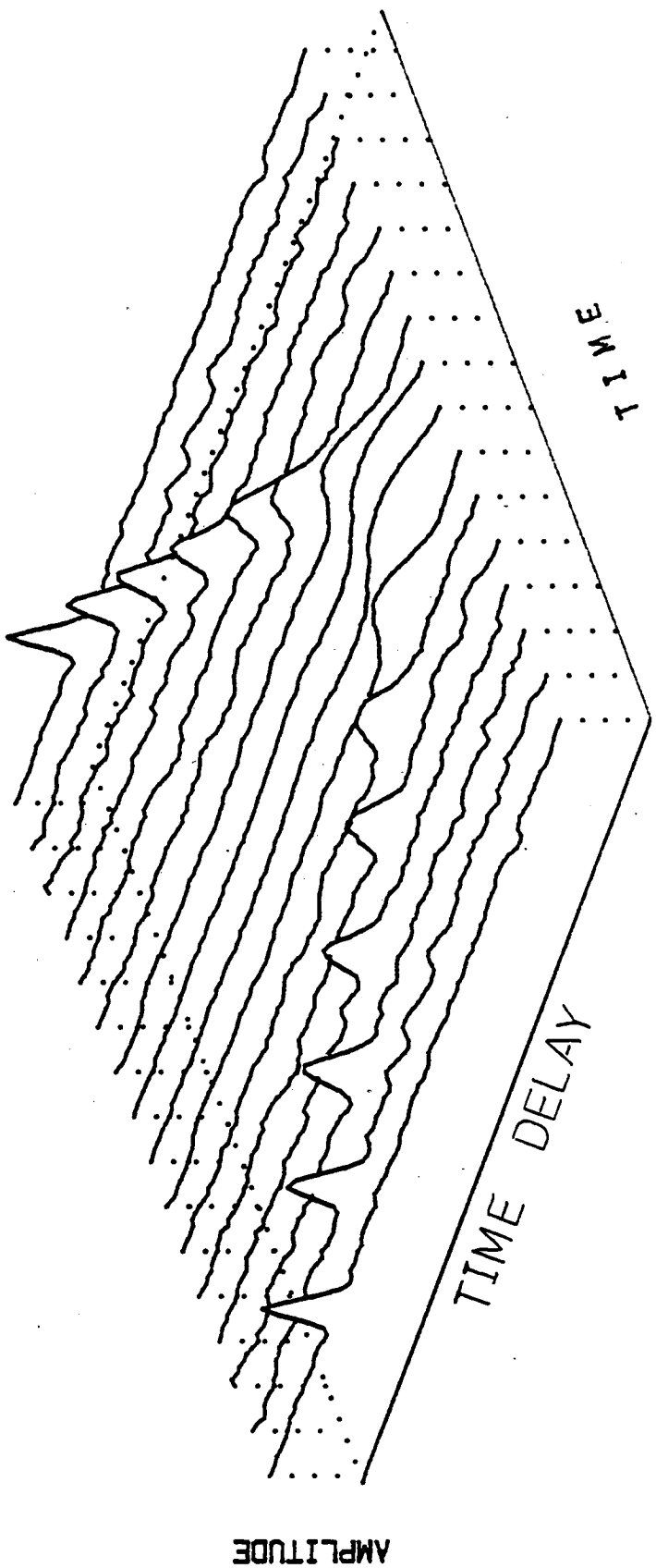

Fig. 5-39 CORRELATION FUNCTION PEAK POSITION SWEEP.

to estimate accurately the period of input signal time delay change. The 2 channel transient recorder shown in figure 5-2 with a sample clock period of 50 msecs were used to sample and store the output response of the ICPT correlator (output of the frequency to voltage convertor with smoothing filter time constant of 2 seconds).

Since the memory space of the transient recorder for each channel is limited to 2048 locations with a maximum sample clock period of 50 msecs, the complete output response of the ICPT correlator cannot be captured by the transient recorder if the period of the input signal time delay change exceeds 1 second. Therefore the HP-85 computer was used to sweep the input signal time delay backward and forward at a period slower than 1 second and the output of the ICPT correlator was recorded through a digital voltmeter by the HP-85 computer after each time delay setting. The internal timer of the HP-85 computer was used to estimate the period of the input signal time delay change.

Initially the period of the input signal time delay change was set to 90 msecs and was swept backward and forward over a 24 to 1 range. The above experiment was repeated by decreasing the period of the input signal time delay change to 227, 454, 673 msecs and finally 30 seconds. Figure 5-40 describes the output response of the ICPT correlator recorded by the transient recorder and the HP-85 computer at the above different periods. Note that when the period of the input signal time delay change is equal to 30 seconds the ICPT correlator tracks very closely the input

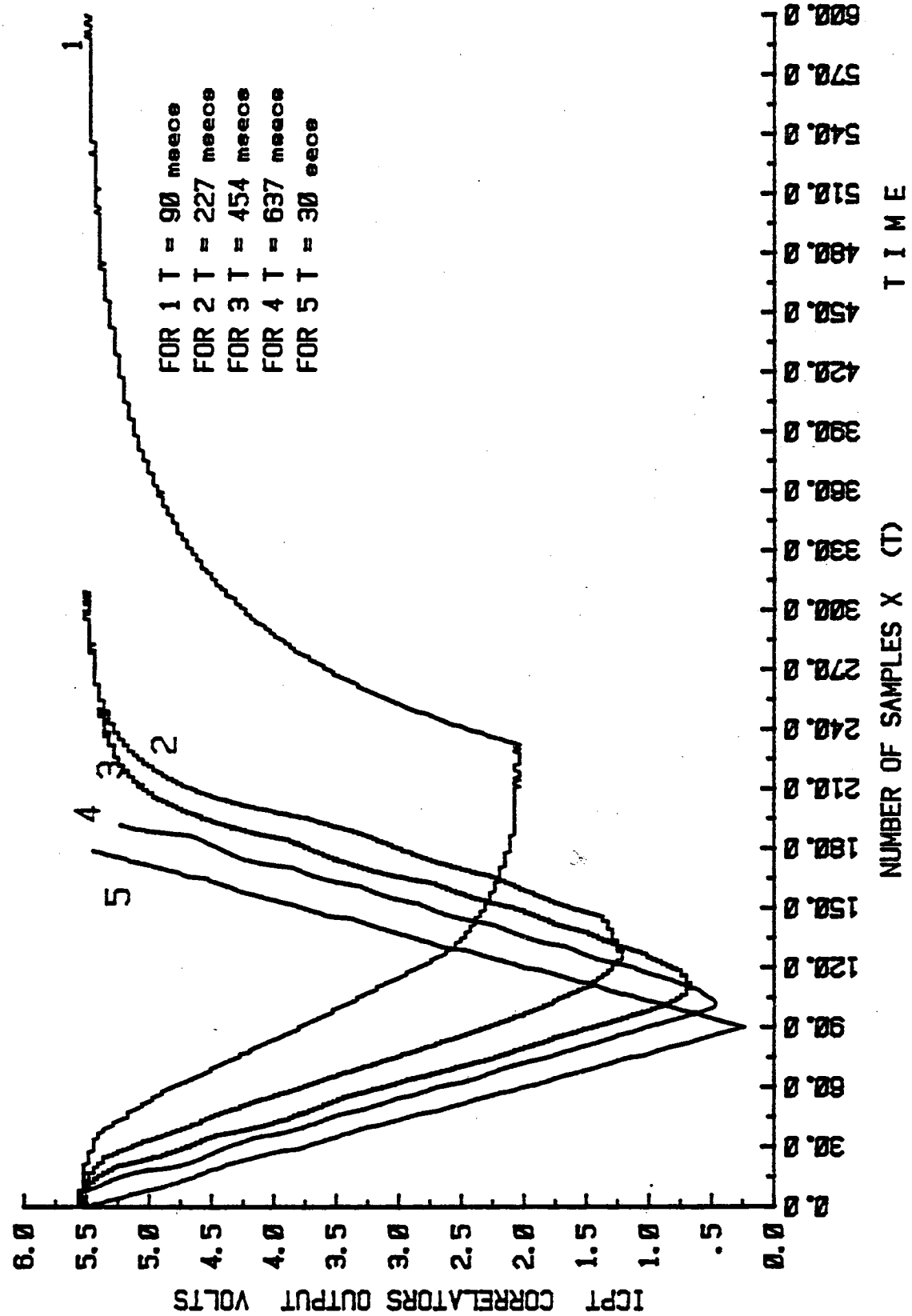

Fig. 5-40 RESPONSE OF THE ICPT CORRELATOR TO THE INPUT SIGNAL TIME DELAY SWEEP.

signal time delay change. From figure 5-40 it will be seen that as the period of the input signal time delay change increases the ICPT correlator tracks the peak of the correlation function more accurately, and its response approaches the case when the input signal time delay was changed with a 30 seconds period. In addition the output response of the ICPT correlator approximately follows the direction of the input signal time delay change and its output is a ramp function.

5-4-2 Static performance of the ICPT correlator

The static performance of the ICPT correlator was investigated using signals derived from the flow noise simulator over an input signal bandwidth of 50 to 500 Hz and 32 to 1 time delay range, (1.64 to 52.48 msecs). The percentage repeatability of the ICPT correlator was computed using equation 5-1 and taking 200 readings at each flow rate settings. The input signal time delay over a 32 to 1 range was divided to correspond to 24 equally spaced flow velocities. The measurement time between each input signal time delay settings was equal to 50 seconds.

Figure 5-41 describes the linear relationship between the input signal time delay settings and the tracking loops frequency to voltage convertors output with smoothing filter time constant of 2 seconds. From figure 5-41 it will be seen that the ICPT correlator can track the peak of the correlation function linearly over an input signal time delay range of 32 to 1. The percentage output reading error of the ICPT correlator over the above time delay range is shown in figure 5-42, and approximately is of order

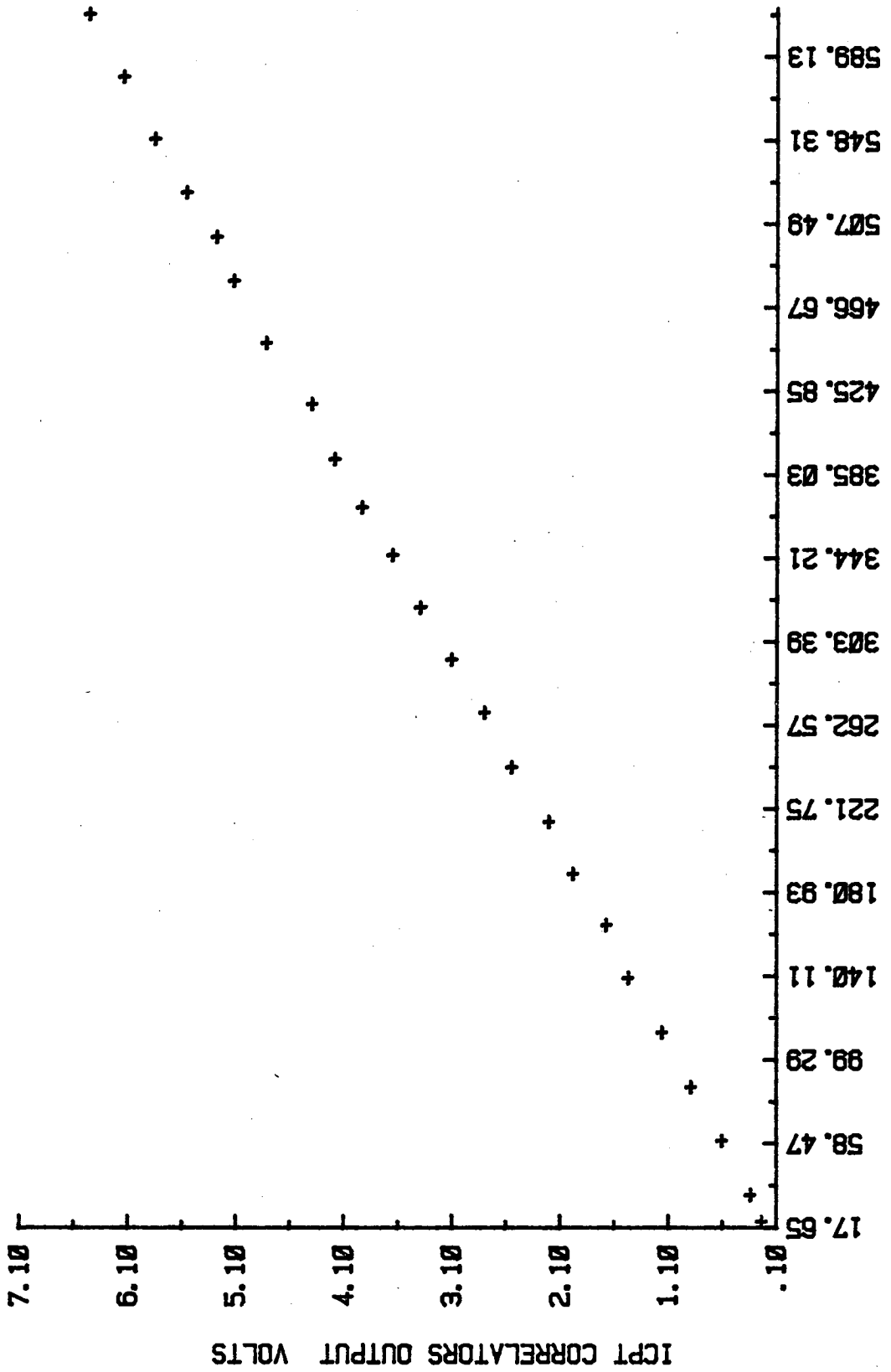

Fig. 5-41 PERFORMANCE OF THE ICPT CORRELATOR UNDER STATIC SIGNAL CONDITIONS

of $\pm$1.5%.

The percentage repeatability of the ICPT correlator over the above input signal time delay range is shown in figure 5-43. From figure 5-43 it will be seen that the percentage repeatability of the ICPT correlator is approximately of order of +1.8%, and increases as the input signal bandwidth decreases. From the experimental results given in this section and section 5-2-2 the performance of the tracking loop under static signal conditions can be summerised as below:-

Input signal time delay range = 32 to 1 .

Input signal bandwidth range = 50 to 500 Hz.

Percentage resolution = 0.6 % .

Percentage output reading error = $\pm$ 1.5 % .

Percentage repeatability = +1.8 % .

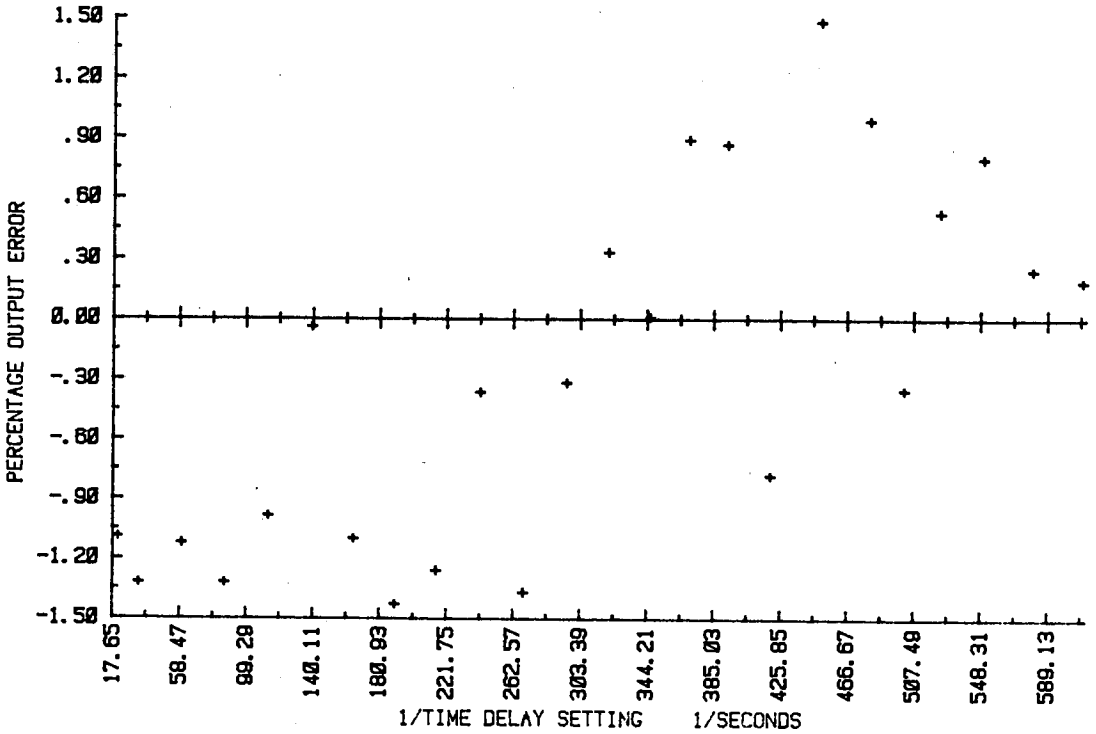

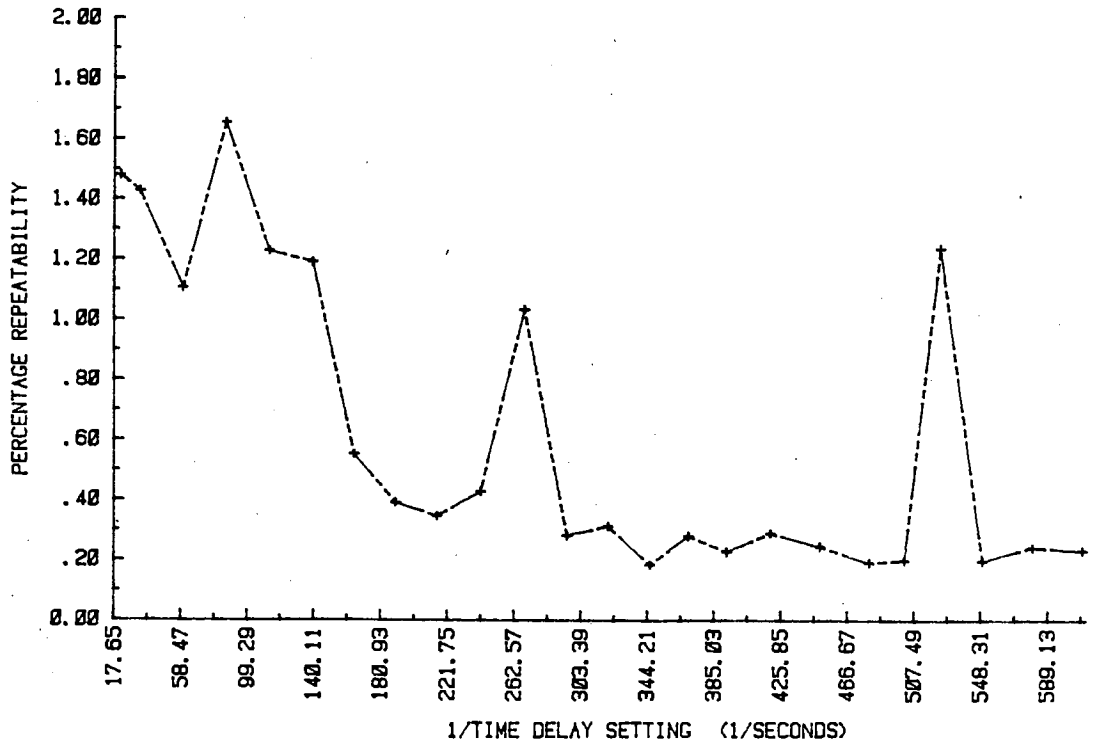

Fig. 5-43 PERCENTAGE REPETABILITY OF THE ICPT CORRELATOR

CHAPTER 6 CONCLUSIONS and RECOMMENDATIONS

The primary objective of the programme of research described in this thesis was to investigate methods for improving the accuracy and dynamic performance of correlation based time delay measurement system, particularly under changing signal conditions. As a result, the improved constrained peak tracking ,ICPT, correlator was designed and constructed and its performance was evaluated. The performance of the ICPT correlator under changing signal conditions was found to offer an industrially acceptable performance, when tested with signals derived from a flow noise simulator.

In broad terms, the work described in this thesis can be divided into three parts. First a review of significant parameters affecting the performance of the correlation based measurement systems, as well as necessary theoretical and practical background are presented. The second and major part of this thesis is concerned with the development and evaluation of the ICPT correlator, intended for flow measurement applications. Finally the third part of the thesis describes a programmable flow noise simulator which was designed, constructed, and used to evaluate the performance of the ICPT correlator.

Published works related to the algorithms available to estimate correlation function, both theoretical and practical were reviewed. It has been found that for applications where the

position of the peak of the correlation function is of great importance, i.e. correlation flow-meter, the digital polarity algorithms and in particular slow sampling technique described by Kam, Shore, and Feher (1975), will simplify the implementation and the cost of the correlator. The review of the reported single chip correlators has revealed that, the current running project by Jordan and Blackly (1983), to implement 512 stage overloading counter correlator on a single chip is of great importance. Such a device will find a large application area and hence its cost will probably be acceptably low. Some of the reported algorithms for implementation on an 8-bit micro-computer were reviewed. The implementation of the correlation function algorithm on a micro-computer reduces the cost and complexity compared with the available hardware techniques. A micro-computer correlator is suitable for applications where the speed of the correlation function estimate is not of prime importance.

The sources of errors which influences the accuracy and dynamic performance of the correlation based measurement systems, and in particular the correlation flow-meters were reviewed in chapter 2. Since the study of the transducer system was not required in this research programme, the sources of errors due to the transducer system were not considered. Some of the major problems experienced with the correlation measurements, results from the assumption made in correlation function analysis that the data being analysed are generated by the stationary processes. A review of the published work describing the performance of correlation based measurement systems under non-stationary signal

conditions has been included. The performance of the correlation based measurement systems under non-stationary signal conditions requires further investigations.

The measurement time of the coarsely quantised time delay axis based correlation flow-meter is requiered to be of order of 2 to 20 seconds, over an input signal bandwidth of 50 to 500 Hz, (Taylor Instrument Ltd., 1976). Such a measurement time will lead to a display which jumps in discrete steps. The review of tracking correlators presented in chapter 2, has indicated that under non-stationary signal conditions these correlators may perform better than coarsely quantised correlators using summation operation to implement the required integration operation. Consequently the major part of this thesis was concerned with the development and evaluation of the performance of the ICPT correlator to the point where the feasibility of this method was established.

The ICPT correlator described in this thesis is most suitable for flow measurement applications, simple to implement and can reliably track the most significant peak of the correlation function. The ICPT correlator is constrained to track the most significant peak of the correlation function by a peak position estimate obtained from a 6809 based coarse correlator.

To design a highly reliable and accurate tracking system, the detailed circuit diagram of the negative feedback loop was considered with great care. The required number of discrete

components was reduced and its performance was maintained.

The previously reported possibility of losing the most significant peak of the correlation function and tracking spurious peak, as well as the tracking loops output response jitter are eliminated by the ICPT correlator. The negative feedback loop of the ICPT correlator is free to track the most significant peak of the correlation function with high resolution defined with its components. The delay shift register of the tracking loop is set by the peak position estimate of the 6809 based coarse correlator through a coarse position latch. The coarse position latch is enabled by the output of a window comparator, through a logic control, once the tracking loops error voltage is beyond its linear lock range. This arrangement has eliminated the previously reported, Manook 1981, output response jitter of the loop as well as the possibility of tracking spurious peak or tracking the peak of the function inaccurately. It should be noted that the performance of the loop is not affected by the poor percentage repeatability of the peak position estimate of the 6809 based coarse correlator.

The output of an additional serial correlator was used to detect no flow conditions (i.e. low significance peaks) and the out of lock mode when the input signal time delay suddenly changes over a large range. This situation is not very common in industrial flow measurement applications, since the rate of change of the flow velocity is determined by the valves and the pumping system used in flow stream, (Taylor Instrument Ltd. 1982).

The small signal analysis method was used to derive the first order transfer function of the tracking loop, and is given by equation 4-6 of chapter 4. This transfer function was used to predict the dynamic chracteristic of the loop, and was achieved by applying a perturbing square wave signal to the input terminal of the tracking loops smoothing filter. The predicted results derived from the transfer function of the loop were clearly verified. The prototype model of the loop was found to operate exactly as predicted by its first order transfer function. The results obtained indicated that the first order transfer function of the loop can be used to predict the tracking loops time constant as well as the output voltage variation of the tracking loops smoothing filter, (error voltage), within its linear lock range.

The dynamic response of the loop to the simulated flow noise signal time delay change,(within its linear lock range), was investigated. The results obtained were compared with the estimated results derived from the first order transfer function of the loop, and found to be identical. Therefore once again, these results indicate that the dynamic characteristic of the loop can be predicted by its first order transfer function.

It has been shown that the closed loop time constant of the tracking correlator is inversely proportional to its delay shift register length, percentage setting of the gain control potentiometer, slope of the differentiated correlation function (polarity), and is proportional to the time constant of the

tracking loops smoothing filter. The closed loop time constant of the loop with relatively small and large delay shift register length over an input signal bandwidth of 50 to 500 Hz was approximately equal to .5 and .2 seconds respectively.

The performance of the tracking loop under changing signal conditions was investigated by sweeping the input signal time delay at different rates in both directions. The results obtained indicated that the tracking range of the loop is directly dependent on the direction of the input signal time delay sweep. In addition it has been found that, regardless of the direction of the input signal time delay sweep, the loop can track the peak of the correlation function linearly within a range smaller than its tracking range and this was called the linear lock range of the loop.

Under changing signal conditions the first order transfer function of the loop was used to estimate the output voltage swing of the tracking correlators error voltage within its linear lock range. The predicted results derived from the first order transfer function of the loop were verified clearly by the experimental results obtained. Therefore it has been concluded that the first order transfer function of the loop can be used to predict the linear lock range of the tracking correlator under changing signal conditions.

The performance of the serial correlator was investigated and from the results obtained it was concluded that, the output of

the serial correlator can not be used to indicate the linear lock range of the loop. The output of the serial correlator can only be used to indicate tracking and out of lock mode of the negative feedback loop.

The tracking performance of the ICPT correlator under static signal conditions over a simulated flow noise signal time delay range of 32 to 1 was investigated. The percentage repeatability and output error of the ICPT correlator over the above time delay range and an input signal band width of 50 to 500 Hz, was found to be equal to 1.8% and $\pm$1.5% respectively. It has been shown that the percentage repeatability of the ICPT correlator is inversely proportional to the bandwidth of the simulated flow noise signal over an input signal bandwidth of 50 to 500 Hz.

A large number of experiments have been carried out to investigate the dynamic performance of the system. Additional improvements made to the basic tracking loop, has indicated that these correlators can be designed to offer a reliable performances, with high accuracy and low cost. The results obtained indicate that the ICPT correlator is suitable for correlation flow measurement applications, and can be designed to offer industrially acceptable performances. The performance of the ICPT correlator over a simulated flow noise signal bandwidth of 50 to 500 Hz, and time delay range of 32 to 1 is summerised

as below:-

i)The closed loop time constant of the tracking correlator to input signal time delay change within its linear lock range is approximately .2 to .5 seconds.

ii)The response time of the loop to settle within a tolerance bandwidth of $\pm$1% when the input signal time delay change is beyond its linear lock range is approximately 1.5 seconds.

iii)The percentage output error of the ICPT correlator is of order of $\pm$1.5%.

iv)The percentage repeatability of the ICPT correlator is of order of 1.8%.

To investigate the performance of the prototype model of the ICPT correlator a noise generator which simulates very closely the flow generated noise signals was required. The reported publications relevant to noise simulation were reviewed. The flow noise simulator described in chapter 3 was designed and constructed in such a way that it can be programmed to satisfy the non-stationary signal requirements of the research programme. The following parameters of the signals derived from the flow noise simulator can be adjusted through the HP-85 computer:-

i) Time delay

ii) Bandwidth

iii) Significance of the correlation function relating the signals derived from the noise simulator.

The results presented in chapter 3 has indicated that the signals derived from flow noise simulator have characteristics very close to practical flow noise signals. In addition the flow noise simulator can be calibrated to simulate a flow noise signals with the required characteristics. Further programmability and flexibility was introduced by interfacing the flow noise simulator through the IEEE bus to the HP-85 computer used as a experiment controller.

The programmability of the noise simulator and the interface of the measurement system through the IEEE bus to the HP-85 computer has lead to collection of repeatable, reliable and consistent results. The measurement system has operated reliably over the past two years.

The programme of the work on the ICPT correlator is continuing with the main effort being concentrated on the implementation of the hardware involved on a single chip, using Microfabrication Facility of the Edinburgh University. This will lead to a single board correlation system complete with a single chip micro-processor capable of reliably covering a very wide delay range.

Replacement of the tracking loops analogue VCO with an all digital VCO will be a major step towards all digital implementation of the ICPT correlator. This will improve the accuracy and reliability of the tracking correlator.

A review of the published works describing the performance of correlation based measurement systems has indicated that very little work has been reported. It would be of great theoretical and practical importance to be able to predict how the slope of the estimated correlation function and its differentiated function is affected by non-stationary signal conditions.

REFERENCES

Antoniou A. (1979),
"Digital filters analysis and design", McGrawhill, 1979.

Al-Chalabi L.A.M. (1980),
"Fast polarity correlation using zero-crossing times for flow measurement and signal processing", Ph.D. Thesis, University of Bradford, 1980.

Adams W.B., Kuhn J.P., Whyland W.P. (1980),
"Correlator compensation requierments for passive time delay estimation with moving source or receivers", IEEE Trans., Vol.ASSP-28, No.2, 1980.

Butterfield M.H., Brigand G.F., Downing J. (1961),
"A new method of strip-speed measurement using random waveform correlators", Trans S.IT, pp 111-126, 1961.

Beck M.S. (1969),
"Powder and fluid flow measurement using correlation techniques", Ph.D. Thesis, University of Bradford, 1969.

Beck M.S. (1974),
"Adaptive control - fundamental aspects and their application", Proceedings of the First Annual Advanced Control Conference, Purdue University, pp 1-26, 1974.

Battye J.S. (1976),
"An industrial correlation flowmeter", Ph.D Thesis, University of Bradford, 1976.

Bell D.A., Rosie A.M. (1960),
"A low-frequency noise generator with Gaussian distribution", Electronic technol, Vol.37, pp 241-260, 1960.

Berndt H. (1963),
"Estimation of time varying correlation functions", Ph.D. disertation, University of Prudue, 1963.

Berndt H., Cooper G.R. (1966),
"Estimates of correlation functions on nonstationary random processes", IEEE Trans., Vol.IT-12, No.1, pp 70-72, 1965.

Berndt H., Cooper G.R. (1965),
"An optimum observation time for estimates of time varying correlation functions", IEEE Trans., Vol.IT-11, No.2, pp 307-310, 1965.

Boonstoppel F., Veltman B., Vergouwen F. (1968),
"The measurement of flow by cross correlation techniques", Proc. Conf. on industrial measurement techniques for on-line computers, London, IEE Conf. Pub. No. 43, pp 110-124, 1968.

Bendat J.S., Piersol A.G. (1980),
"Engineering applications of correlation and spectral analysis", John Wiley & Sons, N.Y., 1980.

Bohman J., Meyr H., Spies G. (1982),
"A digital signal processor for high precision non-contact speed measurement of rail guided vehicles", 32nd IEEE vehicular technology conference, California, pp 454-462, 1982.

Browne M.A., Deloughry R.J., Green R.G., Thorn R. (1982),
"state sequenced cross-correlator", Electronics letters, Vol.18, No.12, pp 528-530, 1982.

Bendall C.J. (1981)
"High speed correlation interface circuit", BSc Hons. project report HSP-267, Elec. Eng. Dept., University of Edinburgh, 1981.

Cumming J.G. (1967),
"Auto-correlation function and spectrum of filtered pseudo random binary sequence". Proc. IEE, Vol.114, No.9, pp 1360-1362, 1967.

Clinch J.M. (1969),
"Measurements of the wall pressure field at the surface of a smooth-walled pipe containing turbulent water flow", J. Sound Vib., Vol.9, No.3, pp 398-419, 1969.

Cernuschi-Frias B., Rocha L.F., (1981),
"A delay-lock period estimator", IEEE Trans., Vol. ASSP-29, No.4, pp 912-914, 1981.

Davies A.C. (1971),
"Properties of waveforms obtained by non-recursive digital filtering of pseudo random binary sequences", IEEE Trans., Vol.C-20, No.3, pp 270-281, 1971.

Douce J.L. (1968),
"Delayed version of m-sequences", Electronics letters, Vol.4, No.12, p254, 1968.

Davies J.T (1972),
"Turbulence phenomena", Academic Press, 1972.

Elias C.M. (1980),
"An ultrasonic pseudo-random signal correlation system", IEEE Trans., Sonics and ultrasonics, Vol. SU-27, No.1, pp 1-7, 1980.

Eldon J. (1981)
"Correlation - A powerful technique for digital signal Processing", TRW LSI Products Publication, California, 1981.

Fisher M.J., Davies P.O.A.L. (1963),
"Correlation measurement in a non-frozen pattern of turbulence", Journal of Fluid Mech., Vol.18, pp 97-116, 1963.

Finnie H.J. (1965),
"Digital correlation techniques for identifying dynamic systems", Ph.D. Thesis, University of Edinburgh, 1965.

Forrest J.R., Price D.J. (1978),
"Digital correlation for noise radar systems", Electronics Letters, Vol.14, No.18, 1978.

Fell R. (1982),
"Micro-processor-based cross-correlators using the skip algorithm", conference on the influence of micro-electronics on measurements, instruments and transducer design at University of Manchester, Umist., Institute of electronic and radio engineers publication, pp 25-32, 1982.

Fog C. (1982),
"The coincidence tracker-electronic equipment for a time of flight wind- speed measurement system", J. Phys. E; Sci. Instrum., Vol.15, pp 1184-1187, 1982.

Golomb S.W. (1964),
"Digital communications with space applications", Englewood Cliffs, N.J., Prentice-Hall, 1964.

Golomb S.W. (1967),
"Shift register sequences", Holden Day Inc., San Franscisco, 1967.

Godfery K.R., Devenish M., (1968)
"An experimental investigation of continuous gas chromatography using pseudo random binary sequences", Measurement and Control, Vol.2, p 228, 1968.

Gray D.F. (1978),
"The analysis of error variances in cross-correlation flow measurement devices", Ph.D. Thesis, University of Brunel, 1978.

Greenshield G., Jordan J.R. (1980),
"A programmable pseudo random noise generator", Micro-electronics Journal, Vol.11, No.9, pp 25-26, 1980.

Gardiner A.B. (1965),
"Logic PRBS delay calculator and delayed-version generator with automatic delay changing facility", Electronic letters, Vol.1, No.5, p 123, 1965.

Geranin V.A., Kozlov I.I., Shlyaktsu M.I. (1973),
"Correlation analysis of ergodic nonstationary random processes", Sov. Autom. Control, Vol.6, No.4, pp 1-5, 1973.

Greaves C.J. (1970),
"Study of Random processes theory", Technical Report, Cornell Aeronautical Laboratory Inc., CAL No. XM-1970-B-2, U.S.A., 1969

Gupta S.C (1975),
"Phase-Locked loops", Proc. IEEE, Vol.63, No.2, pp 291-306, 1975.

Hayes A.M. (1975),
"Cross-correlator design for flow measurement", Ph.D. Thesis, University of Bradford, 1975.

Hayes A.M., Musgrave G. (1973),
"Correlator design for flow measurement", The radio and electronic engineer, Vol.43, No.6, pp 363-368, 1973.

Henry R.M., Al Chalabi L. (1979),
"Microprocessor applications to velocity measurement by cross correlation", ACTA IMEKO, Moscow, pp 87-95, 1979.

Haykim S.S., Thorsteinson C. (1968),
"A quantised delay lock discriminator", Proc. IEEE, pp 1092-1093, 1968.

Hassab J.C., Boucher R.E., (1979),
"Optimum estimation of time delay by a generalised correlator", IEEE Trans., , Vol.ASSP-27, No.4, pp 373-380, 1979.

Hammond J.K. (1981),
"Non-stationary and nonlinearity in data analysis", AGARD report on modern data analysis techniques noise and vibration problems, No.700, pp 107-116, 1981.

Hewlett-Packard Journal (1967),
"Pseudo random and random test signals", Vol.19, No.1, September 1967.

Hewlett-packard Co. Ltd. (1968),
"HP 3721A Correlation Computer", Operating and service manual, 1968.

Hewlett-Packard Co. Ltd. (1981),
"Curve fitting - Auto-regression", HP-85 Standard PAC, 1981.

Honeywell Co. Ltd. (1970),
"Honywell Saicor Correlator", Instruction manual, 1970.

Hoffman G. (1971),
"Binary sequences", English Universities Press, London, 1971.

Hughes M.T.G. (1968),
"Transition matrix constructions for PRBS generators", Electronics letters, Vol.4, No.19, p 417,1968.

Ito R., Hirata Y., Kita O., Seno S., Omadaka K., Fukui R. (1977),
"Experimental study on behaviour of turbulence in a fully developed pipe flow", Journal of chemical engineering of Japan, Vol.10, No.3, pp 194-199, 1977.

Integlietta M., Tompkins W.R. (1971),
"System for measurement of velocity of microscopic particles in liquids", IEEE Trans., Vol.BME-18, pp 376-377, 1971.

Ireland B., Marshall J.E. (1968A),
"Matrix methods to determine shift register connections for delayed PRBS", Electronics letters, Vol.4, No.15, p 309, 1968.

Ireland B., Marshall J.E. (1968B),
"Matrix methods to determine shift register connections for delayed PRBS", Electronics letters, Vol.4 , No.21, p 254 , 1968.

Ireland B., Marshall J.E. (1976),
"New method of generation of shifted linear pseudo-random binary sequences", Proc. IEE, Vol.123, No.2, p 182, 1976.

Jordan A.E., David C.M. (1973),
"On the distribution of sums of successive bits of shift-register sequences", IEEE Trans., Vol.C-22, No.4, pp , 1973.

Jordan J.R. (1973),
"Correlation function and time delay measurement", Ph.D. Thesis, University of Bradford, 1973.

Jordan J.R., Kelly R.G. (1976),
"Integerated circuit correlator for flow measurement", Trans. Inst. measurement and control, Vol.9, pp 267-270, 1976.

Jordan J.R. (1979),
"A correlation interface circuit for microprocessor systems", Microelectronics Journal, Vol.10, No.1, pp 54-56, 1979.

Jordan J.R., Manook B.A. (1981A),
"Correlation function peak detector", Proc. IEE, Part E, Vol.28, No.2, pp 74-78, 1981.

Jordan J.R., Manook B.A. (1981B),
"A correlation function peak tracking system", Trans. Inst. measurement and control, Vol.3, No.2, pp 66-70, 1981.

Jordan J.R., Kiani-Shabestari B. (1982),
"FIR filter for generating multilevel signals from single-bit noise sequences", Electronics Letters, Vol.18, No.17, pp 739-740, 1982.

Jordan J.R., Kiani-Shabestari B. (1983),
"Deriving delayed sequences from pseudo-random-noise generators using exclusive-NOR feedback", Proc. IEE, Vol.130, Pt. G, No.3, 1983.

Jordan J.R., Blackley W. (1983),
"Private discussion",University of Edinburgh, Electrical Eng. Dept., The Kings Buildings, Edinburgh, June 1983.

Kaghazchi B., Beck M.S. (1977),
"Remote level and velocity measurement of rivers and open channels by analysis of random signals from surface waves", IEE Conference Publication, No.159, 1977.

Kramer C. (1965),
"A low-frequency pseudo-random noise generator", Electronic Engineering, pp 465-467, July 1965.

Komiya Kin-ichi. (1966),
"Flow measurement by using correlation techniques", Bulletin of N.R.L.M., Series No. 12, p 64,1966.

Kashiwagi H. (1968),
"Paper strip paper measurement using correlation technique", Trans. Soc. Instrum. Control Engnrs. (Japan), Vol.4, pp 304-312, 1968.

Korn G.A. (1966),
"Random process simulation and measurements", McGraw Hill, London, 1966.

Kam Z., Shore H.B., Feher G. (1975),
"Simple schemes for measuring auto-correlation functions", Rev. Sci. Instrum., Vol.46, No.3, pp 269-277, 1975.

Kostic L. (1981),
"Local steam transit time estimation in a boiling water reactor", IEEE Trans., Vol.ASP-29, No.3, pp 555-560, 1981.

Knapp C.H., Carter G.C. (1976),
"The generalised correlation method for estimation of time delay", IEEE Trans., Vol.ASSP-24, No.4, pp 320-327, 1976.

Keech R.P., (1982),
"The KPC multichannel correlation signal processor for velocity measurement", Tran. Inst. measurement and control, Vol.4, No.1, pp 43-52, 1982.

Lange F.H. (1967),
"Correlation techniques", Ilford Books Ltd., London, 1967.

Lampel A., Eastman W.L., (1971),
"High-speed generation of maximal legnth sequences", IEEE Trans., Vol.C-20, No. , pp 227-229, 1971.

Latawjec K.J., (1976),
"New method of generation of shift register linear pseudo-random binary sequences", Proc.IEE, Vol.123, No.2, p 182, 1976.

Larrowe V.L. (1966),
"A theory and method for correlation analysis of non-stationary signals", IEEE Trans., Vol.EC-15, Review no. R66 60, p 841, 1966.

Leavell W.H., Shahrokhi F. (1977),
"Tracking non-stationary velocity", Trans. Am. Nucl. Soc., Vol.26. p 332, 1977.

Leitner J.R. (1980),
"A microprocessor based cross-correlation flow-meter", Conference on " Applications of microprocessors in devices for instrumentation and automatic control", London, 1980.

Leitner J.R. (1979),
"Slurry flow measurement using correlation techniques", Ph.D Thesis, University of Cape Town, S.A., 1979.

Mitchell R.L., McPherson D.A. (1981),
"Generating non-stationary random sequences", IEEE trans., Vol.AES-17, No.4, 1981.

Maritsas D.G. (1973A),
"On the statistical properties of a class of linear feedback shift-register sequences", IEEE Trans., Vol.C- , No. , pp 961-962, 1973.

Maritsas D.G. (1973B),
"The auto-correlation function of the two feedback shift-register pseudo random source", IEEE Trans., Vol.C- ,No. ,pp 962-964, 1973.

Mesch F., Fritsche R., Kipphan H. (1974),
"Transit time correlation- A survey on its applications to measuring transport phenomena", Trans. of ASME, Journal of dynamic systems, Meas. and Control, pp 414-420, 1974.

Meyer H. (1976),
"Delay lock tracking of stochastic signals", IEEE Trans., Vol.COM-24, No.3, pp 331-339, 1976.

Manook B.A. (1981),
"A high resolution cross-correlator for industrial flow measurement", Ph.D. Thesis, University of Bradford, 1981

Meyer H., Spies G., Bohmann J. (1982),
"Real time estimation of moving time delay", International Conference on acoustics,speech,and signal processing, Paris, IEEE publ., Vol.1, pp 383-386, 1982.

Miller J. (1961),
"Air and space navigation system uses cross-correlation detection techniques", Electronics, pp 55-59, Dec.15, 1961.

Mix D.F., Sheppard J.G. (1973),
"Average correlation functions in on line testing of linear systems", IEEE Trans., Vol.AES-9, No.5, pp 665-669, 1973.

Massen R. (1982),
"Correlation measurement technique in brief", Series A, Introduction to theory and technical implementation, Endress+Hauser Co. publication, 1982.

Massen R. (1982),
"Private discussion at Edinburgh University", 1982.

Newland D.E. (1976),
"Introduction to random vibration and spectral analysis", Longmen, 1976.

Ong K.H (1975),
"Haydrolic flow measurement using ultrasonic transducers and correlation techniques", Ph.D. Thesis, University of Bradford, (1975).

Page C.H. (1952),
"Instantaneous power spectra", Journal of Applied Physics, Vol.23, No.1, pp 103-106, 1952.

Priestley M.B. (1965),
"Evolutionary spectra and non-stationary processes", J.R.Statistical Soc., Series B, Vol.27, No.2, pp 204-237, 1965.

Priestley M.B. (1966),
"Design relations for non-stationary processes", J.R. Statistical Soc., Series B, Vol.28, No.1, pp 228-240, 1966.

Priestley M.B. (1971A),
"Some notes on the physical interpetation of spectra of non-stationary stochastic processes", J. Sound Vib., Vol.17, No.1, pp 51-54, 1971.

Priestley M.B. (1971B),
"Time dependent spectral analysis and its application in prediction and control", J. Sound Vib., Vol.17, No.4, pp 517-534, 1971.

Papoulis A. (1965),
"Probability, random variables, and stochastic processes", McGraw-Hill, International student edition, Tokyo-Japan, 1965.

Roberts P.D.,Davies R.H. (1966),
"Statistical properties of smoothed maximum length binary sequences", Proc. IEE, Vol.113, No.1, pp 190-196, 1966.

Reticon (1978),
"Product summary discrete time analogue signal processing devices", Reticon Corporation USA,1978.

Rocha F.L. (1982),
"Adaptive delay tracking with a delay lock estimator", Conference on acoustics, speech, and signal processing, IEEE Paris, Vol.1, pp 424-427, 1982.

Schobi P. (1981),
"Memory structure speeds generation of pseudo noise sequences", Computer Design, pp 130-142, March 1981.

Spilker J.J., Magill D.T. (1961),
"The delay lock discriminator - An optimum tracking device", Proc. IRE, Vol.49, pp 1403-1416, 1961.

Spilker J.J. (1963),
"Delay lock tracking of binary signals", IEEE Trans., Vol.SET-9, pp 1-8, 1963.

Sykes D. (1976),
"Gas flow measurement using correlation techniques", Ph.D. Thesis, University of Bradford, 1976.

Scarbrough K., Ahmed N., Carter G.C. (1981),
"On simulation of a class of time delay estimation algorithms", Vol.ASSP-29, No.3, pp 534-540, 1981.

Sheppard J.G. (1973),
"On-line testing of linear electronic systems using average correlation functions", Ph.D. dissertation, University of Arkansas, 1973.

Tompkins W.R., Intaglietta M. (1971),
"Circuit for approximate computation of reciprocal of time delay to maximum cross correlation", Rev. Scientific Instruments, Vol.42, No.5, pp 616-618, 1971.

Tompkins W.R., Monti R., Intaglietta M. (1974),
"Velocity measurement by self-tracking correlator", Rev. Sci. Instrum., Vol.45, No.5, pp 647-649, 1974.

Thorn R. (1979),
"A low cost industrial cross correlation flowmeter", Ph.D. Thesis, University of Bradford, 1979.

Townsend A.A. (1947),
"The measurement of double and triple correlation derivatives in isotropic turbulence", Proc. Camb. Phil. Soc., Vol.43, pp 560-573, 1947.

Taylor Instrument Ltd. (1976),
"Summary of correlation flow-meter development", Confidential Report, 1976.

Taylor Instrument Ltd. (1982),
"Private communications", 1982.

Van Vleck J.H., Middleton D. (1966),
"The spectrum of clipped noise", Proc. IRE, Vol.54, No.1, pp 2-19, 1966

Veselova G.P., Gribanov Yu.I. (1969),
"The relay method of determining correlation coefficients", UDC 681.142.5, Obininsk, pp 187-194, 1969, Translated from Avtomatika i Telemekhanika, No.2, pp 31-39,1969.

Wolf J.K. (1963),
"On the applications of some digital sequences to communication", IEEE Trans, Vol. CS-11, pp 422-427, 1963.

Watts D.G. (1962),
"A general theory of amplitude quantisation applications to correlation determination", Proc.IEE, Vol.109, Pt. C, pp 209-218, 1962.

Widrow B. (1956),
"A study of rough amplitude quantisation by means of Nyquist sampling theory", IRE Trans., Vol.VCT-3, p 266, 1956.

Widrow B. (1961),
"Statistical analysis of amplitude-quantised sample data systems", IEEE Trans., Vol.VAI-79, pp 555-568, 1961.

White Jr.R.C. (1967),
"Experiments with digital computer simulations of pseudo random noise generators", IEEE Trans. (short notes), Vol.EC-16, pp 355-357, 1967.

Weatherburn C.E. (1952),
"A first course in mathematical statistics", Cambridge University Press, Second Edition, England, 1952.

Wierwille W.W. (1963),
"A new approach to the spectrum analysis of nonstationary signals", IEEE Trans. Application & Industry, Vol.82, pp 322-327, 1963.

Wierwille W.W. (1965),
"A theory and method for correlation analysis of nonstationary signals", IEEE Trans., Vol.EC-14, No.6, pp 909-919, 1965.

Wierwille W.W. (1968),
"Off-line correlation analysis of nonstationary signals", IEEE Trans., Vol.C-17, No.6, pp 525-536, 1968.

Wierwille W.W., Knight J.R. (1970)
"Study of random process theory", Technical Report, Cornell Aeronautical Laboratory Inc., CAL No. XM-1970-B-3, 1970.

A P P E N D I X 1

" Deriving Delayed Sequences From Pseudo Random Binary Noise Generators using Exclusive-NOR Feedback."

)eriving delayed sequences from pseudo-random-noise generators using exclusive NOR feedback

J.R. Jordan, D.I.C., M.Sc., Ph.D., C.Eng., M.I.E.E., M.I.M.C., and B. Kiani-Shabestari, M.Sc.

Indexing terms: Circuit theory and design, Computer applications, Noise and interference.

Abstract: The generation of delayed sequences from pseudo-random-noise generators, using exclusive-OR feedback, is briefly reviewed. A method for obtaining delayed sequences from circuits using exclusive-NOR feedback is presented. A microcomputer-controlled implementation of a delayed-sequence generator is described.

Introduction

veral methods have been devised for generating delayed juences from pseudo-random-noise generators using exclu-e-OR feedback connections [1, 2, 4, 5]. In this paper, the :thod of Ireland and Marshall [2, 3, 7] is reviewed and ex-ıded to cover the case when exclusive-NOR feedback is used.

prototype microcomputer-controlled delayed sequence nerator has been constructed using available components d has been successfully evaluated. The prototype circuit has en designed to produce test signals for investigating the ıcking performance of correlators used in correlation-based easurement systems.

Theory

)nsider a pseudo-random-noise generator having an n-stage ift register and exclusive-OR feedback defined by

$$X(t+1) = T \cdot X(t) \tag{1}$$

here mod-2 arithmetic is used and the transition matrix T defined by

$$T = \begin{bmatrix} C_1 & C_2 & \cdots & C_n \\ 1 & 0 & \cdots & 0 \\ 0 & 1 & 0 \cdots 0 & 0 \\ \vdots & & & \vdots \\ \cdots & \cdots & 1 & 0 \end{bmatrix}$$

nd $X(t) = [x_1 \ldots, x_n]^{tr}$ is the state of the register at time and $C_1 \ldots, C_n$ defines the feedback connections. After P hifts,

$$X(t+P) = T^P \cdot X(t) \tag{2}$$

The product of the first row of T^P with $X(t)$ gives the alue of x_1 after P shifts, i.e. $x_1(t+P)$, or, equivalently, it s the value of x_1, delayed by $(L-P)$ shifts, i.e. $x_1(t-(L-P))$, where $L = 2^n - 1$. The position of the ones in the first ow of T^P indicates the shift register outputs that must be nod-2 added to give an output-sequence phase advanced by P shifts (or delayed by $(L-P)$ shifts) with respect to the)utput $x_1(t)$.

Eqn. 2 can be rewritten to show the sequence of events resulting from shifting the register a further $n-1$ terms after the pth shift; i.e.

$$\begin{aligned} X(t+P) &= T^P X(t) \\ X(t+P+1) &= T^P X(t+1) \\ X(t+P+n-1) &= T^P X(t+n-1) \end{aligned}$$

Let column vectors $X(t+P)$ to $X(t+P+n-1)$ be represented by an $n \times n$ matrix Φ_p and the column vectors $X(t)$ to $X(t+n-1)$ be represented by an $n \times n$ matrix Φ_0. Then

$$\Phi_p = T^P \cdot \Phi_0$$

and

$$T^P = \Phi_p \cdot \Phi_0^{-1} \tag{3}$$

where

$$\Phi_0 = \begin{bmatrix} x_1(t) & x_1(t+1) & x_1(t+n-1) \\ x_1(t-1) & x_1(t) & x_1(t+n-2) \\ \vdots & \vdots & \vdots \\ x_1(t-n+1) & x_1(t-n+2) & x_1(t) \end{bmatrix}$$

By defining the initial condition to be $X(t) = [100\ldots0]^{tr}$, Ireland and Marshall [3] used the following recursion relation to derive the matrix Φ_0^{-1}:

From eqn. 1,

$$x_1(t+1) = C_1 x_1(t) \oplus C_2 x_2(t) \ldots \oplus C_n x_n(t)$$

But C_n is always 1, hence

$$x_n(t) = x_1(t+1) \oplus C_1 x_1(t) \oplus C_2 x_2(t) \ldots \oplus C_{n-1} x_{n-1}(t)$$

Replacing t by $t-1$ and rewriting the above equation in terms of x_1 gives:

$$x_1(t-n) = x_1(t) \oplus C_1 x_1(t-1) \ldots \oplus C_{n-1} x_1(t-n+1) \tag{4}$$

Similarly

$$x_1(t-n+1) = x_1(t+1) \oplus C_1 x_1(t) \ldots \oplus C_{n-1} x_1(t-n+2)$$

Paper 2441G, first received 25th June and in revised form 8th December 1982

The authors are with the Department of Electrical Engineering, University of Edinburgh, School of Engineering, The King's Buildings, Edinburgh EH9 3JL, Scotland

If the initial condition is $X^{tr} = [1\,0\,0\,0\ldots]$ then $x_1(t-n) = 1$, and

$$[1\,0\,0\ldots] = [1 \quad C_1 \quad C_2 \ldots C_{n-1}]\Phi_0$$

Eqn. 4 may be rearranged to give

$$x_1(t-n) \oplus C_{n-1}x_1(t-n+1) = x_1(t) \oplus C_1x_1(t-1)\ldots \oplus C_{n-2}x_1(t-n+2)$$

Hence,

$$x_1(t-1-n) \oplus C_{n-1}x_1(t-n) = x_1(t-1) \oplus C_1x_1(t-2) \ldots \oplus C_{n-2}x_1(t-n+1)$$

Hence,

$$[0\ 1\ 0\ 0\ldots] = [0\ 1\ C_1\ C_2\ldots C_{n-2}]\Phi_0$$

This process is repeated to give

$$I = \begin{bmatrix} 1 & C_1 & C_2 & \ldots & C_{n-1} \\ 0 & 1 & C_1 & \ldots & C_{n-2} \\ \vdots & & & & \vdots \\ \ldots & \ldots & \ldots & \ldots & \end{bmatrix} \cdot \Phi_0$$

where I is the identity matrix.

Therefore,

$$\Phi_0^{-1} = \begin{bmatrix} 1 & C_1 & C_2 & \ldots & \ldots & C_{n-1} \\ 0 & 1 & C_1 & C_2 & \ldots & C_{n-2} \\ 0 & 0 & 1 & C_1 & \ldots & \\ \vdots & & & & & \vdots \\ \ldots & \ldots & \ldots & \ldots & \ldots & \end{bmatrix} \quad (5)$$

The first row of T^P defines the connections required to achieve a sequence, phase advanced by P shifts. This is obtained by taking the first row of Φ_p and multiplying by Φ_0^{-1}. The first row of Φ_p is the content after $P+n-1$ shifts, written in reverse order.

Consider a 4-stage shift register with mod-2, exclusive-OR, feedback from stages 3 and 4. The transition matrix for this connection is

$$T = \begin{bmatrix} C_1 & C_2 & C_3 & C_4 \\ 1 & 0 & 0 & 0 \\ 0 & 1 & 0 & 0 \\ 0 & 0 & 1 & 0 \end{bmatrix}$$

$$= \begin{bmatrix} 0 & 0 & 1 & 1 \\ 1 & 0 & 0 & 0 \\ 0 & 1 & 0 & 0 \\ 0 & 0 & 1 & 0 \end{bmatrix}$$

Table 1a shows the shift-register sequence for this feedback arrangement.

Table 1: State sequences for 4-stage shift register with Ex-OR feedback and Ex-NOR feedback from stages three and four

a Ex-OR feedback, *b* Ex-NOR feedback

	a				*b*							
	$T^PX(t)$				$T^PX(t) \oplus X_N(t+P-1)$				First row of T^P			
P	x_1	x_2	x_3	x_4	x_1	x_2	x_3	x_4	1	2	3	4*
0	1	0	0	0	1	0	0	0	1	0	0	0
1	0	1	0	0	1	1	0	0	0	0	1	1*
2	0	0	1	0	1	1	1	0	0	1	1	0*
3	1	0	0	1	0	1	1	1	1	1	0	0*
4	1	1	0	0	1	0	1	1	0	1	0	1*
5	0	1	1	0	1	1	0	1	0	1	0	1*
6	1	0	1	1	0	1	1	0	1	0	1	0*
7	0	1	0	1	0	0	1	1	0	1	1	1
8	1	0	1	0	1	0	0	1	1	1	1	0
9	1	1	0	1	0	1	0	0	1	1	1	1*
10	1	1	1	0	1	0	1	0	1	1	0	1
11	1	1	1	1	0	1	0	1	1	0	0	1*
12	0	1	1	1	0	0	1	0	0	0	0	1
13	0	0	1	1	0	0	0	1	0	0	1	0
14	0	0	0	1	0	0	0	0	0	1	0	0
15	1	0	0	0	1	0	0	0	1	0	0	0

Also, the matrix Φ_0^{-1} becomes

$$\Phi_0^{-1} = \begin{bmatrix} 1 & C_1 & C_2 & C_3 \\ 0 & 1 & C_1 & C_2 \\ 0 & 0 & 1 & C_1 \\ 0 & 0 & 0 & 1 \end{bmatrix}$$

$$= \begin{bmatrix} 1 & 0 & 0 & 1 \\ 0 & 1 & 0 & 0 \\ 0 & 0 & 1 & 0 \\ 0 & 0 & 0 & 1 \end{bmatrix}$$

Then, for example, for $P = 7$, the first row of $\Phi_p = 0\ 1\ 1\ 1$ and the first row of

$$T^7 = [0\ 1\ 1\ 1] \begin{bmatrix} 1 & 0 & 0 & 1 \\ 0 & 1 & 0 & 0 \\ 0 & 0 & 1 & 0 \\ 0 & 0 & 0 & 1 \end{bmatrix}$$

and therefore the first row of T^7 is 0 1 1 1. Hence, $x_1(t+7)$ is obtained from

$$x_1(t+7) = x_2(t) \oplus x_3(t) \oplus x_4(t)$$

The connections required to generate $x_1(t-d)$ are obtained by evaluating the first row of T^{L-d}. For example, when $d = 3, L-d = 12$ and the first row of $T^{12} = [0\,0\,0\,1] \cdot \Phi_0^{-1} = 0\,0\,0\,1$. Therefore, $x_1(t-3) = x_4(t)$, as expected. Table 1b shows the first row of T^P for $1 \leqslant P \leqslant 15$.

A look-up table is an attractive way to achieve a programmable delayed ouput. However, for long sequences, a lookup table storing all delay connections will be excessively long.

is generated by masking appropriate shift-register stage outputs and addressing the exclusive-OR gates with only the stage outputs which are required to be modulo-2 added to form the desired delayed output. The details of the programmable sequence length control will not be given.

An on-line routine to calculate the settings for a particular delay could be based directly on the Ireland and Marshall [2] method. A software implementation of eqn. 1 is required, with the equivalent register set initially to $X = [1\,0\,\ldots,0]^{tr}$. After $P+n-1$ shifts, the resulting state vector $X(P+n-1)$ is written in reverse order as a row vector and postmultiplied by Φ_0^{-1}. The resulting row vector has a nonzero element corresponding to each stage to be added modulo-2 to generate the basic sequence, phase advanced by P shifts. This is a time-consuming operation.

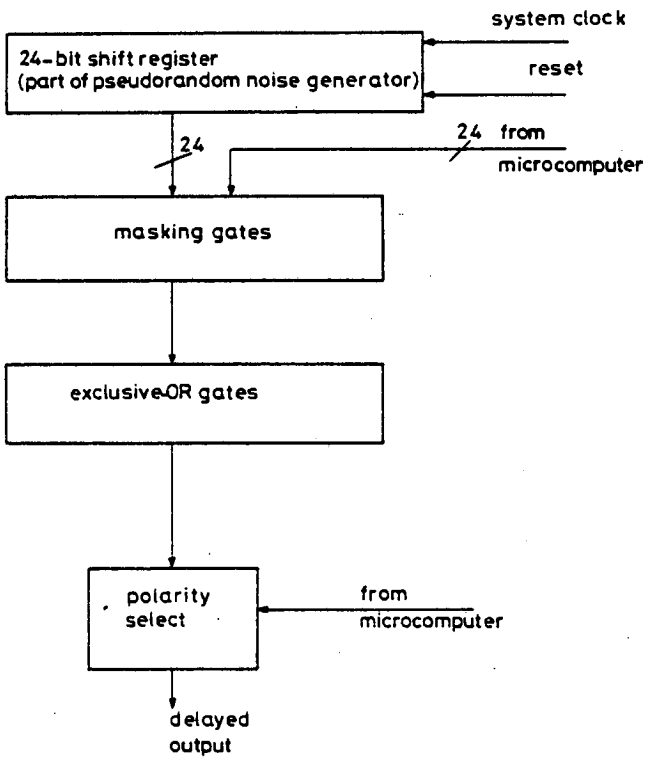

Fig. 1 *Block diagram of circuit used to generate delayed outputs*

In the prototype system, the full range of delay settings for each sequence length was divided by an appropriately large number and the selected delay settings stored to form a coarse delay setting lookup table. The coarse calculations can be carried out off-line and the results stored in ROM or initial calculations can be carried out on-line and the result stored in RAM.

Intermediate delays are derived by interpolating from the nearest point in the coarse-delay table. Ireland and Marshall's method [2] requires the knowledge of an $n \times n$ matrix, Φ_0^{-1}, and to obtain the full range of delay settings for a particular sequence length, the contents of the shift register should be reversed and multiplied by the Φ_0^{-1} matrix after each shift. An interpolation routine has been devised to considerably increase the speed of calculation of delay settings. The interpolation routine is based on eqn. 6, i.e. if $[r_1, r_2 \ldots r_n]$ are the delay connections derived from T^P, then the delay connections required for T^{P+1} are defined by

$$(r_1C_1 \oplus r_2), (r_1C_2 \oplus r_3) \ldots (r_1C_n)$$

Consider the particular case of a 9-bit shift register with feedback from stages 4 and 9 i.e. $C_4 = C_9 = 1$. Then the next phase-advanced setting is defined by

$$r_2, r_3, r_4, (r_1 \oplus r_5), r_6, r_7, r_8, r_1$$

Hence, the algorithm for generating the next phase-advanced setting is

(i) Rotate to the right the previous setting by one position.
(ii) New position 4 equals new position 9 exclusive-OR'ed with position-4 value after the rotate operation.

An algorithm to generate the next delayed setting can be derived by considering:

$$\text{First row of } T^P = r_1, r_2, r_3, r_4, \ldots, r_9$$

and

$$\text{First row of } T^{P+1} = r_2, r_3, r_4, (r_1 + r_5), r_6, r_7, r_8, r_9, r_1$$

First row of T^P is obtained from first row of T^{P+1} by:

(i) Making the position 4 of the first row of T^{P+1} equal to the modulo-2 addition of position 4 with position 9.
(ii) Then rotate to left the result by one position.

When Ex-NOR feedback is used, an additional inversion will be required if the first row of T^P contains an odd number of ones.

If coarse delay settings are selected, so that they are separated by 50 delay steps, the maximum delay setting time for the 6809-based prototype circuit was approximately 0.15 ms when the sequence length was set to $2^{24}-1$. In this case, the maximum setting time corresponds to phase advancing or delaying by 25 steps, and 3 bytes of memory are required to store each delay setting. Sequences of less than $2^{16}-1$ and less than 2^8-1 will require, for each delay, setting 2 bytes and 1 byte of memory, respectively, and hence a shorter delay setting time is obtained.

Coarse delay settings have been calculated, using the extrapolation algorithm for generating the next phase-advanced delay setting. For the prototype system, these calculations were carried out off-line and the results stored in an EPROM. A 2K byte EPROM can, for example, store 682 coarse delay settings for a $2^{24}-1$ sequence. An on-line routine could be used as part of a power-on initialisation procedure. For the $2^{24}-1$ sequence, the calculation time to establish 682 coarse delay settings covering a delay range of 34 100 (i.e. 682 x 50) steps is approximately 200 ns.

4 Conclusions

Shift registers used in pseudo-random-noise generators are most conveniently designed to be reset to the all zero state. It is necessary, therefore, to consider the use of exclusive-NOR feedback, since the all-zero state is the forbidden state for generators using exclusive-OR feedback. Ireland and Marshall's method for deriving delay sequences from pseudo-random-noise generators has been extended to apply to circuits using exclusive-NOR feedback connections. Algorithms have been derived defining the connections necessary to obtain intermediate delay settings from a table of connections defining a range of coarse delay settings. A prototype noise generator, using exclusive-NOR feedback, with programmable delayed outputs, has been constructed and successfully controlled by a 6809 microcomputer.

5 Acknowledgments

The support of SERC and Taylor Instruments Ltd. is gratefully acknowledged.

It will be more convenient to store a smaller number selected at regular steps throughout the complete table and then to derive intermediate values by extrapolating, using

$$T^{P+1} = T^P T$$

where only the first row of T^P needs to be multiplied by T to generate the first row of T^{P+1}.
Let the first row of T^P be $r_1 \ldots, r_n$. Then,

$$T^{P+1} = \begin{bmatrix} r_1 & \cdots & r_n \\ \cdot & \cdots & \cdot \\ \cdot & \cdots & \cdot \\ \cdot & \cdots & \cdot \end{bmatrix}$$

$$\times \begin{bmatrix} C_1 & C_2 & \cdots & C_n \\ 1 & 0 & \cdots & 0 \\ 0 & 1 & 0 \cdots & \cdot \\ \cdot & \cdots & 1 & 0 \end{bmatrix}$$

Hence, first row of $T^{P+1} = (r_1 C_1 \oplus r_2), (r_1 C_2 \oplus r_3), \ldots$

$$\ldots (r_1 C_{n-1} \oplus r_n), r_1 C_n. \quad (6)$$

When the exclusive-NOR feedback connection is used, the operation of the circuit is described by:

$$X^1(t+1) = T \cdot X(t)$$

where

$$X^1 = [\bar{x}_1, x_2 \ldots, x_n]^{tr}$$

and

$$X = [x_1, x_2 \ldots, x_n]^{tr}$$

and where the exclusive-NOR function is defined by the complement of the exclusive-OR function.
But

$$X(t+1) = X^1(t+1) \oplus N^{tr}$$

where

$$N = [1\ 0\ 0\ 0 \ldots, 0]$$

Therefore,

$$X(t+1) = TX(t) \oplus N^{tr}$$

and

$$X(t+2) = T^2 X(t) \oplus TN^{tr} \oplus N^{tr}$$

In general,

$$X(t+P) = T^P \cdot X(t) \oplus T^{P-1} N^{tr} \ldots \oplus TN^{tr} \oplus N^{tr}$$

or

$$X(t+P) = T^P X(t) \oplus X_N(t+P-1) \quad (7)$$

where

$$X_N(t+P-1) = T^{P-1} N^{tr} \oplus \ldots \oplus TN^{tr} \oplus N^{tr} \quad (8)$$

Eqn. 7 differs from the equation for the exclusive-OR circuit (eqn. 2) by the exclusive-OR'ed term $X_N(t+P-1)$. This term will be a column vector, but only the first element is of interest.

From eqn. 7, it follows that, to obtain advanced sequences from pseudo-random-noise generators using exclusive-NOR feedback, the first row of T^P will be used as before, but an inversion will be required if the first element of $X_N(t+P-1)$ is 1. Note that $X_N(t+P-1)$ is the content of the register after $P-1$ clock pulses, assuming that the initial state was $[1\,0\,0 \ldots 0]$.

For commonly used exclusive-NOR feedback connections, the outputs requiring inversion are identified by the parity of the word formed from the first row of T^P, i.e. from the word defining the register outputs that must be combined to form the required delayed output. This may be explained as follows.

Consider two shift registers, one with exclusive-OR feedback, and the other with exclusive-NOR feedback and initial conditions having complementary bit values. When feedback is derived from an even number of stages, with each generator using the same feedback connections, the sequences generated will be complementary, since, for any even number of variables $a_1 \oplus a_2 \oplus \ldots a_n = \bar{a}_1 \oplus \bar{a}_2 \ldots \oplus \bar{a}_n$. Pseudo-random-noise generators, using exclusive-NOR feedback over an even number of stages, will generate a complementary sequence having the same general character as the sequence generated by exclusive-OR feedback. The major difference is that the all-ones state will never occur and a run of $N-1$ ones and N zeros will occur (the opposite conditions are obtained from noise generators, using exclusive-OR feedback).

Consider now the generation of delayed outputs from pseudo-random-noise generators, using exclusive-NOR feedback, derived from two stages (i.e. an even number of stages) of the shift register. Complementary sequences will be generated and, therefore, if an even number of outputs is combined to form a delayed output, an unwanted inversion will be obtained, since $a \oplus b = \bar{a} \oplus \bar{b}$. Hence, in this case, when the first row of T^P is used to define the connections for a particular delay, an additional inversion is required if the word forming the first row of T^P has even parity. If the first row of T^P has odd parity, then, for example, $a \oplus b \oplus c = \bar{a} \oplus \bar{b} \oplus \bar{c}$ and therefore an additional inversion is not required. Application of the parity condition or eqn. 7 will show that, for the example illustrated by Table 1*b*, the outputs that must be inverted are indicated by an asterisk.

3 Implementation

A prototype noise generator using exclusive-NOR feedback has been constructed. The circuit has been designed to be controlled by a 6809 microcomputer and allows sequences of length up to $2^{24}-1$ to be generated with full range of delayed outputs. The noise generator is being used to investigate the performance of cross-correlators under varying time delay conditions. Very fine control of the peak position of the cross-correlation function is possible when the longer sequence lengths are selected.

The pseudo-random-noise generator was based on three 8-stage shift registers. In common with other available shift registers, it was only possible to simultaneously reset all stages to zero. Consequently, exclusive-NOR feedback was selected, since the all zero state would then be a permitted state in the generated sequences. Fig. 1 shows a block diagram of the delayed output generator. Delayed pseudorandom noise

6 References

1 GARDINER, A.B.: 'Logic PRBS delay calculator and delayed-version generator with automatic delay changing facility', *Electron. Letts.*, 1965, 1, (5), p. 123.

2 IRELAND, B., and MARSHALL, J.E.: 'Matrix methods to determine shift-register connections for delayed PRBS', *ibid.*, 1968, 4, (15), p. 309

3 IRELAND, B., and MARSHALL, J.E.: 'Matrix methods to determine shift-register connections for delayed PRBS', *ibid.*, 1968, 4, (21), p. 467

4 HUGHES, M.T.G.,: 'Transition matrix constructions for PRBS generators', *ibid., 1968*, 4, (19), p. 417

5 DOUCE, J.L.: 'Delayed version of *m*-sequences', *ibid.*, 1968, 4, (12), p.254

6 LATAWJEC, K.J.: 'New method of generation of shifted linear pseudorandom binary sequences', *Proc. IEE*, 1974, 121, (8), pp. 905–906,

7 IRELAND, B., and MARSHALL, J.E.: 'New method of generation of shifted linear pseudo-random binary sequences', *ibid.*, 1976, 123, (2), p. 182

Bijan Kiani-Shabestari was born in Tehran, Iran, in 1955. He received the B.Sc. degree in electrical engineering in 1979 and the M.Sc. degree in electronic control engineering in 1980, both from the University of Salford. He is presently working towards a Ph.D. degree in electrical engineering at the University of Edinburgh. His research interests include digital signal processing and its applications to noise simulation and correlation-based measurement systems.

James R. Jordan received the M.Sc. degree from the University of Surrey in 1967 and the Ph.D. degree from the University of Bradford in 1973. He joined the Department of Electrical Engineering, University of Edinburgh in 1969 after industrial engineering experience with EMI Electronics Ltd. and teaching experience at Teeside Polytechnic. He is now a Senior Lecturer and specialises in teaching system theory and electronic instrumentation to undergraduate courses and reliability and fault detection methods to postgraduate courses. His principal research interest is the application of LSI circuits and microelectronic fabrication techniques to electronic instrumentation and transducers.

A P P E N D I X 2

" A FIR Filter For Generating Multilevel

Signals From Single Bit Noise Sequences."

Acknowledgment: The authors are grateful to R. Pierzina for carrying out some of the computations, and the Fraunhofer-Gesellschaft for financial support.

M. CLAASSEN
W. HARTH

Lehrstuhl für Allgemeine Elektrotechnik und Angewandte Elektronik
Technische Universität München
Arcisstraße 21, D-8000 München 2, W. Germany

12th July 1982

References

1 GOKGOR, H. S., DAVIES, I., HOWARD, A. M., and BROOKBANKS, D. M.: 'High-efficiency millimetre-wave silicon impatt oscillators', *Electron. Lett.*, 1981, **17**, pp. 744–745
2 READ, W. T., JUN.: 'A proposed high-frequency, negative-resistance diode', *Bell Syst. Tech. J.*, 1958, **37**, pp. 401–446
3 TAGER, A. S.: 'The avalanche-transit diode and its use in microwaves', *Sov. Phys.-Usp.*, 1967, **9**, pp. 892–912
4 MISAWA, T.: 'Negative resistance in *p-n* junctions under avalanche break-down conditions. Part I', *IEEE Trans.*, 1966, **ED-13**, pp. 137–143
5 GIBLIN, R. A., SCHERER, E. F., and WIERICH, R. L.: 'Computer simulation of instability and noise in high power avalanche devices', *ibid.*, 1973, **ED-20**, pp. 404–418
6 DECKER, D. R.: 'Impatt diode quasi-static large-signal model', *ibid.*, 1974, **ED-21**, pp. 469–479
7 ELTA, M. E., and HADDAD, G. I.: 'Large-signal performance of microwave transit-time devices in mixed tunneling and avalanche breakdown', *ibid.*, 1979, **ED-26**, pp. 941–948

0013-5194/82/170737-03$1.50/0

FIR FILTER FOR GENERATING MULTI-LEVEL SIGNALS FROM SINGLE-BIT NOISE SEQUENCES

Indexing terms: Circuit theory and design, Finite-impulse-response filters

A ROM-based circuit is described for the implementation of finite-impulse-response (FIR) filters used to generate multi-level Gaussian noise signals from pseudorandom binary noise signals. A particular advantage of the circuit is that it can be constructed from readily available, standard components.

Introduction: Gaussian noise signals can be obtained by smoothing maximal-length linear binary sequences.[1] Since the signal to be smoothed is digital, single-bit, the FIR[2,3] filter offers the most convenient way to implement the lowpass smoothing function. A number of commercial noise generators have been produced using this technique (for example, see the Hewlett-Packard HP3722 pseudorandom noise generator*). In this letter an implementation method for FIR filters is described which uses standard, low-cost, components.

Implementation: The block diagram of a conventional FIR filter for single-bit data sequences is shown in Fig. 1. The impulse response of the filter is obtained when a single logic 1 is clocked along the shift register. Hence each stage of the shift register will correspond with an analogue voltage output level. Consequently, resistor values $R_1, \ldots, R_n$ must be chosen to give the required impulse response, and therefore a wide range of, probably nonstandard, values is required.

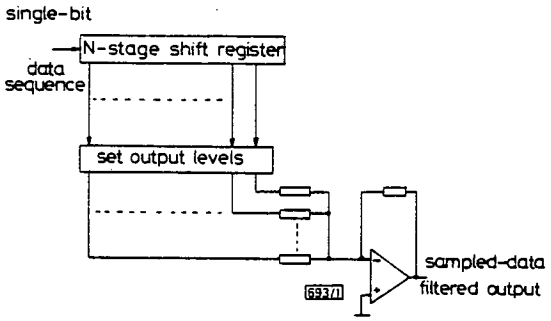

Fig. 1 *Conventional FIR filter*

* 'Operating and service manual' (Hewlett-Packard Co., 1967)

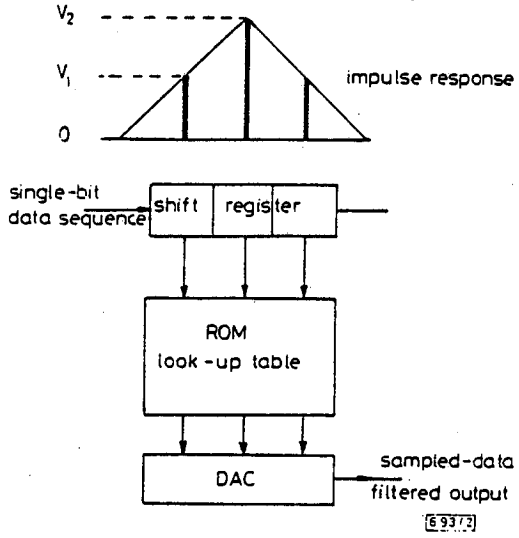

Contents of register ROM address	Filter output	ROM output
0 0 0	$0 = 0$	0 0 0
0 0 1	$V_1 = V_1$	0 0 1
0 1 0	$V_2 = 2V_1$	0 1 0
0 1 1	$V_1 + V_2 = 3V_1$	0 1 1
1 0 0	$V_1 = V_1$	0 0 1
1 0 1	$2V_1 = 2V_1$	0 1 0
1 1 0	$V_1 + V_2 = 3V_1$	0 1 1
1 1 1	$2V_1 + V_2 = 4V_1$	0 0 0

Fig. 2 *3-stage FIR filter using table-look-up output generation*

Fig. 2 shows the simplified block diagram of an alternative implementation using readily available low-cost EPROMs and DACs (digital/analogue convertors) which eliminates the requirement for an array of nonstandard resistors. A practical realisation will require several EPROMs, with each EPROM addressed by a part of the shift register. The EPROMs are programmed to output a word proportional to the analogue voltage defined by the address bit pattern and the required shape of the impulse response.

A prototype FIR filter has been constructed using a 32-bit shift register, three 2 k-byte EPROMs and three DACs. A block diagram of the circuit is shown in Fig. 3. The ROMs were addressed by shift register stages 1 to 11, 12 to 21 (where only 1 k-byte of the ROM is used) and 22 to 32. A computer program was developed to relate the ROM addresses to the

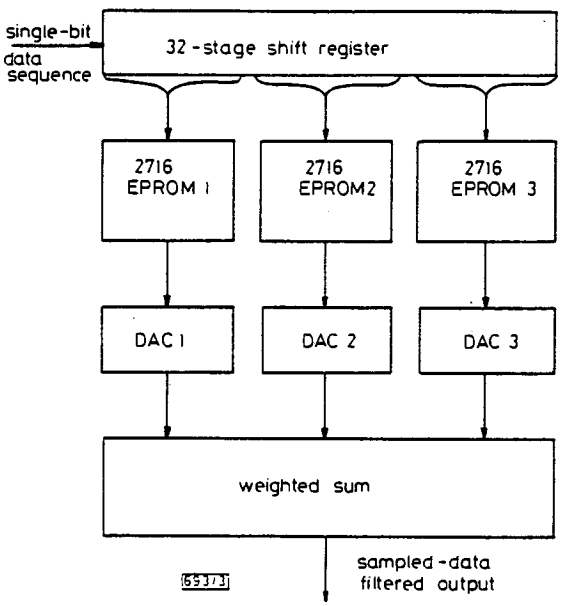

Fig. 3 *FIR filter using EPROMs and DACs*

analogue values of a desired impulse response. This is illustrated by the Table shown in Fig. 2. All computed values are offset by a positive constant to remove negative values in the look-up table due to the impulse response side lobes. The main (significant) part of the impulse response is stored in ROM 2, while ROMs 1 and 3 mainly store the lower valued, sidelobe information. To improve the use of ROMs 1 and 3 a scaling factor was used to increase the magnitude of the stored words. A weighted-summing circuit was used as an output stage to remove the scale factor and the offset voltage.

Results: A prototype circuit was designed such that the first null of the FIR filter impulse response occurred at nine clock periods, i.e. the cutoff frequency was 1/18 of the clock frequency. This is shown in Fig. 4, where the width of the centre lobe of the impulse response of the filter is approximately equal to 1/18 of the clock frequency applied to the filter. Fig. 5 shows the output of the FIR filter when a pseudorandom binary sequence (PRBS) is used as an input to the filter, and Fig. 6 shows the typically bell-shaped Gaussian probability distribution of the multilevel signal obtained when the PRBS was passed through the FIR filter. The lowpass action of the FIR filter can be observed by comparing the autocorrelation function of a PRBS before and after filtering. Figs. 7 and 8 show typical results. (A Hewlett Packard correlation computer was used to obtain the probability distributions and correlation functions.)

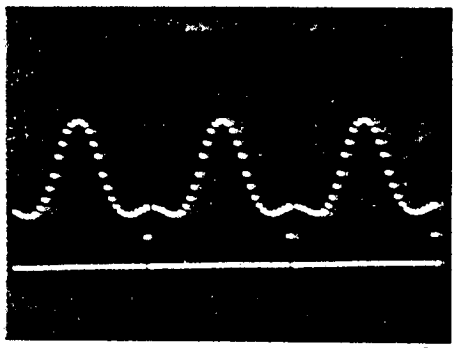

Fig. 4 *Impulse response of prototype circuit*

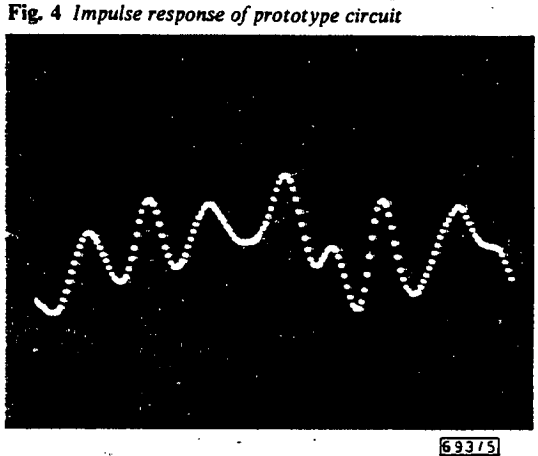

Fig. 5 *Output from filter with PRBS input*

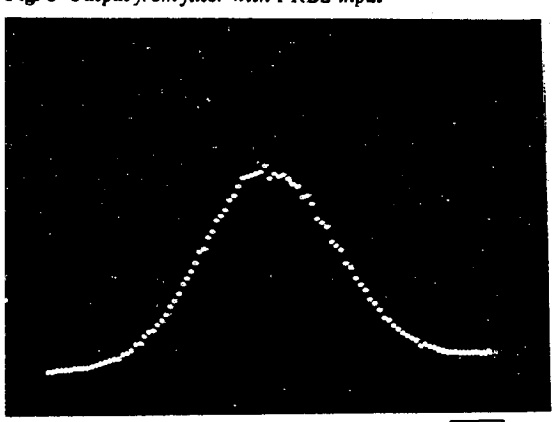

Fig. 6 *Probability distribution of FIR-filtered pseudorandom digital signal*

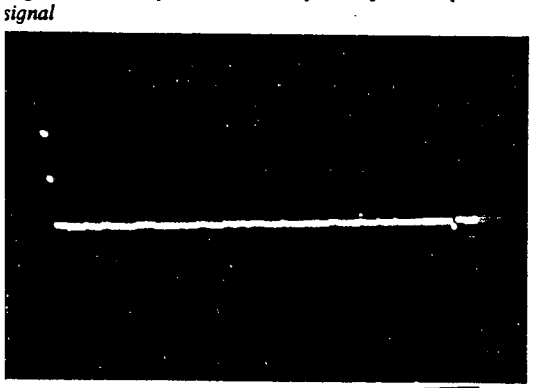

Fig. 7 *Autocorrelation of PRBS*

Fig. 8 *Autocorrelation of PRBS filtered by prototype FIR filter*
Same time base as Fig. 7

Conclusions: The prototype circuit performed as expected and demonstrated that the ROM-based, table-look-up method of generating multilevel Gaussian noise from pseudorandom binary noise is easy to implement. Commercially available shift registers, EPROMs and DACs were used and allowed a maximum clock rate of 2 MHz to give a maximum noise bandwidth of approximately 200 kHz. The number of DACs used can be reduced by the use of digital adders to combine the EPROM outputs.

Acknowledgments: The support of the UK SERC and Taylor Instruments Ltd. is gratefully acknowledged.

J. R. JORDAN
B. KIANI-SHABESTARI

Department of Electrical Engineering
University of Edinburgh
The King's Buildings, Edinburgh EH9 3JL, Scotland

1st July 1982

References

1 ROBERTS, P. D., and DAVIES, R. H.: 'Statistical properties of smoothed maximal-length linear binary sequences', *Proc. IEE*, 1966, **113**, (1), pp. 190–196
2 DAVIES, A. C.: 'Properties of waveforms obtained by non-recursive digital filter of pseudo random binary sequences', *IEEE Trans.*, 1971, **C-20**, pp. 270–281
3 ANTONIOU, A.: 'Digital filters—analysis and design' (McGraw-Hill, 1979)

0013-5194/82/170739-02$1.50/0

EFFICIENT WAVEGUIDE BRAGG-DEFLECTION GRATING ON $LiNbO_3$

Indexing terms: Integrated optics, Diffraction grating, Proton exchange

An efficient Bragg-deflection grating on x-cut $LiNbO_3$, using proton exchange in benzoic acid through an aluminium grating mask, has been demonstrated. A deflection efficiency of 90% has been measured.

Periodic structures play an important role in the field of integrated optics.[1] Such structures have been realised on $LiNbO_3$

A P P E N D I X 3

"An assembled listing of the program used to estimate and find the peak of the correlation function using 6809 based micro-computer."

Note that extensive software has been written for this project but for reason of space limitation only this routine has been included in this thesis. A separate report has been produced to document the software developed.

```
                ; Program developed to estimate 128 coefficients of the
                ; correlation function.
                ;
                ;
                ;
                ;
                ;
        3800            org     x'3800
        0100            pointer equ     x'0100
        0110            first   equ     x'0110
        0111            second  equ     x'0111
        0120            mdata   equ     x'0120
3800    1A 50   initi:  orcc    %x'50           ;mask IRQ & FIRQ
3802    4F              clra                    ;
3803    B7 5F62         sta     x'5f62          ;port A input down-stream signal
3806    B7 5F63         sta     x'5f63          ;port B input down-strean signal
3809    B7 5F53         sta     x'5f53          ;port A input upstream
380C    86 FF           lda     %x'ff           ;
380E    B7 5F52         sta     x'5f52          ;port B, peak position
                                                ;
                                                ;
                                                ;
3811    8E 2000 start1: ldx     %x'2000         ;clear 128 locations
                                                ;
3814    4F      start2: clra                    ;
3815    A7 84           sta     0,x             ;
3817    30 01           leax    1,x             ;
3819    8C 2080         cmpx    %x'2080         ;
381C    26 F6           bne     start2          ;
                                                ;
                                                ;
                                                ;
381E    4F              clra                    ;
381F    B7 0101         sta     pointer+1       ;this location will be compared
                                                ;with the measurement time
                                                ;
                                                ;
3822    1A 50           orcc    %x'50           ;mask IRQ and FIRQ
3824    8E 2000 start3: ldx     %x'2000         ;
                                                ;
                                                ;
                                                ;
                                                ;
3827    1A 40           orcc    %x'40           ;enable IRQ only
3829    3C EF           cwai    %x'ef           ;wait for IRQ
                                                ;and goto sync mode
382B    32 6C           leas    12,s            ;clear stack pointer
                                                ;
                                                ;
                                                ;
382D    B6 5F61         lda     x'5f61          ; content of the port A
                                                ; first 8 samples of up-stream
                                                ; signal
3830    B7 0110         sta     first           ;
3833    B6 5F60         lda     x'5f60          ; content of port B
                                                ; last 8 samples of up-stream
                                                ; signal
3836    B7 0111         sta     second          ;
                                                ;
                                                ;at this stage 16 samples of
                                                ;up-stream data are taken
                                                ;
                                                ;
3839    7E 3840         jmp     modi            ; sample down stream signal
                                                ;
                                                ;
                                                ;
383C    3C BF   start:  cwai    %x'bf           ; wait for FIRQ
383E    32 6C           leas    12,s            ;clear stack pointer
                                                ;
                                                ;
                                                ;
3840    B6 0110 modi:   lda     first           ;
```

```
3843  B8 5F51          eora    x'5f51      ;up-stream signal
                                           ;result stored in accumulator A
3846  F6 0111          ldb     second      ;
3849  F8 5F51          eorb    x'5f51      ;result stored in accumulator B
                                           ;
                                           ;
                                           ;
384C  1A 50            orcc    %x'50       ;mask IRQ and FIRQ
                                           ;check coincidence
                                           ;1
384E  1C 50    next1:  andcc   %x'50       ;clear carry
3850  44                lsra               ;check first bit
3851  25 02            bcs     next2       ;
3853  6C 84              inc     0,x        ;
                                           ;2
3855  1C 50    next2:  andcc   %x'50       ;
3857  44                lsra               ;
3858  25 02            bcs     next3       ;
385A  6C 08              inc     8,x        ;
                                           ;3
385C  1C 50    next3:  andcc   %x'50       ;
385E  44                lsra               ;
385F  25 03            bcs     next4       ;
3861  6C 8810            inc     16,x       ;
                                           ;4
3864  1C 50    next4:  andcc   %x'50       ;
3866  44                lsra               ;
3867  25 03            bcs     next5       ;
3869  6C 8818            inc     24,x       ;
                                           ;5
386C  1C 50    next5:  andcc   %x'50       ;
386E  44                lsra               ;
386F  25 03            bcs     next6       ;
3871  6C 8820            inc     32,x       ;
                                           ;6
3874  1C 50    next6:  andcc   %x'50       ;
3876  44                lsra               ;
3877  25 03            bcs     next7       ;
3879  6C 8828            inc     40,x       ;
                                           ;7
387C  1C 50    next7:  andcc   %x'50       ;
387E  44                lsra               ;
387F  25 03            bcs     next8       ;
3881  6C 8830            inc     48,x       ;
                                           ;8
3884  1C 50    next8:  andcc   %x'50       ;
3886  44                lsra               ;
3887  25 03            bcs     next9       ;
3889  6C 8838            inc     56,x       ;
                                           ;at this stage all 8-bit content
                                           ;of accumulator A is checked
                                           ;ACCUMULATOR B
                                           ;
                                           ;
                                           ;9
388C  1C 50    next9:  andcc   %x'50       ;
388E  54                lsrb               ;
388F  25 03            bcs     next10      ;first bit of accumulator B
3891  6C 8840            inc     64,x       ;
                                           ;10
                                           ;
3894  1C 50    next10: andcc   %x'50       ;
3896  54                lsrb               ;
3897  25 03            bcs     next11      ;
3899  6C 8848            inc     72,x       ;
                                           ;11
389C  1C 50    next11: andcc   %x'50       ;
389E  54                lsrb               ;
389F  25 03            bcs     next12      ;
38A1  6C 8850            inc     80,x       ;
```

```
                                                    ;12
38A4  1C 50     next12: andcc   %x'50               ;
38A6  54                lsrb                        ;
38A7  25 03             bcs     next13              ;
38A9  6C 8858           inc     88,x                ;
                                                    ;13
38AC  1C 50     next13: andcc   %x'50               ;
38AE  54                lsrb                        ;
38AF  25 03             bcs     next14              ;
38B1  6C 8860           inc     96,x                ;
                                                    ;14
38B4  1C 50     next14: andcc   %x'50               ;
38B6  54                lsrb                        ;
38B7  25 03             bcs     next15              ;
38B9  6C 8868           inc     104,x               ;
                                                    ;15
38BC  1C 50     next15: andcc   %x'50               ;
38BE  54                lsrb                        ;
38BF  25 03             bcs     next16              ;
38C1  6C 8870           inc     112,x               ;
                                                    ;16
38C4  1C 50     next16: andcc   %x'50               ;
38C6  54                lsrb                        ;
38C7  25 03             bcs     here                ;
38C9  6C 8878           inc     120,x               ;
                                                    ;
                                                    ;
                                                    ;
                                                    ;
                                                    ;
38CC  30 01     here:   leax    1,x                 ;
38CE  7C 0100           inc     pointer             ;
38D1  B6 0100           lda     pointer             ;
38D4  81 08             cmpa    %08                 ;8 samples of down-stream
                                                    ;data taken?
38D6  10 26FF62         lbne    start               ;
38DA  4F                clra                        ;
38DB  B7 0100           sta     pointer             ;
                                                    ;
                                                    ;
                                                    ;
38DE  7C 0101           inc     pointer+1           ;
38E1  B6 0101           lda     pointer+1           ;
38E4  B1 0123           cmpa    mdata+3             ;measurement time completed
38E7  10 26FF39         lbne    start3              ;
38EB  8E 2000           ldx     %x'2000             ;routine to find peak
                                                    ;position of the function
38EE  A6 80             lda     0,x+                ;
38F0  A1 80     back:   cmpa    0,x+                ;
38F2  22 05             bhi     forwd               ;
38F4  A6 1F             lda     -1,x                ;
38F6  BF 0000           stx     x'0000              ;
                                                    ;
38F9  8C 2080   forwd:  cmpx    %x'2080             ;
38FC  26 F2             bne     back                ;
38FE  7A 0001           dec     x'0001              ;
3901  74 0001           lsr     x'0001              ;multiply by two
3904  B6 0001           lda     x'0001              ;
3907  B7 5F50           sta     x'5f50              ;port B output peak position
390A  7E 3811           jmp     start1              ;start again

pointe  0100    first   0110    second  0111    mdata   0120
initi   3800    start1  3811    start2  3814    start3  3824
modi    3840    start   383C    next1   384E    next2   3855
next3   385C    next4   3864    next5   386C    next6   3874
next7   387C    next8   3884    next9   388C    next10  3894
next11  389C    next12  38A4    next13  38AC    next14  38B4
next15  38BC    next16  38C4    here    38CC    back    38F0
forwd   38F9
```